

**PREPARATION AND CHARACTERIZATION OF MICRO AND NANO  
FIBER REINFORCED NATURAL RUBBER COMPOSITES  
BY LATEX STAGE PROCESSING**

*Thesis submitted to*  
*Cochin University of Science and Technology*  
*in partial fulfillment of the requirements*  
*for the award of the degree of*  
*Doctor of Philosophy*  
*under the*  
*Faculty of Technology*

*by*

**Bipinbal P. K.**



**Department of Polymer Science and Rubber Technology  
Cochin University of Science and Technology  
Kochi- 682 022, Kerala, India  
<http://psrt.cusat.ac.in>**

**October 2012**

# **Preparation and characterization of micro and nano fiber reinforced natural rubber composites by latex stage processing**

*Ph. D Thesis*

*Author*

**Bipinbal P. K.**

Department of Polymer Science and Rubber Technology  
Cochin University of Science and Technology  
Cochin- 682 022, Kerala, India  
E-mail: bipinbal@cusat.ac.in

*Guide:*

**Dr. Sunil K Narayanankutty**

Professor  
Department of Polymer Science and Rubber Technology  
Cochin University of Science and Technology  
Cochin- 682 022, Kerala, India  
E-mail: sunil@cusat.ac.in

October, 2012



*Department of Polymer Science and Rubber Technology*  
*Cochin University of Science and Technology*

**Kochi - 682 022, Kerala, India**  
**<http://psrt.cusat.ac.in>**

---

**Dr. Sunil K Narayanankutty**  
Professor

Mob: +91 9995300093  
E-mail:sunil@cusat.ac.in

---

## *Certificate*

This is to certify that the thesis entitled “**Preparation and characterization of micro and nano fiber reinforced natural rubber composites by latex stage processing**” is an authentic report of the original work carried out by Mr. Bipinbal P. K., under my supervision and guidance in the Department of Polymer Science and Rubber Technology, Cochin University of Science and Technology, Kochi – 682 022. No part of the work reported in this thesis has been presented for the award of any degree from any other institution.

Kochi- 22  
18/10/12

*Dr. Sunil K. Narayanankutty*  
(Supervising Guide)



## *Declaration*

I hereby declare that the thesis entitled “**Preparation and characterization of micro and nano fiber reinforced natural rubber composites by latex stage processing**” is the original work carried out by me under the guidance of Dr. Sunil K Narayanankutty, Professor, Department of Polymer Science and Rubber Technology, Cochin University of Science and Technology, Kochi 682 022, and no part of the work reported in this thesis has been presented for the award of any degree from any other institution.

Kochi – 22  
18/10/12

*Bipinbal P. K,*



*Dedicated to My Father*

## *Acknowledgement*

---

*The thesis would not have been completed successfully but by the sincere help of others. As such, it is only appropriate that I express my sincere gratitude to them at this juncture.*

*I would like to express my deep sincere gratitude to my supervising guide, Prof. Dr. Sunil K. Narayanan Kutty, Professor and Head of the Department of Polymer Science and Rubber Technology, Cochin University of Science and Technology for providing guidance and support to carry out my research. He will always be there to help me with inspirations. I extended my gratitude to all other members of teaching faculty in the department for their valuable help and suggestions. I am also thankful to all non-teaching staff for the support I received from them.*

*I thank all my friends in the research fraternity in the department for their companionship and helps rendered especially Abhilash, Jabin Teacher and Teena. I am grateful to Prof. Jayaraj of Dept. of Physics, CUSAT and his students Arun, Vikas and Hasna for helping with nanofiber characterization, Prof. Mohanan of Dept. of Electronics, CUSAT and his student Nijaz for allowing me to carry out microwave characterization, Prof. Jayalakshmi of Dept. of Physics CUSAT and her students Sreekanth and Anand for their help in conductivity measurements, Soney Varghese, Asst. Prof. and his student Subhash for helping me with morphology studies, Lovely Mathew, Associate Prof. in the Dept. of Chemistry, Newman college, Thodupuzha and her students Cintil, Jitin, Lyju for their help in the preparation of nano fibers. I am indebted to Joby and his supervisor Prof. Lars Berglund of the Wood Science Center, Royal Institute of Technology, Stockholm, Sweden for their help in research and career. I extend my warm gratitude to Rejil,*

*Shibu, Bijoy, Aneurin, Chinju and Azeem. I extend my thanks to scientists of the Sophisticated Tests and Instrumentation center, Kochi especially Melbin and Shibu for analysis.*

*I sincerely acknowledge Dr. Joseph Makkolil, IUCND, CUSAT for his novel ideas, suggestions and encouragement. Last but not the least I express my gratitude to my mother for being a pillar of support.*

***Bipinbal P.K.***

## **Preface**

*Use of short fibers as reinforcing fillers in rubber composites is on an increasing trend. They are popular due to the possibility of obtaining anisotropic properties, ease of processing and economy. In the preparation of these composites short fibers are incorporated on two roll mixing mills or in internal mixers. This is a high energy intensive time consuming process. This calls for developing less energy intensive and less time consuming processes for incorporation and distribution of short fibers in the rubber matrix. One method for this is to incorporate fibers in the latex stage. The present study is primarily to optimize the preparation of short fiber- natural rubber composite by latex stage compounding and to evaluate the resulting composites in terms of mechanical, dynamic mechanical and thermal properties. A synthetic fiber (Nylon) and a natural fiber (Coir) are used to evaluate the advantages of the processing through latex stage. To extract the full reinforcing potential of the coir fibers the macro fibers are converted to micro fibers through chemical and mechanical means.*

*The thesis is presented in 7 chapters. The introductory chapter of the thesis reviews the state of the art research in the area of short fiber-elastomer composites reinforced with both natural and synthetic fibers. The scope and objectives of the present work are also discussed.*

*The second chapter of the thesis gives a detailed description of the materials used and the experimental techniques for characterization used in the study.*

*Third chapter presents the features of an alternate green method with less energy and time consumption for the preparation of short nylon fiber- natural rubber composites. The effect of adhesion promoters such as HRH bonding system*

*and maleic anhydride grafting is also described. Cure characteristics and mechanical properties of the composites are carried out. Strain sweep studies in RPA are conducted to evaluate fiber agglomeration and matrix–fiber interaction. Thermal analysis of the composites with and without adhesion promoters is carried out.*

*The fourth chapter discusses the preparation of micro fibers from a natural renewable material (Coir) by chemical and mechanical treatments. Morphological investigation of the microfibers is carried out. The use of coir micro fibers as an effective reinforcement in natural rubber composites prepared through latex stage processing is also presented. The composites are characterized for cure parameters, mechanical, dynamic mechanical and thermal properties.*

*Fifth chapter of the thesis describes the preparation of cellulosic nanofiber from coir through a simple and cost effective process of bleaching and homogenization. Dimensions of the nanofiber are determined by scanning electron microscopy and atomic force microscopy. Nanofibrillated cellulose is incorporated into natural rubber through latex stage processing. Characterization of the resultant composites is carried out.*

*Sixth Chapter reports the preparation of conducting elastomer composites by latex stage processing. Aniline is polymerized insitu in the latex containing micro and nano fibers so that polyaniline is coated on fibers and get dispersed in the matrix at the same time. The conducting composites are investigated for mechanical properties, DC electrical conductivity and microwave characteristics. The last chapter summarizes the main findings of the study and present the conclusions reached.*

## *Abstract*

In the present study short nylon fiber- natural rubber composites were prepared by latex stage processing. The composite was compared with composite prepared in the conventional processing method of dry rubber compounding. The mechanical properties of the composites were better for latex stage composites. To improve the interaction between the fiber and the matrix HRH bonding system and maleation of the matrix together with the surface hydrolysis of the fibers were carried out. The composites were evaluated with respect to mechanical, dynamic mechanical and thermal properties. The HRH bonding system was found to be better in improving the properties of the composites. A lignocellulosic fiber (Coir) was also used as a natural source for reinforcement in the preparation of short fiber composites through latex stage processing. The fibers in the macro form reduced the properties of the composites. Coir fibers were subjected to chemical and mechanical treatment to convert them to micrometer dimensions. The micro fibers reinforced the rubber matrix even at low fiber content. The dynamic mechanical and thermal characterizations of the composites were carried out. Agglomeration of fibers at higher loadings was revealed in strain sweep studies. Thermal stability of the composites decreased with increasing fiber content. In the next phase nano cellulosic fibers were extracted from coir by a simple and cost effective process. These nano fibers were used to prepare rubber composites by latex stage processing. The nano cellulosic fibers reinforced the rubber matrix at even lower loadings. Fiber agglomeration at higher loadings and reduction of thermal stability were seen in the case of nano composites also. Latex stage processing was utilized for the preparation of conducting elastomer composites. Polyaniline was coated insitu on micro and nanofibers dispersed in the latex.



# Contents

## Chapter 1

### INTRODUCTON ..... 01 - 41

1.1	Classification of Composites -----	02
1.2	Fiber composites -----	03
1.3	Why short fiber composites? -----	04
1.4	Short fiber elastomer composites -----	05
1.5	Reinforcement mechanism in short fiber composites -----	06
1.6	Factors influencing the properties of short fiber - elastomer composites -----	08
1.6.1	Type and Aspect Ratio of Fiber -----	08
1.6.2	Fiber Dispersion -----	09
1.6.3	Fiber Orientation -----	10
1.6.4	Fiber Matrix Adhesion-----	11
1.7	Natural rubber short fiber composites -----	14
1.8	Fibers used in short fiber composites -----	16
1.8.1	Nylon fiber -----	17
1.8.2	Coir fiber -----	18
1.8.3	Nanocellulosic fiber -----	18
1.9	Types of composites-----	20
1.9.1	Short Nylon Fiber – Elastomer Composites -----	20
1.9.2	Short Coir fiber -Elastomer composites -----	21
1.9.3	Nanocellulosic fiber – Elastomer composites -----	22
1.9.4	Conducting fiber elastomer composites -----	22
1.10	Applications of short fiber composites -----	24
1.11	Processing of short fiber elastomer composites -----	26
1.11.1	Mixing -----	26
1.11.2	Latex stage compounding -----	27
1.12	Scope and objective of the present work -----	28
	References -----	

## Chapter 2

### EXPERIMENTAL TECHNIQUES ..... 43 - 53

2.1	Materials-----	43
2.2	Chemicals -----	45
2.3	Processing-----	46
2.3.1	Compounding -----	46
2.3.2	Cure Characteristics -----	46
2.3.3	Vulcanization -----	48
2.4	Physical Properties-----	48
2.4.1	Tensile Strength, Modulus and Elongation at Break -----	49

2.4.2	Tear Strength	49
2.4.3	Hardness	49
2.4.4	Abrasion Resistance	49
2.4.5	Rebound Resilience	50
2.4.6	Compression Set	50
2.5	Dynamic Mechanical Analysis	51
2.5.1	Strain sweep studies in RPA	51
2.5.2	Studies in DMA	51
2.6	Thermal Analysis	51
2.7	Scanning Electron Microscopy (SEM)	52
2.8	Atomic force microscopy	52
2.9	X-ray diffraction	52
2.10	Lignin content	52

### **Chapter 3**

## **NATURAL RUBBER-NYLON MICRO FIBER COMPOSITES..... 55 - 122**

### **Part -A**

#### **Mechanical properties of NR- Nylon Micro Fiber Composites**

3.A.1	Introduction	55
3.A.2	Experimental	57
3.A.2.1	Materials Used	57
3.A.2.2	Processing	58
3.A.3	Results and discussions	61
3.A.3.1	Evaluation of Processing Energy	61
3.A.3.2	Fiber breakage analysis	62
3.A.3.3	Cure characteristics	63
3.A.3.3.1	<i>Composites without adhesion promoters</i>	63
3.A.3.3.2	<i>Composites with adhesion promoters</i>	65
3.A.3.4	Mechanical properties	71
3.A.3.4.1	<i>Composites without adhesion promoters</i>	71
3.A.3.4.2	<i>Composites with adhesion promoters</i>	76
3.A.3.5	Ageing resistance	90
3.A.3.6	SEM Analysis	92
3.A.4	Conclusions	94

### **Part -B**

#### **Dynamic mechanical properties of NR- Nylon Micro Fiber Composites**

3.B.1	Introduction	95
3.B.2	Experimental	96

3.B.3 Results and discussion -----	97
3.B.3.1 Strain sweep studies in RPA -----	97
3.B.3.1.1 Composites with HRH -----	97
3.B.3.1.2 MANR – Treated Nylon composites -----	99
3.B.3.2 Studies in DMA -----	101
3.B.3.2.1 Temperature sweep -----	101
3.B.3.2.2 Frequency sweep studies -----	104
3.B.4 Conclusions -----	109

### **Part -C**

#### **Thermal studies of NR- Nylon Micro Fiber Composites**

3.C.1 Introduction -----	110
3.C.2 Experimental -----	111
3.C.3 Results and discussion -----	112
3.C.3.1 Thermogravimetry -----	112
3.C.3.1.1 NR-Nylon composites with HRH bonding -----	112
3.C.3.1.2 MANR-Treated Nylon Composites -----	117
3.C.3.2 Differential Scanning Calorimetry -----	118
3.C.4 Conclusions -----	120
<b>References -----</b>	<b>120</b>

## **Chapter 4**

### **COIR MICROFIBER REINFORCED NATURAL RUBBER COMPOSITES.... 123 - 167**

#### **Part -A**

#### **Mechanical Properties of Coir Microfiber Reinforced Natural Rubber Composites**

4.A.1 Introduction -----	123
4.A.2 Experimental -----	125
4.A.2.1 Materials Used -----	125
4.A.2.2 Processing -----	125
4.A.3 Results and Discussion -----	128
4.A.3.1 Fiber characterization -----	128
4.A.3.1.1 Lignin content -----	128
4.A.3.1.2 SEM analysis -----	128
4.A.3.2 Composite characterization -----	129
4.A.3.2.1 Composites of macro fibers -----	129
4.A.3.2.2 Composites of micro fibers -----	133
4.A.4 Conclusions -----	145

## **Part -B**

### **Dynamic Mechanical Studies of Coir Microfiber Reinforced Natural Rubber Composites**

4.B.1 Introduction-----	147
4.B.2 Experimental-----	148
4.B.3 Results and discussion-----	149
4.B.3.1 Strain sweep in RPA-----	149
4.B.3.2 Studies in Dynamic Mechanical Analyzer-----	151
4.B.3.2.1 <i>Temperature sweep studies</i> -----	151
4.B.3.2.2 <i>Frequency sweep</i> -----	153
4.B.4 Conclusions-----	156

## **Part -C**

### **Thermal Studies**

4.C.1 Introduction-----	157
4.C.2 Experimental-----	158
4.C.3 Results and discussion-----	158
4.C.3.1 Thermogravimetry-----	158
4.C.3.2 Differential Scanning Calorimetry-----	164
4.C.4 Conclusion-----	165
References-----	165

## **Chapter 5**

### **NANOCELLULOSIC FIBER REINFORCED NATURAL RUBBER COMPOSITES**

..... 169 – 217

## **Part -A**

### **Mechanical properties of NR- Nanocellulosic Fiber Composites**

5.A.1 Introduction-----	169
5.A.2 Experimental-----	172
5.A.2.1 Materials Used-----	171
5.A.2.2 Processing-----	171
5.A.2.2.1 <i>Bleaching and homogenization</i> -----	171
5.A.2.2.2 <i>Preparation of composites</i> -----	172
5.A.2.2.3 <i>Scanning electron microscopy</i> -----	172
5.A.2.2.4 <i>Atomic force microscopy</i> -----	173
5.A.2.2.5 <i>X-ray diffraction</i> -----	173
5.A.3 Results and discussions-----	174
5.A.3.1 Fiber characterization-----	174
5.A.3.1.1 <i>Lignin content</i> -----	174

5.A.3.1.2 Infrared spectroscopy	175
5.A.3.1.3 Scanning electron microscopy	175
5.A.3.1.4 Atomic force microscopy	177
5.A.3.1.5 X-ray diffraction	179
5.A.3.2 Composite characterization	179
5. A.3.2.1 Cure characteristics	180
5.A.3.2.2 Mechanical properties	182
5.A.3.2.3 Ageing resistance	190
5.A.3.2.4 SEM Analysis	191
5.A.4 Conclusions	192

### **Part -B**

#### **Dynamic mechanical properties of NR- Nanocellulosic Fiber Composites**

5.B.1 Introduction	194
5.B.2 Experimental	195
5.B.3 Results and Discussion	195
5.B.3.1 Strain sweep studies in RPA	195
5.B.3.2 Studies in DMA	199
5.B.3.2.1 Temperature sweep studies	199
5.B.3.2.2 Frequency sweep studies	201
5.B.4 Conclusions	205

### **Part -C**

#### **Thermal studies of NR- Nanocellulosic Fiber Composites**

5.C.1 Introduction	206
5.C.2 Experimental	207
5.C.3 Results and discussion	207
5.C.3.1 Thermogravimetry	207
5.C.3.2 Differential Scanning Calorimetry	214
5.C.4 Conclusions	216
References	216

## **Chapter 6**

### **POLYANILINE COATED MICRO AND NANO FIBER CONDUCTING COMPOSITES BASED ON NATURAL RUBBER PREPARED THROUGH LATEX PROCESSING.....219 -**

6.1 Introduction	219
6.2 Experimental	221
6.2.1 Materials	221
6.2.2 Preparation of composites	222
6.2.3 DC electrical conductivity	223
6.2.4 Measurement of microwave properties	223

6.3	Results and Discussion -----	225
6.3.1	SEM Analysis -----	225
6.3.2	Mechanical properties -----	<b>226</b>
	6.3.2.1 Tensile strength -----	226
	6.3.2.2 Modulus -----	228
	6.3.2.3 Elongation at break -----	228
6.3.3	DC electrical conductivity-----	229
6.3.4	Microwave characteristics-----	231
	6.3.4.1 Dielectric permittivity-----	231
	6.3.4.2 Dielectric loss -----	223
6.4	Conclusions -----	234
	<b>References -----</b>	<b>235</b>

*Chapter 7*

<b>SUMMARY AND CONCLUSIONS .....</b>	<b>237 - 244</b>
--------------------------------------	------------------

**ABBREVIATION**

**LIST OF PUBLICATIONS**

.....❧.....

## *Abbreviations*

ASTM	American society for testing and materials
AFM	Atomic Force microscopy
CBS	N-cyclohexyl-2-benzothiazyl sulphenamide
$\mu\text{m}$	Micrometer
D	Dry rubber
DMA	Dynamic mechanical analysis
DSC	Differential scanning calorimetry
DTG	Derivative thermogravimetry
E'	Storage modulus
E''	Loss modulus
Hexa	Hexa methylene tetramine
Hr	Hour
HRH	Hexa methylene tetramine- resorcinol- hydrated silica
Hz	Hertz
ISNR	Indian standard natural rubber
L	Latex
lc	Critical fibre length
MH	Maximum torque
min	Minutes
ML	Minimum torque
mm	millimetre
MPa	Mega Pascal
N	Newton
Nm	Newton meter
RPA	Rubber Proess Analyzer
TGA	Thermogravimetric Analyzer
XRD	X-ray diffraction
ZDBC	Zinc dibutyl dithiocarbamate



## *List of Publications*

### **International Peer Reviewed Journals**

- [1] A Comparative Study of Short Nylon Fiber–Natural Rubber Composites Prepared from Dry Rubber and Latex Masterbatch **Bipinbal P.K** and Sunil K. N. kuty, *Journal of Applied Polymer Science*, Vol. 109, 1484–1491 (2008)
- [2] Enhanced electrical conductivity of polypyrrole/polypyrrole coated short nylon fiber/natural rubber composites prepared by in situ polymerization in latex D.S. Pramila Devi, **P.K. Bipinbal**, T. Jabin, Sunil K.N. Kutty, *Materials and Design* Vol. 43, 337-347 (2013). (Published online) <http://dx.doi.org/10.1016/j.matdes.2012.06.042>
- [3] Lignocellulosic microfiber reinforced Natural rubber composites **Bipinbal P. K.**, Joseph M. J. and Sunil K. N. Kutty *Composites Science and Technology (Communicated)*
- [4] Preparation of nanocellulosic fibers from coir **Bipinbal P. K.**, Teena Thomas ,Joseph M. J. and Sunil K. N. Kutty, *Journal of Applied Polymer Science (Communicated)*
- [5] Preparation and characterization of polyaniline coated nano and microfiber – natural rubber composites. **Bipinbal P. K.**, Teena Thomas ,Joseph M. J. and Sunil K. N. Kutty, *Polymer Plastics Technology and Engineering (Communicated)*

### **International conferences, seminars**

- [1] Thermal Analysis of Short Nylon-6 Fiber/ Natural Rubber Composite Prepared by Latex Stage Compounding **Bipinbal P.K** and Sunil K. N. Kutty, *POLYCHAR 16- World Forum on Advanced Materials*, 2008, Lucknow, India

- [2] Short nylon fiber – natural rubber composite prepared by latex masterbatching: cure characteristics and mechanical properties  
**Bipinbal P.K** and Sunil K. N. Kutty, *International Conference on Advances in Polymer Technology*, September 25-27, 2008, Cochin, India
- [3] A Study on Short Nylon Fiber – Natural Rubber Composite Prepared By Latex Masterbatching, Using Rubber process Analyser. International Conference on Materials Science Research and Nanotechnology-2008, Kodaikanal, Tamilnadu, India
- [4] Natural Rubber- Cellulose Microfiber Composites by Latex Masterbatching **Bipinbal P. K.**, Joseph M. J. and Sunil K. N. Kutty International Conference on Materials for The New Millenium-MATCON 2010, Cochin, India
- [5] Cellulose microfiber-Natural rubber composites prepared by latex masterbatching: Processing characteristics and mechanical properties  
**Bipinbal P. K.**, Joseph M. J. and Sunil K. N. Kutty International Conference on Advances in Polymer Technology, Feb. 26-27, 2010, India, Page No.300

### **National conferences, seminars**

---

- [1] Novel Method for Preparing Short Nylon Fiber – Natural Rubber Composite. **Bipinbal P.K.**; Kutty S.K.N, Proceedings of the 17<sup>th</sup> AGM, Materials Research Society of India, 2006, Lucknow.

## INTRODUCTON

<b>Contents</b>	1.1	<i>Classification of Composites</i>
	1.2	<i>Fiber composites</i>
	1.3	<i>Why short fiber composites?</i>
	1.4	<i>Short fiber elastomer composites</i>
	1.5	<i>Reinforcement mechanism in short fiber composites</i>
	1.6	<i>Factors influencing the properties of short fiber - elastomer composites</i>
	1.7	<i>Natural rubber short fiber composites</i>
	1.9	<i>Types of composites</i>
	1.10	<i>Applications of short fiber composites</i>
	1.11	<i>Processing of short fiber elastomer composites</i>
	1.12	<i>Scope and objective of the present work</i>

Composite materials have been in existence for many centuries. Some of the earliest records of their use date back to the Egyptians, who are credited with the introduction of plywood, and the use of straw in mud for strengthening bricks. Similarly, the ancient Inca and Mayan civilizations used plant fibers to strengthen bricks and pottery. Bamboo, bone, and celery are examples of cellular composites that exist in nature. Muscle tissue is a multidirectional fibrous laminate. There are numerous other examples of both natural and man-made composite materials.

In today's world composite materials have been gaining wide use in commercial, military and space applications. High strength and stiffness, high toughness and low weight are the most important characteristics of an ideal engineering material. Conventional engineering materials, metals and their

alloys are strong and tough, but not light. Polymeric materials are light but lack strength. Fiber reinforced composites have all the ideal properties for engineering materials, leading to their rapid development and successful use in many applications over the last few decades. However, the potential advantages of these fiber filled polymer composites are far from being fully realized and continued growth is anticipated in their use for many years to come.

By definition, composite material consists of two or more chemically distinct constituents or phases with a distinguishable interface between them and some of their properties are radically different from their constituents. Composite consists of a continuous phase called matrix in which a discontinuous phase is embedded. The discontinuous phase, which is harder and stronger than matrix, is called reinforcement. The properties of the composites are strongly influenced by the properties of their constituent materials, their distribution and interaction among them. Composite properties may be either the sum of the properties of the distinct phases, or it may be the resultant property of the synergic action of constituent phases.

## **1.1 Classification of Composites**

The strengthening mechanism of composites strongly depends on the geometry of the reinforcement. Based on the geometry of reinforcement the classification of the composites is shown in the Fig. 1.1 [1].

A composite whose reinforcement is a particle, is called particle reinforced composites. Particle fillers are widely used to improve or modify the matrix properties such as thermal and electrical conductivities, performance at elevated temperatures, wear and abrasion resistance, machinability, surface hardness and to

reduce friction and shrinkage. In many cases they are simply used to reduce the cost.

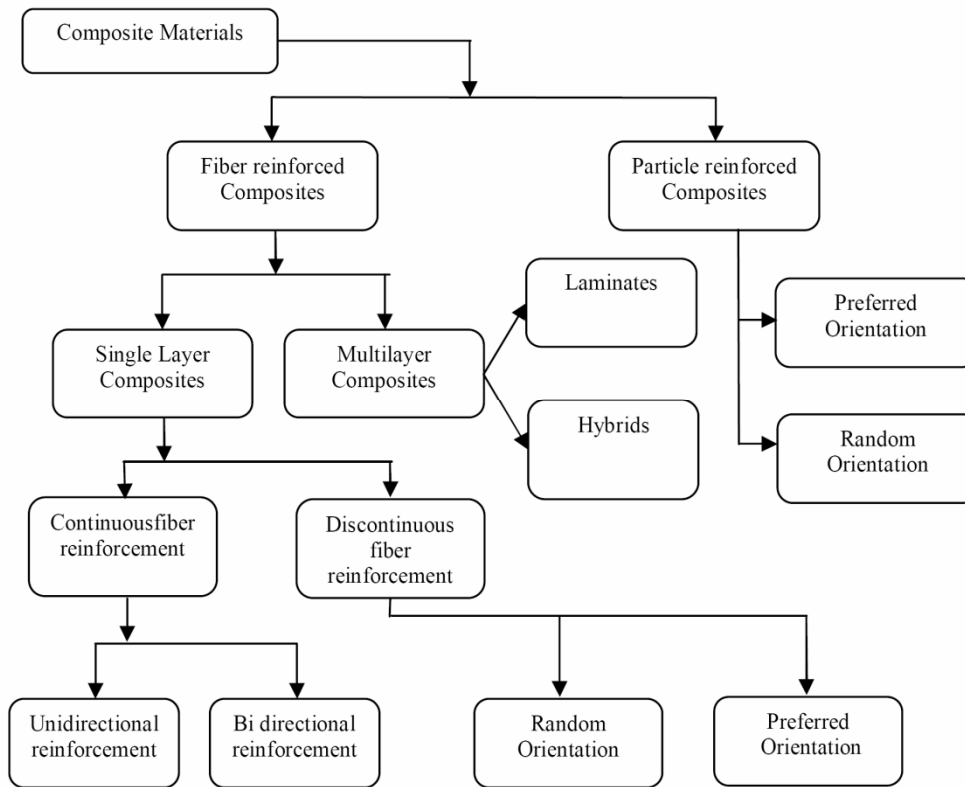


**Figure 1.1 Classification of Composites**

## 1.2 Fiber composites

In the fiber form the material will typically contain very few microscopic flaws, from which cracks may initiate to produce catastrophic failure. Therefore, the strength of the fiber is greater than that of the bulk material. Individual fibers are hard to control and form into useable components. Without a binder material to separate them, they can become knotted, twisted, and hard to separate. The binder (matrix) material must be continuous and surround each fiber so that they are kept distinctly separate from adjacent fibers and the entire material system is easier to handle and work with. In

composites, fibers are the main load carriers. Matrix holds the fibers together and maintains the desired fiber orientations and transfers the load to the fibers. Matrix also protects the fibers against environmental attack and damage due to handling.

The most commonly used matrices are carbon, ceramic, glass, metal, and polymer. Polymer matrices can be thermoplastic, thermoset or rubber. Reinforcing fibers can be either organic or inorganic. Nylon, cellulose, polypropylene and graphite fibers are examples of organic fibers. They can be generally characterized as lightweight, flexible, elastic and heat sensitive. Inorganic fibers such as glass, tungsten and ceramics, in general, have very high strength, heat resistance and rigidity and low, energy absorption and fatigue resistance. Yet another classification of fibers is into natural and manmade. Cellulose, jute, sisal, cotton etc. are examples of natural fibers. Carbon, aramid, polyester, nylon, boron, glass etc are the man made fibers. Composites with long fibers are called continuous fiber reinforcement and composites in which short or staple fibers are embedded in the matrix are termed as discontinuous fiber reinforcement.

### **1.3 Why short fiber composites?**

The fiber reinforced composites with best mechanical properties are those with continuous fiber reinforcement. Such materials cannot be adapted easily to mass production and are generally confined to products in which the property benefits outweigh the cost penalty. Short fiber reinforced composites can be processed in a manner similar to the matrix. Thus Reinforced natural and synthetic rubbers can be processed by the usual rubber processing methods such as calendaring, extrusion and injection moulding, and uneconomic methods such as dipping, wrapping and laying are not required.

Many of the rubber processing operations cause fiber alignment, which is often beneficial.

Part of the property advantage of long fiber composites derives from the continuous nature of the reinforcement but part is a consequence of the highly parallel fiber orientation. Though in short fiber composites the fiber orientation distribution is far less perfect and is often random, and as a result, the degree of anisotropy is generally less than that in continuous fiber composites, it is often very significant. Moreover processing windows can be quite narrowly defined so that the required fiber orientation distribution is obtained.

#### **1.4 Short fiber elastomer composites**

Reinforcement of thermosetting plastic materials with short fibers has been practiced for quite some time. However the adoption of this technology to rubbery and thermoplastic materials have been very gradual, mainly due to the success in using continuous cord reinforcement in industrial elastomeric articles, imparting strength without sacrificing flexibility. While short fiber reinforced rubber combines the characteristics of flexible rubber matrix and the stiffness and tenacity of the reinforcing fiber, the short fiber reinforcement is still insufficient to replace continuous cord reinforcement. Nevertheless the improvements imparted by short fibers to elastomeric matrices are so substantial that their use in rubber products is on an upward swing.

Because short fibers can be incorporated directly into most rubber compounds along with the other additives using standard mixing equipment and because the resulting composites can be processed in standard rubber processing steps (extrusion, calendaring, as well as compression, injection and transfer moulding), economical high volume output are feasible. This is a

significant advantage over the slower processes required for the incorporation and placing of continuous fibers, cords and fabrics. Thus the penalty of sacrificing noticeable reinforcing strength with discontinuous fibers is counterbalanced by processing economies. In addition, short fibers significantly outperform simple particulate materials as reinforcements. They impart drastic changes to the mechanical, thermal and viscoelastic properties of compounded rubber. These changes – even at low fiber concentrations – go far beyond the levels obtainable with the rubber industry’s traditional reinforcement, the carbon black.

Typical advantages associated with short fibers as fillers in polymer matrices apart from ease of processing and production economy, are design flexibility, high low-strain modulus, good damping and anisotropy in technical properties and stiffness. Fibers can also improve thermochemical properties of polymer matrices to suit specific areas of applications. Moreover short fibers provide high green strength, high dimensional stability during fabrication, improved creep resistance, tear strength, impact strength and good ageing resistance [2]. The manufacture of complex shaped engineering articles, which are impractical for formation from elastomers reinforced with continuous fiber, can easily be accomplished with short fibers.

### **1.5 Reinforcement mechanism in short fiber composites**

In a fiber-polymer composite the fibers are stiffer than the matrix and the proportion of the load that they support is greater than their volume fraction. The overall elastic properties of a composite are relatively easy to compute from the elastic properties of the components when the fibers are continuous and parallel [3]. For a perfectly aligned and properly bonded unidirectional continuous fiber composite the rule of mixture is applicable and is given by

$$\sigma_{cu} = \sigma_f V_f + \sigma_m V_m \text{ ----- (1.1)}$$

where,

$\sigma_{cu}$  = ultimate composite strength,  $\sigma_f$  = ultimate fiber strength,  $\sigma_m$  = matrix strength at the maximum fiber strength,  $V_f$  = volume fraction of fiber and  $V_m$  = volume fraction of matrix.

In composites, loads are not directly applied on the fibers, but are applied to the matrix material and transferred to the fibers through the fiber ends and also through the cylindrical surface of the fiber nearer the ends. When the length of a fiber is much greater than the length over which the transfer of stress takes place, the end effects can be neglected and the fibers may be considered to be continuous. The stress on a continuous fiber can thus be assumed constant over its entire length. In the case of short fiber composites the end effect cannot be neglected and the composite properties are a function of fiber length. A portion of the end of each finite length fiber is stressed at less than the maximum fiber stress.

A critical fiber length is required to obtain the transfer of maximum load from the matrix to the fiber. When the fibers are smaller than a critical length, the maximum fiber stress is less than the average fiber strength so that fibers will not fracture and the composite failure occurs when the matrix or interface fails. When the fiber length is greater than the critical length the fibers can be stressed to their average strength and fiber failure initiates when the maximum fiber stress is equal to the ultimate strength of the fibers.

Longitudinal and transverse moduli of the aligned short fiber composites given by Halpin Tsai equation are,

$$E_L/E_m = \frac{1 + 2l/d\eta_L V_f}{1 - \eta_L V_f} \text{-----(1.2)}$$

and

$$E_T/E_m = \frac{1 + 2\eta_T V_f}{1 - \eta_T V_f} \text{-----(1.3)}$$

where,

$$\eta_L = \frac{E_f/E_m - 1}{E_f/E_m + 2l/d} \text{-----(1.4)}$$

$$\eta_T = \frac{E_f/E_m - 1}{E_f/E_m + 2} \text{-----(1.5)}$$

$E_L$  and  $E_T$  are the longitudinal and transverse moduli of an aligned short fiber composite having the same aspect ratio and fiber volume fraction as the composite under consideration.  $E_f$  and  $E_m$  are the modulus of fiber and matrix respectively. The Halpin- Tsai equation predicts that the transverse modulus of an aligned short fiber composite is not influenced by the fiber aspect ratio  $l/d$ .

## 1.6 Factors influencing the properties of short fiber - elastomer composites

### 1.6.1 Type and Aspect Ratio of Fiber

The aspect ratio of fibers is a major parameter that controls the fiber dispersion, fiber matrix adhesion, and optimum performance of short fiber polymer composites. An aspect ratio in the range of 100 – 200 is essential for high performance fiber rubber composites for good mechanical properties. For synthetic fibers an aspect ratio of 100 – 500 is easily attained as they are available in the diameter range of 10 – 30  $\mu\text{m}$ . Considerable fiber breakage occurred during mixing of fibers with high aspect ratio (as high as 500) resulting in reduction in aspect ratio [4]. O'Connor [5] studied the extent of

fiber breakage after processing and after vulcanization and concluded that fiber breakage and distribution of fiber length occur in the uncured stock during processing and not during curing. For certain type of fibers like glass and carbon the fiber breakage was such that the resulting aspect ratio was too low to give good performance as reinforcement for rubber [6,7]. Chakraborty et al. [8] have observed that an aspect ratio of 40 gave optimum reinforcement in XNBR reinforced with short jute fiber. Murty and De [9,10] reported that for jute fiber filled rubbers good reinforcement could be obtained with aspect ratio of 15 and 32 for NR and SBR respectively.

An excellent treatment on the importance of aspect ratio especially with respect to the modulus of the matrix is given by Abrate [11]. Significant breakage of short Kevlar fibers during mixing in Brabender plasticorder in TPU matrix was reported by Kutty et al. [12,13]. Varghese et al. [14] reported that an aspect ratio in the range of 20-60 was sufficient for reinforcement for NR-short sisal fiber composites. A series of short fiber reinforced SBR composites were studied by Prasanthakumar et al. [15] with sisal fibers of different lengths and a fiber length of 6 mm was found to be optimum.

### **1.6.2 Fiber Dispersion**

Good dispersion of fibers in the matrix is one of the major factors which affect the high performance of the composite. Good dispersion implies there will be no clumps of fibers in the finished products, ie, the fiber will be separated from each other during the mixing operation and surrounded by the matrix. Aramid and nylon fibers tend to clump together and do not disperse easily [16]. A pre-treatment of fibers is necessary to reduce the interaction between fibers and to increase interaction between fiber and rubber. The pre-treatments include making dispersions and formation of a soft film on the

surface. Leo and Johanson [17] described pre dispersions of chopped polyester, glass and rayon fibers in neoprene latex for better mixing in to CR or SBR rubber. It has been reported that cellulose pulp may be dispersed directly into a concentrated rubber masterbatch or into a final compound, if it is sufficiently wetted to reduce fiber to fiber hydrogen bonding [18]. Intensive mixing has been done with cellulose fibers in an elastomer matrix. [19,20] Effect of shear rate, ram pressure, fill factor, power input and mixing time on fiber dispersion were studied. The effect of fiber dispersion on modulus and strength was studied by Shen and Rains [21]. They have stated a dimensionless dispersion number  $N_R$ , which is a function of rotor length, rotor diameter, rotor tip clearance, mixing chamber volume, rotor speed and mixing time, can be a reliable scale up parameter for short fiber mixing in polymers. Derringer [22] recommended that organic fibers be first incorporated into a concentrated masterbatch where high shear force can be established between the aggregates. These can later be broken down to the desired compound formulation in order to optimise dispersion.

### 1.6.3 Fiber Orientation

The preferential orientation of fibers in the matrix is the key to the development of anisotropy in the matrix. During processing of rubber composites, the fibers tend to orient along the flow direction causing mechanical properties to vary in different directions [23]. Enormous benefits would be possible, if methods could be developed for exercising tight control over the fiber orientation in moldings made from short fiber polymer composites. The dependence of composite properties on fiber orientation and alignment is well documented [24]. Milling and calendering are perhaps the most commonly used processing methods in which fibers tend to orient along the mill direction. A large shear flow during milling forces fibers to orient

along mill direction [25]. For a continuous flow through a fixed mill opening, all the possible fiber orientation is achieved during the first pass. Flow pattern is not expected to change during subsequent mill passes. A high degree of fiber orientation could be achieved by repetitive folding and passing through a two-roll mill as reported by Boustany and Coran [26]. Akthar et al. [27] found a small nip gap and single pass in the mill to be the best. A rubber mill was used by Foldi [28] to orient various organic filaments into several types of rubber stock. Senapati et al. [29] reported that two passes through tight nip gave optimum mechanical properties for short PET/NR composites. The effect of mill opening and the friction ratio of the mill and temperature of the rolls on the orientation of short Kevlar fibers in TPU matrix has been described by Kutty et al. [30] It was observed that the lower the nip gap, the higher the anisotropy in tensile strength, implying greater orientation of fibers. The orientation of short fibers in polymer matrices has been reviewed in detail by McNally [31].

#### **1.6.4 Fiber Matrix Adhesion**

The bond between fiber and matrix at the interface is known to play an important role in composites since it is through this interfacial bond the load is transferred to the fiber. The load transfer is dependent on fiber to polymer adhesion and the fiber aspect ratio. The adhesion between low modulus polymer and high modulus fiber prevents the independent deformation of the polymer at the interface. Different techniques have been employed to achieve a strong interfacial bond between fiber and matrix. These include HRH systems, RFL dips, fiber surface grafting and use of coupling agents.

The improvement in reinforcement obtained by enhancing fiber-matrix adhesion through the incorporation of a bonding system has been widely

studied in the case of rubber vulcanizates [32-34] Kondo has reviewed the selection of adhesives for bonding short fiber reinforcements in SBR and NR compounds [35]. Derringer [36] evaluated the HRH system with various fibers in nitrile and natural rubber and good adhesion was obtained. He concluded that the HRH system was not effective with polyester fibers in any elastomeric matrix. O'Connor [37] compared the HRH system with RH and hexa methoxy methyl melamine (HMMM) alone in various short fiber natural fiber composites. It has been reported that the presence of tri-component bonding system (HRH) is essential for the promotion of adhesion between fiber and rubber matrix [38-44,206]. Some researchers have found that the replacement of silica by carbon black in the tri-component bonding system leads to essentially similar adhesion level [45-46]. The mechanism of action of coupling agents to improve the fiber-matrix interface properties has been studied by Mukherjea et al. [47] Arumugam et al. [48] reported that HRH system was effective in improving the adhesion between coconut fiber and rubber matrix.

Kutty and Nando[49] have reported that chemically treated polyester cord-NR vulcanizates exhibit lower Goodrich heat build up than untreated PET cord-NR composites. Also NR matrix compounded with HRH dry bonding agent gave lower heat generation than even chemically treated fiber-rubber composites owing to better interfacial adhesion between fiber and matrix. HRH bonding material was effective for short fiber reinforced butadiene rubber also [50]. Ashida, [51] in a review has mentioned about adhesives used for short fibers. The effect of surface treatment of nylon short fiber with RFL bonding agent was analysed for NR and EPDM rubbers [52]. Owing to surface treatment, there was some improvement in mechanical properties. A two-component system of resorcinol and hexamethylene tetramine was found to be better than tri-component HRH system for NR-short

sisal fiber composites [53]. The effect of addition of HRH system/RH system on the properties of short polyester fiber- reclaimed rubber composites has been reported [54].

To improve adhesion between fibers and NR, polyallyl acrylate was grafted on cellulose fibers by Yano et al. [55]. Ibarra [56] used 1,4 carboxyl benzene sulfonyl diazide as adhesive agent for PET-SBR composites and obtained enhanced properties. The effect of fiber-matrix interfacial adhesion on viscoelastic properties of short sisal fiber NR composites was evaluated by Siby et al. [57]. Interfacial adhesion between coir fiber and NR was improved by treating the fiber with alkali and NR solution and by incorporating HRH/RH system [58-59].

Suhara et al. [60] reported that in the presence of HRH bonding system the water liberated during resin formation caused hydrolysis of urethane linkages and hence HRH system could not be used as interfacial bonding agent for polyurethane-short polyester fiber composite. Effect of urethane based bonding agent on the cure and mechanical properties of short fiber-PU elastomer composites has been reported [61-62]. Improvement of interfacial adhesion of poly (m-phenylene isophthalamide) short fiber-thermoplastic elastomer composite was achieved with N-alkylation of fiber surface [63]. Sreeja et al. [64-65] reported the urethane based bonding agent for short Nylon-6 reinforced NBR ad SBR rubber composites. Rajeev et al. [66] studied the effect of dry bonding system in improving the adhesion between fiber and matrix of short melamine fiber –nitrile rubber composite. Deet al [67] found that in alkali treated grass-fiber-filled natural rubber composites rubber/fiber interface was improved by the addition of resorcinol formaldehyde latex (RFL) as bonding agent. Effect of an epoxy-based bonding agent on the cure characteristics and mechanical properties of short-nylon-fiber-reinforced

acrylonitrile-butadiene rubber and neoprene rubber composites was studied by Seema et al [68-69]. Maya et al [70] found that chemically treated sisal-oil palm hybrid fiber-natural rubber green composites are possessing enhanced mechanical properties. Fibers were treated with varying concentrations of sodium hydroxide solution and different silane coupling agents. Leny Mathew[71-72] studied short nylon-6 fiber reinforced natural rubber and NBR composites were nanosilica act as a dry bonding system component and as reinforcement. The introduction of the nanosilica improved interfacial adhesion and the properties of composites.

### **1.7 Natural rubber short fiber composites**

Short fibers find application in essentially all conventional rubber compounds, examples are NR, EPDM, SBR, neoprene and nitrile rubber. Various speciality elastomers like silicone rubber, fluoro elastomer, ethylene vinyl acetate, thermoplastic elastomer and polyurethane have also been found utility as composite matrices [73-77]. Here for the sake of brevity only natural rubber composites reinforced with short fibers will be discussed.

Derringer[78] incorporated different short fibers such as rayon, nylon and glass into NR matrix to improve young's modulus of vulcanizates. Short jute fiber reinforced NR composites have been studied by Murty et al. [79-80]. Mukherjea [81] studied the role of interface in fiber reinforced polymer composites with special reference to natural rubber.

Kikuchi [82] used nylon short fibers with 0.2-0.3  $\mu\text{m}$  diameter and 100-200  $\mu\text{m}$  length to reinforce NR and found that tires made from it showed reduced weight and rolling resistance. Short silk fiber reinforced NR have been described by Setua et al. [83-84]. Effect of chemical treatment, aspect ratio, concentration of fiber and type of bonding system on the properties of

NR-short sisal fiber composites were evaluated by Varghese et al.[85]. Dynamic mechanical properties of NR reinforced with untreated and chemically treated short sisal fibers were studied and the effect of fiber-matrix interfacial adhesion on viscoelastic properties were evaluated[86]. Natural rubber-coir fiber composite was studied by Geethamma et al. [87-88].

Effect of fiber loading, orientation, abrasion load and thermal ageing on the abrasion behaviour of NR reinforced with aramid short fibers were reported by Zheng et al. [89]. Incorporation of short poly (p-phenylene terephthalamide) into NR compound resulted in improved tensile strength, modulus, 'on-end' abrasion, thermal stability and in 30-60% lower energy loss after shock loads compared to reference compound[90].

Short polyester fiber-NR composites were studied by Senapati et al[91] and the effect of fiber concentration, orientation and L/D ratio on mechanical properties were examined. Ibarra et al [92] investigated the effect of several levels of short polyester fiber on mechanical properties of uncured and cured NR compounds and found that the addition of fiber markedly reduced maximum swelling of the composites. Joseph et al. prepared Natural rubber-oil palm fiber composites [93]. Stress induced crystallization and dynamic properties of NR reinforced with short syndiotactic 1,2 polybutadiene fibers and with very fine nylon 6 fibers were discussed in a review[94]. Effect of various parameters on the mechanical properties of short-isora-fiber-reinforced natural rubber composites were evaluated by Lovely et al. [95]. Short sisal/oil palm hybrid fiber reinforced natural rubber composites were studied for the effects of fiber concentration and modification of fiber surface [96-97].

## 1.8 Fibers used in short fiber composites

Both synthetic and natural fibers were used for the reinforcement of elastomers, natural as well as synthetic rubbers. The generally available synthetic fibers are polyester, aramid, nylon, rayon and acrylic. It is possible to improve the properties of composites by using high performance fibers such as carbon, glass or aramid. In the case of soft rubbery composites cellulose fiber has been found to give better reinforcement than glass or carbon fibers [98]. This may be probably due to the fact that the flexibility of cellulose fibers results in less breakage during processing than that happens with the brittle glass or carbon fiber. A review of various types of short fibers highlighting their properties and shortcomings as reinforcements for polymers is given by Milewski [99]. Various natural materials which are potential reinforcements for rubber compounds are coir, jute [100], bagasse [101-102] and pineapple leaf fiber [103]. Goodloe et al. [104-105] were the first to use short cellulose fibers in elastomer matrix and found that the tendency of the rubber to shrink was reduced in presence of short fibers. The use of asbestos, flax, glass and cotton fibers to reinforce various types of rubber is reviewed by Zuev et al. [106]. Manceau [107] compared cellulose, glass and nylon fibers as reinforcement for SBR rubber. Coconut fiber reinforced rubber composites have been reported by Arumugam et al. [108] Acrylic fiber reinforced rubber has been prepared by Moyama et al. [109]. The use of a polyolefin based fiber as reinforcement in SBR has also been reported [110]. Boustany and Coran [111] showed improved performance of hybrid composites comprising cellulose in conjunction with a chopped textile fiber. The in situ generation of plastic reinforcing fibers within an elastomeric matrix has been disclosed in literature [112-113]. This method has been used by Coran and Patel [114] to reinforce chlorinated polyethylene with nylon fibrils.

### 1.8.1 Nylon fiber

Nylon was the first commercially successful synthetic fiber. Nylon, like many synthetics, was developed by Wallace Carothers at the DuPont Chemical Company. They are prepared by reacting diamines with dibasic acids, by self-condensation of an amino-acid or by opening of a lactam ring. The most common versions are nylon 6,6 and nylon 6 and they account for nearly all of the polyamides used for fiber applications. Nylon 6,6 is made by the condensation reaction between adipic acid and hexamethylene diamine. Nylon 6 is preferred over nylon 6,6 in Europe and in India. Ring opening polymerization of caprolactam is used for the manufacture of Nylon 6. The polyamide is melt spun and drawn after cooling to give the desired properties for each intended use. The fiber has outstanding durability and excellent physical properties. The main features are exceptional strength, high elastic recovery, abrasion resistance, lusture, washability, resistance to damage from oil and many chemicals, high resilience, and colourability. The typical physical properties of Nylon fibers are given below (Table 1.1).

**Table 1.1 Typical physical properties of Nylon fibers**

Property	Continuous filament	Staple
Tenacity at break, N/tex, 65% Rh, 21 <sup>o</sup> C	0.40 - 0.71	0.35 - 0.44
Extension at break, % 65% Rh, 21 <sup>o</sup> C	15 - 30	30 - 45
Elastic Modulus, N/tex, 65% Rh, 21 <sup>o</sup> C	3.5	3.5
Moisture regain at 65% Rh, %	4.0 - 4.5	4.0 - 4.5
Specific Gravity (g/cc)	1.14	1.14
Approx. volumetric swelling in water, %	2 - 10	2 - 10

### 1.8.2 Coir fiber

Coir is an important lignocellulosic fiber obtained from the fibrous mesocarp of coconut, the fruit of coconut trees (*cocos nucifera*), which is cultivated extensively in Kerala, the southern state of India. The traditional production of fibers from the coconut husk is as follows. After manual separation of the nut from the husk, the husks are processed by various retting techniques, generally in ponds of brackish waters (for three to six months) or in salt backwaters or lagoons. By retting the fibers they are softened and can be decorticated and extracted by beating, which is usually done by hand. After hackling, washing and drying (in the shade) the fibers are loosened manually and cleaned.

The chemical composition of the coir fiber is given in Table 1.2

**Table 1.2 Chemical composition of Coir**

Cellulose	32–43%
Lignin	40–45%
Hemi-cellulose	0.15–0.25%
Pectins and related compounds	3–4%
Moisture Content	8%

### 1.8.3 Nanocellulosic fiber

Cellulose is one of the most abundant natural materials. Because of its renewability, biodegradability, abundance and low cost, cellulose has been tried to be used for many different applications [204]. One of the main areas where extensive research is being carried out is replacing petroleum derived synthetic materials with cellulose [202]. Depletion of the petroleum reserves and danger of global warming has put great thrust on efforts in the substitution of synthetic

polymers with natural alternatives. The high strength and mechanical properties of the cellulose makes it a suitable substitute for synthetic fibers.

According to Meier [115] and Heyn [116] elementary fibrils of diameter 3.5 nm formed from the cellulose molecules are universal structural units of natural cellulose. Blackwell and Kolpak [117] also reported the occurrence of elementary fibrils with diameters of approximately 3.5 nm in cotton and bacterial cellulose, thus giving supportive evidence about the basic fibrillar unit in cellulose microfibrils. According to Meier, microfibrils are agglomerates of elementary fibrils and always have diameters which are multiples of 3.5 nm. The bundling of elementary fibrils into microfibrils is caused by a pure physical coalescence as a mechanism of reducing the free energy of the surfaces [118]. The maximum diameter of a microfibril was proposed to be 35 nm.

Natural fibres have been applied as the raw material for the production of a fibrillated material, [201,203,205,207] which was introduced and defined as microfibrillated cellulose (MFC) by Turbak et al. [119] and Herrick et al. [120]. Several modern and high-tech nano-applications have been envisaged for MFC.

Cellulosic nanofibril whiskers were synthesized from banana fibers by the process of steam explosion in alkaline medium followed by acidic treatment [121]. Henrickson et al. prepared high toughness cellulose nanopaper from wood fibrils [122].

Over the years, the fibrillated material have been endowed with various nomenclatures, such as nanofibrillated cellulose, nanofibers, nanofibrils, microfibrils and nanocellulose [123-127]. Here the individual fibrils in nanometer dimensions will be referred to as nanofibrillated cellulose. In this

study nanofibrillated cellulose prepared from coir fibers is used to make composites based on natural rubber.

## **1.9 Types of composites**

### **1.9.1 Short Nylon Fiber – Elastomer Composites**

Studies on various aspects of short nylon fiber reinforced elastomers have been carried out by many researchers. Brokenbrow et al. [128] reported the preparation of a composite with good mechanical properties by incorporating nylon fibers in a low molecular weight non-terminally reactive liquid SBR and subsequently cross-linking it. Sreeja et al. [129-131] studied short Nylon –6 reinforced NR, NBR SBR composites and found that short Nylon –6 is enhancing the mechanical properties of these rubbers. Senapati et al. [132] investigated the effect of short nylon fibers on the mechanical properties of NR vulcanizates. Saad and Younan. [133] studied the rheological and electrical properties of NR-white filler mixtures, reinforced with short nylon-6 fiber with respect to filler loading. Dynamic viscoelastic properties of nylon short fiber reinforced composites were studied by Chen et al. [134]. They reported that the storage modulus and loss modulus increased with fiber loading. Short nylon fiber reinforced SBR compounds for V-belts applications were reported by King et al. [135]. Factors affecting the elastic modulus of short nylon fiber-SBR rubber composites were studied by Li et al. [136]. Ye et al. [137] incorporated short nylon fibers into SBR and BR matrices and reported that the vulcanization time increased with fiber content. Zhou et al. [138] studied the effect of fiber pre-treatment on properties of short nylon fiber-NBR composites. Kikuchi [139] reported that tires made from short nylon fiber having 0.2-0.3  $\mu\text{m}$  diameter and 100-200  $\mu\text{m}$  length in proper direction and NR showed reduction in cost and rolling resistance. The reinforcement and orientation behavior of short nylon fibers in NR, SBR and

CR were studied with emphasis on the determination of ideal aspect ratio for fibers by Bhattacharya [140]. Mechanical properties of nylon short fiber reinforced SBR/NR composites were studied in detail by Ma et al. [141]. Rajesh et al. [142] studied cure and mechanical properties of short Nylon fiber NBR composites. The influences of fiber length, loading and rubber crosslinking systems on the properties of the composites were analyzed. Sreeja et al [143] studied the short Nylon-6 fiber reinforced natural rubber/reclaimed rubber blends and found that most of the mechanical properties of NR were improved by the presence of nylon fibers. Leny Mathew [144] studied short nylon-6 fiber/natural rubber composite with nanosilica as dry bonding system component and as reinforcement.

### **1.9.2 Short Coir fiber -Elastomer composites**

Coir fiber is considered to be a poor reinforcing fiber in rubber because of its low interfacial adhesion with the matrix and lack of physical characteristics that are essential for a reinforcing fiber. Geethamma et al. made attempts to improve the interfacial interaction between coir and natural rubber by chemical treatment of the coir fibers, coating with NR solution and by the incorporation of HRH/RH bonding systems [145]. Mechanical properties of the composites were found to be decreasing with increase in fiber content even with the presence of bonding agents. The same group conducted studies on other characteristics of short coir fiber natural rubber composites. Diffusion of water and artificial sea water through the composites were evaluated and found that chemically treated fibers reduced water intake [146]. Stress relaxation studies of the composites were also conducted [147]. The not so encouraging results of these studies may be the reason behind the absence of any further attempts to try coir fiber as reinforcement for elastomers. In our study, effect of chemical and mechanical treatments in reducing the size of the

coir macro fibers to micro fiber and ensuing changes in the reinforcing potential of the micro fibers are investigated in detail.

### **1.9.3 Nanocellulosic fiber – Elastomer composites**

Studies on cellulosic nanofiber-reinforced elastomer composites have been very few. Only a limited amount of work is reported in literature. Visakh et al. [148] studied the effect of cellulose nanofibers isolated from bamboo pulp residue on vulcanized natural rubber. Banana nanofibers obtained by the process of steam explosion were incorporated in matrices like polylactic acid and natural rubber latex to form composites [149]. Nanocomposites of potato starch nanocrystal and natural rubber latex was prepared by Bouthegourd et al. [150] In both of the latter works vulcanization of the rubber matrix was not carried out to make the rubber elastic and usable. In the present work nanofibrillated cellulose composites prepared through latex stage processing is vulcanized in conventional moulds so that an elastic matrix is obtained which could be used for conventional applications.

### **1.9.4 Conducting fiber elastomer composites**

During the past two decades, conducting polymers and conducting polymer composites have been the subject of intensive research and development. Polyaniline (PANI) is one of the most studied conducting polymers due to its high electronic conductivity, redox and ion-exchange properties, excellent environmental stability and ease of preparation from common chemicals [151-154]. PANI is suitable for manufacture of electrically conducting yarns, antistatic coatings and flexible electrodes. Conducting polymers are also suitable for shielding electromagnetic radiation and reduction or elimination of electromagnetic interference because of their relatively high conductivity and dielectric constant and ease of tuning of these

properties through chemical processing and doping [155-157]. Reports on the high shielding efficiency of polyaniline, in comparison with that of copper triggered active research in tuning of it by chemical processing with different dopants [158-159].

There have been efforts to get conducting polymers in fiber form. For this either the conducting polymers were made into fibers or fibers were coated with conducting polymers [210,211]. Conductive coating of the fibers has been prepared by direct surface coating or by in situ polymerization on textile substrates [160-162,208]. Polyamides, polyesters, carbon fibers and Kevlar are commonly used to produce conducting fibers. Commonly used conductive materials are polythiophene, polyaniline or polypyrrole [163]164].

Incorporation of conducting additives into an elastomer matrix will combine electronic conductivity of the additive with elasticity and other useful mechanical properties of the rubber matrix [165,209]. Conducting blends of elastomer and polyaniline have several potential applications, especially as pressure sensors. A blend of PANI and nitrile rubber (NBR) has been prepared by coating a platinum working electrode with a thin film of nitrile rubber and polymerizing aniline by the potentiodynamic method [166]. Nitrile rubber and polyaniline were also blended by cold mixing in a 'calender'.

Studies have been conducted on the incorporation of conducting polymer coated short fibers into the elastomer matrix to impart good mechanical and electrical properties to the composites. Saritha et al. prepared composites of natural and chloroprene rubbers with conducting short nylon fibers [167-168]. Polypyrrole coated short nylon fibers were also used to prepare elastomeric composites based on natural rubber [169].

In all these works conducting polymer and coated fiber were incorporated to the dry rubber. If both of these additives are added in the latex stage advantages in terms of better dispersion of conducting polymer and short fiber and lower breakage of the short fibers could be achieved. So efforts have been made to polymerize insitu the conducting polymer in the latex containing short fibers. Our own group earlier reported the polypyrrole coated short nylon fiber/natural rubber composites prepared by in situ polymerization in latex [170].

In this work the insitu polymerization of polyaniline in latex containing fibers, to prepare conducting elastomer composites is discussed. Fibers used were separated from coir in micro and nano dimensions.

### **1.10 Applications of short fiber composites**

Nowadays short fiber reinforced elastomer composite find a wide variety of applications in various fields and can even replace the continuous reinforcement in some applications as they offer flexibility in both design and processing besides imparting advantageous properties. The manufacture of articles of complex shape cannot be easily accomplished with a continuous fiber reinforced elastomer. On the other hand the preparation of intricate shaped products is possible with short fibers as reinforcements since they can be processed in similar manner to the matrix. The main application areas for short fiber composites are in hose, belting, solid tires and pneumatic tire components. Short fiber reinforcements in the production of hoses, V-belts, tire tread, spindle drive wheel and complex shaped mechanical goods have been studied by many workers [171-174].

An important application that utilizes the full reinforcing potential of short fibers in a load-bearing application is as a replacement for continuous

cord in rubber hose. The major advantages associated with short fiber reinforcement are easy processing, economy and higher production rate. These find applications in the automotive industry [175] as well as for general purpose utility hoses. A high-tech hose for a high-tech car turbo engine was developed by Schroden et al. [176].

Power transmission belts, more precisely V-belts, represent an extreme dynamic application of rubber-fiber composites. A V-belt running over pulleys is subjected to very severe stresses when bent and flexed at a frequency of thousands of cycles per minute. Tensile stresses resulting from static tensioning and load transmission are supported by the textile reinforcing cord. The compressive sidewall pressures are supported mainly by the base rubber. The ideal material for this part of the V-belt must exhibit high modulus in the transverse direction and low modulus coupled with high flexibility in the axial direction. Such complex properties can best be achieved in an anisotropic rubber-short fiber composite. Rogers. [177] and Yagnyatinskaya et al. [178] discussed the use of short cellulose fiber along with polyester fibers as reinforcements for V-belt compounds. Tear resistant short fiber reinforced conveyor belts were manufactured by Arata et al. [179]. The use of CR reinforced with aramid short fiber for transmission belts have been discussed by Ichithani et al. [180].

The use of short fibers in tire treads to improve wear characteristics has received much attention [181-182]. Arnhem et al.[183] reported that a small amount of short fibers in the tread of a truck tyre reduced the rolling resistance considerably. A reduction in crack propagation rate is obtained with the addition of 1% cellulose fibers to the tread compound. [184] Another application of short fibers in tires involves the circumferential reinforcement of the tread to improve strength against the centrifugal forces developed according to Dubetz [185]. Marzocchi et al. [186] claimed improved tire

stability when a random short glass fiber mat was incorporated under the tread. Short fiber containing pneumatic tires having good balance of abrasion and ice/snow–skid resistance were prepared by Midorikawa et al. [187]. Kikuchi [188] used nylon short fibers with 0.2-0.3  $\mu\text{m}$  diameter and 100-200  $\mu\text{m}$  length to reinforce NR and found that tyres made from it showed reduced weight and rolling resistance.

Seals and gaskets are potentially large markets for short fiber reinforcement. Short fiber reinforcement will impart excellent creep resistance to seals and gaskets, especially at elevated temperatures. Development of sealing materials of jute fiber reinforced cork and butadiene acrylonitrile rubber was described by Xie et al. [189]. The use of fiber reinforcement in dock fenders and methods to fabricate them have been discussed by Goettler et al. [190]. Sheet roofing can benefit greatly from short fiber reinforcement.

Chopped nylon fibers were used to improve the wear of crepe shoe soles [191]. De and co workers [192] investigated the potential of using carbon fibers in neoprene to shield against electromagnetic interference (EMI) and found that 30-40 phr carbon fiber loading was sufficient to make the composite a potential EMI shielding material in the electronic industry. Spherical vibrational dampers having low expansion at high temperature and good dimensional stability and shape maintenance were prepared by mixing rubbers with short fibers in their length direction. [193]. Additional applications claimed are [194] hard roll covers, oil well packings, bearings and bushes.

## **1.11 Processing of short fiber elastomer composites**

### **1.11.1 Mixing**

The processing advantage of short fiber reinforced elastomer composites is that short fibers can be incorporated directly into rubber compounds along

with the other additives using standard mixing equipment [195] and the resulting composites can be processed in standard rubber processing steps like extrusion, calendaring, as well as compression, injection and transfer moulding. Mixing is the process carried out to masticate rubber into a softer and flowable form and to incorporate compounding ingredients into rubber. Mixing of rubber is accomplished using mills and internal mixing machines. The mixing of ingredients in rubber is occurring in four phases namely, subdivision, incorporation, dispersion and distribution. During subdivision larger lumps or agglomerates are broken down into smaller aggregates suitable for incorporation. Then these aggregates are absorbed or incorporated into the rubber. During mixing, shearing of the rubber generate shearing stresses in rubber mass which in turn imposes shear stress on aggregates and breaks these down into their ultimate fine size. This is known as dispersion. Distribution is the moving of particles from one point to another, without further size reduction, to increase the randomness of the mixture. As soon as the ingredients get absorbed distribution and dispersion processes takes place simultaneously. Brittle fibers like glass or carbon require more distributive mixing but for fibers such as nylon and natural cellulosic fibers dispersive mixing is preferred since these fibers tend to agglomerate during mixing procedure.

### **1.11.2 Latex stage compounding**

Latex stage compounding is a processing method practiced for the mixing of compounding ingredients into rubber. Latex-carbon black masterbatch is prepared by mixing carbon black dispersed in water with latex and coagulating the latex-carbon black mixture [196-197], Rajamma et al. prepared latex stage compounds by mixing rubber and compounding ingredients in the

latex stage followed by coagulation and drying. Compounding ingredients are added as either dispersions or emulsions to a latex mixed with stabilizer.

During the dispersive mixing in rubber mixing machinery, considerable breakage of short fibers is a certain possibility [198-200]. If the breakage is so severe that the fibers are broken down into lengths lower than their critical fiber lengths, the stress transfer from the matrix to the fiber may not be sufficient. So the full reinforcing potential of the short fibers will not be realised. To restrict the reduction of fiber length to a minimum an effective tool will be the adoption of latex stage compounding technique for the preparation of short fiber elastomer composites.

### **1.12 Scope and objective of the present work**

In rubber compounding fillers are incorporated on two roll mixing mills or in internal mixers. Fillers being the major volume component, it takes more time to disperse uniformly. Consequently it takes up about 60 – 70% of the total energy input of the mixing operation. Any reduction in the energy requirement, even to the extent of 10-20% can be economically very attractive. A reduced mixing cycle can also be very advantageous in terms of improved production volume. This calls for developing less energy intensive and less time consuming processes for incorporation and distribution of short fibers in the rubber matrix. One method for this is to incorporate fibers in the latex stage. Latex can then be coagulated and processed into sheet or block rubber. The composite can then be compounded on two-roll mill or internal mixers. The present study is primarily to optimize the preparation of short fiber- natural rubber composite by latex stage compounding and to evaluate the resulting composites in terms of mechanical, dynamic mechanical and thermal properties. A synthetic fiber (Nylon) and a natural fiber (Coir) would be used to evaluate the advantages of the processing through latex

stage. To extract the full reinforcing potential of the coir fibers the macro fibers will be converted to micro fibers through chemical and mechanical means.

Extraction of nanocellulosic fibers from coir fiber, obtained from the fibrous mesocarp of coconut, the fruit of coconut trees (*cocos nucifera*), which is cultivated extensively in Kerala, the southern state of India, is also tried. The nano fibers being high in modulus will impart better mechanical properties to the elastomer composites prepared through latex stage processing. One of the important problems in the preparation of nanocellulosic composites, namely agglomeration of the nano fibers in the matrix by strong hydrogen bonding, would also be resolved through latex stage processing.

The micro and nano fibers obtained from coir would be characterized by different techniques.

To determine the energy efficiency of the proposed process a detailed study of the energy input required for the mixing process is necessary. For this a prototype internal mixer which is capable of measuring the energy or the mixing process would be used. By measuring the torque generated the efficiency of the mixing process could be evaluated.

Another advantage expected from the latex stage compounding is the lower fiber breakage resulting from the reduced shear history of the rubber compound due to lower mixing time. When the average length of the fibers after milling, increases, the stress transfer between the rubber and fiber will be more efficient leading to better mechanical properties of the composites. Mechanical properties of the composites prepared in the new method would be compared with the properties of the composites prepared by conventional dry stage mixing. Scanning electron microscopic studies of the tensile fracture

surfaces of the composites would reveal the interfacial adhesion between fiber and matrix and the failure mode of the composites.

Viscoelastic properties of the composites would be investigated by dynamic mechanical analysis. Effect of temperature and frequency on storage modulus, loss modulus and  $\tan\delta$  of the composites would be evaluated.

Thermal stability of the composites can be influenced by the shear history of the composites. Thermal stability is also greatly dependent on the type of the fiber used as reinforcement. So evaluation of thermal properties of the new composites and comparison with conventional composites would be carried out.

## References

- [1] Bhagwan D. Agarwal and Larence J. Broutman., Analysis and Performance of Fiber Composites., Jhon Wiely Publications., 1980
- [2] Coran A.Y., Boustany K. and Hanned P. Rubbr Chem. Technol., **47** (1974) 396.
- [3] Piggott M.R., Load Bearing Fiber Composites, Pergamon, Oxford (1980).
- [4] Stickney P.B. and Falb R.D., Rubber Chem. Technol., **37** (1964) 1299.
- [5] O' Connor J.E., Rubber Chem. Technol., **50** (1977) 945.
- [6] Goettler L.A. and Shen K.S., Rubber Chem. Technol., **56** (1983) 619.
- [7] Ashida M., Nippon Gomu Kyokaishi, **56** (1983) 768.
- [8] Chakraborty S.K., Setua D.K. and De S.K., Rubber Chem. Technol., **55** (1982) 1286.
- [9] Murty V.M. and De S.K., J. Appl. Polym. Sci., **27** (1982) 4611.
- [10] Murty V.M. and De S.K., J. Appl. Polym. Sci., **29** (1984) 1355.
- [11] Abrate S., Rubber Chem. Technol., **59** (1986) 384.

- [12] Kutty S.K.N. and Nando G.B., *Plast. Rub. Comp.*, **19**(2) (1993) 105.
- [13] Kutty S.K.N., Nando G.B., *J. Appl. Polym. Sci.*, **43** (1991) 1913.
- [14] Varghese Siby, Kuriakose Baby, Thomas Sabu and Koshy Alex T., *Indian J. Nat. Rubber Res.*, **4**(1) (1991) 55.
- [15] Prasantha Kumar R., RamaMurthy K., Schit S.C. and Thomas Sabu, *Macromol..... New Front , Proc. IUPAC Int. Symp. Adv. Polym. Sci. Technol.*, **2** (1998) 793.
- [16] O' Connor J.E., *Rubber Chem. Technol.*, **50** (1977) 945.
- [17] Leo T.J. and Johanson A.M., US patent, 4,263,184 (to Wyrrough and Loser Inc.) April 21, 1989.
- [18] Murty V.M., Bhowmick A.K., De, S.K., *J. Mater. Sci.*, **17** (1982) 709.
- [19] Goettler L.A., US Patent 4,248,743, Feb 3, 1981.
- [20] Anthocne G., Arnold R.L., Rains R.K. and Shen K.S., *International Rubber Conference, Brighton, England* (1977).
- [21] Shen K.S. and Rains R.K., *Rubber Chem. Technol*, **52** (1979) 764.
- [22] Derringer G.C., *Rubber World*, **165** (1971) 45
- [23] Moghe S. R., *Rubber Chem. Technol.*, **47** (1974) 1074.
- [24] Derringer G.C., *J. Elastoplast.*, **3** (1971) 230.
- [25] Moghe. S.R., *Rubber Chem. Technol.*, **49** (1976)1160.
- [26] Boustany K. and Coran A.Y., (to Monasanto Co) US 3,697, 364, (Oct 10,1972).
- [27] Akthar S., De P.P. and De S.K., *J. Appl. Polym. Sci.*, **32** (1986) 5123.
- [28] Foldi A.P., *Rubber Chem. Technol.*, **49** (1976) 379.
- [29] Senapati A.K., Kutty S.K.N., Pradhan B. and Nando G.B., *Int. J. Polym. Mater.*, **12** (1989) 203.
- [30] Kutty S.K.N. and Nando G.B., *Plast. Rub. Comp.*, **19**(2) (1993) 105.

- [31] McNally D.L., Polym. Plast. Technol. Eng., **8** (1977) 101.
- [32] Lee L.H., J. Polym. Sci., **5** (1967) 751.
- [33] Dunnom D.D., Rubber Age, **100** (1968) 49.
- [34] Hewitt N.L., Rubber Age, **104** (1972) 59.
- [35] Kondo A., Selchaku, **22** (5) (1978) 13.
- [36] Derringer G.C., J. Elastoplast., **3** (1971) 230.
- [37] O' Connor J.E., Rubber Chem. Technol., **50** (1977) 945.
- [38] Murty V.M. and De S. K., Rubber Chem. Technol., **55** (1982) 287.
- [39] Chakraborty S.K., Stua D.K. and De S.K., Rubber Chem. Technol., **55** (1982) 1286.
- [40] Setua D.K. and Dutta B., J. Appl. Polym. Sci., **29** (1984) 3097.
- [41] Akthar S., De P.P. and De S.K., J. Appl. Polym. Sci., **32** (1986) 5123.
- [42] Creasy J.R. and Wagner M.P., Rubber Age, **100** (10) (1968) 72.
- [43] Morita E., Rubber Chem. Technol., **53** (1980) 795.
- [44] Setua D. K. and De S. K., J. Mater. Sci., **19** (1984) 983.
- [45] Goettler L.A. and Shen K.S., Rubber Chem. Technol., **56** (1983) 619
- [46] Manas-Zloczorver I., Nir A. and Tadmor Z., Rubber Chem. Technol., **57** (1984) 583.
- [47] Mukherjea R.N., Pal S.K. and Sanyal S.K., J. Polym. Mater. **1** (1984) 69.
- [48] Arumugam N., Tamere Selvy K. and Venkata Rao K., J. Appl. Polym. Sci., **37** (1989) 2645.
- [49] Kutty S.K.N. and Nando G.B., Kautschuk Gummi Kunststoffe, **43** (1990) 189.
- [50] Ye L., Pan J. and Li D., Jixie Gong Cheng Xuebao, **26** (4) (1990) 68.
- [51] Ashida M., Nippon Gomu Kyokaishi, **63** (11) (1990) 694
- [52] Kutty S.K.N. and Nando G.B., Kautschuk Gummi Kunststoffe, **43** (1990) 189.

- [53] Varghese S., Kuriakose B., Thomas S. and Koshy A. T., *Indian J. Nat. Rubber Res.*, **4**(1) (1991) 55.
- [54] Zhanxun, Fu Shenjin Wang Kexin and Xu Shuzhen, *Heching Xiangjiao Gongye*, **14** (5) (1991) 323.
- [55] Yano Shoichiro, Stenberg and Bingth Flink, *Per. Nihon Reoroji Gakkarshi*, **20** (3) (1992) 132.
- [56] Ibarra L., *J. Appl. Polym. Sci.*, **49** (9) (1993) 1593.
- [57] Varghese S., Kuriakose B., Thomas S. and Koshy A. T., *Indian J. Nat. Rubber Res.*, **5** (1- 2) (1992) 18.
- [58] Geethamma V.G., Reethamma J. and Thomas S., *J. Appl. Polym. Sci.*, **55**(4) (1995) 583.
- [59] Geethamma V.G., Thomas M.K., Lakshminarayanan R. and Thomas S., *Polymer*, **39** (1998) 6.
- [60] Suhara F., Kutty S.K.N. and Nando G.B., *Plast. Rub. Comp. Proces. Appl.*, **24** (1995) 37.
- [61] Suhara F., Kutty S.K.N. and Nando G.B., *Int. J. Polym. Mater.* **38** (1997) 205.
- [62] Suhara F., Kutty S. K. N. and Nando G. B. *Polym. Plast. Technol. Eng*, **37** (2) (1998) 241.
- [63] Chantaratcharoen Anongnuch, Sirisinha Chakrit, Amorn Sukchai Taweechai, Buclek Limcharoen Sauvarop and Meesiri Wiriya, *J. Appl. Polym. Sci.*, **74** (10) (1999) 2414.
- [64] Sreeja T.D. and Kutty S.K.N. *Prog. In Rubber Plast. & Recyling Technol.* **18** (4) (2002) 283.
- [65] Sreeja T.D., Kutty S.K.N *Advances in Polymer Technology*, **20** (4) (2001) 281.
- [66] Rajeev, R.S; Bhowmick A. K., De, S.K and Bandyopadhyay, S., *J. Appl. Polym. Sci.* **90**(2) (2003) 544.
- [67] De, D., De, D. and Adhikari, B., *J. Appl. Polym. Sci.*, **101** (2006) 3151

- [68] Seema, A. and Kutty, S.K.N., J. Appl. Polym. Sci., **99** (2006) 532.
- [69] Seema, A. and Kutty, S.K.N., Polym.-Plast. Technol. Eng., **44**, (2005)1139.
- [70] John, M.J., Francis, B., Varughese, K.T. and Thomas, S., Composites, Part A, **39** (2008) 352.
- [71] Mathew, L. and Narayanankutty, S.K., Polym.-Plast. Technol. Eng., **48** (2008) 75.
- [72] Mathew, L. and Narayanankutty, S.K., J. Appl. Polym. Sci., **112** (2009) 2203.
- [73] Warick E.L., Pierce O.R., Polmanteer K.E. and Saam J.C., Rubber Chem. Technol., **52** (1979) 437.
- [74] Novikova L.A., Kolensnikovu N.N. and Tolstukhina F.S., Kauch Rezina, **6** (1978) 19.
- [75] Felterman M.Q., J. Elastomers Plast., **9** (1977) 226.
- [76] Kane R.P., J. Elastomers Plast., **9** (4) (1977) 416.
- [77] Sheelerz J.W., J. Elastomers Plast., **9** (3) (1977) 267.
- [78] Derringer G.C., Rubber World, **165** (1971) 45
- [79] Murty V.M. and De S.K., Polym. Eng. Revs., **4** (1984) 313.
- [80] Murty V.M. and De S.K., J. Appl. Polym. Sci., **27** (1982) 4611.
- [81] Mukherjea R.N., Pal S.K. and Sanyal S.K., J. Polym. Mater. **1** (1984) 69.
- [82] Kikuchi, Naohike, Rubber World, **214**(3) (1996) 31.
- [83] Setua D.K. and Dutta B., J. Appl. Polym. Sci., **29** (1984) 3097.
- [84] Setua D.K. and De S.K., Rubber Chem. Technol., **56** (1983) 808.
- [85] Varghese S., Kuriakose B., Thomas S. and Koshy A. T., Indian J. Nat. Rubber Res., **4**(1) (1991) 55.

- [86] Varghese S., Kuriakose B., Thomas S. and Koshy A. T., *Indian J. Nat. Rubber Res.*, **5** (1- 2) (1992) 18.
- [87] Geethamma V.G., Reethamma J. and Thomas S., *J. Appl. Polym. Sci.*, **55**(4) (1995) 583.
- [88] Geethamma V.G., Thomas M.K., Lakshminarayanan R. and Thomas S., *Polymer*, **39** (1998) 6.
- [89] Zheng Yuansuo, Song Yue Xian Zhang Wen, Wang Youdav and Jin Zhihao, *Xiang Jiaotong Daxue Xuebao*, **32**(10) (1998) 88.
- [90] Van der Pol J.F., *Rubber World*, **210** (3) (1994) 32.
- [91] Senapati A.K., Kutty S.K.N., Pradhan B. and Nando G.B., *Int. J. Polym. Mater.*, **12** (1989) 203.
- [92] Ibarra L. and Chamorro Celia, *J. Appl. Polym. Sci.*, **43** (10) (1991) 1805.
- [93] Joseph S., Joseph K. and Thomas S., *Int. J. Polym. Mater.*, **55** (2006) 925
- [94] Yamamotos, *Compos. Polym.* **1**(5) (1998) 371.
- [95] Mathew L. and Joseph R., *J. Appl. Polym. Sci.*, **103** (2007) 1640.
- [96] John, M.J., Francis, B., Varughese, K.T. and Thomas, S., *Composites, Part A*, **39** (2008) 352.
- [97] Jacob M., Thomas S. and Varughese K.T., *Compos. Sci. Technol.*, **64** (2004) 955.
- [98] Murty V.M. and De S.K., *Polym. Eng. Revs.*, **4** (1984) 313.
- [99] Milewski J.W., *Plast. Compd.*, May/June (1982) 53.
- [100] Murty V.M. and De S. K., *Rubber Chem. Technol.*, **55** (1982) 287.
- [101] Usmani A.M., Salyer I.O., Ball G.L.III and Schewndeman J.L., *American Chem. Soc. Div. Org., Coatings and Plastics Chem. Papers*, **45** (1981) 466.
- [102] Usmani A.M., Salyer I.O., Ball G.L.III and Schewndeman J.L., *J. Elast. Plast.*, **13** (1981) 46.

- [103] Bhattacharya T.B., Biswas A.K. and Chatterjee J., *Plast. Rub. Comp. Proces. Appl.*, **6** (1986) 119.
- [104] Goodloe P.M., Mc Murtie D.H. and van Nostrand R.J., *Rubber Age*, **67**(1950) 687.
- [105] Goodloe P.M., Reiling T.L. and Mc Murtie, *Rubber Age*, **61** (1947) 697.
- [106] Zeuv Y.S., Karpovich T.I. and Bukhina M.F., *Kauch Rezina*, No.6 (1978) 28.
- [107] Manceau F., *Rev. Gen. Caoulch Plast.*, **56** (592) (1974) 95.
- [108] Arumugam N., Tamere Selvy K. and Venkata Rao K., *J. Appl. Polym. Sci.*, **37** (1989) 2645.
- [109] Moyama Tomoko and Nakkahara Akihiro, *Eur. Pat. Appl.*, JP 511,838,04 Nov. 1992.
- [110] Blanc D. and Evrand G., *5<sup>th</sup> Conf. Envr. Plast. Caoutch*, **2** (1978) D15.
- [111] Boustany K. and Coran A.Y., (to Monasanto Co.) US 3,709,845 (Jan. 9, 1973).
- [112] Anon, *Res. Disel.*, **177** (1979) 19.
- [113] Duhbar J.A. and Pope G.A., *Chem. Abstracts*, **90** (1979) 88581 g.
- [114] Coran A.Y. and Patel R., *Rubber Chem. Technol.*, **56** (1983) 210.
- [115] Meier H., *Pure Appl. Chem.*, **5** (1962) 37.
- [116] Heyn A.N., *J. Ultrastruct. Res.*, **26** (1969) 52.
- [117] Blackwell J. and Kolpak F.J., *Macromolecules* **8**(3) (1975) 322.
- [118] Peterlin A. and Ingram P., *Text. Res. J.*, **40**(4) (1970) 345.
- [119] Turbak A.F., Snyder F.W. and Sandberg K.R., *J. Appl. Polym. Sci. Appl. Polym. Symp.*, **37** (1983) 815.
- [120] Herrick F.W., Casebier R.L., Hamilton J.K. and Sandberg K.R., *J. Appl. Polym. Sci. Appl. Polym. Symp.*, **37** (1983) 797.

- [121] Cherian B.M., Pothan L.A., Nguyen-Chung T. et al., *J. Agric. Food Chem.*, **56** (2008) 5617.
- [122] Henrickson M., Berglund L.A., Isaksson P. et al. *Biomacromolecules*, **9**(2008) 1579.
- [123] Siqueira G., Bras J. and Dufresne A., *Biomacromolecules* **10**(2) (2009) 425.
- [124] Mörseburg K. and Chinga-Carrasco G. *Cellulose* **16**(5) (2009) 795.
- [125] Ahola S., Österberg M. and Laine J., *Cellulose* **15**(2) (2008) 303.
- [126] Gardner D.J., Oporto G.S., Mills R. and Samir MASA, *J. Adhesion Sci. Techn.*, **22** (2008) 545.
- [127] Abe K., Iwamoto S. and Yano H., *Biomacromolecules*, **8**(10) (2007) 3276.
- [128] Brokenbrow B.E., Sims D. and Stokoe A.G., *Rubber J.*, **151**(10) (1969) 61.
- [129] Sreeja, T.D. and Kutty S.K.N., *J. Elastomers Plast.*, **34** (2) (2002) 157.
- [130] Sreeja T.D. and Kutty S.K.N., *J. Elastomers Plast.*, **33** (3) (2001) 225
- [131] Sreeja T.D. and Kutty S.K.N., *Int. J. Polym. Mater.*, **52** (3) (2003) 239.
- [132] Senapati A.K., Nando G.B. and Pradhan B., *Int. J. Polym. Mater.*, **12**(1988) 73.
- [133] Saad A.L.G. and Younan A.F., *Polym. Degrad. Stab.*, **50** (2) (1995) 133.
- [134] Li Chen, Liu Bo and Zhou Yanhao, *Fuhe Cailiao Xuebao*, **6**(4) (1989) 79.
- [135] King Chang Kee, Shin Gui Sook and Kim Byung Kyu, *Pollimo*, **14**(5) (1990) 456.
- [136] Li Chen and Zhou Yanhao, *Fuhe Cailiao Xuebao*, **7** (4) (1990) 53.
- [137] Ye L., Pan J. and Li D., *Jixie Gong Cheng Xuebao*, **26** (4) (1990) 68.
- [138] Zhou Yanhao, Chen Tao, Li Chen and Li Donghong, *Heching Xiangjiao Gongye*, **15** (2) (1992) 294.
- [139] Kikuchi, Naohike, *Rubber World*, **214**(3) (1996) 31.

- [140] Bhattacharya J.K., Rubber India, **46** (9) (1994) 13,3
- [141] Ma Peiyu, Zhao Jan, Tang Jiansheng and Dai Guihua, Guofenzi Cailiao Kexue Yu Gongcheng, **10** (6) (1994) 55.
- [142] Rajesh C., Unnikrishnan G., Purushothaman E., Thomas M.S., J. Appl. Polym. Sci., **92** (2004) 1023.
- [143] Srjeea T.D. and Kutty S.K.N., Polym. Plast. Technol. Eng., **42** (2), (2003), 239.
- [144] Leny Mathew and Kutty S. K. N., J. Appl. Polym. Sci., 112 (2009) 2203
- [145] Geethamma V.G., Thomas Mathew, K., Lakshminarayanan, R. and Thomas S., Polymer **39** (1998) 1483
- [146] Geethamma V.G. and Thomas S., Polym. Compos. **26** (2005) 136
- [147] Geethamma V.G., Pothan L. A., Rhao B., Neelakantan N.R. and Thomas S., J. Appl. Polym. Sci., **94** (2004) 96
- [148] Visakh et al. Bio Resources **7**(2) (2012) 2156
- [149] Abraham E., Pothan L.A., and Thomas S. In Proceedings of the Fibre Reinforced Composites Conference, Port Elizabeth, South Africa, December 2007.
- [150] Bouthegourd E., Rajisha K.R., Kalarical N., Saiter J.M. and Thomas, S., Mater. Lett., **65** (23-24) (2011) 3615
- [151] Gospodinova N. and Terlemezyan L., Prog. Polym. Sci., **23** (1998) 1443
- [152] Kang E., Prog. Polym. Sci., **23** (1998) 277
- [153] Trivedi D.C., in Handbook of Organic Conductive Molecules and Polymers, vol. 2, ed. by Nalwa HS. Wiley, Chichester, pp. 505–572 (1997).
- [154] Stejskal J., in Dendrimers, Assemblies, Nanocomposites, MML Series, vol. 5, ed. by Arshady R and Guyot A. Citus Books, London, pp. 195–281 (2002).

- [155] Joo J., Oh E-J, and Epstein A.J., *Molecular Electronics & Devices*, 107-118, (1995).
- [156] Joo.J. and Epstein. A.J., *Proc. Conference on Plastics for Portable Electronics*, Las Vegas, NV, 5-6 January 1995, 140-149 (1995).
- [157] Kohlman R.S., Min. Y.G., MacDiarmid A.G. and Epstein. A.J., *Proc. Soc. of Plastics Engineers Annual Technical Conference (ANTEC)* 1412-1416, (1996).
- [158] Lee C.Y. et al., *Synth. Met.* **102** (1999) 1346.
- [159] Joo, J. et al., *Mol. Cryst. Liq. Cryst. Sci. Technol., Sect. A*, **316** (1998) 367.
- [160] Gregory R.V., Kimbrell W.C. and Kuhn H.H., *Synth. Met.*, **28** (1989) 823.
- [161] Gregory R.V., Samuels R.J. and Hanks T., *National Textile Center annual report*. <http://www.furman.edu/~hanks/ntc/>.
- [162] SarithaChandran, A. and Narayanankutty, S.K., *J. Mater. Res.*, **24** (2009) 2728.
- [163] Heisey C.L., Wightman J.P., Pittman E.H. and Kuhn H.H., *Text. Res. J.*, **63**, (1993) 247-256.
- [164] Byun S.W. and Im S.S., *Synth. Met.*, **57** (1993) 3501.
- [165] Anand J., Palaniappan S. and Sathyanarayana D., *Prog. Polym. Sci.*, **23** (1998) 993.
- [166] Tassi E.L. and De Paoli M.-A., *J. Chem. Soc., Chem. Commun.*, (1990) 155. doi:10.1039/c39900000155
- [167] A. S.C. and Narayanankutty S.K., *Polym.-Plast. Technol. Eng.*, **50** (2011) 443.
- [168] Saritha Chandran A. and Narayanankutty S.K., *Eur. Polym. J.*, **44** (2008) 2418.
- [169] Pramila Devi D.S., Jabin T. and Kutty S.K.N., *Polym.-Plast. Technol. Eng.* **51**(8) (2012) 823.

- [170] Pramila Devi D.S., Bipinbal, P.K., Jabin, T. and Kutty S.K.N., *Mater. Des.* **43** (2013) 337.
- [171] Goettler L.A. and Lambright A.J., US Patent 4,056, 591 (to Monasanto Co.) Nov.1 1977.
- [172] Beatly J.R. and Hamed P., Paper Presented at the ACS Meeting, Rubber Div., Montreal, Quebec, Canada, May 1978.
- [173] Patent to Bridge Stone Co. *Chem. Abstr.*, 96 219182f (1982).
- [174] Anonymous, *Gummi Asbest. Kunst, Int. Polym. Sci. Technol.*, **10** (2) (1983) 35.
- [175] Anon, High Strength Automotive Hose Reinforced with Short Fibers, *Design Eng.* 24 May 1980.
- [176] Schroden Thomas and Keuper Dieter, *Kaust. Gummi Kunstst.*, **44**(9) (1991) 878.
- [177] Rogers J.W., *Rubber World*, **183**(6) (1981) 27.
- [178] Yagnyatinskaya S.M., Goldberg B.B., Dubinker E.M. and Pozdnyakova LV., *Kauch Rezina*, **32**(7) (1973) 28.
- [179] Hasegawa Arata, Koga Toshiaki, Mizuno Takahido Takashima Hidesuke, Matsuo Yasunori and Ookawa Hiroshi, *Jpn. Kokai Tokkyo Koho*, JP 08 55,512 (9655,512) 27 (1996).
- [180] Ichitani Ru, Tachibana Firoyuki and Kerada Mitsumori, *Jpn. Kokai Tokkyo Koho*, JP 05, 262,919 (93,262,916) 12, (1993).
- [181] Beatly J.R. and Hamed P, *Elastomers*, **110** (8) (1978) 27.
- [182] Anon, *Product Eng.*, **39** (18) (1968) 107.
- [183] Rijpkema B., *Arnhem Kautschuk Gummi Kunststoffe*, 47, Jahrgang Nr. 10/94.
- [184] Beatly J.R. and Hamed P, *Elastomers*, **110** (8) (1978) 27.

- [185] Dubetz A. et al., (to The Firestone Tire and Rubber Co.) US 3, 05, 389 (1962).
- [186] Marzoechi A. et al. (to Owens Corning Fiber glass Corp.) US 3,315,722 (1967).
- [187] Midorikawa Shingo, Kondo Takanori and Harada Masaaki, Jpn. Kokai Tokkyo Koho, JP 06, 328, 905 (94, 328, 905) 29 Nov. 1994.
- [188] Kikuchi, Naohike, Rubber World, **214**(3) (1996) 31.
- [189] Xie Sujiang, Lu Renliang and Zhou Hujun, Runhera Yu Mifeng, **3** (1995) 14.
- [190] Goettler L.A. and Swiderski Z, in Composite Applications, The Role of Matrix, Fiber and Interface, Eds. Vigo T.L. and Kinzip B.J., VCH Publishers, New York, (1992) 333.
- [191] Anon, Plast. Rubbers, Textiles **1**(3) (1970) 115
- [192] Jana P.B., Mallick A.K. and De S.K., Composites, **22** (1989) 451.
- [193] Yokobori Shizno and Ondo Kenji, Jpn. Kokai Tokkyo, JP 07 24 960 (95,24,960) 27 Jan. 1995.
- [194] Georgieva V.S. and Vinogradva G.C., Kozh-Obuyn Prom-st, **22**(4) (1980) 45.
- [195] Boustany K., Coran Y., US patent No. 33 679 364 (1972)
- [196] Janssen H.J.J. and Weinstock K.V., Rubber Chem. Technol., **34**(5) (1961) 1485.
- [197] Gopalakrishnan K.S., Kuriakose B. and Thomas E.V., Rubber Board bulletin **13**(3) (1976).
- [198] Goettler L.A. and Shen K.S., Rubber Chem. Technol., **56** (1983) 619.
- [199] Stickney P.B. and Falb R.D., Rubber Chem. Technol., **37** (1964) 1299.
- [200] Ashida M., Nippon Gomu Kyokaishi, **56** (1983) 768.
- [201] Kaushik A., and Singh M., Carbohydr. Res., **346**(1) (2011) 76.

- [202] Abdul Khalil H. P. S., Bhat A. H. and Ireana Yusra A. F., *Carbohydr. Polym.*, **87**(2) (2012) 963.
- [203] Abraham E., Deepa B., Pothan L. A., Jacob M., Thomas S., Cvelbar U., and Anandjiwala R., *Carbohydr. Polym.*, **86**(4) (2011) 1468.
- [204] Thomas S., Paul S. A., Pothan L. A., Deepa B., Kalia S., Kaith B. S. and Kaur I., in *Cellulose Fibers: Bio- and Nano-Polymer Composites*, Eds. Kalia S., Kaith B. S. and Kaur I., Springer Berlin Heidelberg, Berlin, Heidelberg, (2011) 3.
- [205] Bittencourt E. and Camargo, M. De., *Alternatives*, (2011) 18.
- [206] Khalil A. M., El-Nemr K. F. and Khalaf A. I., *J. Polym. Res.*, **19**(6) (2012).
- [207] Tonoli G. H. D., Teixeira E. M., Corrêa A. C., Marconcini J. M., Caixeta L. A., Pereira-da-Silva M. A. and Mattoso L. H. C., *Carbohydr. Polym.*, **89**(1) (2012) 80.
- [208] Zhang R., Deng H., Valenca R., Jin J., Fu Q., Bilotti E. and Peijs T., *Sens. Actuators, A*, **179** (2012) 83.
- [209] Sahoo B. P., Naskar K., Choudhary R. N. P., Sabharwal S. and Tripathy D. K., *J. Appl. Polym. Sci.*, **124**(1) (2012) 678.
- [210] Park M., Im J., Shin M., Min Y., Park J., Cho H., Park S. et al., *Nat. Nanotechnol.*, **7**(12) (2012) 803.
- [211] Saini P., Choudhary V., Vijayan N. and Kotnala R. K., *J. Phys. Chem. C*, **116**(24) (2012) 13403.



**EXPERIMENTAL TECHNIQUES**

<b>Contents</b>	2.1. <i>Materials</i>
	2.2. <i>Chemicals</i>
	2.3. <i>Processing</i>
	2.4. <i>Physical properties</i>
	2.6. <i>Thermal analysis</i>
	2.7. <i>Scanning electron microscopy</i>

This chapter deals with the description of the materials used, the methods of sample preparation and the experimental techniques adopted in the present investigations.

**2.1 Materials****Dry natural rubber**

Natural rubber (NR) used for the study was ISNR 5 obtained from Rubber Research Institute of India, Kottayam, Kerala.

Dirt content	0.05% by mass
Volatile matter	0.5% by mass
Nitrogen	0.3% by mass
Ash	0.4% by mass
Initial plasticity number, P0	30
Plasticity retention index, PRI	60

### Concentrated natural rubber latex

Natural rubber (NR) used for the study was ISNR 5 obtained from NJavallil Latex Pvt. Ltd., Ernakulam, Kerala.

Dry Rubber Content (%)	60.00
Total Solids (%)	61.22
Ammonia Content (%)	0.75
Non-Rubber Contents (%)	1.22
Specific Gravity	0.946
Volatile Fatty Acid No.	0.020
KOH Number	0.48
Mechanical Stability	1015''
Coagulam Content (%)	0.004
Sludge content (%)	0.002

**Short Nylon Fiber (Nylon-6)** fibers obtained from M/s SRF Ltd., Chennai was chopped to approximately 6mm. Specifications of nylon fiber are given below.

Breaking strength	28.3 kg - 31.5 kg
Elongation at break	27.5% - 36.5%
Twist	S 392 - 374
Denier	3656 – 3886

**Coir** is an important lignocellulosic fiber obtained from the fibrous mesocarp of coconut, the fruit of coconut trees (*cocos nucifera*), which is cultivated extensively in Kerala, the southern state of India. The chemical

composition of the coir fiber is given below. Coir fibers procured locally were chopped to approximately 6 mm and used.

Cellulose	32–43%
Lignin	40–45%
Hemi-cellulose	0.15–0.25%
Pectins and related compounds	3–4%
Moisture Content	8%

## **2.2 Chemicals**

### **Maleic anhydride**

Maleic anhydride was obtained from S D Fine-Chem Limited, India.

### **Hexamethylene tetramine (Hexa)**

Hexamethylene tetramine used was laboratory grade supplied by M/S E-Merck, Mumbai., India.

### **Resorcinol**

Resorcinol was supplied by M/S E- Merck Mumbai., India.

### **Silica**

Commercial grade silica supplied by M/S Minar Chemicals, Kochi, was used

### **Aniline**

Aniline was supplied by M/S E- Merck Mumbai., India.

**Hydrochloric acid, Sulphuric acid, Sodium hydroxide, Ammonium persulphate, Sodium chlorite and Acetic acid** were supplied by M/S E-Merck Mumbai., India.

**Valcastab VL** was obtained from Rubber Research Institute of India

**Other Compounding ingredients** used for the work were

Zinc oxide, supplied by M/S Meta Zinc Ltd. Mumbai; Stearic acid, supplied by M/S Godrej Soap (P) Ltd. Mumbai; N-Cyclohexyl-2-Benzothiazole Sulphenamide (CBS), supplied by M/S Polyolefins Industries Ltd. Mumbai; Tetramethyl-thiuramdisulphide (TMTD) procured from M/S NOCIL, Mumbai, 1,2-dihydro-2,2,4-trimethylquinoline (TQ), supplied by M/S Bayer India Ltd. Mumbai; Zinc diethyl dithiocarbamate (ZDBC), supplied by Merchem Ltd, Kerala and Sulfur, supplied by M/S Standard Chemicals Company, Pvt. Ltd., Chennai.

## **2.3 Processing**

### **2.3.1 Compounding**

The mixing was done as per ASTM D 3182 on a two roll laboratory size mixing mill (150 x 330 mm). Once a smooth band was formed on the roll, the ingredients were added in the following order: fibers (in dry rubber mixes), activators, bonding agent mixture, anti oxidant, accelerators and finally sulphur. After complete mixing the stock was passed six times through the tight nip and finally sheeted out at a fixed nip gap so as to orient the fibers preferentially in one direction. Sheets were cut out and stacked one over the other till the required volume is reached.

### **2.3.2 Cure Characteristics**

Cure characteristics at 150°C were determined by using Rubber Process Analyzer, RPA 2000. The machine has two directly heated, opposed biconical dies that are designed to achieve a constant shear gradient over the entire sample chamber. The specimen was kept in the lower die, which was oscillating through a small deformation angle ( $\pm 0.2^\circ$ ) at a frequency of 50 oscillations per

minute. The torque transducer on the upper die senses the force being transmitted through the rubber. A typical cure curve is shown in figure 2.1.

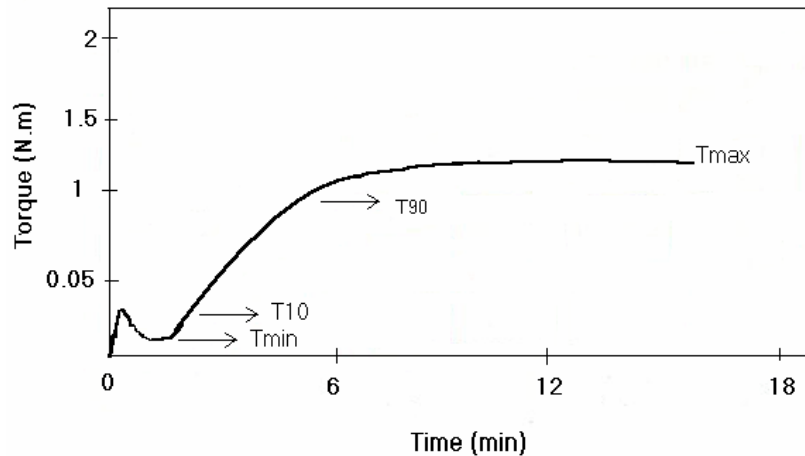


**Figure 2.1. A typical cure curve**

The following data can be obtained from the cure curve.

**Minimum torque (Tmin):** It is the lowest torque shown by the mix at the test temperature before the onset of cure.

**Maximum torque (Tmax):** It is the maximum torque recorded when curing of the mix is completed.

**Differential (Maximum – Minimum) torque:** It is the difference between maximum torque and minimum torque during vulcanization. It represents improvement in the degree of crosslinking on vulcanization, i.e. it is a measure of final cross link density of the vulcanizate.

**Scorch time (T<sub>10</sub>):** It is taken as the time for 10% rise in torque from the minimum torque.

**The optimum cure time T<sub>90</sub>:** Corresponds to the time to achieve 90% of maximum cure which was calculated using the formula

$$\text{Torque at optimum cure} = 0.9 (T_{\max} - T_{\min}) + T_{\min}$$

where  $T_{\max}$  and  $T_{\min}$  are the maximum and minimum torques, respectively.

### 2.3.3 Vulcanization

Test specimens marked with the mill grain direction were vulcanized at  $150 \pm 2^\circ\text{C}$  and at a pressure of  $180\text{kg/cm}^2$  in an electrically heated hydraulic press to their respective cure times. For thicker samples, sufficient extra cure time was given to obtain satisfactory mouldings. Mouldings were cooled quickly in water at the end of the curing cycle and stored in a cold dark place for 24 hours and were used for subsequent property measurements.

## 2.4 Physical Properties

The vulcanizates were tested for different mechanical properties according to the relevant ASTM standards. Mechanical properties like tensile strength, tear strength, elongation at break, and abrasion resistance were tested using samples with the fibers oriented along (Longitudinal direction) and across (Transverse direction) the sample length. Schematic representation of fiber orientation in different test samples is given in figure 2.2. For ageing studies, the samples were kept in an air oven for 48 hours at  $100^\circ\text{C}$  (ASTM 573 – 88). The properties were measured after 24 hours on the completion of ageing.

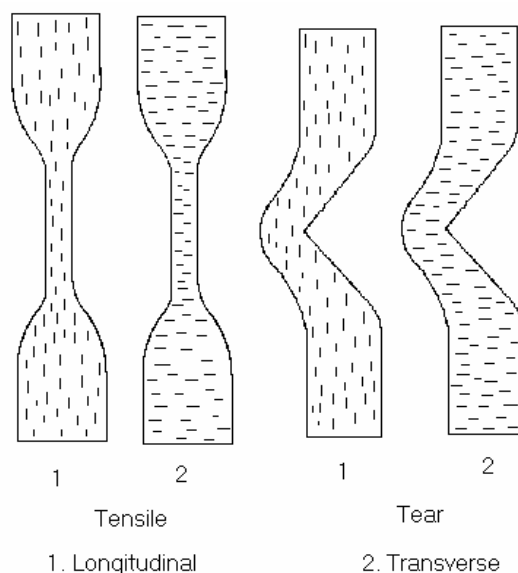


**Figure 2.2. Schematic representation of fiber orientation**

#### **2.4.1 Tensile Strength, Modulus and Elongation at Break**

Tensile properties were measured using Shimadzu Universal Testing Machine Model AG-I 10 KN according to ASTM D 412. Samples were punched out from the moulded sheets both along and across the grain direction with a dumb-bell die (die E). The grip separation speed was 500 mm/min. The ultimate strength, modulus at different elongations and ultimate elongation were noted.

#### **2.4.2 Tear Strength**

The tear strength was determined using Shimadzu Universal Testing Machine Model AG-I 10 KN according to ASTM D 624 (die C). The samples were punched from the moulded sheets along and across the direction of fiber orientation. The test speed was 500 mm/min.

#### **2.4.3 Hardness**

The hardness of the sample (Shore A) was determined using Mitutoyo Hardmatic hardness tester according to ASTM D 2240 – 86. Samples having dimensions of 12 mm diameter and minimum 6 mm thickness were used. Readings were taken 10 seconds after the indenter had made a firm contact with the specimen.

#### **2.4.4 Abrasion Resistance**

Abrasion resistance of the samples was measured using a DIN abrader based on DIN 53516, both in the longitudinal and transverse directions. Samples having a diameter of  $12 \pm 0.2$  mm and a thickness of 16 - 20 mm was placed on a rotating holder and a load of 10 N was applied. A pre-run was given for conditioning the sample and the sample weight was taken. Weight after the test was also noted. The difference in weight is the weight loss of the

test piece after its travel through 40 m on a standard abrasive surface. The results were expressed as volume loss per hour.

$$V = \frac{\Delta M \times 27.27}{\rho}$$

where V = Abrasion loss in cm<sup>3</sup>/hr, Δ M = mass loss and ρ = density of the sample.

#### 2.4.5 Rebound Resilience

Rebound resilience was determined by vertical rebound method according to ASTM D 2832 - 88. In this method, a plunger suspended from a given height (400 ± 1mm) above the specimen was released and the rebound height was measured. The resilience scale was marked in 100 equally spaced divisions and hence the rebound height is equal to the resilience (%).

#### 2.4.6 Compression Set

Compression set at constant strain was measured according to ASTM D 395 – 86 method B. Samples with 6.25 mm thickness and 18 mm diameter were compressed to constant strain (25%) and kept for 22 hours in an air oven at 70°C. At the end of the test period the test specimens were taken out, kept at room temperature for 30 minutes and the final thickness was measured. The compression set in percentage was calculated as follows.

$$\text{Compression set (\%)} = \frac{T_i - T_f}{T_i - T_s} \times 100 \text{ ----- (2.1)}$$

where T<sub>i</sub> and T<sub>f</sub> are the initial and the final thickness of the specimen respectively and T<sub>s</sub> is the thickness of the space bar used.

## **2.5 Dynamic Mechanical Analysis**

### **2.5.1 Strain sweep studies in RPA**

Rubber process Analyzer (RPA 2000) also act as a dynamic mechanical rheological tester (DMRT). RPA 2000 measures the viscoelastic properties of rubber compounds in torsional shear. Strain sweep tests were performed on RPA. 5 cm<sup>3</sup> of the uncured fiber mixes were cut using a punch and placed in the sealed biconical cavity of the Rubber Process Analyzer. The samples were kept at the test temperature of 60 °C for a preheating time of 4 minutes. It was then subjected to a strain sweep with varying strains of 0.05, 0.1, 0.2, 0.5, 1, 2, 3, 5 and 7 degrees in a single sweep. The complex modulus values obtained were plotted against strain in degrees. For strain sweep studies in cured state, uncured samples were first vulcanized to their respective cure times at 150 °C. The temperature was then reduced to 60 °C and the sample was subjected to strain sweep as above.

### **2.5.2 Studies in DMA**

TA Instruments DMA Q800 was used to conduct dynamic mechanical analysis. Test specimens having a dimension of 30 mm x 3 mm x 2 mm were used in tension mode. Temperature sweep and frequency sweep experiments were conducted. Temperature sweep experiments of the composites were performed from -80°C to +40°C. Frequency was set at 1 Hz and strain amplitude 15 µm. Frequency sweeps were conducted over a frequency range of 1Hz to 30 Hz at 40 °C. The amplitude was fixed at 15 µm.

## **2.6 Thermal Analysis**

Thermogravimetric analyses of the gum and composites were carried out on TA Instruments TGA Q50 with a heating rate of 20°C/min under nitrogen atmosphere. The following characteristics were determined from the

thermogravimetric curves: the temperature of onset of degradation, the temperature at peak rate of decomposition and the peak rate of degradation. Using Friedman method, the activation energy and the order of the degradation reaction of the composites were calculated.

## **2.7 Scanning Electron Microscopy (SEM)**

Scanning electron microscope studies were carried out using SEM model 6390LA JEOL instrument. To find fiber dimensions a drop of fiber dispersion was placed on the carbon tape and allowed to evaporate the water completely. The samples were gold plated to suppress specimen charging. To study the failure mode, the surfaces were carefully cut from the failed test specimens without touching the fracture surface and were sputter coated with gold. The orientation of the samples was kept constant in a particular mode of failure.

## **2.8 Atomic force microscopy**

AFM was used to study the surface morphology of nano fibers. Dispersion of the nanofibrillated material after homogenization process was cast into a sheet. The smooth surface of the sheet was probed with AFM in non contact mode. The instrument used was Agilent 5500 AFM.

## **2.9 X-ray diffraction**

High Resolution XRD was done using the instrument PANalytical XPert Pro High Resolution X-Ray diffractometer. The scan range was from 5 to 80  $2\theta$ .

## **2.10 Lignin content**

0.5g of the sample was weighed ( $W_1$ ) and 7.5 ml 72 %  $H_2SO_4$  added. Kept at room temperature for 2 hours by stirring at every 15 minutes.

Transferred the contents to a 500ml RB flask and diluted with 280ml of deionised water. Heated the liquid to a gentle boil and refluxed for 4 hours. Filtered solution through previously ignited filtering crucible. Dried the crucible and contents at  $105 \pm 3^\circ\text{C}$  for 2 hours. Cooled in a desiccator and weighed ( $W_2$ ). Placed the crucible and contents in the muffle furnace and ignited at  $575 \pm 25^\circ\text{C}$  for 3 hours. Cooled in a desiccator and weighed ( $W_3$ ).

$$\% \text{ lignin} = \frac{W_2 - W_3}{W_1}$$

.....



**NATURAL RUBBER-NYLON MICRO FIBER COMPOSITES**

<b>C</b> <b>o</b> <b>n</b> <b>t</b> <b>e</b> <b>n</b> <b>t</b> <b>s</b>	<b>Part -A</b>
	<i>Mechanical properties of NR- Nylon Micro Fiber Composites</i>
	<b>Part B</b>
	<i>Dynamic mechanical properties of NR- Nylon Micro Fiber Composites</i>
	<b>Part C</b>
	<i>Thermal studies of NR- Nylon Micro Fiber Composites</i>

**Part -A****Mechanical properties of NR- Nylon Micro Fiber Composites****3.A.1 Introduction**

Short fibers are used as reinforcing fillers in rubber compounds to get products with improved properties. They became very popular due to the possibility of obtaining anisotropic properties, ease of processing and economy [3-5]. In rubber compounding fillers are incorporated on two roll mixing mills or in internal mixers. Typical mixing process involves incorporation, distribution and dispersion. These are achieved by continuous shearing of the material. The use of short fibers such as glass, rayon, aramid, asbestos and cellulose as reinforcing fillers in natural, as well as synthetic rubber have been investigated by many researchers[1-10]. The effect of fiber-matrix adhesion,

aspect ratio of fiber, fiber dispersion and orientation, nature of the matrix, and type of fiber on the extent of reinforcement is also studied [11-16]. All of these studies utilized the traditional mode of fiber incorporation at the time of mixing. Preparation of homogeneous compounds with well dispersed fibers is time consuming and highly energy intensive. Fillers being the major ingredient in a rubber compound, it takes about 60-70% of the total energy input of a mixing operation. This calls for development of a less time consuming process for incorporation and distribution of fibers in the rubber matrix.

One method is to incorporate the fibers in the rubber latex itself and then process the latex into conventional sheet form. In this chapter the features of such an alternate method is reported. The cure characteristics and the mechanical properties of these composites are compared with that of the composites prepared by conventional method. The effect of a conventional dry bonding system based on hexamethylene tetramine, resorcinol and hydrated silica (HRH) also have been investigated.

In order to obtain better interaction between the matrix and fiber another adhesion promotion mechanism using maleic anhydride grafting was also tried. To make the interaction more effective nylon fiber was surface hydrolysed with NaOH. The free-NH<sub>2</sub> groups will combine with the grafted maleic anhydride in the matrix at cure temperature increasing the reinforcement [17]. A schematic representation of the reaction mechanism is shown in figure 3.1.

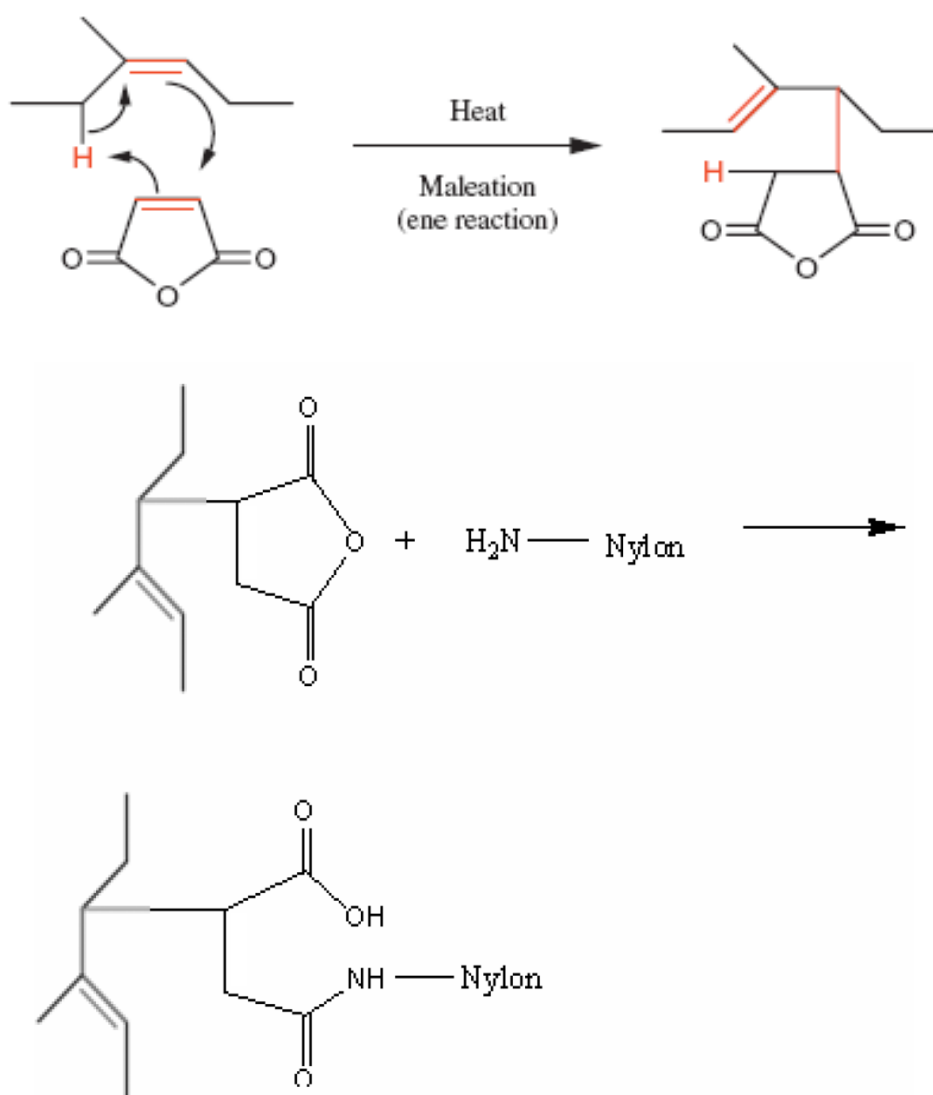


Figure 3.1. Reaction mechanism of treated nylon with maleated natural rubber

### 3.A.2 Experimental

#### 3.A.2.1 Materials Used

Concentrated natural rubber latex (60 DRC) was procured from Njavally Latex Pvt Ltd. Block rubber (ISNR-5) was obtained from the Rubber Research Institute of India, Kottayam. Nylon fibers manufactured by SRF Ltd., Chennai, were chopped to approximately 6mm length. Zinc oxide, stearic acid, TQ

(1,2-dihydro-2,2,4-trimethylquinoline), MBTS (Mercptobenzthiazyldisulfide), TMTD (tetramethylthiuram disulfide), sulfur, hexa (hexamethylenetetramine), resorcinol and hydrated silica used were of commercial grade.

### 3.A.2.2 Processing

The concentrated latex was diluted to 12.5% dry rubber content (DRC). A sandwich of alternating layers of latex and short fibers cut to 6 mm length was made and the latex was coagulated using dilute acetic acid. The coagulum obtained was squeezed between rollers to remove water. The sheet obtained was dried in an air oven at 40°C for three days. Fiber loadings were adjusted to get 10, 20 and 30 phr fiber in the final composites. The composites were then processed like conventional sheet rubber.

Formulation of the mixes is given in Table 3.1. Formulation of the mixes modified for improved interfacial adhesion through HRH dry bonding system and maleic anhydride grafting are given in table 3.2 and table 3.3 respectively. The mixes were prepared according to ASTM D 3182 on a laboratory size two-roll mixing mill. Fibers were extracted by dissolving out the matrix in a solvent and the length distribution of fibers was determined by using stereo microscope and camera.

For maleic anhydride grafting, nylon fibers were treated with 10% NaOH solution for 20 min at ambient temperature. The fiber was then thoroughly washed with distilled water to remove excess sodium hydroxide and dried at 50°C. To prepare a masterbatch of maleic anhydride grafted natural rubber, natural rubber was mixed with 6 phr maleic anhydride in a Brabender Plastograph. 15 phr of the masterbatch thus obtained was incorporated during mixing of the fiber composites.

The energy for mixing was determined by mixing in a Thermo Haake Rheomix. The mixing cycle was limited to 5.5 minutes at 80°C with a fill factor of 0.75. The fibers were incorporated at 1.5 minute and the torque was continuously measured for the remaining time of 4 minutes. Rotor speed was kept constant at 30 rpm during initial loading time of 1.5 minute and then at 60 rpm for the remaining running time of 4 minutes. The integrated energy input for the free mixing cycle was noted.

Cure characteristics were determined by using Rubber Process Analyser model RPA 2000 at 150°C. Fibers were oriented in the mill direction by passing through the tight nip in the mill at the end of the mixing process. The thin sheets obtained were cut in the required dimensions and stacked one above the other to the desired volume. The sheets were vulcanized at 150 °C under a pressure of 180 kg/cm<sup>2</sup> in an electrically heated hydraulic press to their respective cure times. The samples obtained were tested for mechanical properties according to relevant ASTM standards. The test samples were prepared such that the fibers are oriented along and across the direction of application of load during testing. Schematic representation of fiber orientation in tensile and tear test samples is given in Figure 3.2.

**Table 3.1. Formulation of the mixes without bonding agent**

<b>Ingredients</b>	<b>A<sub>1</sub></b>	<b>B<sub>1</sub></b>	<b>C<sub>1</sub></b>	<b>D<sub>1</sub></b>
NR	100	100	100	100
ZnO	4	4	4	4
Stearic acid	2	2	2	2
TQ	1	1	1	1
Fiber	-	10	20	30
MBTS	0.6	0.6	0.6	0.6
TMTD	0.2	0.2	0.2	0.2
Sulphur	2.5	2.5	2.5	2.5

**Table 3.2 Formulation of the mixes with HRH bonding agent**

<b>Ingredients</b>	<b>A<sub>2</sub></b>	<b>B<sub>2</sub></b>	<b>C<sub>2</sub></b>	<b>D<sub>2</sub></b>
NR	100	100	100	100
ZnO	4	4	4	4
Stearic acid	2	2	2	2
TQ	1	1	1	1
Fiber	-	10	20	30
Silica	1.6	1.6	1.6	1.6
Resorcinol	2.5	2.5	2.5	2.5
Hexa	1.6	1.6	1.6	1.6
MBTS	0.6	0.6	0.6	0.6
TMTD	0.2	0.2	0.2	0.2
Sulphur	2.5	2.5	2.5	2.5

**Table 3.3 Formulation for MANR-treated nylon composites**

<b>Ingredients</b>	<b>A<sub>3</sub></b>	<b>B<sub>3</sub></b>	<b>C<sub>3</sub></b>	<b>D<sub>3</sub></b>
NR	100	100	100	100
Maleic anhydride	0.9	0.9	0.9	0.9
ZnO	4	4	4	4
Stearic acid	2	2	2	2
TQ	1	1	1	1
Fiber	-	10	20	30
CBS	1	1	1	1
Sulphur	2	2	2	2

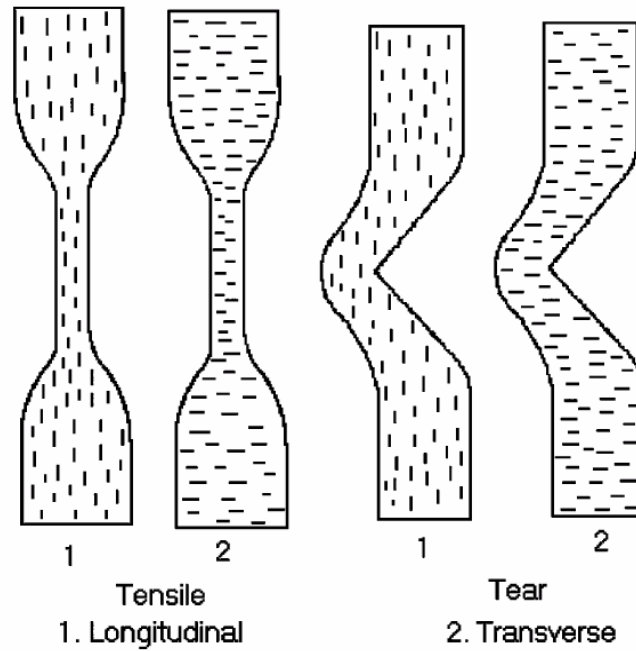


Figure 3.2. Schematic representation of fiber orientation in tensile and tear test samples

### 3.A.3 Results and discussions

#### 3.A.3.1 Evaluation of Processing Energy

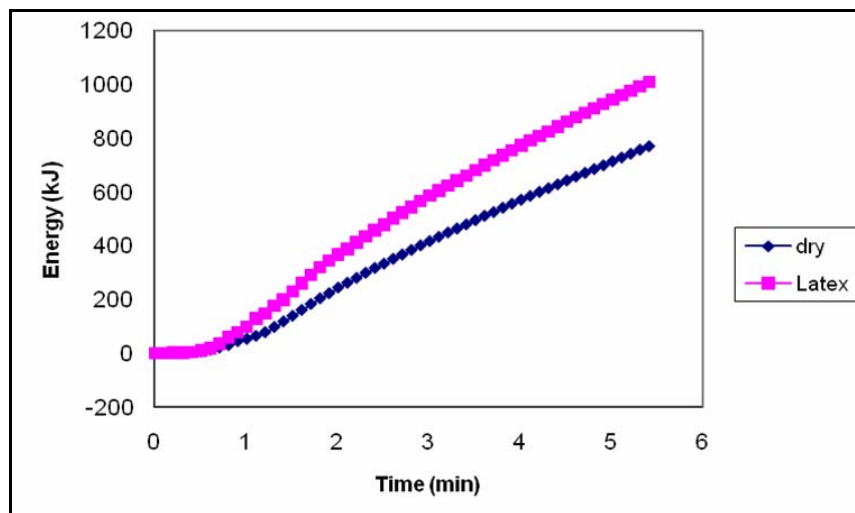


Figure 3.3 Energy input with time of mixing

Figure 3.3 shows the integrated energy input during the mixing process in the Rheocord mixer. The energy input shows almost a linear increase with time. For the latex stage composite energy input at any time is greater than the dry rubber composite. The higher energy for mixing is due to more restrained matrix resulting from better dispersion of fibers. That, higher energy can be input in shorter time shows that the total mixing time is reduced without compromise in the filler dispersion.

### 3.A.3.2 Fiber breakage analysis

The initial average length of the fibers was 6mm. Figure 3.4 compares the distribution of fiber length after milling. The figure shows that average fiber length is 1.5 – 2.5 mm in the case of dry rubber compound where as it is 2.5 – 4.0 in the case of latex stage compound. This confirms lower fiber damage in the case of compounds prepared using latex stage masterbatch. This may be attributed to shorter shear history of the latex masterbatch.

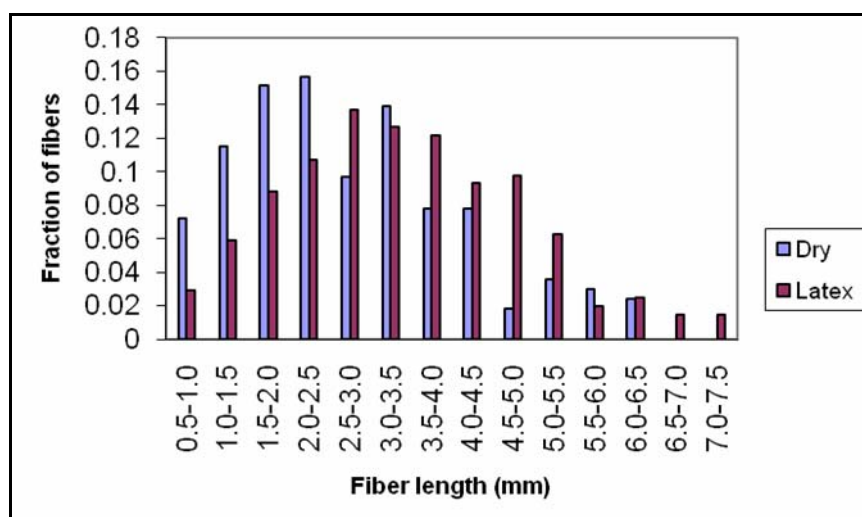


Figure 3.4. Fiber length distribution after milling

### 3.A.3.3 Cure characteristics

#### 3.A.3.3.1 Composites without adhesion promoters

##### a. Minimum torque

Figure 3.5 shows the variation of minimum viscosity measured as torque in RPA at 150°C with fiber loading. The minimum torque increases with fiber loading. The relatively higher viscosity of the latex stage composite may be attributed to higher average fiber length and low level of molecular breakdown due to shorter shear history.

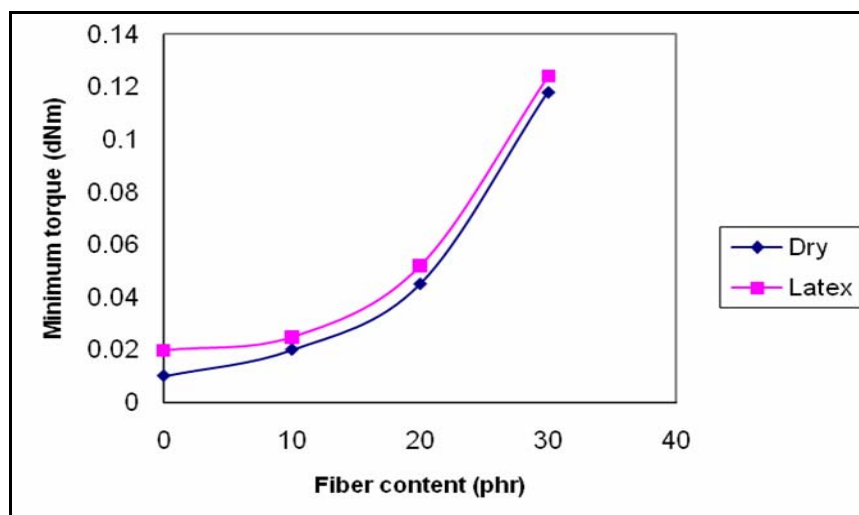


Figure 3.5 Variation of minimum torque with fiber content

##### b. Differential torque

Figure 3.6 compares the differential torque i.e. the difference between maximum torque and the minimum torque values of the composites. The differential torque increases with the fiber loading. This shows an increasingly restrained matrix with fiber loading. Latex stage compounds show marginally higher differential torque compared to dry rubber compounds. This is because of the lower fiber breakage during processing.

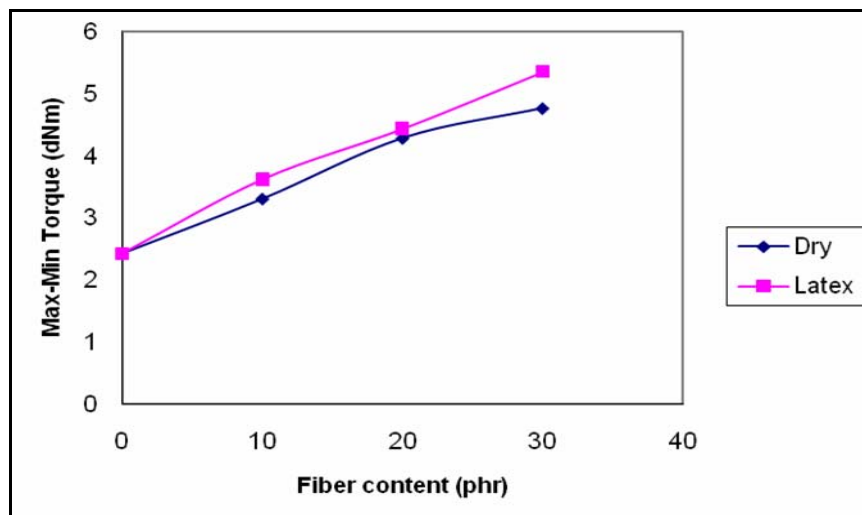


Figure 3.6 Variation of differential torque with fiber content

**c. Cure time & scorch time**

Figures 3.7 and 3.8 show the variation of cure time and scorch time with fiber loading, respectively. Cure time initially remains constant and then increases with fiber loading.

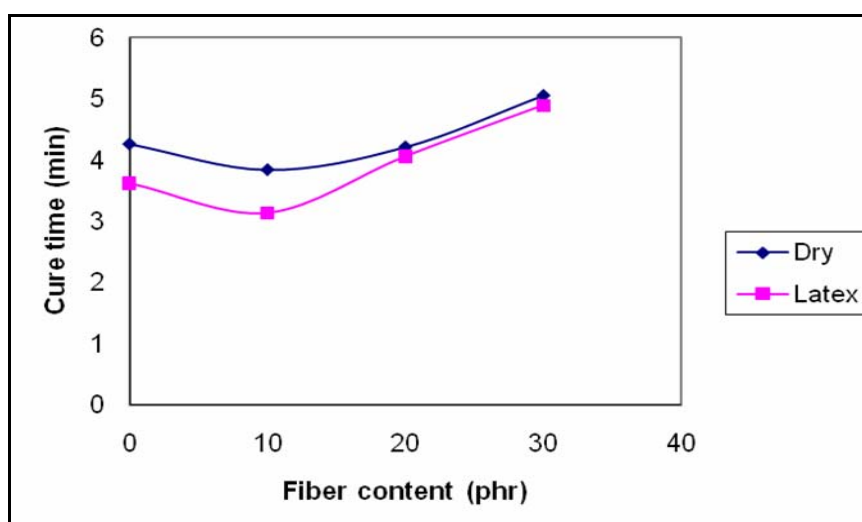
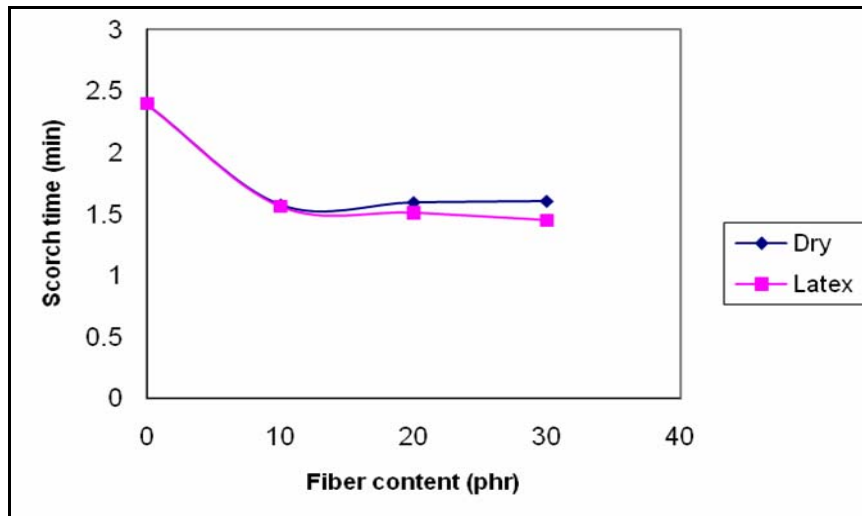


Figure 3.7 Variation of cure time with fiber content



**Figure 3.8 Variation of scorch time with fiber content**

An increase of about 1 minute is observed at 30 phr fiber loading for dry rubber compounds and latex stage compounds. For both types of composites scorch time initially decreases and then remains almost constant. The cure and scorch behaviour shows that at higher loadings of fiber there is retardation of cure rate. This may be due to the adsorption of curatives by the fibers making them unavailable for crosslinking.

### **3.A.3.3.2 Composites with adhesion promoters**

#### **a. HRH Bonding system**

##### **Minimum torque**

Figure 3.9 shows the variation of minimum viscosity measured as torque in RPA at 150°C with fiber loading. The minimum torque increases with fiber loading. The relatively higher viscosity of the latex stage composite may be attributed to higher average fiber length and low level of molecular breakdown due to shorter shear history. The minimum torque values are comparable to that of compounds without HRH (figure 3.5).

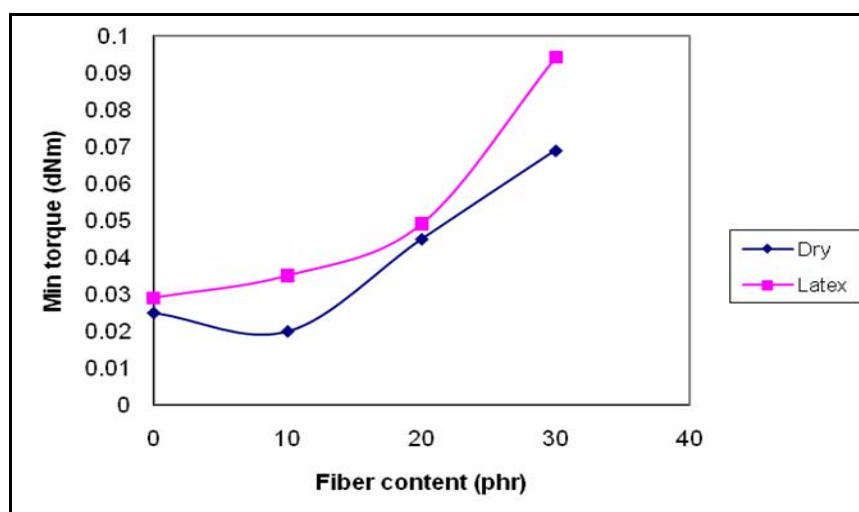


Figure 3.9 Variation of minimum torque with fiber content (Composites with HRH bonding agent)

### Differential torque

The differential torque increases with the fiber loading (Figure 3.10). This shows an increasingly restrained matrix with fiber loading. Differential torque is comparable for dry rubber and latex stage composites of both with HRH and without HRH compounds. (See Figure 3.6)

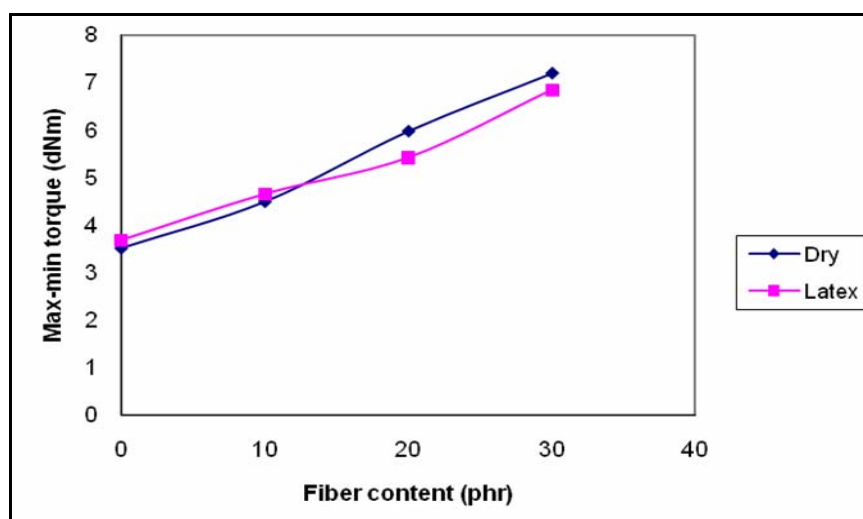
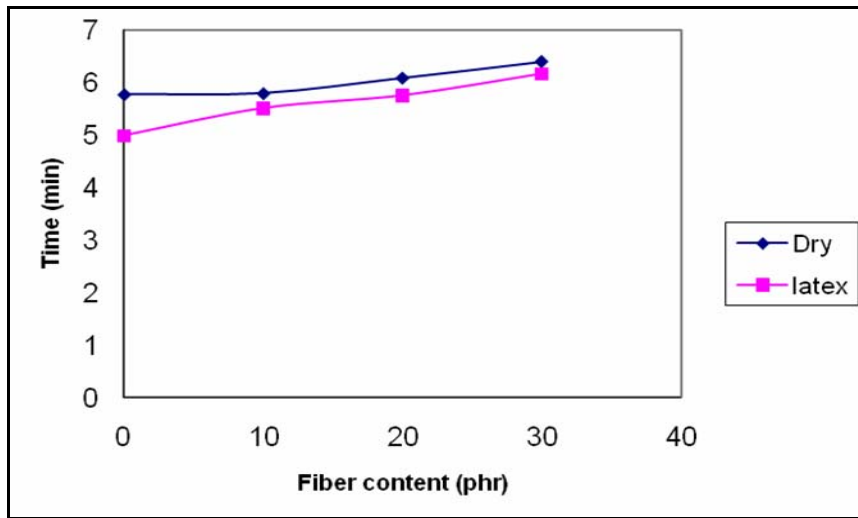


Figure 3.10 Variation of differential torque with fiber content (Composites with HRH bonding agent)

**Cure time & scorch time**

Figures 3.11 and 3.12 show the variation of cure time and scorch time, respectively, with fiber loading. A marginal increase in cure time with fiber loading is observed.



**Figure 3.11 Variation of cure time with fiber content (Composites with HRH bonding agent)**

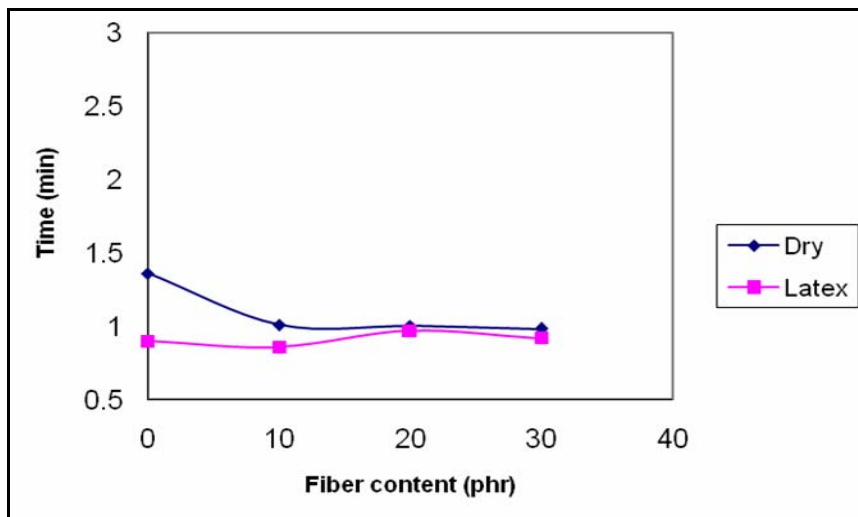


**Figure 3.12 Variation of scorch time with fiber content (Composites with HRH bonding agent)**

At all fiber loadings the latex stage compounds show marginally higher cure time. Scorch time initially decreases and then remains almost constant. The cure and scorch behaviour shows that at higher loadings of fiber there is retardation of cure rate. This may be due to the adsorption of curatives by the fibers making them unavailable for crosslinking. The cure time of composites with HRH are higher than that of composites without HRH. This may be due to the presence of acidic silica in the matrix.

### b. MANR-treated nylon composites

#### Minimum torque

Figure 3.13 shows the variation of minimum viscosity measured as torque in RPA at 150°C with fiber loading. The minimum torque increases with fiber loading. The latex stage composites show slightly higher viscosity compared to dry rubber composites. This may be attributed to higher average fiber length and low level of molecular breakdown due to shorter shear history.

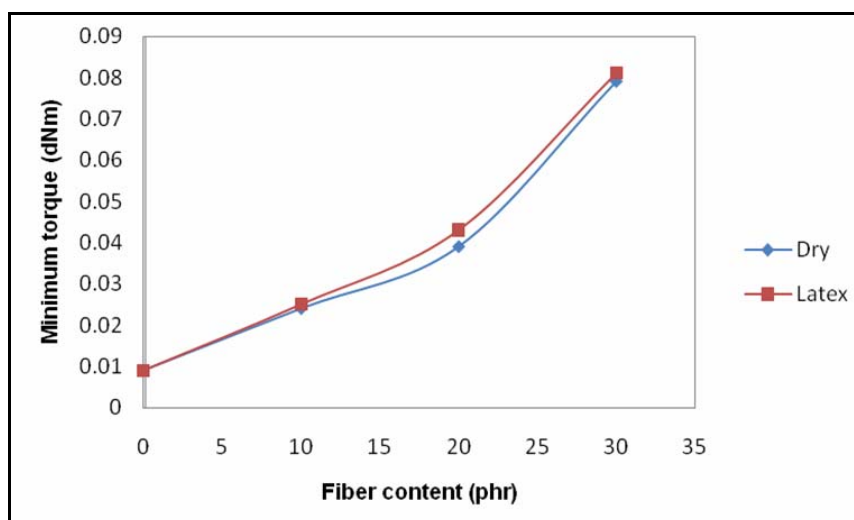


Figure 3.13 Variation of minimum torque with fiber content for MANR-treated nylon composites

### Differential torque

Figure 3.14 compares the differential torque, that is, maximum torque minus the minimum torque values of compounds obtained in Rubber Process Analyzer. The differential torque increases with the fiber loading. This shows an increasingly restrained matrix with fiber loading. Latex stage composites show better differential torque especially at 20 and 30 phr. This may be the result of lower molecular breakdown and fiber breakage of latex compounds compared to dry rubber compounds.

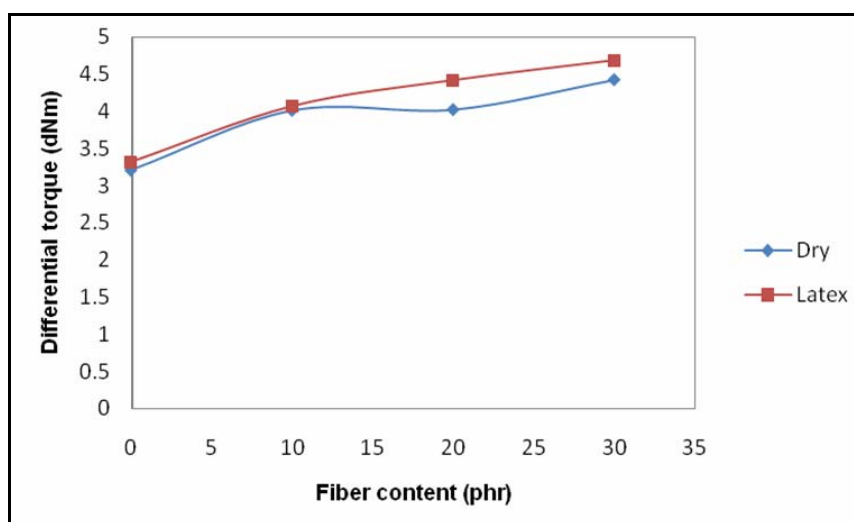


Figure 3.14 Variation of minimum torque with fiber content for MANR-treated nylon composites

### Cure time & Scorch time

Figures 3.15 and 3.16 give the variation of cure time and scorch time, respectively with fiber loading. The maleated matrix will be acidic in nature. This acidic nature will retard the cure reaction rendering a higher cure time. This is reflected in the high cure time of the gum composites compared to composites with and without HRH. For both dry rubber and latex composites the cure time decreases with fiber content. When treated fibers are added to the matrix the free -

NH<sub>2</sub> groups in the uncombined state may accelerate the cure reaction. This may be the reason for the lower cure time of fiber composites compared to gum composite. With the increase in the loading of the fiber the number of uncombined –NH<sub>2</sub> groups increases consequently decreasing the cure time. Latex stage composites show slightly lower cure time than dry rubber composites. Scorch time follows a similar trend as cure time.

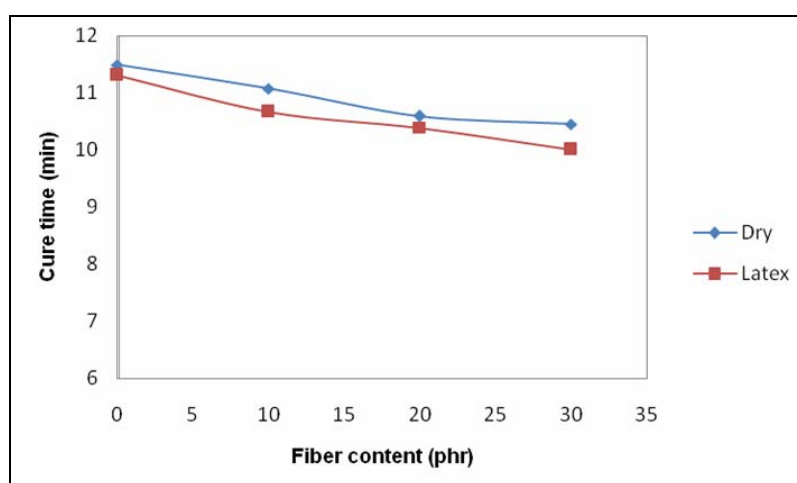


Figure 3.15 Variation of cure time with fiber content for MANR-treated nylon composites

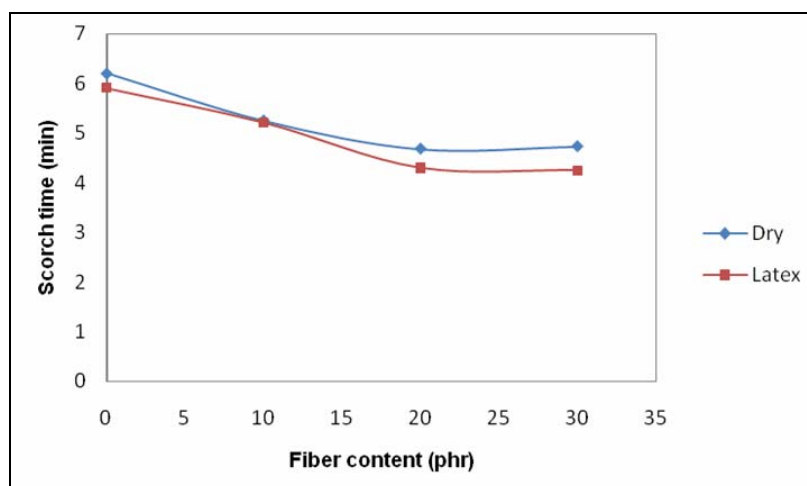


Figure 3.16 Variation of scorch time with fiber content for MANR-treated nylon composites

### 3.A.3.4 Mechanical properties

#### 3.A.3.4.1 Composites without adhesion promoters

##### a). Tensile strength

The variation of tensile strength of the composites in longitudinal and transverse directions is shown in figures 3.17 and 3.18, respectively. In both the directions tensile strength continuously decreases with the fiber loading. Since the natural rubber matrix is non-polar the polar nylon fiber will not develop adequate inter facial adhesion to resist the tensile forces at high elongations. So the fibers get easily pulled out from the matrix. The voids thus developed will act as points of weakness effecting earlier failure and reducing the tensile strength. With increase in fiber content the tensile strength is further reduced. When the fibers are arranged transversely the tensile strength will be provided solely by the matrix. With increase in fiber content the dilution of the matrix will reduce the tensile strength.

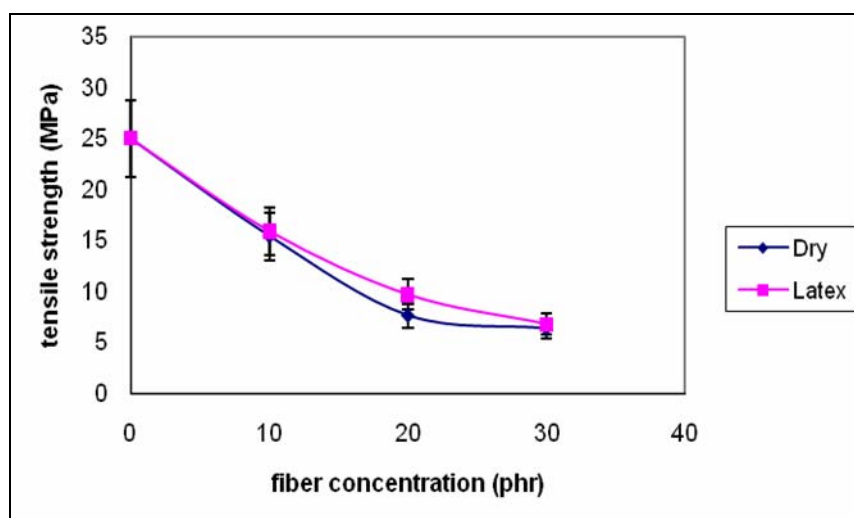


Figure 3.17 Variation of tensile strength (longitudinal) with fiber content

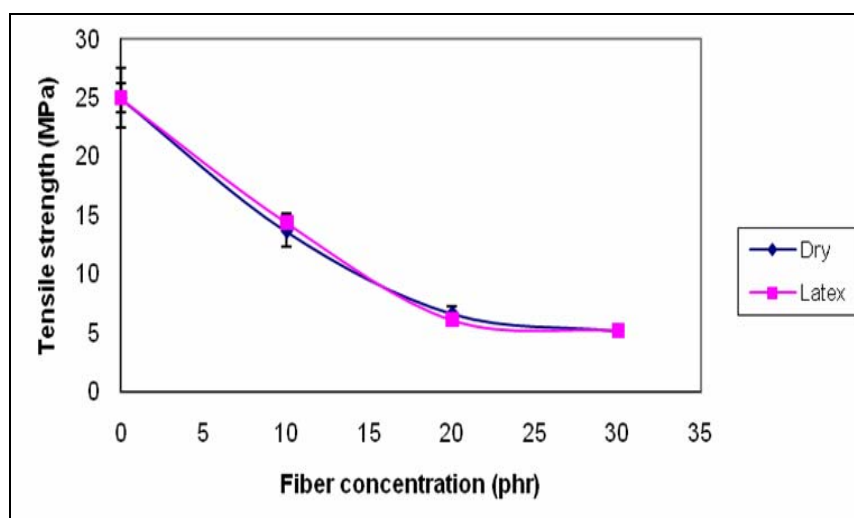


Figure 3.18 Variation of tensile strength (transverse) with fiber content

b). **Modulus**

Figures 3.19 and 3.20 show the variation of modulus at 50% elongation of composites in longitudinal and transverse directions, respectively. In both cases an increase in modulus with fiber content is observed.

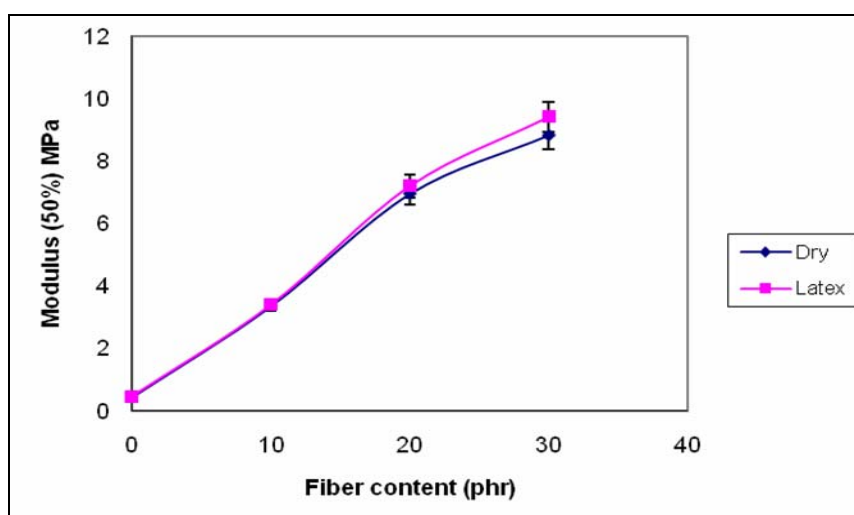
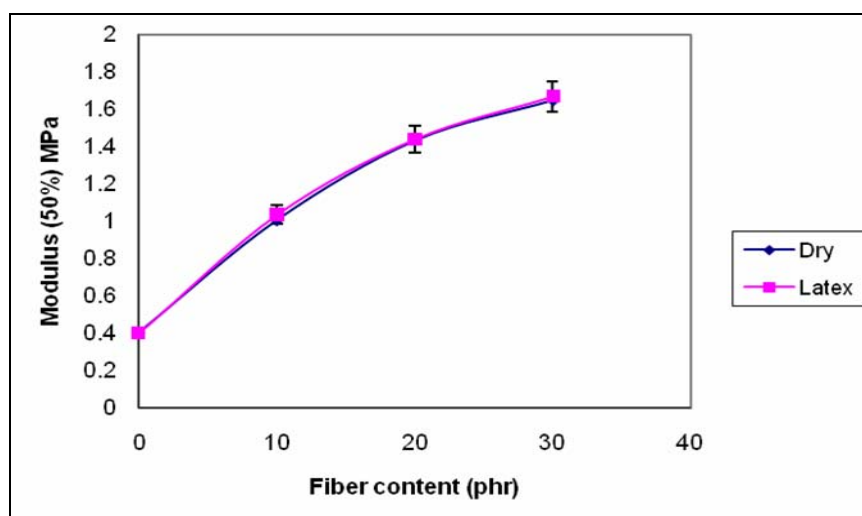


Figure 3.19 Variation of 50% modulus (longitudinal) with fiber content



**Figure 3.20 Variation of 50% modulus (transverse) with fiber content**

In longitudinal direction latex stage composites are marginally better than dry rubber composites especially at 30 phr fiber content. This is attributed to the reduced fiber breakage and lower molecular breakdown of matrix as a result of lower time of mixing cycle. In transverse direction both types of composites show similar values, since the role of fibers in load bearing is minimal.

### c. Tear strength

The figures 3.21 and 3.22 show the variation of tear strength with fiber content. In the longitudinal direction the fibers are oriented perpendicular to the crack propagation. When the fiber content increases there will be more and more hindrance to the crack propagation as is evident from the increase in tear strength. The values are comparable between latex and dry stage composites. In the transverse direction fibers are parallel to the crack front and offer less resistance to crack propagation resulting in lower tear strength values.

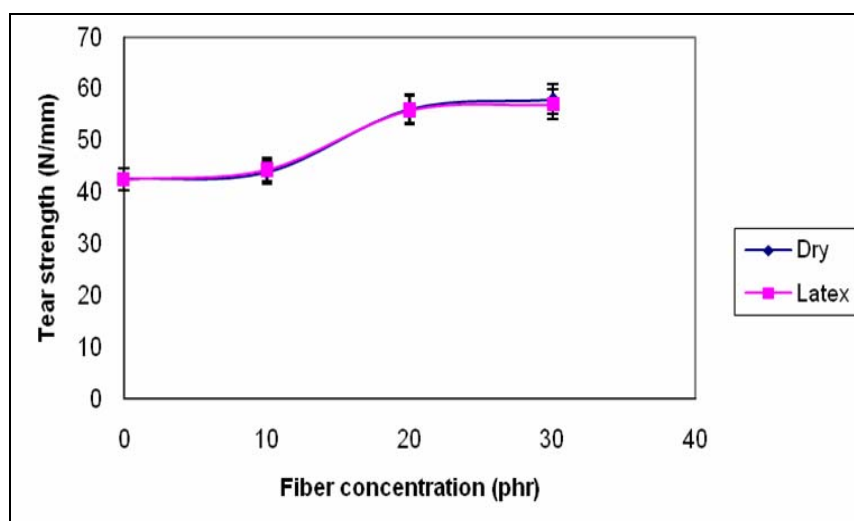


Figure 3.21 Variation of tear strength (longitudinal) with fiber content

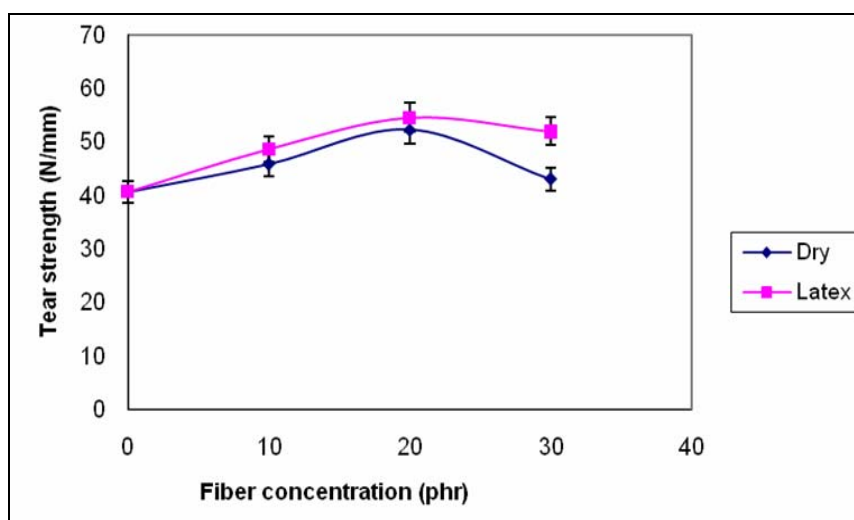


Figure 3.22 Variation of tear strength (transverse) with fiber content

**d). Elongation at break**

Variation of elongation at break with fiber content is shown in figures 3.23, and 3.24, respectively. Elongation at break values exhibit a linear decrease with fiber content for both longitudinal and transverse oriented composites. Since the composites have lower fiber matrix adhesion pull out of

fibers is easier on tensile fracture and the voids thus formed in the matrix will act as defects causing earlier breaking of specimens and reduced elongation at break. The latex masterbatch composites show better values than dry rubber composites since the determining factor is the matrix which encountered lesser shear than the latter.

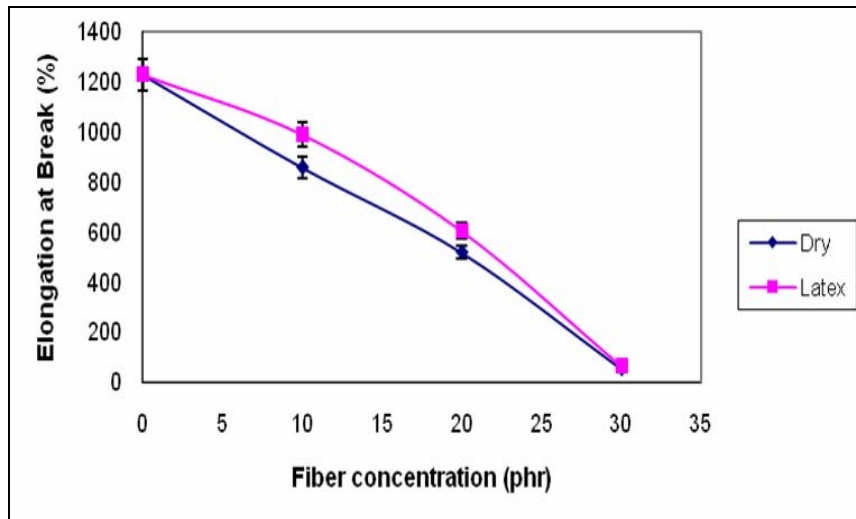


Figure 3.23 Variation of elongation at break (longitudinal) with fiber content

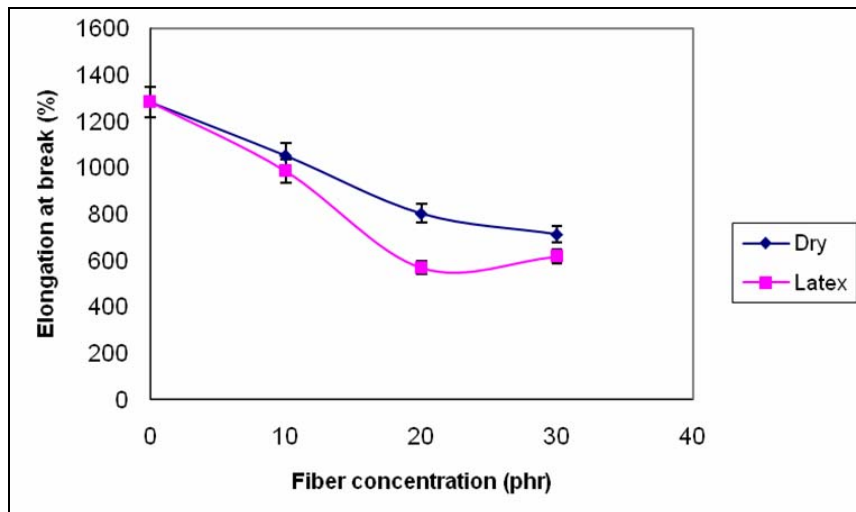


Figure 3.24 Variation of elongation at break (transverse) with fiber content

### 3.A.3.4.2 Composites with adhesion promoters

#### a) HRH Bonding system

##### *Tensile strength*

Variations of tensile strength of composites with fibers oriented in the longitudinal and transverse directions are shown in figures 3.25 and 3.26. Tensile strength in longitudinal direction initially decreases and then increases with the fiber content unlike composites without HRH where the tensile strength goes on decreasing with fiber content. Sreeja et al [18] reported similar results with treated fibers in dry NR. Initial reduction in tensile strength is due to the interruption of stress crystallization of natural rubber by the short fibers. At higher fiber loadings the increased reinforcement will offset the effect of reduction in stress crystallization. The latex stage compound shows higher values than dry stage compound. This is due to less fiber and matrix breakdown as a result of lower mixing cycle. In the transverse direction the tensile strength shows a decrease with fiber content as the matrix strength is lowered by the dilution effect. Here also the latex stage composites exhibit better values due to the lower molecular breakdown of the matrix as a result of lower mixing time.

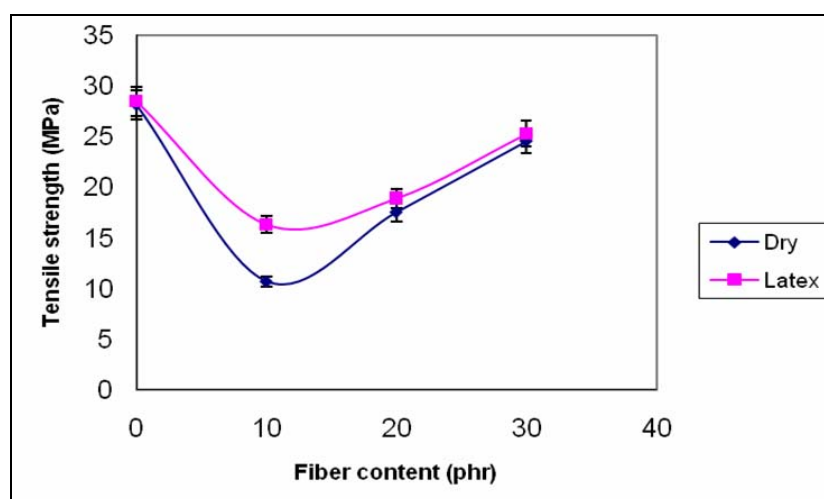


Figure 3.25 Variation of tensile strength (Longitudinal) with fiber content (Composites with HRH bonding agent)

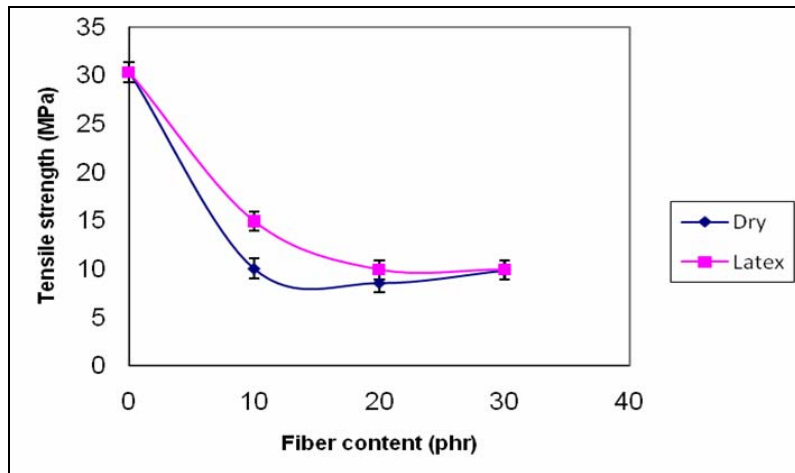


Figure 3.26 Variation of tensile strength (Transverse) with fiber content (Composites with HRH bonding agent)

### Modulus

Figures 3.27 and 3.28 show the variation of modulus at 50% elongation of composites with bonding system in longitudinal and transverse directions, respectively. Modulus values are improved substantially compared to composites without HRH, due to improved interaction between fiber and matrix.

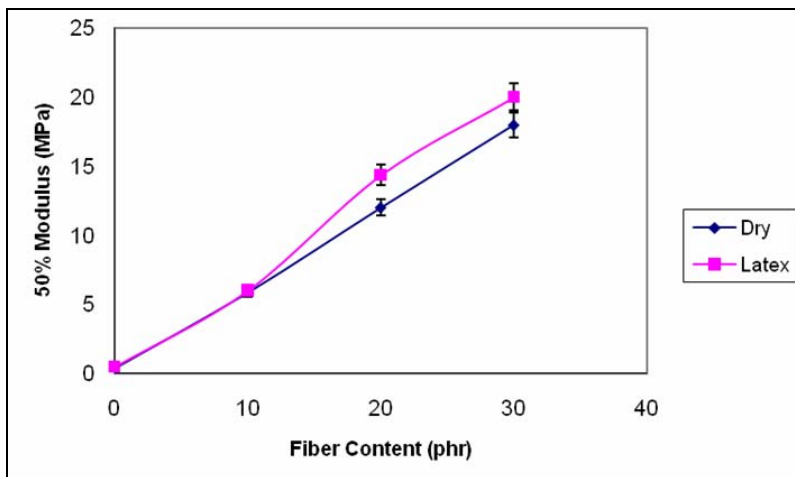
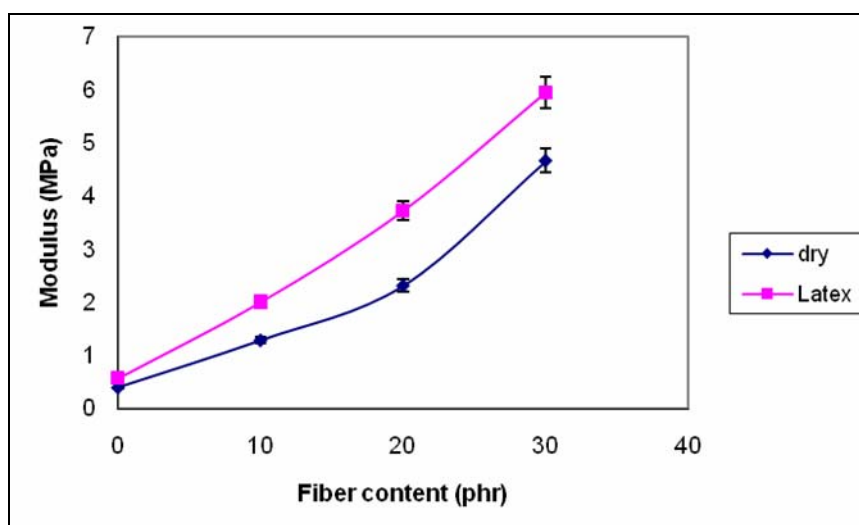


Figure 3.197 Variation of modulus (Longitudinal) with fiber content (Composites with HRH bonding agent)



**Figure 3.28** Variation of modulus (Transverse) with fiber content (Composites with HRH bonding agent)

Composites show an increase in modulus with fiber content. Latex stage composites show better values than the dry rubber composites especially for 20 and 30 phr loadings. This is attributed to the reduced fiber breakage and lower molecular breakdown of matrix as a result of lower time of mixing cycle.

### ***Tear strength***

The figures 3.29 and 3.30 show the variation of tear strength with fiber content for the composites with bonding agent. In the longitudinal direction the fibers are oriented perpendicular to the crack propagation. When the fiber content increases there will be more and more hindrance to the crack propagation as is evident from the increase in tear strength. The composites with bonding agent show higher values compared to those without bonding agent as expected. The tear strength values are comparable between latex and dry stage composites. In the transverse direction fibers are parallel to the crack front and offer less resistance to crack propagation resulting in lower tear strength values.

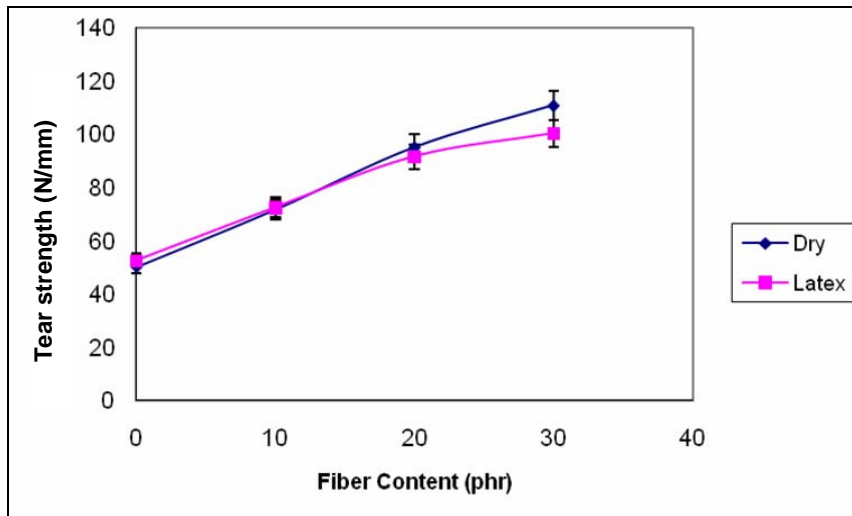


Figure 3.29 Variation of tear strength (Longitudinal) with fiber content (Composites with HRH bonding agent)

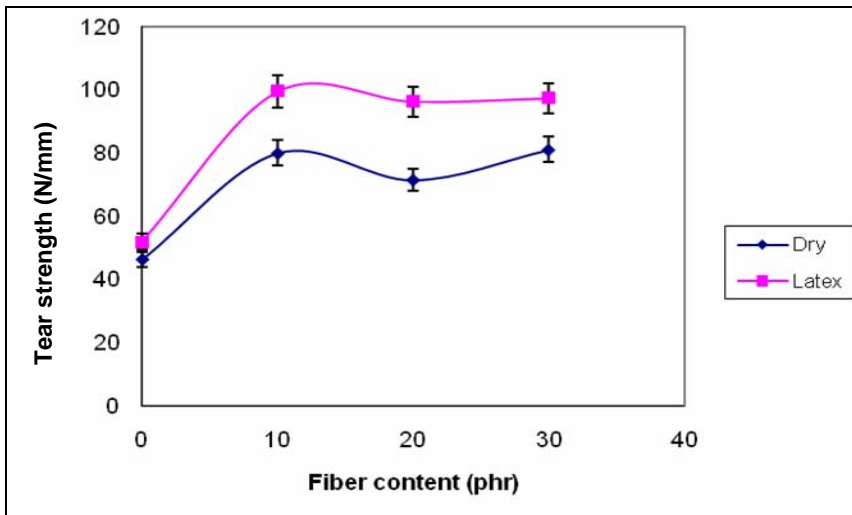
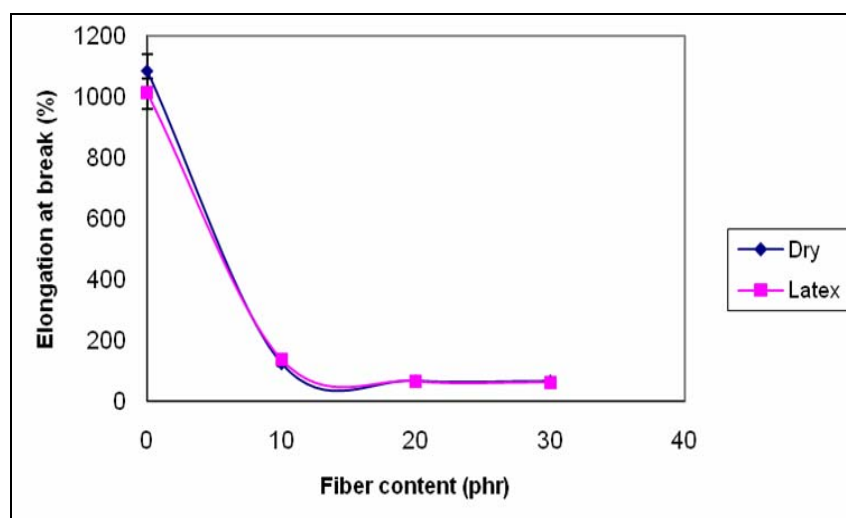


Figure 3.30 Variation of tear strength (Transverse) with fiber content (Composites with HRH bonding agent)

### Elongation at break

Elongation at break values (figures 3.31 and 3.32) exhibit a sharp decrease with fiber content, unlike composites without HRH (figure 3.23). In composites containing bonding agent, the fibers progressively restrict the matrix resulting in a decrease in elongation at break.



**Figure 3.31** Variation of elongation at break (Longitudinal) with fiber content (Composites with HRH bonding agent)

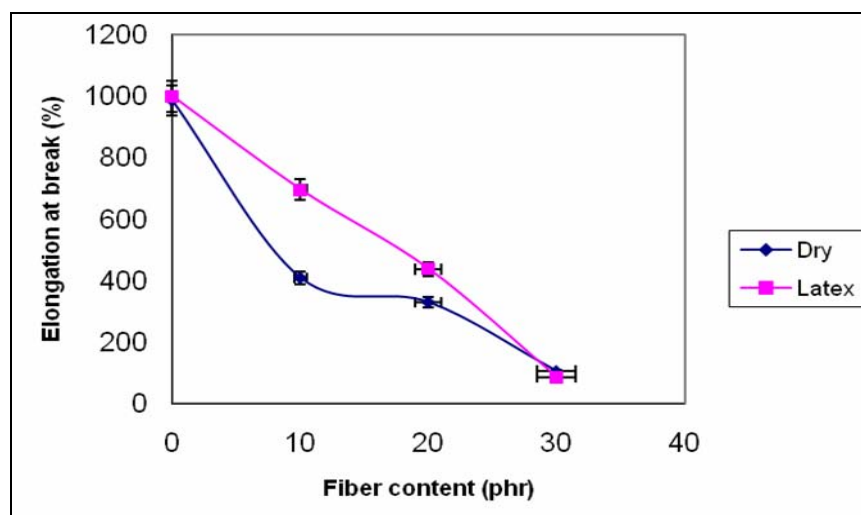


**Figure 3.32** Variation of elongation at break (Transverse) with fiber content (Composites with HRH bonding agent)

### ***Rebound resilience***

Figure 3.33 shows the variation of rebound resilience with fiber concentration. For compounds with bonding agent rebound resilience decreases with the increase in fiber content. The values are similar for both latex stage and dry stage composites.

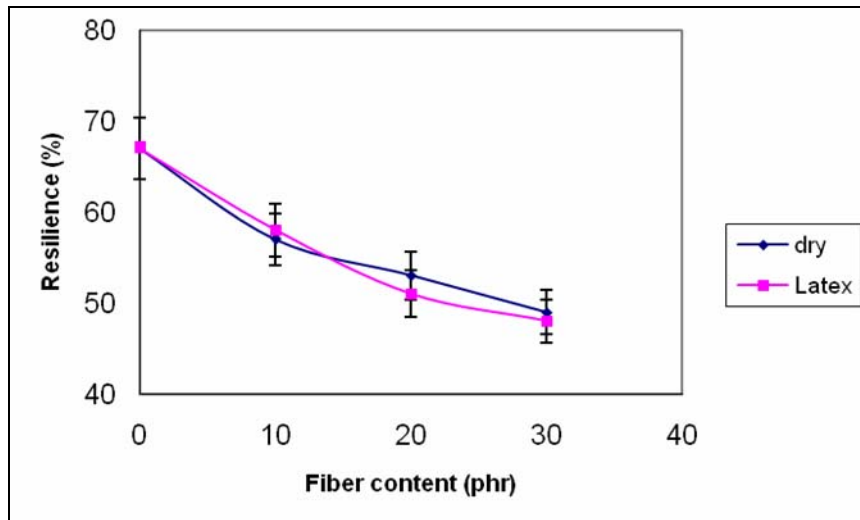


Figure 3.33 Variation of resilience with fiber content (Composites with HRH bonding agent)

*Compression set*

Figure 3.34 compares the compression set values of latex masterbatch and dry rubber composites, both with bonding agent.

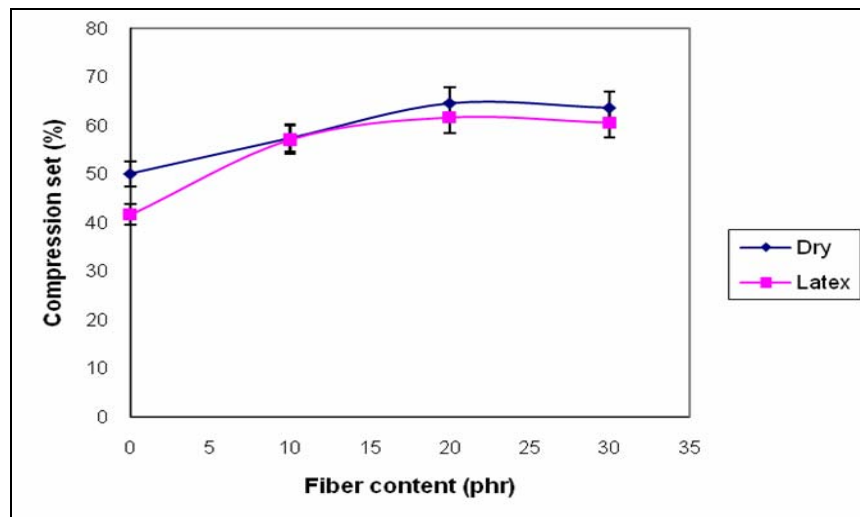


Figure 3.34 Variation of compression set with fiber content (Composites with HRH bonding agent)

Compression set increases with the fiber content. With increase in fiber content reinforcement effect increases. The matrix becomes more restricted. This is reflected in higher compression set of the composites.

### ***Abrasion resistance***

Figure 3.35 compares the abrasion resistance in the longitudinal direction of latex and dry stage composites with fiber content. Abrasion resistance increases with the introduction of fibers in the case of composites with bonding system. There is significant reduction in abrasion loss for latex masterbatch composites compared to dry rubber, especially beyond 10 phr fiber loading.

Figure 3.36 shows the abrasion resistance in the transverse direction. In the transverse direction the abrasion resistance shows an initial decrease and then increases. But in this case better values are for the dry rubber stage composites than for the latex stage composites. In the transverse orientation during abrasion process whole fibers are removed from the sample along with abraded rubber. Consequently abrasion loss will be higher than the samples with longitudinally oriented fibers. In the latex stage compounds the interaction between the fiber and the rubber is more. Due to this interaction more rubber will be bound together with the fiber and will be removed along with fiber. So latex stage compounds will register higher abrasion loss.

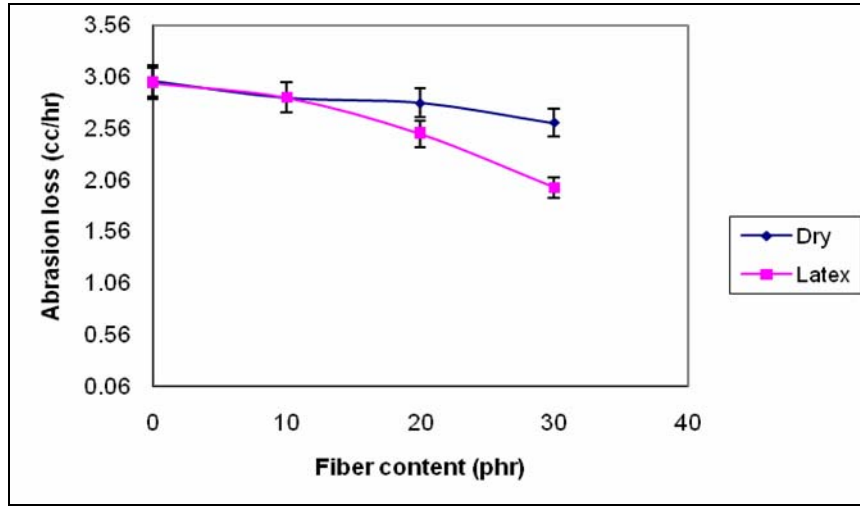


Figure 3.35 Variation of abrasion loss (Longitudinal) with fiber content (Composites with HRH bonding agent)

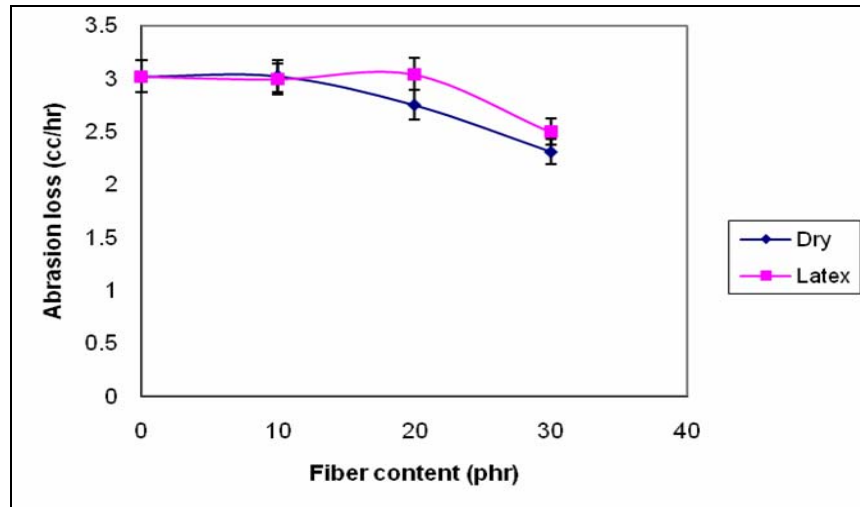


Figure 3.36 Variation of abrasion loss (Transverse) with fiber content (Composites with HRH bonding agent)

### MANR-treated nylon composites

#### *Tensile strength*

Variation of tensile strength of maleated composites is shown in figure 3.37. The improved interaction between the maleated matrix and free  $-NH_2$  groups

on the fiber surface will increase the interfacial adhesion and contribute positively to the tensile strength. Tensile strength initially decreases and then increases with the fiber content. Initial reduction in tensile strength is due to the interruption of stress crystallization of natural rubber by the short fibers. At higher fiber loadings the increased reinforcement will offset the effect of reduction in stress crystallization. The composites with 30 phr fiber loading show better strength than composites with HRH bonding system (figure 3.25). The latex stage compound shows higher values than dry stage compound. This is due to less fiber and matrix breakdown as a result of lower mixing cycle.

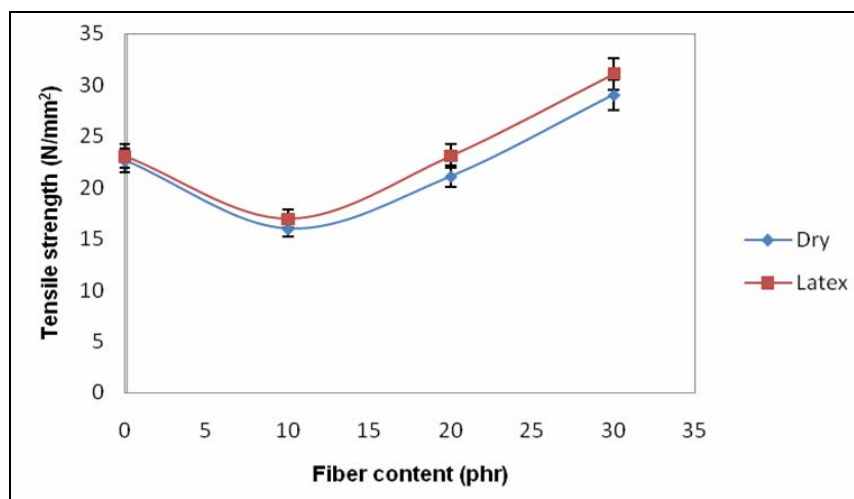
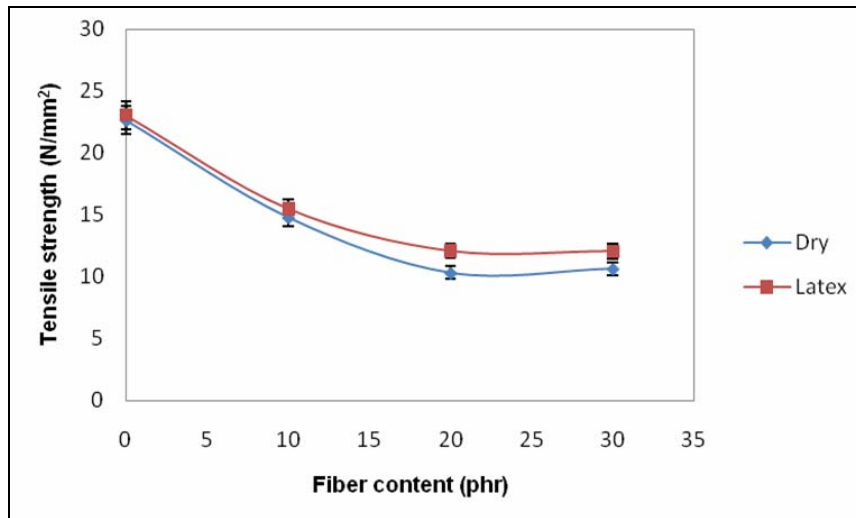


Figure 3.37 Variation of tensile strength with fiber content (Treated nylon composites)

Figure 3.38 shows the variation of tensile strength in transverse direction of the MANR-treated nylon composites, with fiber loading. The tensile strength continually decreases with fiber content. This is due to the dilution effect offered by the fibers arranged in transverse direction. These fibers are not effective in stress transfer and as a result weaken the matrix causing failure at lower stresses. Here also the latex stage composites shows better properties compared to dry rubber composites due to lower fiber and matrix breakage.



**Figure 3.38** Variation of tensile strength (transverse) with fiber content (Treated nylon composites)

### ***Modulus***

Figure 3.39 shows the variation of modulus at 50% elongation of maleated composites. An increase in modulus with fiber content is observed which is due to effective reinforcement of maleated matrix with treated fibers. Latex stage composites show better values than the dry rubber composites. This is attributed to the reduced fiber breakage and lower molecular breakdown of matrix as a result of lower time of mixing cycle. Figure 3.40 gives the variation of modulus in transverse direction. The modulus increases with fiber content but the values are much lower compared to the longitudinal modulus. The fibers being arranged in transverse direction to the tensile force, the restriction of deformation of matrix in the tensile direction is much lower.

### ***Elongation at break***

Figure 3.41 shows the variation of elongation at break with fiber content in longitudinal direction. Elongation decreases with fiber content. Even at 10 phr fiber loading elongation decreases drastically. This shows the effect of

reinforcement imparted to the maleated matrix by treated nylon fiber. Elongation in transverse direction (figure 3.42) also decreases with fiber content. But the decrease is gradual compared to longitudinal composites. This shows the better restraining of matrix by fibers arranged in longitudinal direction.

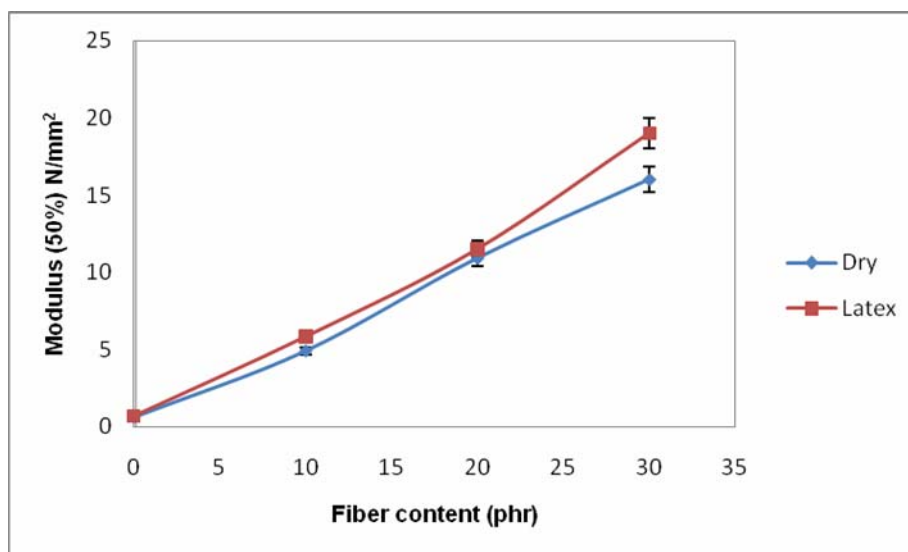


Figure 3.39 Variation of modulus (Longitudinal) with fiber content (Treated nylon composites)

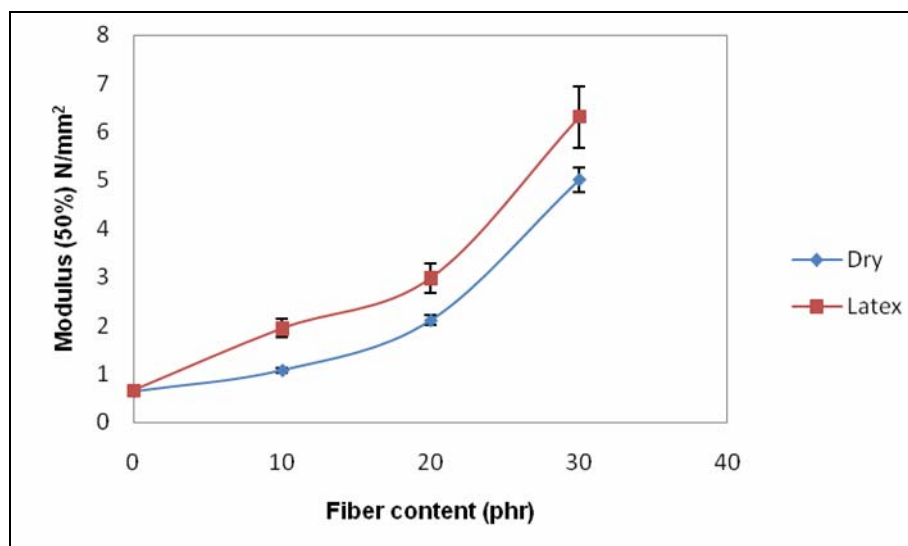


Figure 3.40 Variation of modulus (transverse) with fiber content (Treated nylon composites)

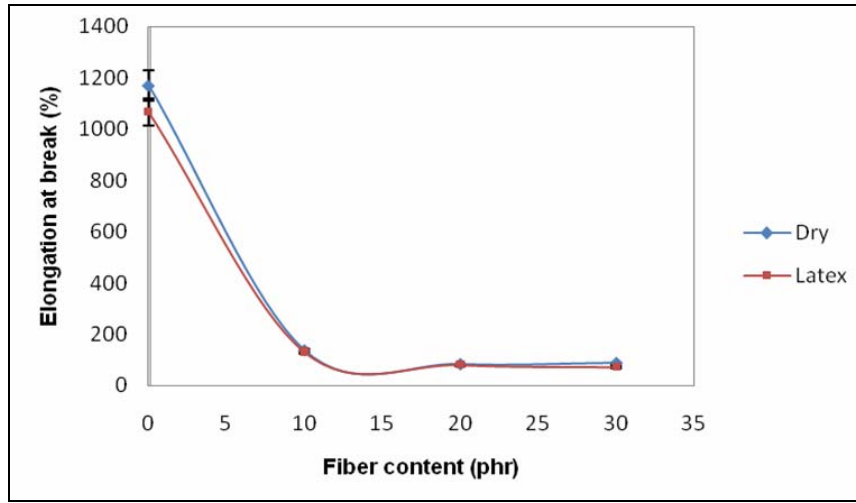


Figure 3.41 Variation of elongation at break with fiber content (Treated nylon composites)

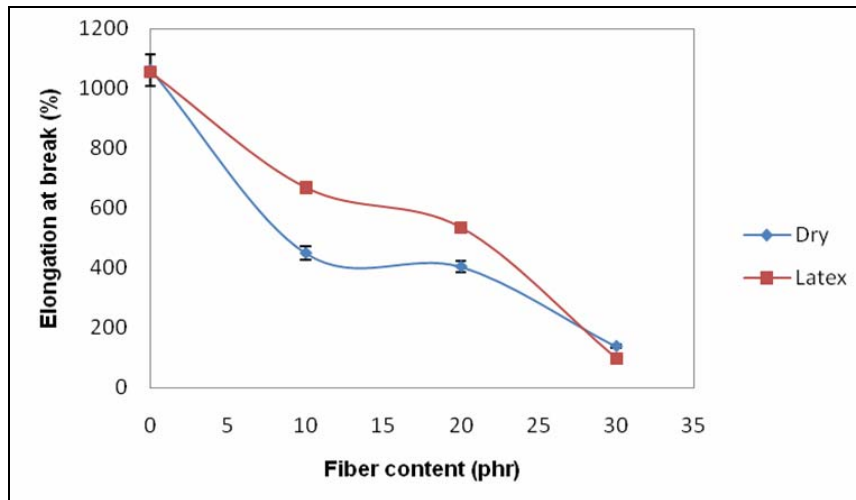


Figure 3.42 Variation of elongation at break (Transverse) with fiber content (Treated nylon composites)

### Abrasion loss

Figure 3.43 compares the abrasion resistance of dry rubber and latex stage composites. Abrasion resistance increases with the introduction of fibers. Latex stage composites show better abrasion resistance than dry rubber composites at all fiber loadings. The lower fiber and matrix breakdown of the

latex stage composites may be binding together more rubber with reinforcing fiber making it difficult to get removed by the abrading action.

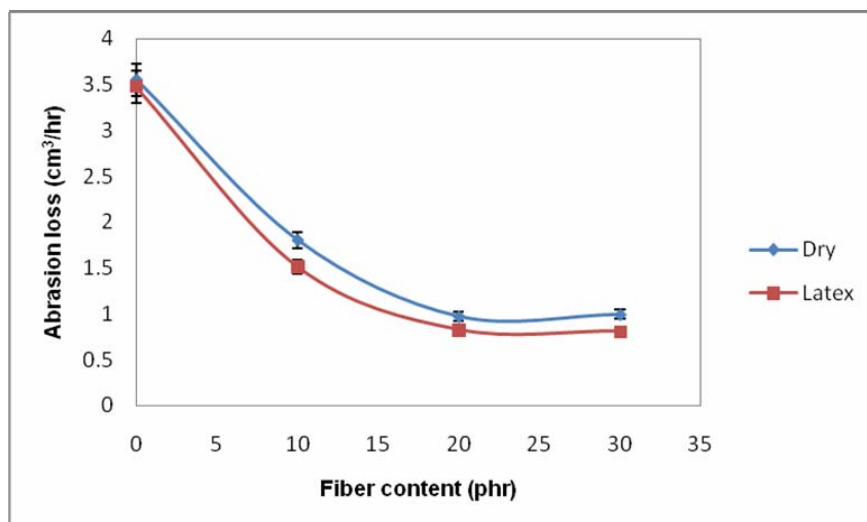


Figure 3.43 Variation of abrasion loss with fiber content

### Hardness

Figure 3.44 shows the hardness of MANR-treated nylon composites. Hardness increases with fiber content indicating higher reinforcement. Hardness is comparable for dry and latex stage composites.

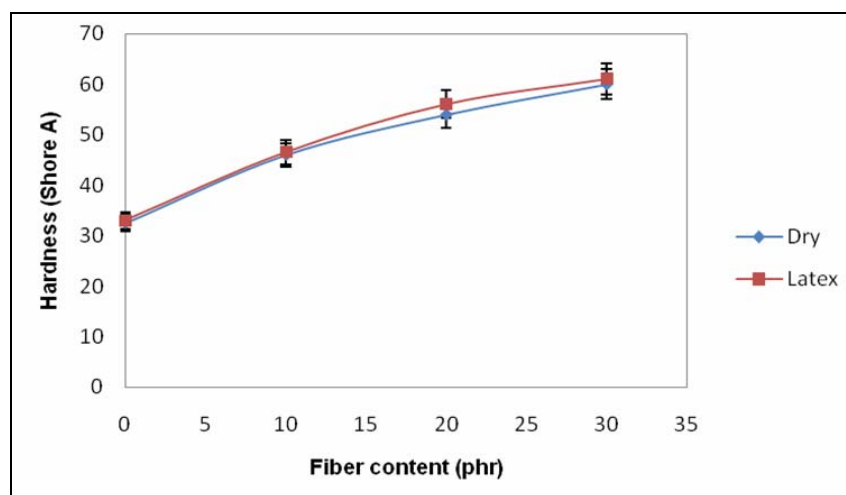
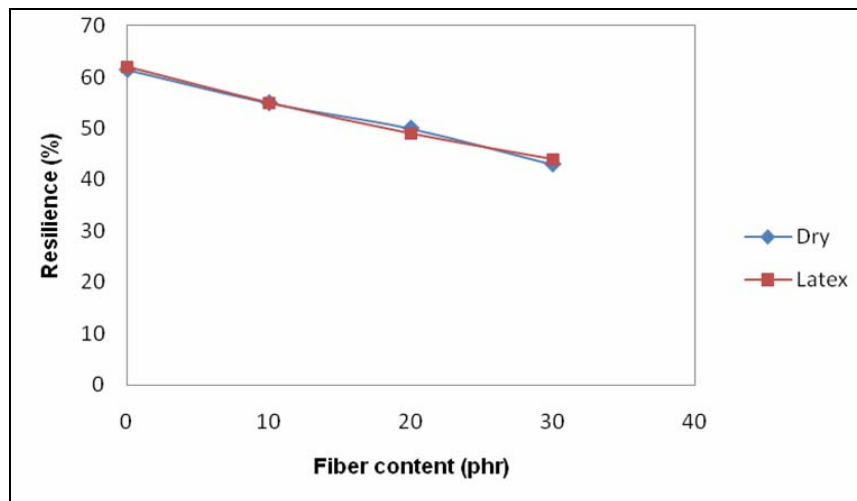


Figure 3.44 Variation of hardness with fiber content

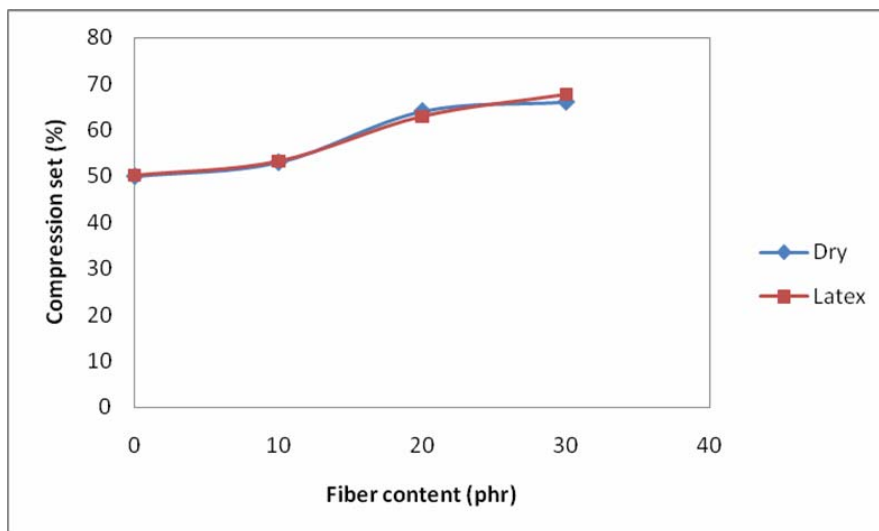
**Rebound Resilience**

Figure 3.45 shows the variation of rebound resilience with fiber content. Resilience decreases with fiber content. Resilience values are similar for both dry rubber and latex stage composites.



**Figure 3.45 Variation of resilience with fiber content**

**Compression set**



**Figure 3.46 Variation of compression set with fiber content**

Figure 3.46 show the compression set of MANR-treated Nylon composites with fiber content. Compression set increases with fiber content. The increase is more pronounced at 20 and 30 phr fiber content. As the filler content increases the viscous loss also increases as energy can dissipate at fiber – matrix interfaces. A more viscous matrix flows easily at elevated temperature under applied stress leading to higher compression set values. Compression set is more or less similar for dry rubber and latex stage composites.

### 3.A.3.5 Ageing resistance

Ageing resistance of the composites with HRH bonding system is shown in the Figures 3.47 and 3.48. Figure 3.47 shows the tensile strength of the composites after ageing and figure 3.48, modulus at 50% elongation. Tensile strength and modulus increases after the ageing. This may be due to the increased fiber matrix adhesion as result of the after cure of the unreacted bonding system. Similar results were reported earlier [6,19].

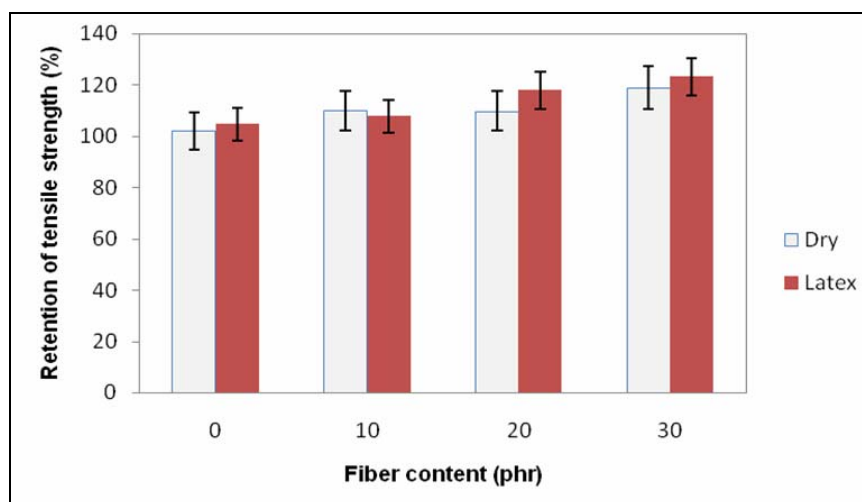
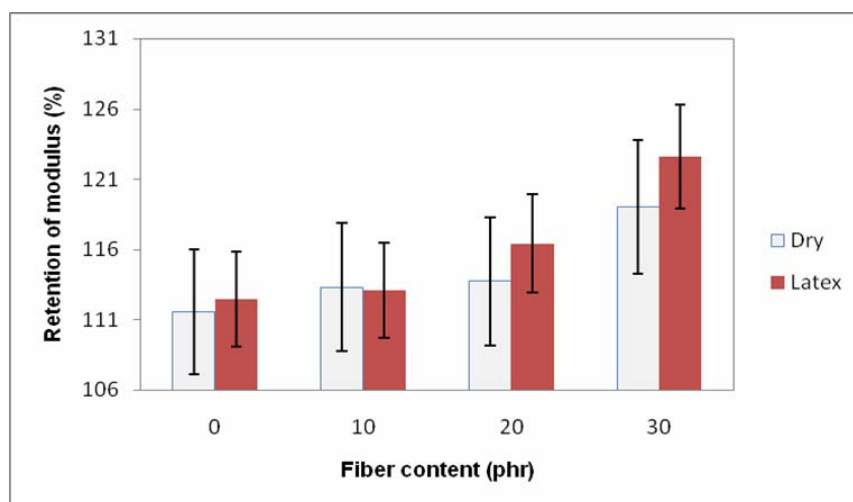


Figure 3.47 Retention in tensile strength of composites with HRHbonding

The retention percentage generally increases with fiber content in both tensile strength and modulus. Compared to dry rubber composites, latex stage composites exhibits marginally higher retention percentage, especially at higher fiber content. This may be due to the lower thermal and shear history of the latex stage composites.



**Figure 3.48 Retention in modulus of composites with HRH bonding**

Figures 3.49 and 3.50 show the ageing resistance of the MANR-treated nylon composites in terms of tensile strength and modulus respectively. Unlike composites with HRH bonding system, ageing properties decrease in the case of MANR-treated nylon composites. Retention percentage of properties improves with increasing fiber content. Here also latex stage composites show better properties in most of the composites.

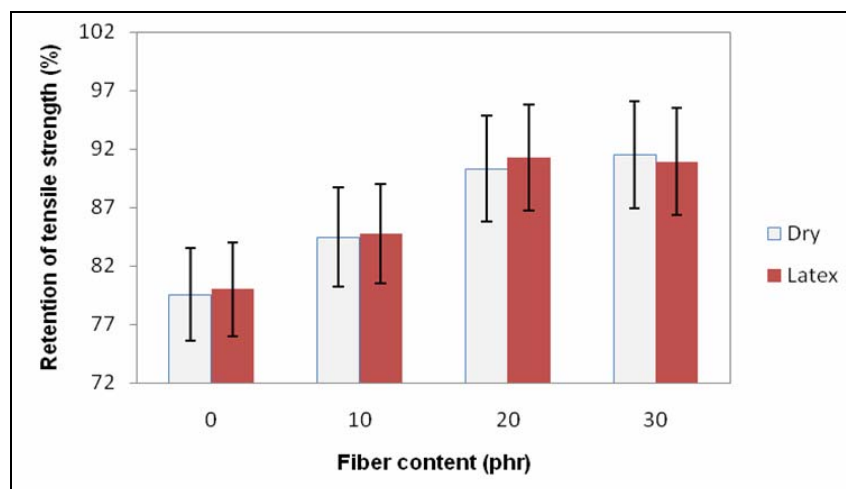


**Figure 3.49** Variation of percentage retention in tensile strength with fiber content for treated nylon composites

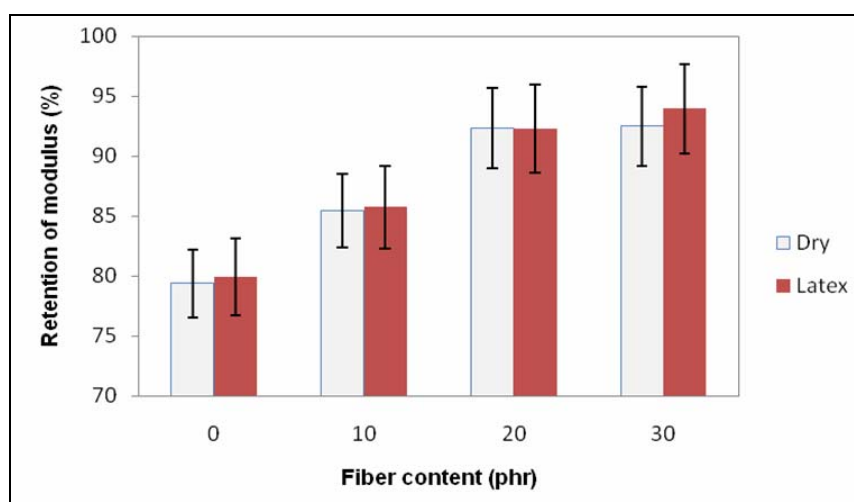


**Figure 3.50** Variation of percentage retention in modulus with fiber content for treated nylon composites

### 3.A.3.6 SEM Analysis

Figures 3.51 and 3.52 show the SEM photographs of the fracture surface of tensile specimens without adhesion promoters, from dry rubber and latex stage composites respectively. From the SEM analysis it is observed that in latex stage composite samples the dispersion is more uniform and there are

less fiber pullouts from the matrix than dry rubber. This proves that the reduction in mixing time is not affecting the dispersion of fibers but positively contribute to the composite performance.



**Figure 3.51 SEM photograph of fracture surface of dry rubber composite**

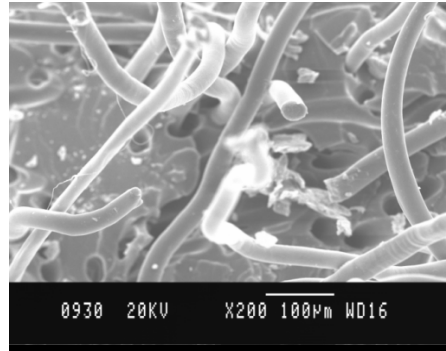


**Figure 3.52 SEM photograph of fracture surface of latex masterbatch composite**

The effect of reduction in mixing time is more pronounced in the samples with bonding agent. Figures 3.53 and 3.54 show the fracture surface of dry rubber and latex masterbatch composites with bonding agent, respectively. In composites with bonding system the adhesion is better compared to those without bonding system, which is apparent from the fracture surface texture.

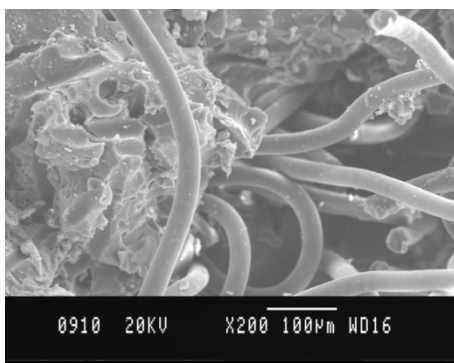


**Figure 3.53 SEM photograph of fracture surface of dry rubber composite with HRH**



**Figure 3.54 SEM photographs of fracture surface of latex masterbatch composite with HRH**

### 3.A.4 Conclusions

Short nylon fiber-natural rubber composites were prepared through latex stage processing and compared with conventional dry rubber composites. The fiber breakage and mixing time were found to be reduced for latex stage processed composites compared to dry rubber composites. The composites prepared by the new method show similar cure characteristics as of the conventional composites. The mechanical properties of the composites found to be decreasing with increasing fiber loading due to insufficient interaction between fiber and matrix. To increase the fiber-matrix interaction two methods were adopted. One, incorporation of HRH bonding system and the other, maleation of the matrix along with surface hydrolysis of the fibers. Of the mechanical properties tested for the composites with HRH bonding agent modulus, tensile strength and abrasion resistance show better values indicating better reinforcement for the latex stage composites. Elongation at break is reduced. Tear strength, resilience and compression set show more or less similar values. Better interaction between matrix and fibers for the new composites is also indicated by the SEM analysis. For maleated composites cure characteristics other than cure time and scorch time were similar to that of composites with HRH bonding system. Cure time and scorch time continuously decreases with fiber content showing acceleration of cure rate. Of the mechanical properties tensile strength and abrasion resistance of the maleated composites were improved compared to HRH composites especially at higher fiber loadings while modulus was better for HRH composites.

The new method of fiber composite preparation proposed is an efficient one to reduce the mixing time and hence to increase the production volume without compromising and mostly enhancing the mechanical properties.

**Part -B**

**Dynamic mechanical properties of NR- Nylon Micro Fiber Composites**

**3.B.1 Introduction**

Dynamic mechanical analysis in a Dynamic Mechanical Analyzer is a very powerful technique which allows for determination of mechanical properties (modulus and damping), detection of molecular motions (transitions), and for the development of morphology relationships (crystallinity, molecular weight, crosslinking, etc) [20]. A number of researchers have dwelled upon the dynamic mechanical properties of short fiber reinforced elastomer composites. Mechanical and dynamic-mechanical properties of tire tread compound reinforced with aramid short fibers were investigated by Kashani and found that tire traction and rolling resistance improved as a result of fiber addition [21]. The effects of short fiber and particulate fillers on viscoelastic damping of SBR composites were compared by Praveen et al [22]. Dynamic mechanical behavior of short coir fiber- natural rubber composites was studied by Geethamma et al. found that interfacial bonding affects damping properties of composites [23]. Pothan et al. [24] analyzed the effect of chemical modification on the dynamic mechanical properties of banana fiber reinforced polyester composites to investigate the interfacial properties. Ibarra et al. [25] reported that the loss modulus values increased with loading of short PET fibers in NR, CR, NBR and SBR compared to their respective gum compounds. Varghese et al. [26] studied the DMA of acetylated short sisal fiber reinforced NR composites and found that composite with poor interfacial bonding dissipated more energy than that with good interfacial bonding.

The RPA 2000 Rubber Process Analyzer is a very versatile dynamic mechanical rheological tester (DMRT). The RPA has been proven to be an

effective raw polymer tester, a processability tester for mixed rubber stocks, an advanced cure meter, and a DMRT for measuring post cure dynamic properties. The RPA 2000 measures the viscoelastic properties of rubber compounds in torsional shear. Thorough rubber compound characterizations are made through frequency, strain, and temperature sweeps. Here we subjected the uncured and cured fiber compounds to varying strains in a single sweep. The complex modulus values of the compounds were plotted against strain.

In this section the dynamic mechanical behavior of the composites prepared by different methods is discussed. The effect of a bonding agent and the effect of chemical modifications of the fiber are also presented.

### **3.B.2 Experimental**

Rubber process analyzer (RPA 2000) was used to study the effect of filler interaction of the compounds in uncured and cured state. 5 cm<sup>3</sup> of the uncured fiber mixes were cut using a punch and placed in the sealed biconical cavity of the Rubber Process Analyzer and subjected to strain sweep program. The samples were kept at the test temperature of 60 °C for a preheating time of 4 minutes. It was then subjected to a strain sweep with varying strains of 0.05, 0.1, 0.2, 0.5, 1, 2, 3 and 7 degrees in a single sweep. The complex modulus values obtained were plotted against strain in degrees. For strain sweep studies in cured state, uncured samples were first vulcanized to their respective cure times at 150 °C. The temperature was then reduced to 60 °C and the sample was subjected to strain sweep as above.

TA Instruments DMA Q800 was used to measure the dynamic mechanical properties of the NR-Nylon composites. Test specimens having a dimension of 30 mm x 3 mm x 2 mm were used in tension mode. Temperature sweep and frequency sweep experiments were conducted. Temperature sweep experiments

of the composites were performed from -80°C to +40°C. Frequency was set at 1 Hz and strain amplitude 15  $\mu\text{m}$ . Frequency sweeps were conducted over a frequency range of 1 Hz to 30 Hz at 40 °C. The amplitude was fixed at 15  $\mu\text{m}$ .

### **3.B.3 Results and discussion**

#### **3.B.3.1 Strain sweep studies in RPA**

##### **3.B.3.1.1 Composites with HRH**

For reinforced elastomers, there exists an important dependence of dynamic mechanical properties upon dynamic strain amplitude. This was investigated by Payne and is called “Payne Effect” [27]. This phenomenon relates to the non-linearity observed in the shear modulus ( $G^*$ ) of materials with the breakdown of the filler network under increasing strain amplitudes. The figures 3.55 and 3.56 show the effect of strain amplitude on the complex modulus for the dry rubber composites in uncured and cured states, while figures 3.57 and 3.58 show that of latex stage composites. In the linear viscoelastic region there will not be much change in modulus with increase in strain [28]. There is a strain amplitude called critical strain above which modulus starts to decrease. For dry rubber composites containing 10 and 20 phr fiber the critical strain starts at 0.1 degree. This may be due to the breakage of the fiber network at that strain. When the fiber content increased to 30 phr the linear viscoelastic region disappears indicating an early breakage of network. The initial modulus increases with fiber content indicating possibility of fiber agglomeration at higher fiber loadings.

The latex stage composites follow similar behavior as that of dry rubber composites. But here the modulus is much higher than dry rubber composites indicating lower shear history of the matrix.

For the composites in cured state the critical strain starts much later, showing Payne effect at a strain of 2 degree. Here also initial modulus increase with fiber content is showing an increasingly restrained matrix. Compared to dry rubber composites latex stage composites show increased initial modulus at all fiber loadings.

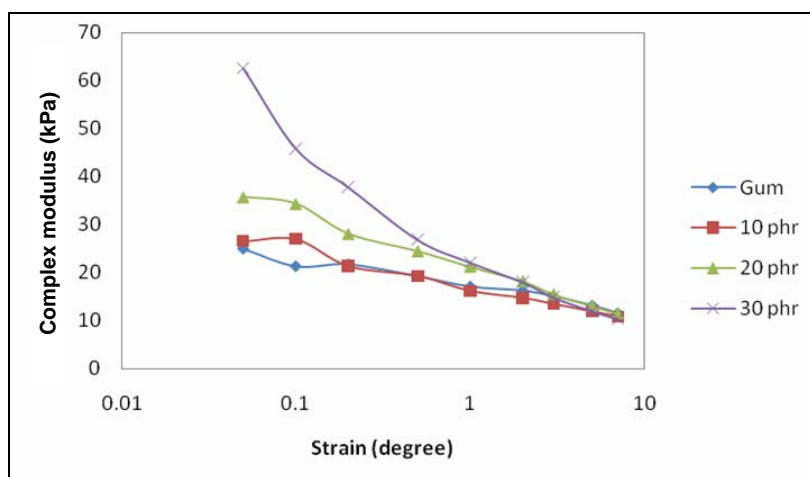


Figure 3.55 Complex modulus Vs strain for dry rubber composites in Uncured state

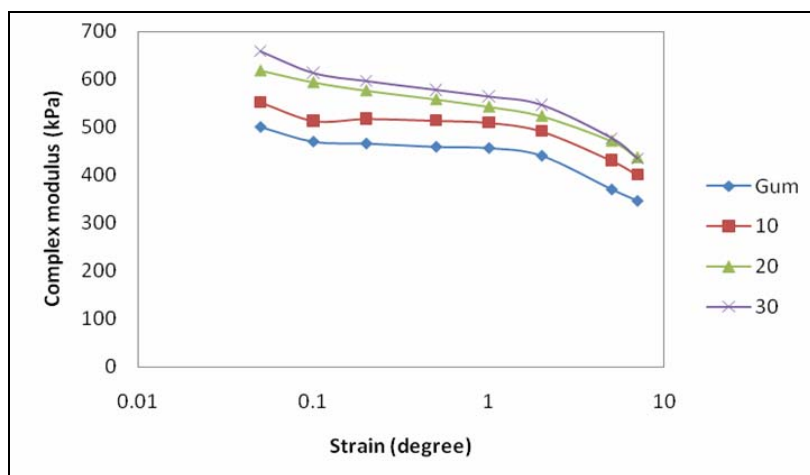


Figure 3.56 Complex modulus Vs strain for dry rubber composites in Cured state

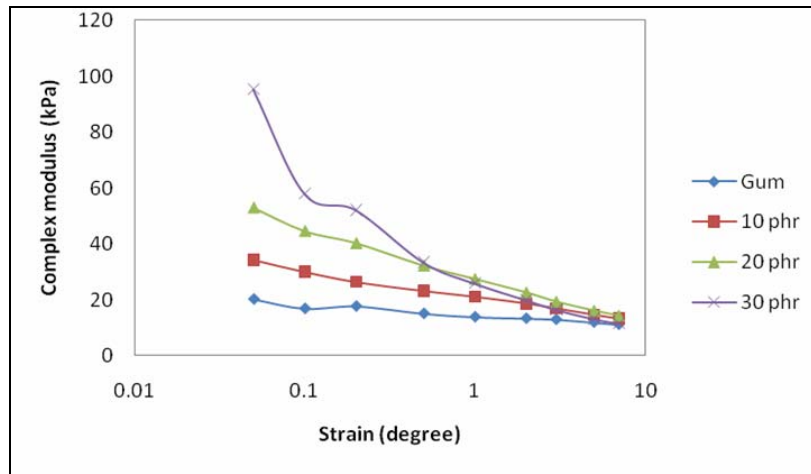


Figure 3.57 Complex modulus Vs strain for latex stage composites in Uncured state

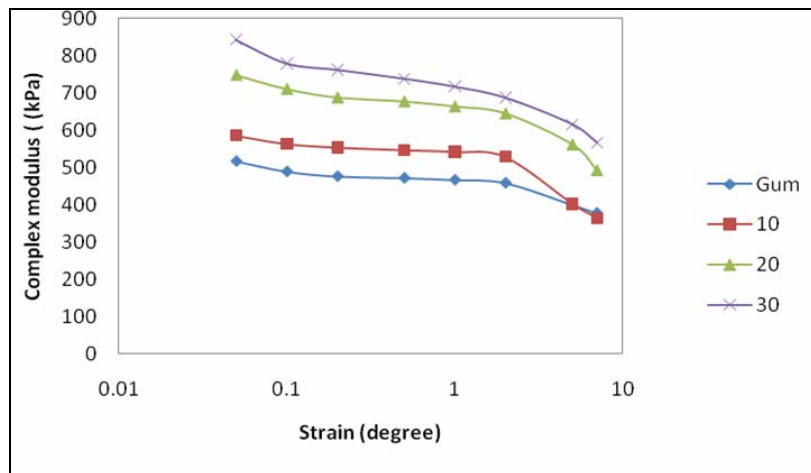


Figure 3.58 Complex modulus Vs strain for latex stage composites in Cured state

### 3.B.3.1.2 MANR – Treated Nylon composites

Figure 3.59 show the strain sweep in uncured state of MANR-treated fiber composites prepared in latex stage. Here also similar behavior as in the case of uncured latex stage composites with HRH bonding system is observed except in the case of gum composites. The gum composites show an initial modulus similar to that of 10 phr composites. But at very low strain the modulus starts decreasing and then stabilizes to a constant value. This higher initial value may be due to

formation of some amount of crosslinked gels within the matrix formed by maleic anhydride. This weak gel network soon breaks decreasing the modulus.

The cured state of MANR-treated nylon composites (figure 3.60) lacks a well defined critical strain especially at 30 phr fiber content. This may be due to the formation of crosslinks formed by the grafted maleic acid in the rubber matrix which breaks down at lower strains.

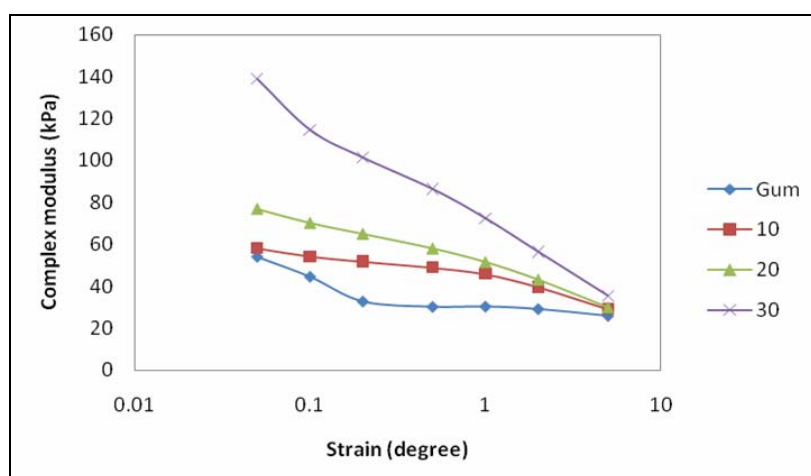


Figure 3.59 Complex modulus Vs strain of treated Nylon composites in Uncured state

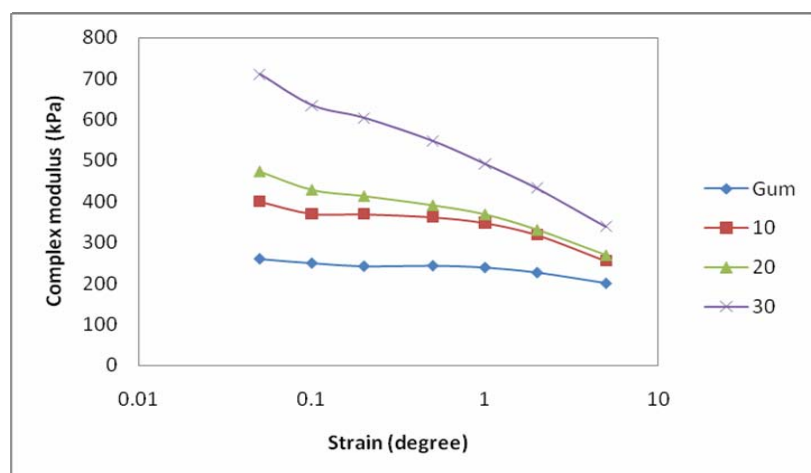


Figure 20.60 Complex modulus Vs strain of treated Nylon composites in Cured state

### 3.B.3.2 Studies in DMA

#### 3.B.3.2.1 Temperature sweep

##### NR-Nylon composites with HRH bonding

Variation of storage modulus with temperature of NR-Nylon composites with HRH bonding are shown in figure 3.61. Storage moduli of composites containing 30 phr of fiber, prepared through dry rubber and latex stage processing, are compared with gum composites. Storage modulus values are high below glass transition temperature which reduces during the glass transition. 30 phr Fiber composites show higher storage modulus than gum composite. Between the fiber composites latex stage composites show higher storage modulus than dry rubber composites. This is in tune with the better reinforcement of the latex stage composites. The lower fiber breakdown and thermal history of the latex stage composites give rise to better modulus. The variation in loss modulus of the composites is shown in figure 3.62.

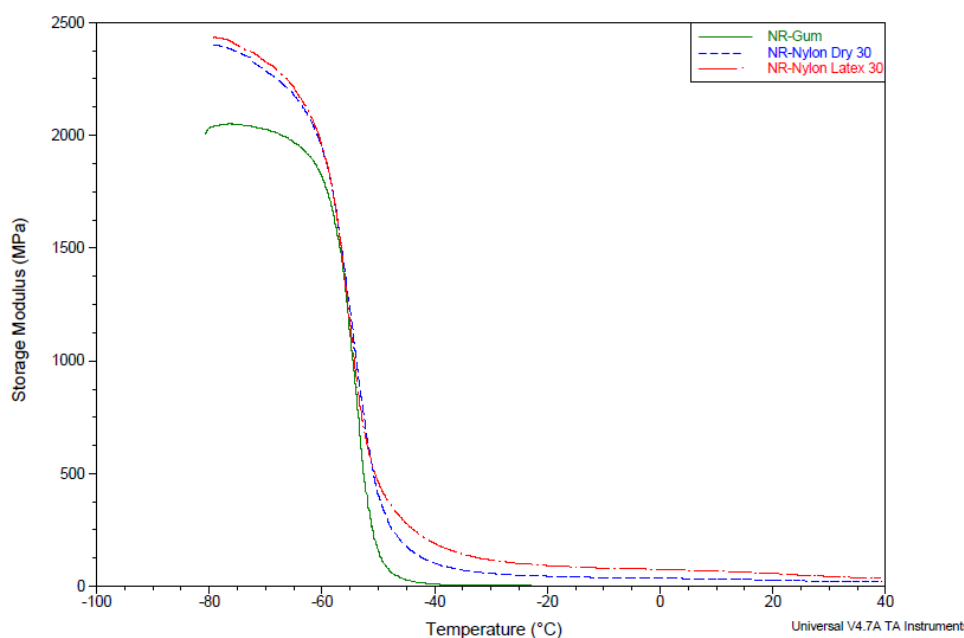
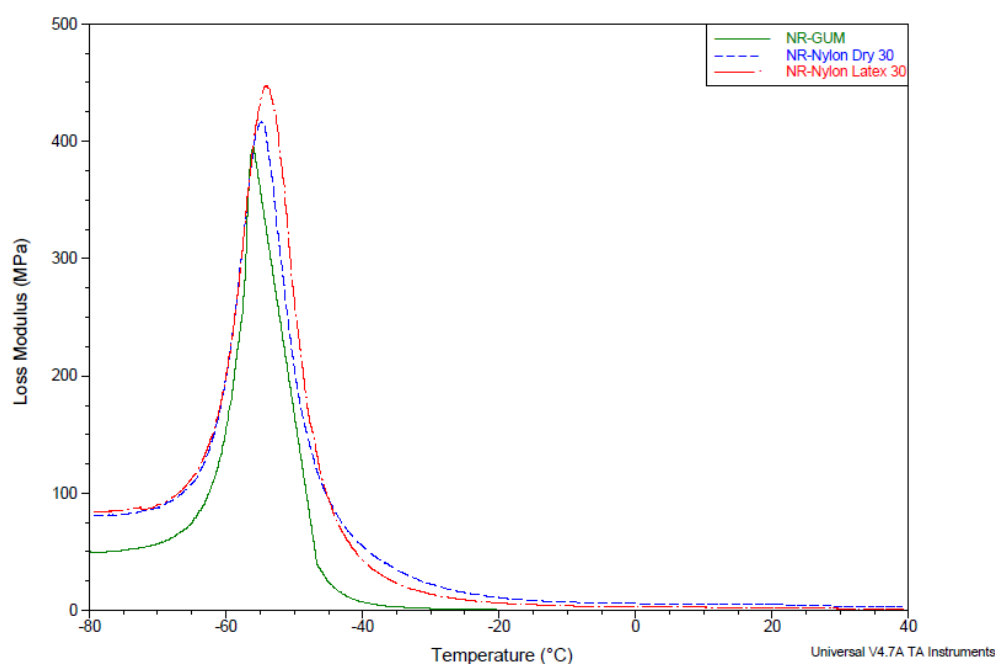


Figure 21.61 Variation of storage modulus with temperature of NR/nylon composites with HRH bonding

The loss modulus shows a peak at the glass transition temperature. There is a slight shift in the peak temperature between the gum and the composites. This shows that the segmental motion of the rubber molecules are more restricted in the stiffer fiber composites. The interaction between the Nylon fibers and the rubber molecules may be the cause for this restriction.

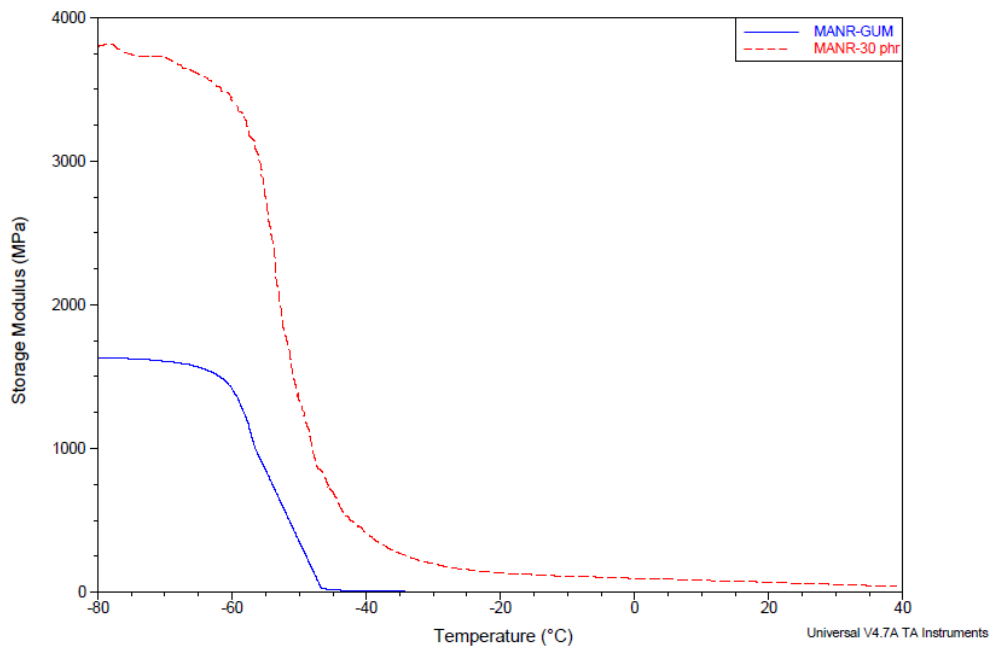


**Figure 3.62** Variation of loss modulus with temperature of NR/nylon composites with HRH bonding

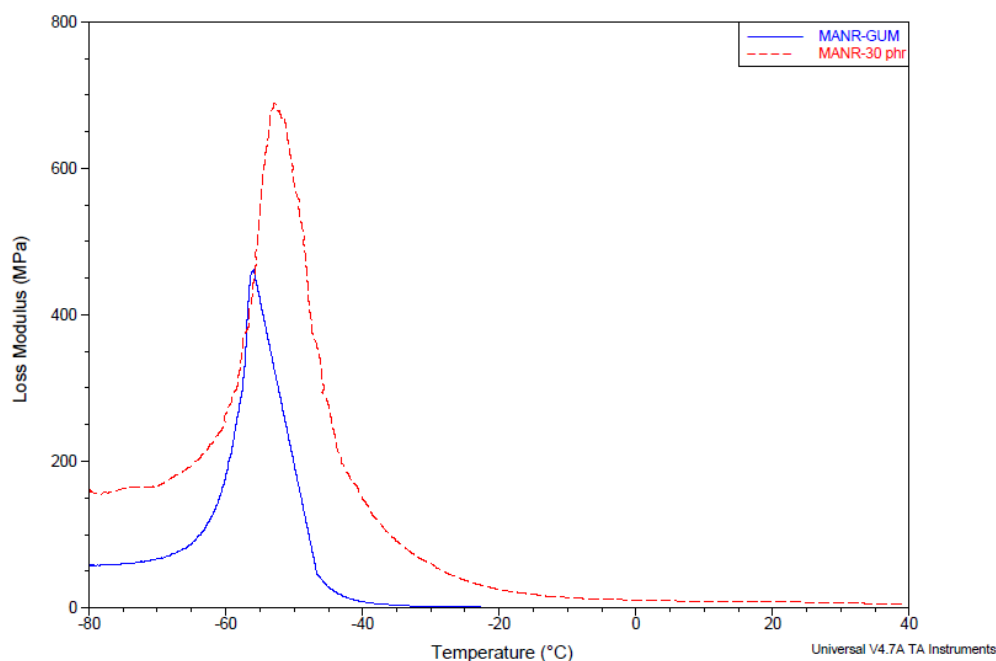
### *MANR-Treated Nylon composites*

Figure 3.63 shows the variation of storage modulus with temperature of MANR-treated nylon composites. There is large difference between gum and fiber composite in the storage modulus below glass transition temperature. This shows a highly restrained matrix in the case of 30 phr fiber composites. Storage modulus above glass transition also is higher for fiber composites. This is due to the high reinforcement imparted by the fiber to the matrix as

evident from mechanical property measurements in the previous section. Figure 3.64 gives the variation of loss modulus with temperature. The loss modulus increased considerably in the case of fiber composites. This may be due to the dissipation of energy at the fiber-matrix interfaces. The peak in loss modulus of the fiber composite at the glass transition temperature is shifted towards higher temperature compared to gum composite. This is due to the reduced segmental mobility of the rubber molecules as a result of improved interaction between fiber and matrix. This confirms the high reinforcing potential of MANR-treated nylon composites.



**Figure 3.63** Variation of storage modulus with temperature (MANR-treated nylon composites)



**Figure 3.64** Variation of loss modulus with temperature (MANR-treated nylon composites)

### 3.B.3.2.2 Frequency sweep studies

#### NR-Nylon composites with HRH bonding

Figures 3.65, 3.66 and 3.67 give the frequency sweep studies of the dry rubber and latex stage composites. ‘D’ and ‘L’ indicate dry rubber and latex stage, respectively. The succeeding digits indicates the fiber content in phr. Gum composites are denoted by ‘Gum’ succeeding ‘D’ or ‘L’.

Figure 3.65 gives the variation of storage modulus ( $E'$ ) with fiber content of the composites. Storage modulus increases with frequency for all composite. Among the composites it can be seen that  $E'$  increases with fiber content for both dry rubber and latex stage composites. With the increase in fiber content the rubber matrix gets more and more restricted and this reflects in the storage modulus values. For every loading of fiber latex stage

composites show higher storage modulus values compared to dry rubber composites. This can be attributed to the lower fiber breakage and matrix breakdown in the case of latex stage composites.

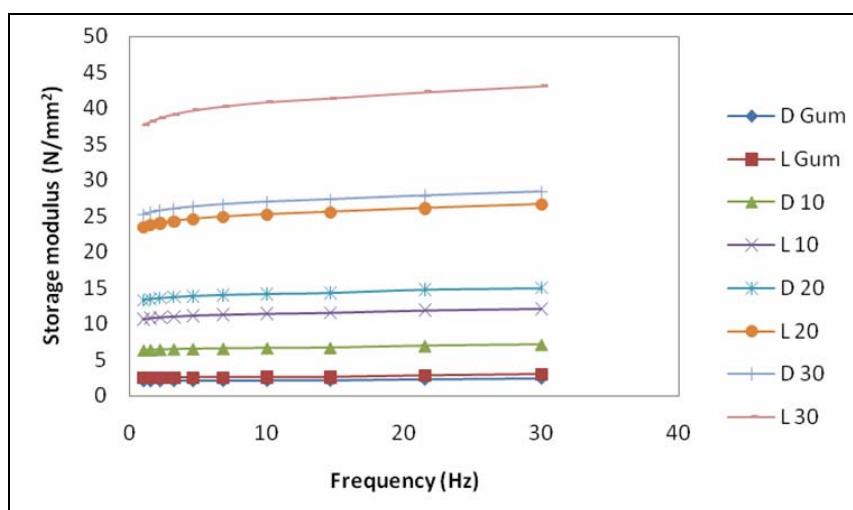


**Figure 3.65 Variation of storage modulus ( $E'$ ) with frequency of composites with HRH bonding**

Figure 3.66 shows the variation of loss modulus ( $E''$ ) with frequency of the composites. For every composite  $E''$  initially shows a gradual increase with frequency upto 14.6 Hz. Thereafter a sharp rise in  $E''$  is noted. Increase in frequency is equivalent to decrease in temp. The effect of increase in frequency reaches such a level similar to the transition temperature of the rubber. Similar to the peak of loss modulus at the glass transition temperature a peak appears at the corresponding frequency. Fiber composites show higher loss modulus than gum composites. The loss modulus increases with fiber content as in the case of storage modulus for both dry rubber and latex stage composites. This may be due to more energy being dissipated at the fiber matrix interface.

Figure 3.67 shows the variation of tan delta with frequency. The tan  $\delta$  varies in a similar pattern as the loss modulus. This is as expected since the increase in loss modulus is higher than the increase in storage modulus in most composites.

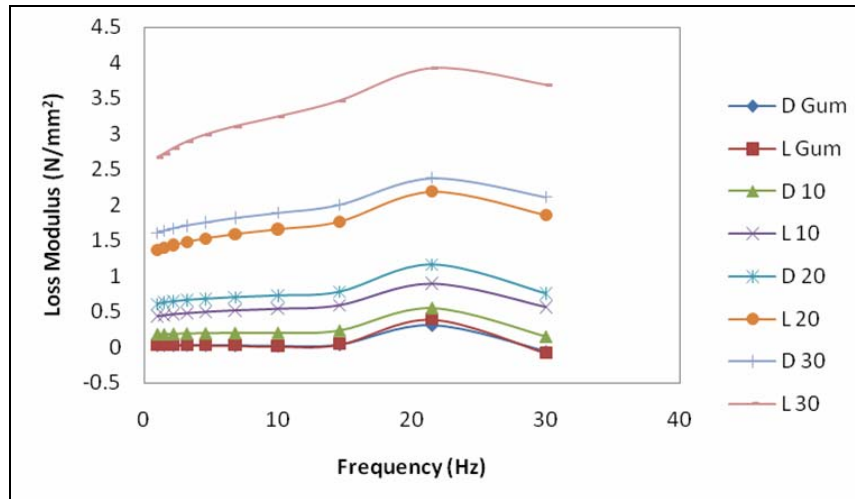


Figure 3.66 Variation of loss modulus ( $E''$ ) with frequency of composites with HRH bonding

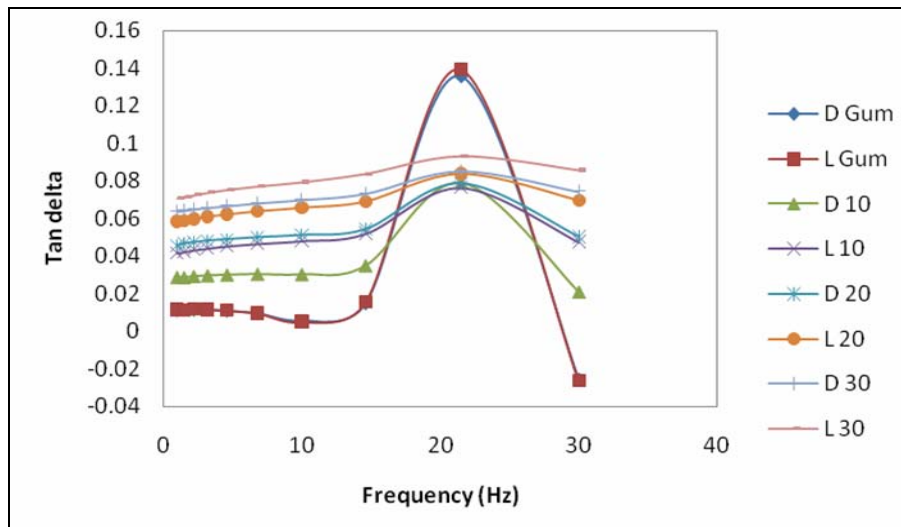
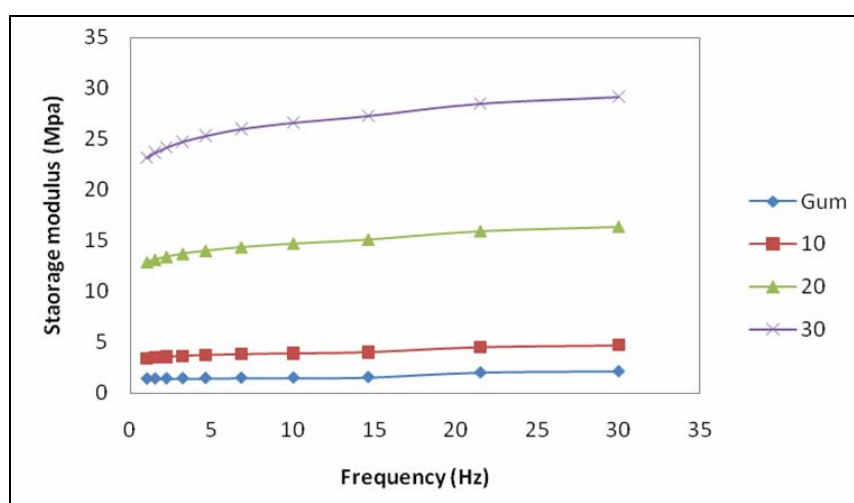


Figure 3.67. Variation of tan  $\delta$  with frequency of composites with HRH bonding

**MANR-Treated Nylon composites**

Figure 3.68, 3.69 and 3.70 show the behavior of storage modulus, loss modulus and tan delta respectively of MANR-treated nylon composites with variation of frequency. Storage modulus continuously increases with frequency as the material becomes more and more rigid. Beyond a frequency of 14.6 there is significant increase in storage modulus especially for composites with higher fiber content. This may be the equivalent of transition region in a temperature sweep experiment. A corresponding behavior is shown in loss modulus in the same frequency region. Loss modulus shows a peak at this frequency indicating a transition region. Similar trend is shown in tan delta plots also confirming the presence of a transition region. Among the composites storage modulus and loss modulus increase with fiber content indicating a progressively restrained matrix. The peak height in the transition region of tan delta plots is maximum for gum composites. Peak height decreases with increasing fiber content. As the matrix get reinforced the rubber molecules are increasingly being restricted in segmental mobility. This is reflected in the decreased tan delta peak height.



**Figure 3.68. Variation of storage modulus with frequency of MANR-treated nylon composites**

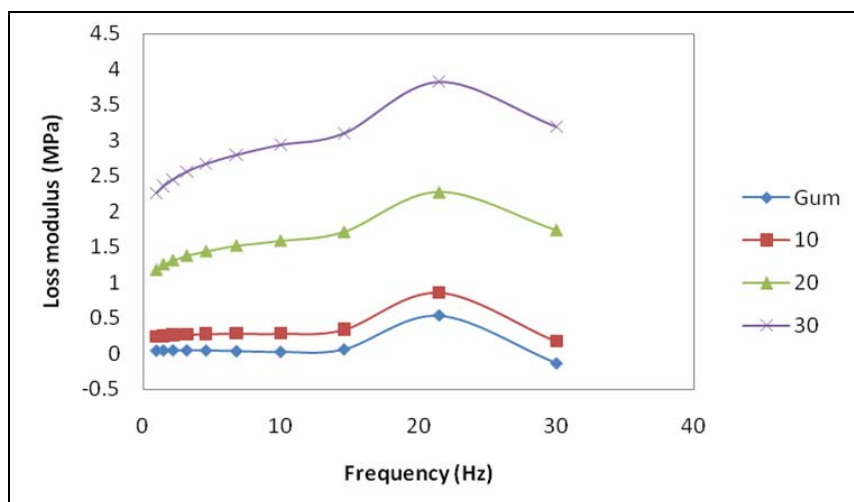


Figure 3.69 Variation of loss modulus with frequency of MANR-treated nylon composites

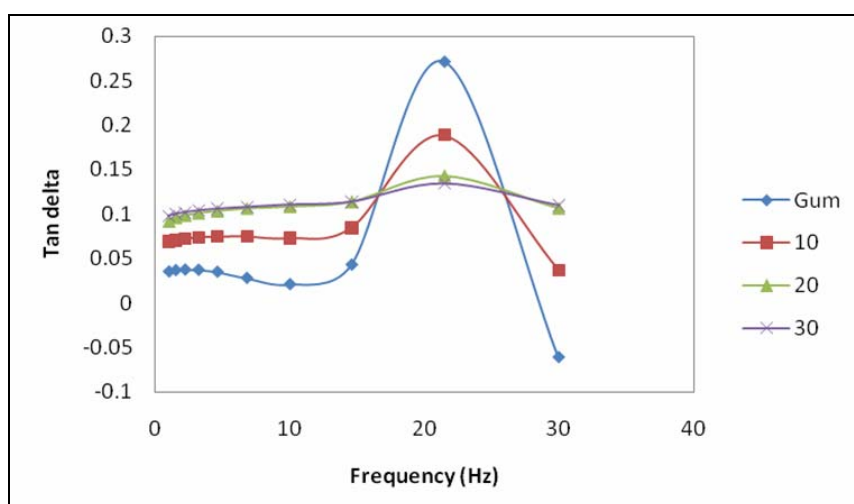


Figure 3.70 Variation of tan delta with frequency of MANR-treated nylon composites

### **3.B.4 Conclusions**

The strain sweep studies were performed in RPA to study the fiber dispersion and interaction between fiber and matrix. The decrease in complex modulus at lower strains in uncured composites, especially at higher fiber loadings, indicates fiber agglomeration at these fiber loadings. The increased modulus values of the fiber composites in cured state indicate better reinforcement of the fiber composite with increase in fiber content. Latex stage composites showed better modulus values in cured state compared to dry rubber composites. Maleated NR-treated nylon composites also show similar behavior. But the linear viscoelastic region in the cured composite is lower compared to HRH composites showing better fiber-matrix interaction in the case of HRH composites.

Temperature sweep studies in DMA showed an increasingly restrained matrix with increasing fiber content, indicating increased reinforcement. In HRH composites latex stage processed composites showed better properties. MANR-treated nylon composites show considerable improvement in reinforcement over the gum composite. The glass transition of the composites increased at higher fiber contents especially in the case of MANR-treated nylon composites. Frequency sweep studies also, indicated the increase of reinforcement with fiber content and better reinforcement in the case of latex stage composites. Frequency sweep profiles show a transition region corresponding to the transition in temperature sweep.

**Part -C**

**Thermal studies of NR- Nylon Micro Fiber Composites**

**3.C.1 Introduction**

Thermal analysis is an important analytical method in polymer technology to investigate the thermal stability of polymers and composites and to understand the effect of structure on thermal properties. It is well established that the thermal stability of polymers can be improved by adding short fibers and strong interaction between fiber and matrix is essential for good thermal stability [29].

Corre<sup>^</sup>a et al. [30] studied the influence of short fibers on the thermal resistance of the matrix and Tg and kinetic parameters of the degradation reaction of thermoplastic polyurethane and found that thermal resistance of aramid fiber-reinforced composite was greater than that of carbon fiber-reinforced composites. The degradation characteristics of Kevlar fiber-reinforced thermoplastics were reported by Kutty et al. [31] Younan et al. [32] studied the thermal stability of natural rubber polyester short fiber composites. Suhara et al. [33] studied thermal degradation of short polyester fiber-polyurethane elastomer composite and found that incorporation of the short fiber enhanced the thermal stability of the elastomer. Rajeev et al. studied thermal degradation of short melamine fiber-reinforced EPDM, maleated EPDM, and nitrile rubber composite with and without bonding agent and found that the presence of melamine fiber in the vulcanizates reduced the rate of decomposition, and the effect was pronounced in the presence of the dry bonding system. [34].

Thermogravimetric studies of short nylon-6 fiber-reinforced NR will provide an insight into the thermal stability and degradation pattern of these

composites. The nylon fiber and other additives will influence the thermal stability of the NR. In this chapter the thermal degradation studies of short nylon-6 reinforced Natural Rubber composites prepared both by the conventional method from dry rubber and by the new method which is incorporation of fibers in the latex stage are presented

### 3.C.2 Experimental

Differential scanning calorimetry of the composites was performed on DSC Q100 of TA Instruments. The experiments were carried out from -80°C to 100°C. The heating rate was 10°C/minute. A nitrogen atmosphere was maintained throughout the experiment.

Thermogravimetric analyses were carried out on TGA Q50 of TA Instruments. The samples were heated from ambient to 800°C with a heating rate of 20°C/minute under nitrogen atmosphere.

In the study of thermal stability and degradation kinetics numerous kinetic schemes and models regarding to the fiber degradation process have been established. In order to characterize thermal degradation kinetics for short fiber composites, the recorded original degradation traces were further allowed to be processed according to the mathematical expression,

$$\frac{d\alpha}{dt} = Z(1 - \alpha)^n \exp\left(-\frac{E}{RT}\right) \text{----- (1)}$$

in which  $\alpha$  is the weight loss of the composites undergoing thermal degradation at an experimental time  $t$ ,  $d\alpha/dt$  is the thermal degradation rate or weight-loss rate,  $Z$  is a frequency factor,  $n$  is the order of thermal degradation reaction,  $E$  represents the thermal degradation reaction activation energy,  $R$  is the gas constant parameter ( $8.3136 \text{ J mol}^{-1} \text{ K}^{-1}$ ) and  $T$  is the absolute temperature (K). A

characterization method proposed by Friedman was used to establish the kinetic parameters. Since there was no assumption in the Friedman model, more reliable analysis might be realized on the basis of TGA measurement [35]. Friedman method utilizes the deduced mathematical Eq. (1) as follows

$$\ln\left(\frac{d\alpha}{dt}\right) = \ln Z + n \ln(1 - \alpha) - \frac{E}{RT}$$

From a mathematical plot of  $\ln(d\alpha/dt)$  or  $\ln(1-\alpha)$  against  $1/T$ , a linear relationship could be obtained with a slope equal to  $-E/R$  or  $-E/(nR)$  [36].

### 3.C.3 Results and discussion

#### 3.C.3.1 Thermogravimetry

##### 3.C.3.1.1 NR-Nylon composites with HRH bonding

Figure 3.71 Shows a typical TGA and DTG profile of the Gum rubber and nylon composites.

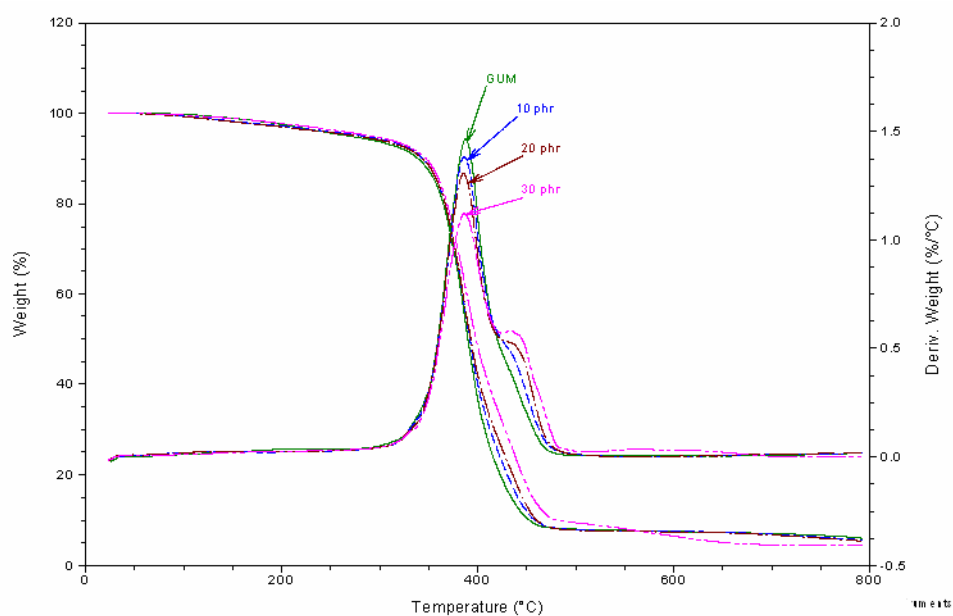


Figure 3.71 TGA and DTG profile of the Gum rubber and nylon composites

Table 3.4, 3.5, 3.6 & 3.7 give the temperature of onset of degradation (Ti), the temperature at which the rate of decomposition is maximum (Tmax) and the peak degradation rate, for both dry rubber and latex stage composites with and without bonding system. It can be seen from the tables that the initiation temperature for the composites with bonding agent is lower than that of composites without bonding agent. This may be due to the degradation of bonding agent preceding the main degradation, which is of rubber. In the case of maximum rate of degradation the composites with bonding agent shows lower values than corresponding composites without bonding agent. This shows that better bonding between the matrix and the fiber results in lower rate of degradation. NR gum vulcanizates degrades in a single step. When nylon fibers are incorporated in NR the rate of degradation is progressively decreasing in both the type of composites, that is composites with and without bonding system. When the fibers are incorporated in the latex stage the rate of degradation is lower compared to the composites prepared from the dry rubber stage. There is a reduction of about 5 % in the rate of degradation for the latex stage composites compared to the dry rubber stage composites. For the composites with bonding agent this reduction is about 8.6%. This can be attributed to the lower shear history of the latex stage composites than dry rubber stage composites. The maximum rate of degradation does not follow a definite trend within the same set of composites.

**Table 3.4 Degradation parameters of Dry rubber composites without bonding agent**

DRY	Ti (°C)	Tmax (°C)	Rate (%/°C)
Fiber content (phr)			
0	313.4	387.0	1.54
10	312.6	386.3	1.46
20	317.4	385.9	1.36
30	309.5	386.4	1.35

**Table 3.5 Degradation parameters of Latex stage composites without bonding agent**

<b>LATEX</b>	<b>Ti (°C)</b>	<b>Tmax (°C)</b>	<b>Rate (%/°C)</b>
<b>Fiber content (phr)</b>			
0	317.1	384.9	1.59
10	317.7	382.2	1.43
20	315.7	385.5	1.39
30	320.3	387.2	1.28

**Table 3.6 Degradation parameters of Dry rubber composites with HRH bonding agent**

<b>HRH-DRY</b>	<b>Ti (°C)</b>	<b>Tmax (°C)</b>	<b>Rate (%/°C)</b>
<b>Fiber content (phr)</b>			
0	299.6	382.8	1.52
10	299.6	386.4	1.37
20	294.5	387.9	1.27
30	295.5	388	1.23

**Table 3.7 Degradation parameters of Latex stage composites with HRH bonding agent**

<b>HRH-LATEX</b>	<b>Ti (°C)</b>	<b>Tmax (°C)</b>	<b>Rate (%/°C)</b>
<b>Fiber content (phr)</b>			
0	294.2	387.5	1.46
10	295.4	386.2	1.38
20	296.6	385.4	1.30
30	282.8	386.7	1.12

Figures 3.72 and 3.73 show typical Friedman method plots. According to the Friedman characterization model, the original TGA data recorded were

allowed to be further processed, and the obtained mathematical plots are shown in Figure. It could be clearly seen that both the  $\ln (d\alpha/dt)$  vs  $1/T$  and the  $\ln (1-\alpha)$  vs  $1/T$  data plots exhibited good linear relationship, and this shows that the thermal degradation of the composites proceeded in good agreement with the Friedman model.

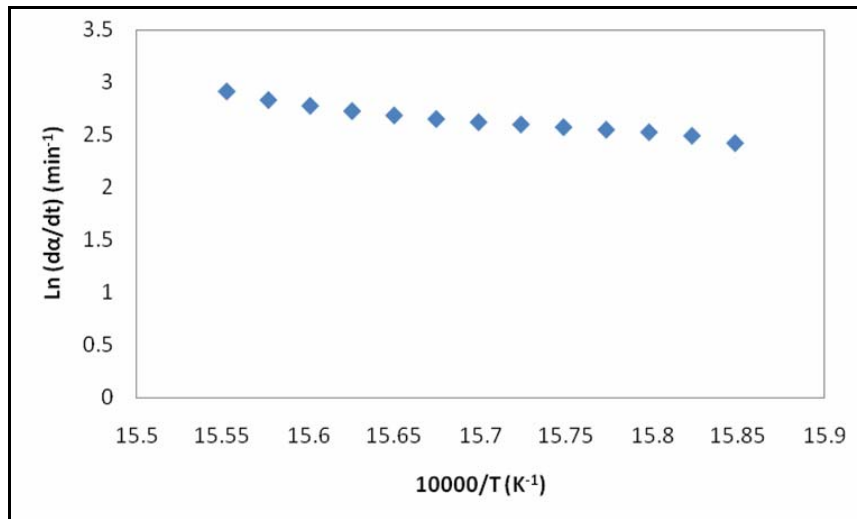


Figure 3.72 Variation of  $\ln (d\alpha/dt)$  with  $1/T$

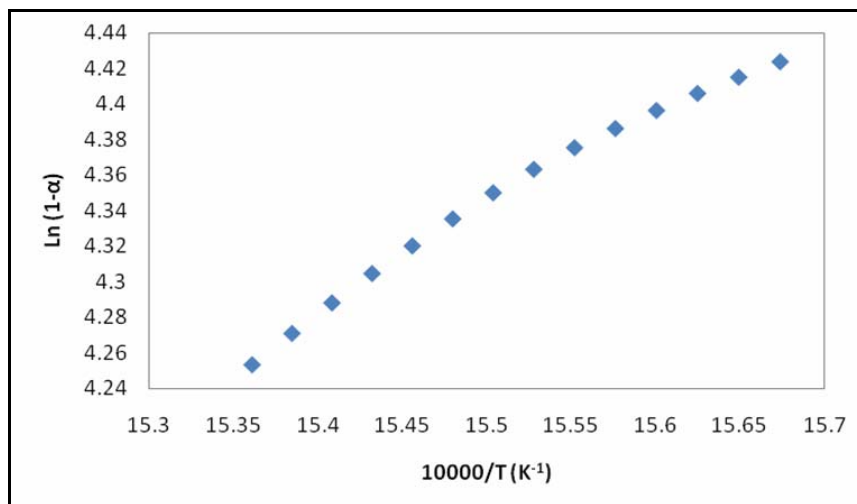


Figure 3.73 Variation of  $\ln (1-\alpha)$  with  $1/T$

Activation energy and order of the degradation reaction of the composites were found from the Friedman plots and are given in Tables 3.8, 3.9, 3.10 and 3.11. It can be seen that the gum composites possess the lowest activation energy. The activation energy steadily increases with the fiber content. The more thermally stable nylon fibers will increase the thermal stability and thus the activation energy of the composites. Between dry rubber and latex stage composites, the latex stage composites exhibit comparatively higher activation energies than dry rubber composites. This may be due to the lower thermal history of these composites during processing in two-roll mill. The presence of bonding agent will affect the thermal stability positively which is evident from the increased activation energy of the composites. Both the dry rubber and latex stage composites with bonding agent exhibit higher activation energy compared to those without bonding agent. The better fiber-matrix interaction in the composites with bonding agent may be the reason for the higher activation energies.

**Table 3.8 Thermal kinetics parameters of Dry rubber composites without bonding agent**

Dry rubber composites/ Without Bonding agent	Activation energy (kJ/mol)	n
Gum	118.5	2.6
10 phr Nylon	129.0	2.4
20 phr Nylon	132.7	2.7
30 phr Nylon	147.4	2.7

**Table 3.9 Thermal kinetics parameters of Latex stage composites without bonding agent**

Latex composites/ Without Bonding agent	Activation energy (kJ/mol)	n
Gum	137.23	2.6
10 phr Nylon	141.33	2.7
20 phr Nylon	142.96	2.6
30 phr Nylon	153.93	2.7

**Table 3.10 Thermal kinetics parameters of Dry rubber composites with HRH bonding agent**

Dry rubber composites/ With Bonding agent	Activation energy (kJ/mol)	n
Gum	149.0	2.6
10 phr Nylon	150.9	2.5
20 phr Nylon	157.8	2.8
30 phr Nylon	161.4	2.7

**Table 3.11 Thermal kinetics parameters of Latex stage composites with HRH bonding agent**

Latex composites/ With Bonding agent	Activation energy (kJ/mol)	n
Gum	150.8	2.7
10 phr Nylon	153.1	2.5
20 phr Nylon	161.7	2.7
30 phr Nylon	163.6	3.0

### 3.C.3.1.2 MANR-Treated Nylon Composites

The thermal degradation parameters of the MANR-treated nylon composites are given in table 3.12. The initiation temperature of degradation and the temperature of maximum degradation did not show any appreciable change on the addition of treated fibers. But the rate of degradation is continually decreasing with fiber content. The improved bonding between the fiber and matrix may be imparting higher thermal stability to the composites. The increase in thermal stability is also confirmed activation energy calculations from Friedman plots.

**Table 3.12 Degradation parameters of MANR-Treated Nylon composites**

Fiber content (phr)	Ti (°C)	Tmax (°C)	Rate(%/°C)
0	308.4	384.6	1.61
10	308.5	386.6	1.48
20	309.5	385.8	1.38
30	306.0	386.2	1.34

**Table 3.13 Thermal degradation kinetics parameters of MANR-treated Nylon composites.**

Fiber content (phr)	Activation energy (kJ/mol)	n
0	157.7	2.1
10	161.5	2.6
20	163.2	2.6
30	164.5	2.6

Activation energy and order of the degradation reaction of the composites from the Friedman plots and are given in Table 3.14. As the fiber content increases activation energy increases. The increased adhesion between the fiber and the matrix through chemical bond formation may be responsible for the increased thermal stability of the composites as observed from the activation energy.

### 3.C.3.2 Differential Scanning Calorimetry

The DSC thermograms of dry rubber and latex stage composites both without filler (gum) and with 30 phr fiber loading are shown in figure 3.74. DSC thermograms of MANR-treated nylon composites without fiber and with 30 phr fiber is shown in figure 3.75. The glass transition temperatures of the composites as obtained from the thermograms are more or less similar for all composites.

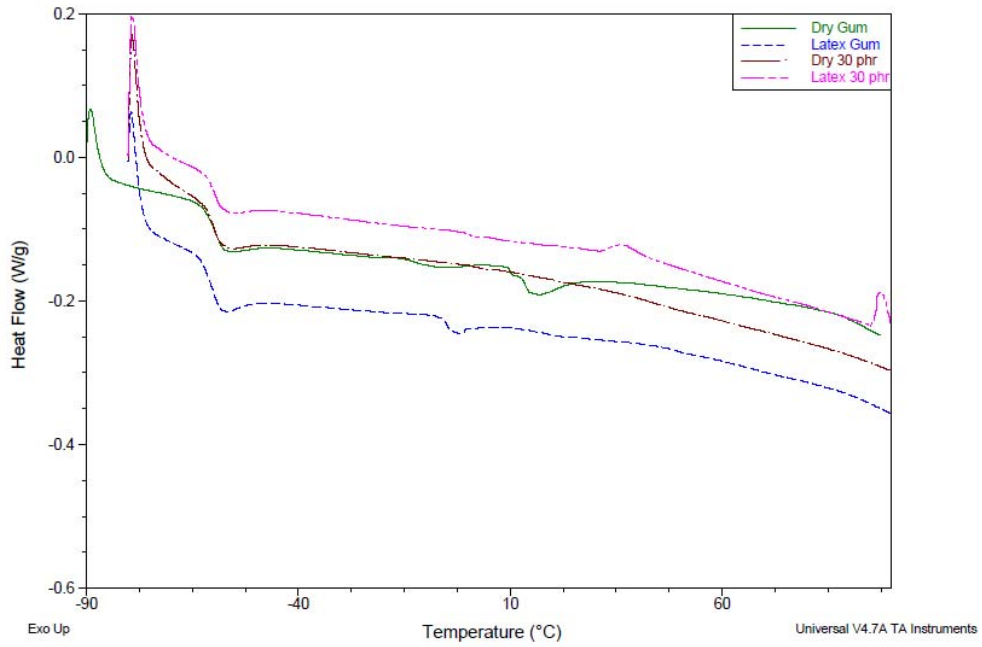


Figure 3.74 DSC thermograms of composites with HRH bonding

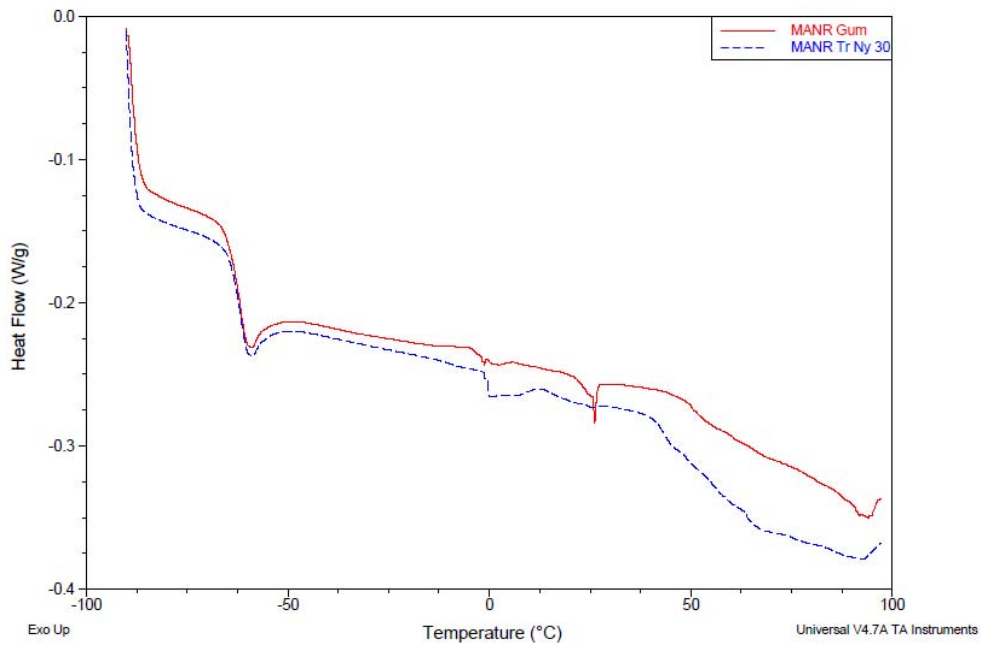


Figure 3.75 DSC thermograms of MANR treated nylon composites

### 3.C.4 Conclusions

Thermal stability and degradation kinetics of the composites were studied. The initiation temperature for the composites with HRH bonding system is lower than that of composites without bonding system. Maximum rate of degradation is lower for the composites with bonding agent than corresponding composites without bonding agent. Better bonding between the matrix and the fiber results in lower rate of degradation. The initiation of degradation and maximum rate of degradation decreases with increase in fiber content. The activation energies for degradation were determined by Friedman kinetics model. The activation energy increases with fiber content. The latex stage composites shows improved activation energy. In MANR-treated nylon composites also rate of degradation continuously decreases with fiber content showing increased thermal stability. Glass transition temperatures obtained through DSC showed no appreciable change.

### References

- [1] Coran A.Y., Boustany K. and Hamed P., *J. Appl. Polym. Sci.*, **15** (1975) 2471.
- [2] Foldi A.P., *Rubber Chem. Technol.*, **49** (1976) 379.
- [3] Chakraborty S.K., Setua D.K. and De S.K., *Rubber Chem. Technol.*, **55**(1982) 1286.
- [4] O' Connor J.E., *Rubber. Chem. Technol.*, **50** (1977) 945.
- [5] Rajesh C., Unnikrishnan G., Purushothaman E. and Thomas S., *J. Appl. Polym. Sci.*, **92** (2004) 1023.
- [6] Rajeev R. S., Bhoumick A. K., De S. K. and Bandyopadhyay S., *J. Appl. Polym. Sci.*, **90**(2) (2003) 544.

- [7] Coran A.Y., Hamed P. and Goettler L.A., *Rubber Chem. Technol.*, **49** (1976) 1167.
- [8] Derringer G.C., *J. Elastoplast.*, **3** (1971) 230.
- [9] Boustany K. and Arnold R.L., *J. Elastoplast.*, **8** (1976) 160.
- [10] Coran A.Y., Boustany K. and Hamed P., *Rubber Chem. Technol.*, **47** (1974) 396.
- [11] Martins M. A. and Mattoso L. H. C., *J. Appl. Polym. Sci.*, **91** (2004) 670.
- [12] Goettler L.A. and Shen K.S., *Rubber Chem. Technol.*, **56** (1983) 619.
- [13] Moghe S.R., *Rubber Chem. Technol.*, **49** (1976) 1160.
- [14] Murthy V.M. and De S.K., *J. Appl. Polym. Sci.*, **29** (1984) 1355.
- [15] Murthy V.M. and De S.K., *Rubber Chem. Technol.*, **55** (1982) 287.
- [16] Seema A. and Kutty S. K. N., *J. Appl. Polym. Sci.*, **99** (2006) 532.
- [17] Amornsakchai T., Sinpatanapan B. and Bualek-limcharoen S., *J. Sci. Soc. Thailand* **40** (1999) 2993.
- [18] Sreeja T.D. and Kutty, S.K.N., *Polym.-Plast. Technol. Eng.*, **42**(2) (2003) 239.
- [19] L. Mathew, *Development of Elastomeric Hybrid Composite Based on Synthesized Nanosilica and Short Nylon Fiber*, PhD thesis (2009)
- [20] Turi, Edith A., *Thermal Characterization of Polymeric Materials*, Second Edition, Volume I., Academic Press, Brooklyn, New York, 1997, P. 980.
- [21] Kashani M. R., *J. Appl. Polym. Sci.*, **113** (2009) 1355.
- [22] Praveen S., Chakraborty B. C., Jayendran S., Raut R. D. and Chattopadhyay S., *J. Appl. Polym. Sci.*, **111** (2009) 264.
- [23] Geethamma V.G., Kalaprasad G., Groeninckx G. and Thomas S., *Composites, Part A*, **36**(11) (2005) 1499.

- [24] Pothan L. A., Oommen Z. and Thomas S., *Compos. Sci. Technol.*, 63(2) (2003) 283.
- [25] Ibarra L. and Chamorro., *J. Appl. Polym. Sci.*, 2 (1991) 1805.
- [26] Varghese S., Kuriakose B., Thomas S. and Koshy A.T., *J. Adhes. Sci. Technol.*, 8 (1994) 235.
- [27] Payne R., *J. Appl. Polym. Sci.*, 6 (1962) 57.
- [28] Dick J. S. and Pawlowski H., *Rubber World*, January, 1995
- [29] Setua D.K. and Mathur G.N., *Polymer*, 79 (2001) 646.
- [30] Corre<sup>^</sup>a R. A., Regina C. R. N. and Vera L. L., *Polym. Degradation Stab.* 52 (1996) 245.
- [31] Kutty, S. K. N., T. K. Chaki, and G. B. Nando. *Polym. Degradation Stab.*, 38 (1992) 187.
- [32] Younan, A. F., M. N. Ismail, and Khalaf A. I., *Polym. Degradation Stab.*, 48 (1995) 103.
- [33] Suhara F., Kutty S. K. N. and Nando G. B., *Polym. Degradation Stab.* 61 (1998) 9.
- [34] Rajeev R. S., De S. K., Bhowmick A. K. and John B., *Polym. Degradation Stab.* 79 (2003) 449.
- [35] Wen W.Y. and Lin J.W., *J. Appl. Polym. Sci.*, 22 (1978) 2285.
- [36] Friedman H.L., *J. Polym. Sci. C*, 6 (1964) 183.

.....❧.....

**COIR MICROFIBER REINFORCED NATURAL RUBBER COMPOSITES**

<b>C</b> <b>o</b> <b>n</b> <b>t</b> <b>e</b> <b>n</b> <b>t</b> <b>s</b>	<b>Part -A</b>
	<i>Mechanical Properties of Coir Microfiber Reinforced Natural Rubber Composites</i>
	<b>Part B</b>
	<i>Dynamic mechanical Studies of Coir Microfiber Reinforced Natural Rubber Composites</i>
	<b>Part C</b>
	<i>Thermal Studies of Coir Microfiber Reinforced Natural Rubber Composites</i>

**Part -A****Mechanical Properties of Coir Microfiber Reinforced Natural Rubber Composites****4.A.1 Introduction**

Short fibers are an important class of reinforcing materials for elastomers because of their ability to impart high strength, tenacity and anisotropic properties [1,2]. Various synthetic fibers have been used successfully as reinforcing filler in many synthetic rubbers as well as in natural rubber [3-10]. However, the use of synthetic polymers, in general, is being discouraged because of its dependency on petroleum resources and other environmental concerns. Already, there is a conscious effort to move to more environment-friendly natural materials. Using cellulosic natural fibers as

reinforcement material in polymer composite is one such step that is attaining wider recognition [11-13].

Cellulose is the most common plant biopolymer, annual production being around  $10^{11}$  tons. The low density of cellulosic fibers together with their superior mechanical properties, environmental benefits and low cost have been the drivers for the use of these fibers as reinforcement in polymers. Using cellulosic fibers in natural rubber – again a natural renewable material- makes an environment friendly composite. Coir is an important lignocellulosic fiber obtained from the fibrous mesocarp of coconut, the fruit of coconut trees (*cocos nucifera*), which is cultivated extensively in Kerala, the southern state of India. The chemical composition of the coir fiber is given in Table 1.2 [14]. Use of coir as reinforcement in rubber has been tried with limited success [15-16]. Upon incorporation of coir fiber, it was seen that the tensile strength of the composite decreased sharply with increase in fiber loading [17]. Making good bonding possible, between the coir fiber and the rubber matrix, is the major problem encountered in this process. The polar fiber surface and the non-polar rubber have a natural tendency for poor interaction [18-19]. The resulting poor bonding between the fiber and the rubber matrix forms weak points in the composite which causes stress concentration during tension and premature failure of the composite. As a result the composites strength decreases with the increasing loading of the coir fiber. As a remedial measure, different bonding agents were tried but without much success. Another problem associated with lignocellulosic fiber/polymer composites is the agglomeration of fibers due to insufficient dispersion, caused by the tendency of fibers to form hydrogen bonds with each other during processing [20].

The problem is approached with a two-pronged strategy. One is by the modifications performed on the fiber in terms of size reduction and chemical

treatments. The other is by improving the fiber dispersion in rubber matrix by adopting latex stage processing. The coir has been found to be a poor reinforcement material because of its large and variable diameter, high microfibrillar angle, and high lignin/hemicellulose content. Reducing the diameter of the coir fibers is expected to improve the reinforcement. Similarly the incorporation of chemically modified fibers to the latex prior to coagulation is expected to improve dispersion [21]. The microfibers with polar hydroxyl groups on the surface will be well wetted by the polar aqueous phase of the natural rubber latex.

This chapter reports the results of a systematic study on the modification of coir fiber by mechanical and chemical means to refine size and the effect of incorporating these modified fibers by a latex stage processing route on the mechanical properties.

## **4.A.2 Experimental**

### **4.A.2.1 Materials Used**

Concentrated natural rubber latex (60 DRC) was procured from Njavally Latex Pvt Ltd. Coir fibers procured locally were chopped to approximately 6mm length. Zinc oxide, stearic acid, HS (1,2-dihydro-2,2,4-trimethylquinoline), CBS (cyclohexylbenzthiazylsulfenamide), sulfur and hydrated silica used were of commercial grade. Hexa (hexamethylenetetramine) and resorcinol were supplied by Merck Ltd, Mumbai. Hydrochloric acid – 3.5 and 5 M solution, Sodium hydroxide – 5% solution.

### **4.A.2.2 Processing**

#### **a. Preparation of macro fiber composites**

The chopped coir fibers were treated with 5% NaOH solution and kept at 50°C for 4 hours for removing a major part of lignin and hemicellulose. It was

then washed free of alkali and treated with 3.5 molar HCl to break the cellwalls thus facilitating easier separation of microfibrills [22]. The fibers were then washed free of acid and incorporated into latex by the method described in the previous chapter. The latex – coir mixture was coagulated, using dilute acetic acid in successive layers. The coagulum obtained was squeezed between rollers to remove water. The sheet obtained was dried in an air oven at 40 °C for three days. Coir loading was adjusted to get 10, 20 and 30 phr coir in the final composites. The composites were then processed like conventional sheet rubber.

**b. Preparation of micro fiber composites**

Another batch of chopped fibers was subjected to the same alkali and acid treatments as in the case of microfiber composites. The fibers were then washed and grinded to convert them into a pulp form. The alkali and acid treatments of water dispersed coir pulp were repeated, but this time using 5 M HCl for removing hemicellulose. The pulp was then washed and solid content was determined. SEM photographs of the coir pulp were taken in 6390LA JEOL instrument to study the surface characteristics and to determine the dimensions. The water dispersion of the coir pulp was then added to concentrated natural rubber latex. It was mixed well and coagulated using dilute acetic acid in successive layers. The coagulum obtained was squeezed between rollers to remove water. The sheet obtained was dried in an air oven at 40°C for three days. Coir loading was adjusted to get 2.5, 5, 10, 20 and 30 phr coir in the final composites. The composites were then processed like conventional sheet rubber.

Formulation of the mixes is given in table 4.1. The mixes were prepared according to ASTM D 3182 on a laboratory size two-roll mixing mill. Cure characteristics of the mixes were determined by using Rubber Process Analyser model RPA 2000 at 150°C. Fibers were oriented in the mill direction by passing through tight nip in the mill at the end of the mixing process. The thin sheets obtained were cut in the required dimensions and stacked one above the other to the desired volume. The sheets were vulcanized at 150°C under a pressure of 180 kg/cm<sup>2</sup> in an electrically heated hydraulic press to their respective cure times. The samples obtained were tested for mechanical properties according to relevant ASTM standards.

**Table 4.1 Formulation of mixes**

Ingredients	Mix No.					
	A	B	C	D	E	F
NR	100	100	100	100	100	100
ZnO	4	4	4	4	4	4
Stearic acid	2	2	2	2	2	2
HS	1	1	1	1	1	1
Fiber	-	2.5	5	10	20	30
Silica	-	0.083	0.166	0.33	0.66	1
Resorcinol	-	0.166	0.333	0.667	1.334	2
Hexa	-	0.166	0.333	0.667	1.334	2
CBS	0.6	0.6	0.6	0.6	0.6	0.6
Sulphur	2.5	2.5	2.5	2.5	2.5	2.5

Lignin content of the samples after alkali treatment of both un-grinded and grinded coir was determined by ASTM D 1105.

### 4.A.3 Results and Discussion

#### 4.A.3.1 Fiber characterization

##### 4.A.3.1.1 Lignin content

Table 4.2 Lignin content

Lignin content (%)		
Untreated coir	After First alkali treatment	After Second alkali treatment
42.9	34.8	22.4

Untreated coir has a lignin content of 42.9%. After the alkali treatment of the fibers in the ungrinded form the lignin content was reduced to 34.8%. After the second alkali treatment in of the fibers in the grinded pulp form, the lignin content was further reduced to 22.4%. In the ungrinded form the lignin removal was 8.1% while in the grinded form a further 10.4% of lignin was removed making a total of 18.5% removal. This substantial removal was possible by the mechanical size reduction of the coir fiber which breaks the cellwalls facilitating easier removal of lignin.

##### 4.A.3.1.2 SEM analysis

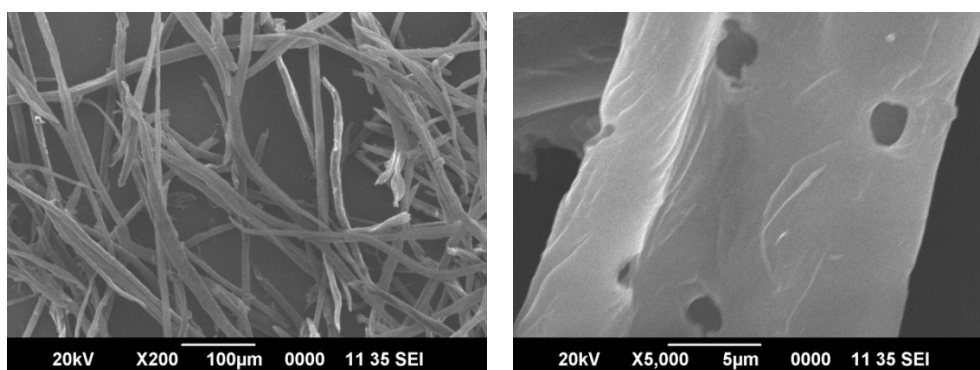


Figure 4.1 & 4.2. SEM photographs of coir microfibers

Figures 4.1 and 4.2 show the SEM photographs of the coir fibers, after chemical and mechanical treatments, in the dispersion. It can be seen from the photographs that the chopped fibers are reduced to microfibers with a diameter range of 8-11 $\mu$ m and length of 350 to 550  $\mu$ m. The aspect ratio of the fibers is in the range 35-65. This is the optimum range for good stress transfer between the fiber and the matrix and corresponding better reinforcement of the composites. Some pit formations and striations are observed on the surface of the fibers. These will promote better mechanical anchorage between the fiber and the rubber matrix thus improving the mechanical properties.

#### 4.A.3.2 Composite characterization

##### 4.A.3.2.1 Composites of macro fibers

###### a) Cure characteristics

###### *Differential torque*

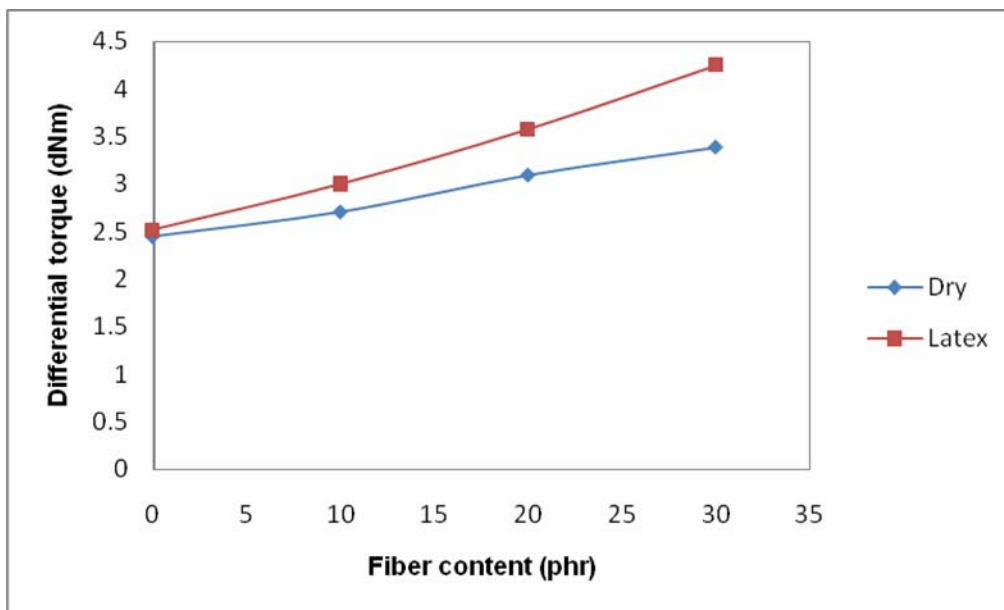
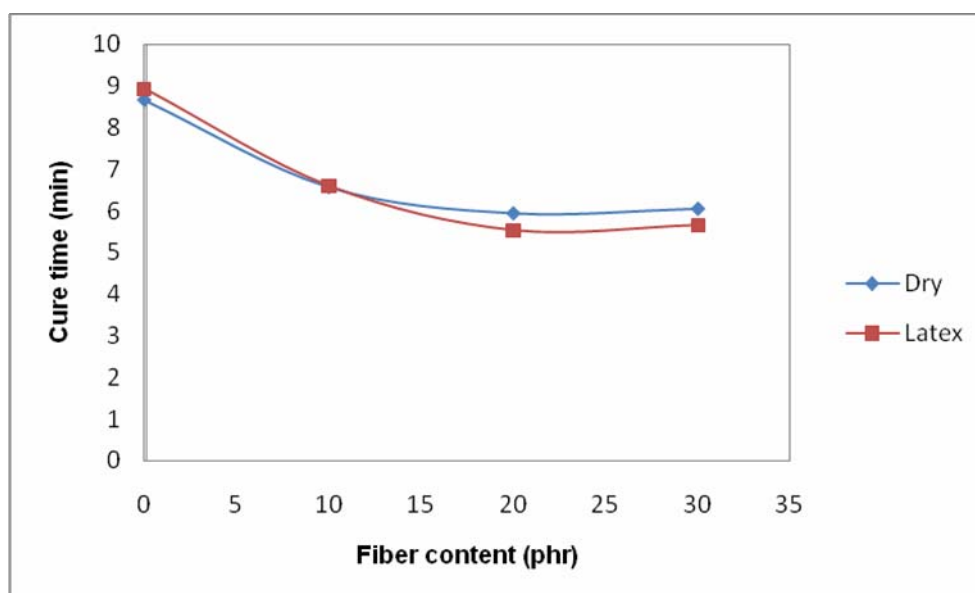


Figure 4.3. Variation of differential torque with ungrinded fiber content

Differential torque is the difference between maximum and minimum torque experienced in Rubber Process Analyzer during the curing process at 150°C. Figure 4.3 shows the variation of differential torque with fiber loading. Differential torque increases with fiber loading for both dry rubber and latex stage composites. This shows, with increase in the amount of fiber, matrix is being increasingly restrained. Differential torque is higher for latex stage composites. This may be due to lower thermal history of the latex stage composites during mixing.

#### *Cure time and scorch time*



**Figure 4.4 Variation of cure time with ungrinded fiber content**

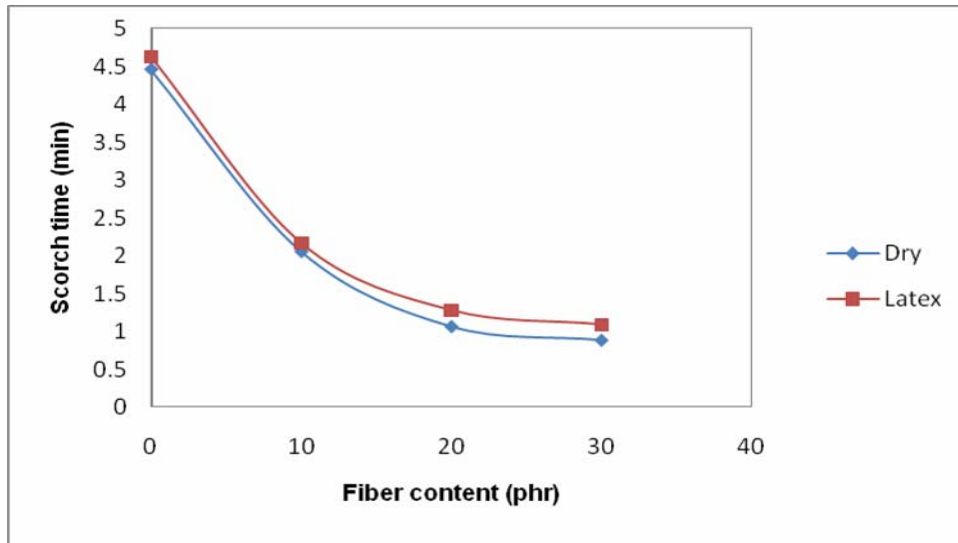


Figure 4.5 Variation of scorch time with ungrinded fiber content

Figures 4.4 and 4.5 show the variation of cure time and scorch time respectively, with fiber loading. Cure time and scorch time decrease with fiber loading.

**b) Mechanical properties**

*Tensile strength*

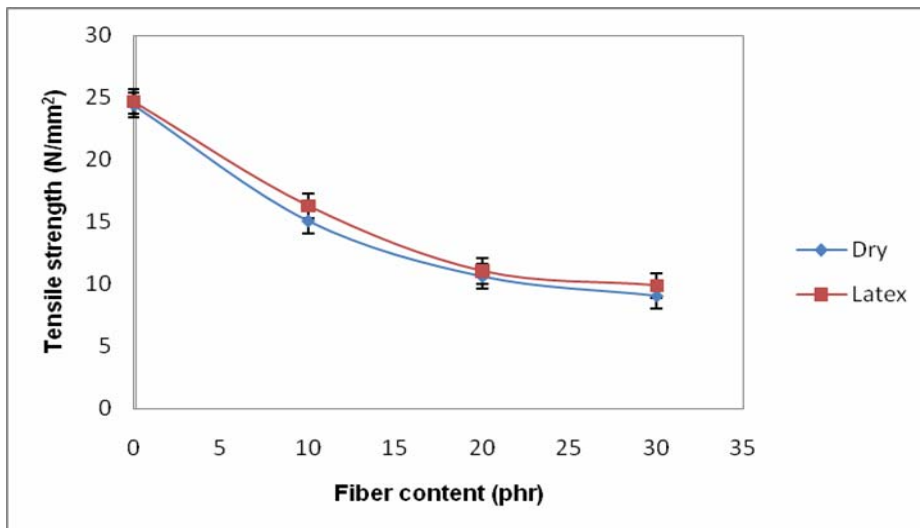


Figure 4.6 Variation of tensile strength with ungrinded fiber content

Figure 4.6 shows the variation of tensile strength of composites in which fibers without size reduction is incorporated after chemical treatment. The tensile strength continuously decreases with fiber content. At every fiber content tensile strength of latex stage composites are slightly better than dry rubber composites.

### Modulus

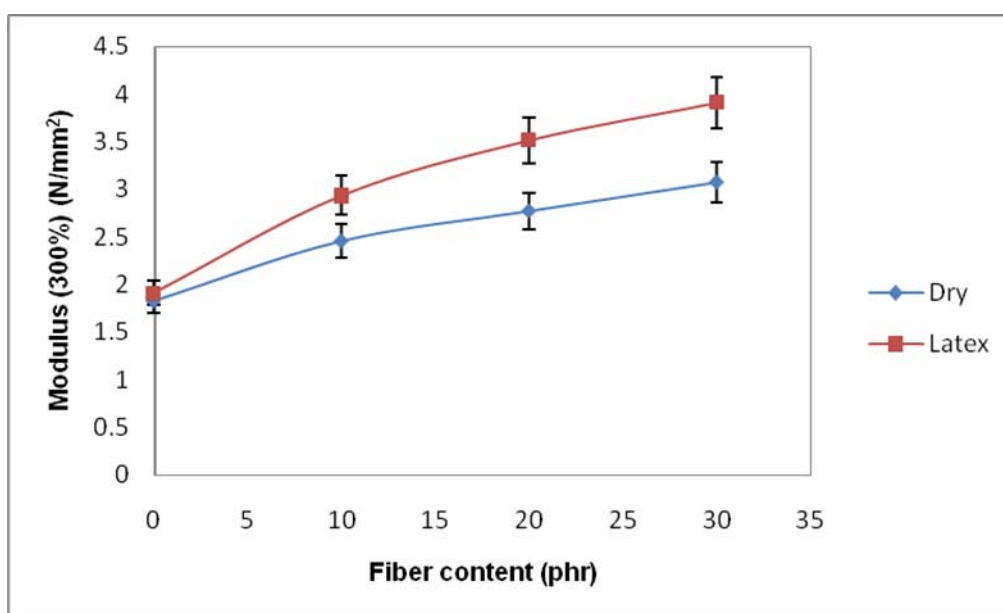
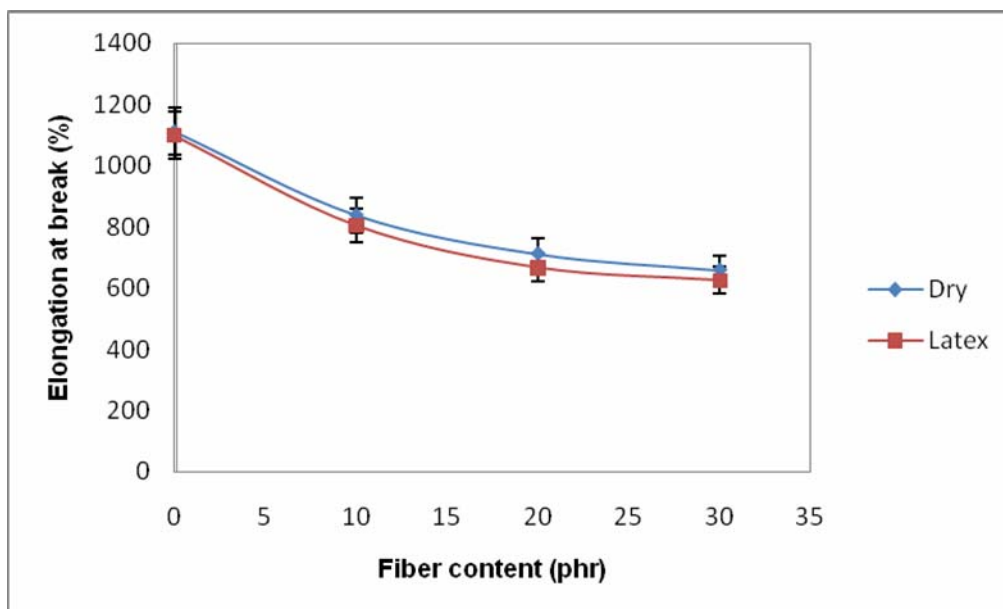


Figure 4.7 Variation of modulus with ungrinded fiber content

Figure 4.7 shows the modulus at 300 % elongation of the composites with fiber loading. The modulus increases with fiber content. Latex stage composites show better modulus at every fiber loading. This shows the superiority of latex stage composites in mechanical properties.

**Elongation at break**

**Figure 4.8 Variation of elongation at break with ungrinded fiber content**

Figure 4.8 shows the effect of coir fibers on the elongation of the composites. Elongation decreases with fiber content. Elongation is lower for latex stage composites. This indicates the better reinforcement offered by the latex stage composites.

#### 4.A.3.2.2 Composites of micro fibers

##### a) Cure characteristics

##### *Differential torque*

Differential torque is the difference between maximum and minimum torque experienced in Rubber Process Analyzer during the curing process at 150°C. Differential torque increases with the fiber loading (Fig 4.9). This shows, with increase in the amount of reinforcing fiber, matrix is being increasingly restrained.

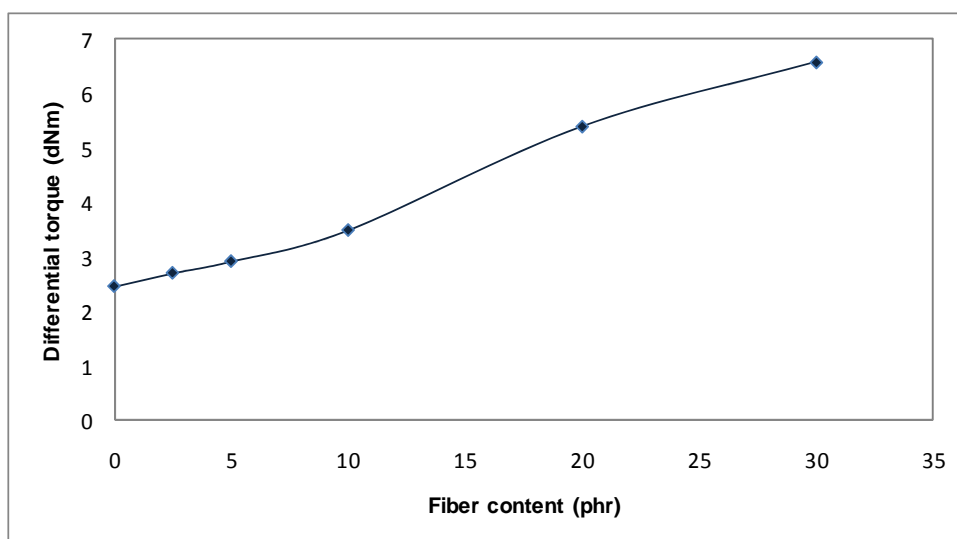


Figure 4.9 Variation of differential torque with fiber content

#### *Cure time & scorch time*

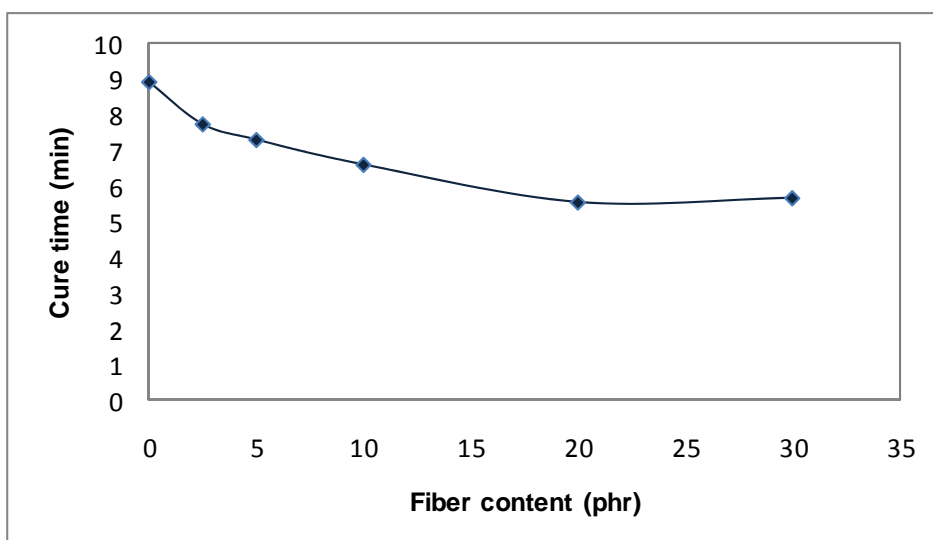


Figure 4.10 Variation of cure time with fiber content

Figs 4.10 and 4.11 show the variation of cure time and scorch time respectively, with fiber loading. Cure time and scorch time decrease with fiber loading. The percent decrease in scorch time is higher compared to cure time. The accelerator used is of delayed action type.

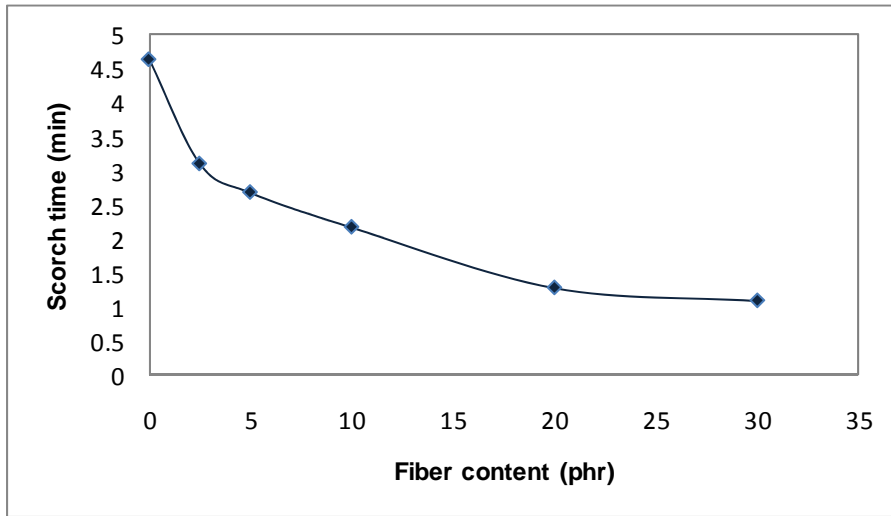


Figure 4.11 Variation of scorch time with fiber content

The scorch behaviour of the composites indicates an early induction of crosslinking for the composites. But the rate of cure remains unchanged or slightly lowered as indicated by the absence of corresponding level of decrease in the cure time.

## b) Mechanical properties

### *Tensile strength*

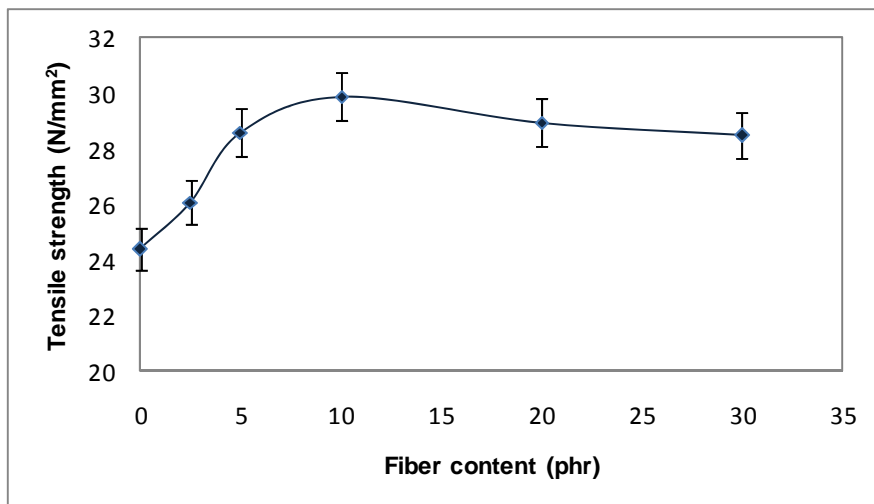
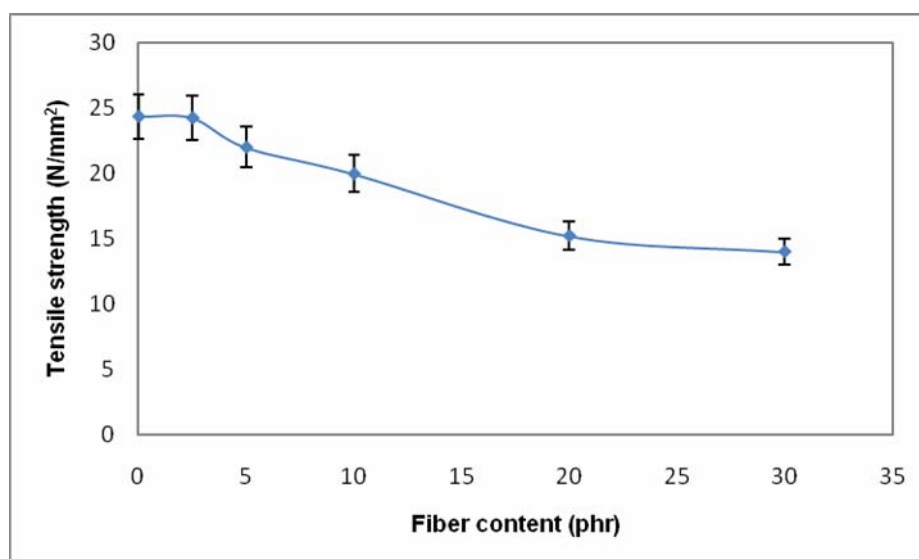


Figure 4.12 Variation of tensile strength (Longitudinal) with fiber content



**Figure 4.13 Variation tensile strength (Transverse) with fiber content**

The variation of tensile strength of the composites with fiber loading is shown in figure 4.12. Tensile strength increases with fiber loading and reaches a maximum at 10 phr fiber loading. At this concentration the tensile strength shows an improvement of 22% on the nonreinforced composite. The increase in tensile strength of the composites can be attributed to improved interaction between the microfibers and rubber matrix, helped by the pit formations and striations on fiber surface, together with the efficient fiber dispersion achieved by latex stage processing. Beyond this loading the tensile strength remains almost unchanged with fiber loading. At higher fiber loadings there may be some agglomerations of the fibers which will act as points of weakness, thus leading to early breakdown of the composites.

Figure 4.13 gives the variation of tensile strength measured in transverse direction to the orientation of fibers. Tensile strength decreases with fiber content. The fibers, when arranged in a direction perpendicular to the application of force, effective stress transfer does not take place. The nonreinforcing fibers only

contribute to the dilution effect on matrix. So with increase in fiber content the matrix gets progressively diluted leading to lower tensile strength values.

**Modulus**

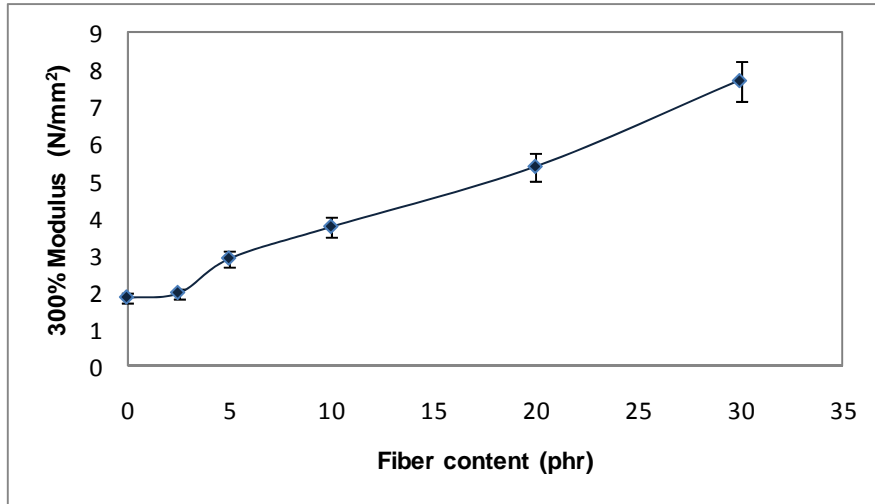


Figure 4.14 Variation of modulus (Longitudinal) with fiber content

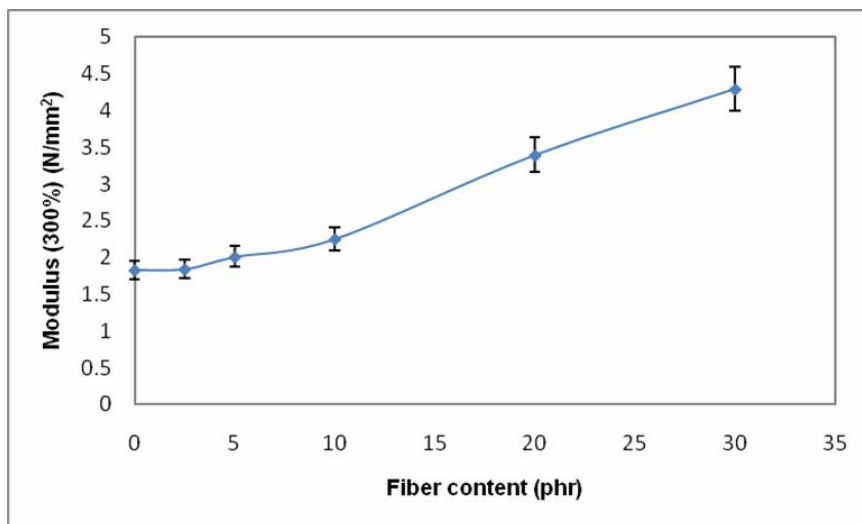
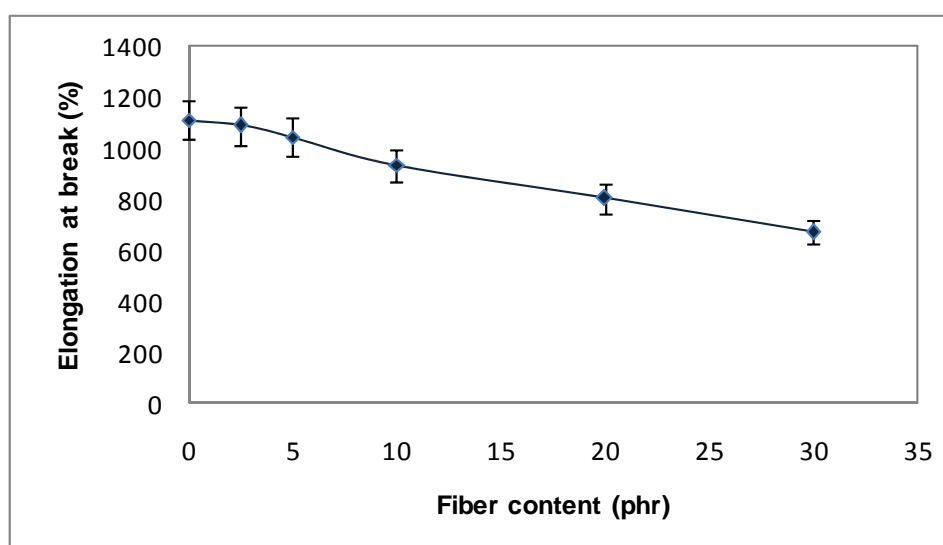


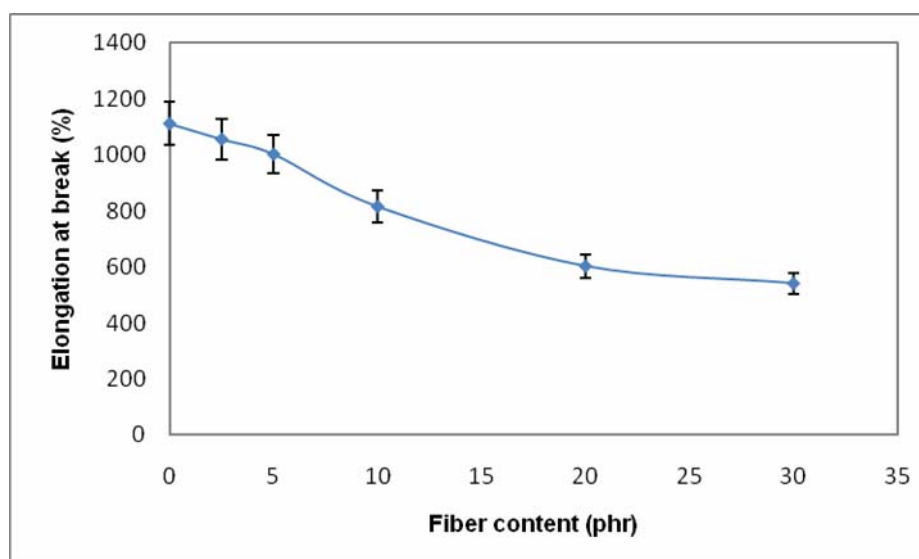
Figure 4.15 Variation of modulus (Transverse) with fiber content

Figure 4.14 shows the variation of modulus at 300% elongation with fiber loading in the longitudinal direction. Modulus increases almost linearly with filler content. At 30 phr fiber content there is an increase of 76% compared to the nonreinforced composite. Higher modulus of the composites indicates that there is effective interaction between the fiber and the matrix. The fiber–matrix interaction remains more or less intact at the strains where the modulus is evaluated. Modulus shows increase in the transverse direction (figure 4.15) also. The incorporation of fibers increases the stiffness of the matrix at lower strains. But the increase in modulus is much lower compared to the modulus in longitudinal direction.

#### ***Elongation at break***

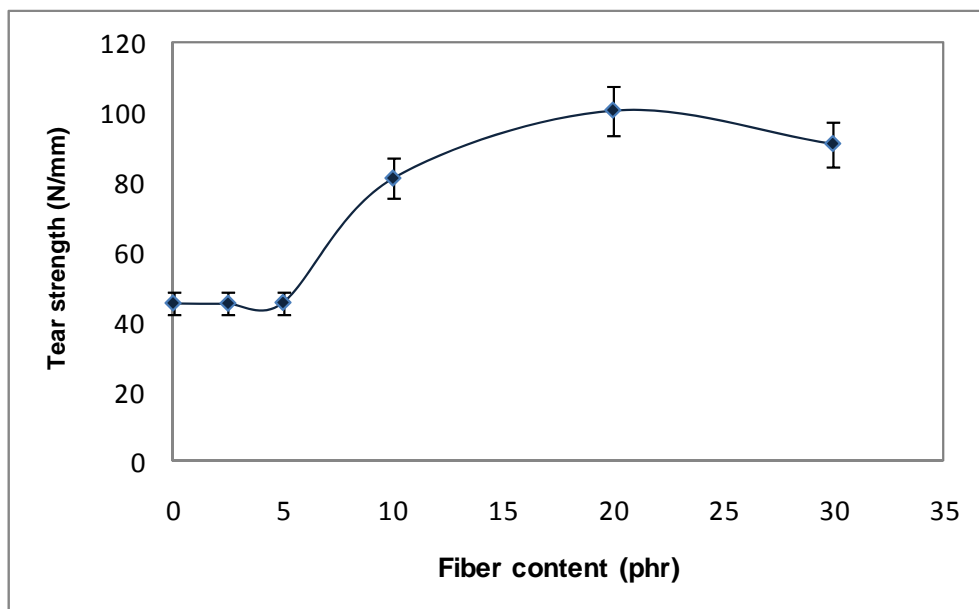


**Figure 4.16 Variation of elongation at break (Longitudinal) with fiber content**



**Figure 4.17** Variation of elongation at break (Transverse) with fiber content

Variation of elongation at break of the composites, with fiber content, is shown in figure 4.16. Elongation at break exhibits a linear decrease with fiber content. Fiber agglomerations at higher fiber contents, cause more fiber-fiber interactions than matrix-fiber interactions. This can result in easier pullout of the fibers from the matrix at high strains. The resulting voids act as defects inducing earlier breakage of the composites and thus reducing elongation at break. Figure 4.17 shows the elongation at break in transverse direction. The elongation decreases with fiber content. The decrease in elongation is higher compared to that in longitudinal direction. The nonreinforcing fibers oriented in the transverse direction are getting separated from the matrix at lower elongations leading to the formation of defects. These defects acts as stress concentration points and cause the failure of the composite at lower elongations.

**Tear strength**

**Figure 4.18 Variation of tear strength with fiber content**

The figure 4.18 shows the variation of tear strength with fiber content. When the compounded rubber is passed through tight mill nip the fibers are oriented in the mill direction. The tear samples were prepared such that the fibers are aligned perpendicular to the crack propagation. When the fiber content increases, there will be more and more hindrance to the crack propagation, thus increasing resistance to tear. Upto 5 phr fiber loading no notable improvement in tear strength is observed. Upto 5 phr, fiber content may not be sufficient to cause considerable obstruction to the crack propagation. Thereafter tear strength increases with fiber content upto 20 phr. At this concentration more than 122% improvement in tear strength is shown compared to unreinforced composites. For composites with 30 phr fiber loading the tear strength registers a reduction, as in the case of tensile strength.

### ***Abrasion loss***

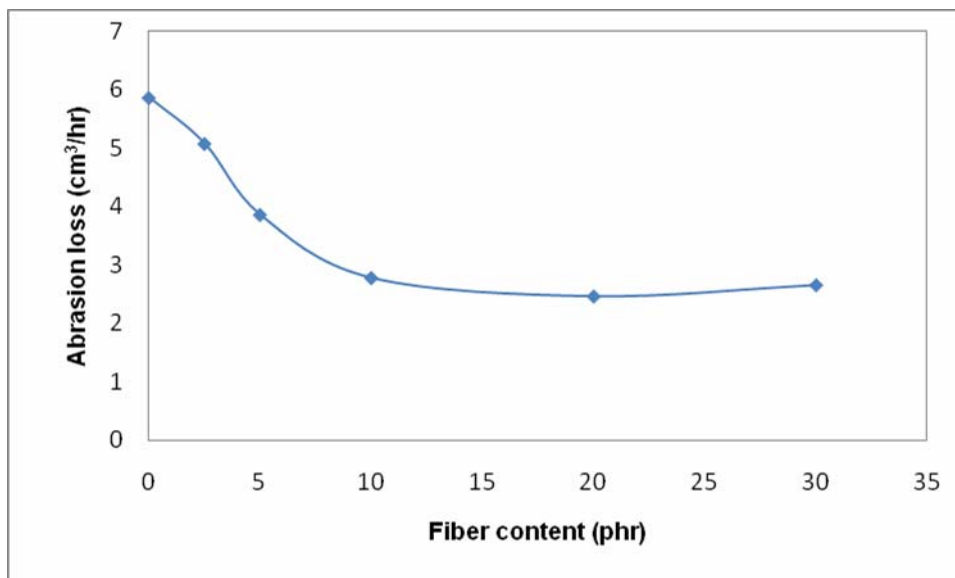


**Figure 4.19** Variation of abrasion loss with fiber content

Figure 4.19 shows the abrasion resistance of coir microfiber reinforced composites. Abrasion loss decreases with increasing fiber content. This shows the reinforcing capacity of the microfibers. Abrasion resistance reaches a maximum at 20 phr fiber loading. Beyond this loading a slight decrease in abrasion resistance is noted. At higher fiber content there is a chance of fiber agglomeration. These agglomerates will weaken the matrix and get removed as large chunks together with the rubber causing an increase in the abrasion loss.

### ***Hardness***

Figure 4.20 gives the hardness of the composites with respect to fiber loading. Hardness increases linearly with fiber content. The incorporation of fibers causes the stiffening of the matrix. This is reflected in the hardness of the composites.

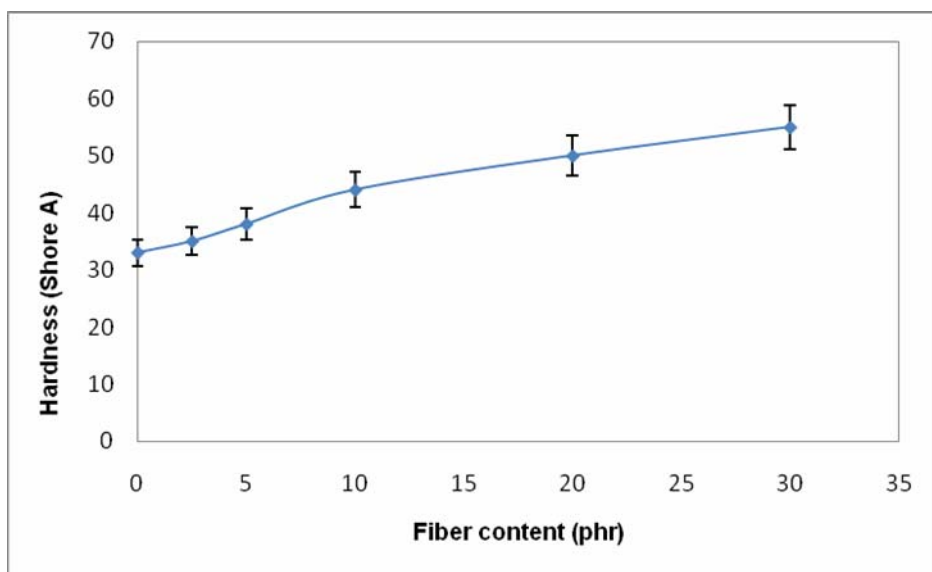


Figure 4.20 Variation of hardness with fiber content

### Resilience

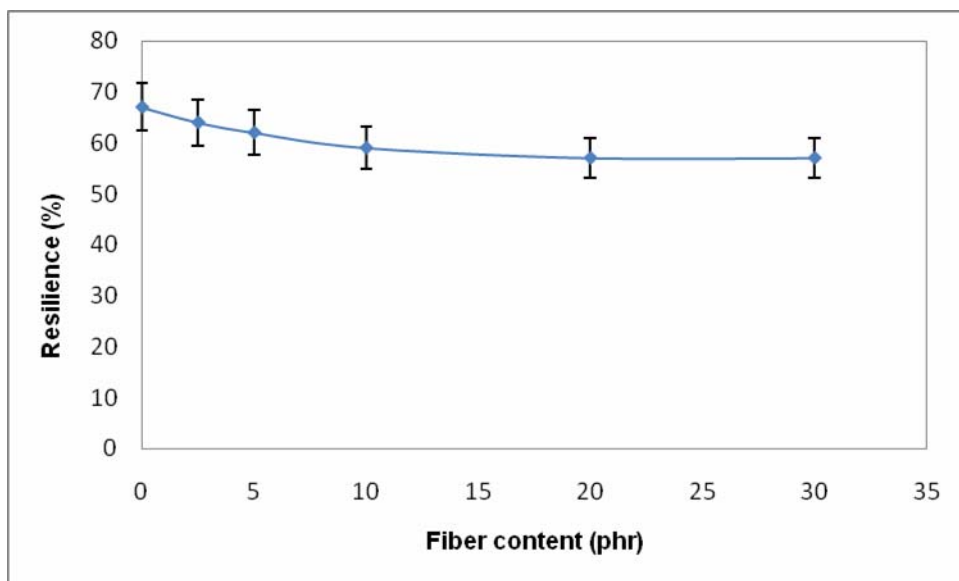
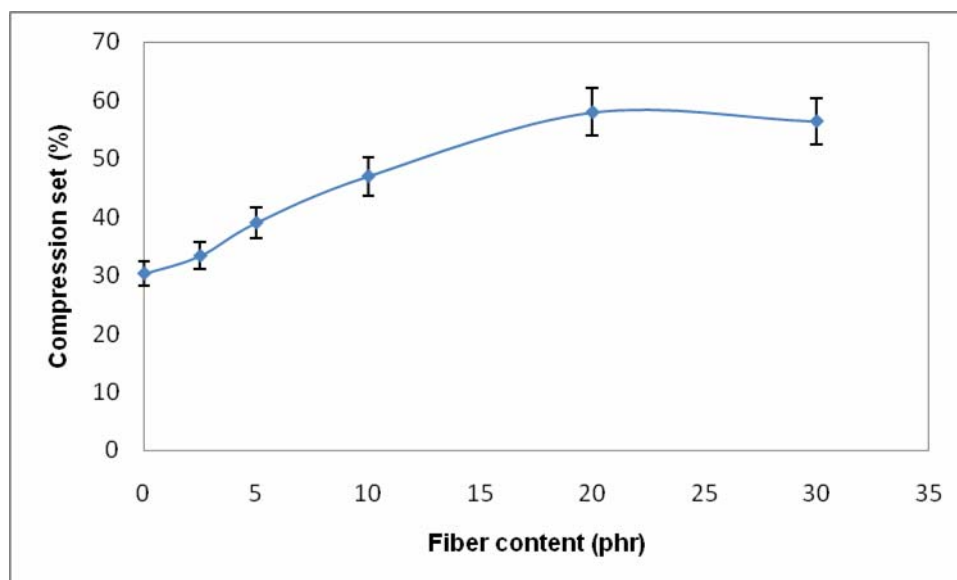


Figure 4.21 Variation of resilience with fiber content

Figure 4.21 change in resilience upon fiber loading. Resilience decreases with fiber content. As the fiber content increases the rubber matrix will get more restricted effecting a decrease in resilience.

### Compression set



**Figure 4. 22 Variation of compression set with fiber content**

Figure 4.22 shows the variation of compression set with fiber content. The compression set shows the opposite trend of resilience showing an increase with fiber content. As the reinforcement increases the compression set increases. Beyond 20 phr fiber loading a decrease in the compression set is observed. The fiber agglomeration at higher loadings will reduce the interaction between fibers and matrix giving lower compression set.

### Ageing resistance

Ageing resistance of the coir microfiber filled composites is given in figures 4.23 and 4.24. Figure 4.23 gives the retention percentage of tensile strength compared to unaged samples and figure 4.24 retention of modulus. The ageing resistance decreases with increasing fiber content. The fiber composites are more prone to degradation as observed in thermal analysis due

to the lower thermal stability of the cellulose compared to gum rubber. This is reflected in the composite performance after ageing.

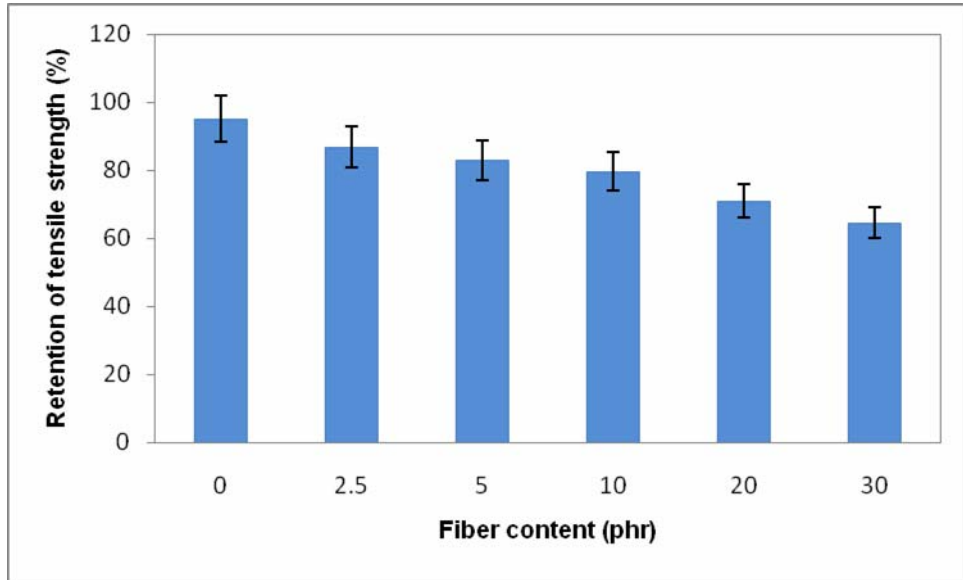


Figure 4.23 Variation of retention in tensile strength with fiber content

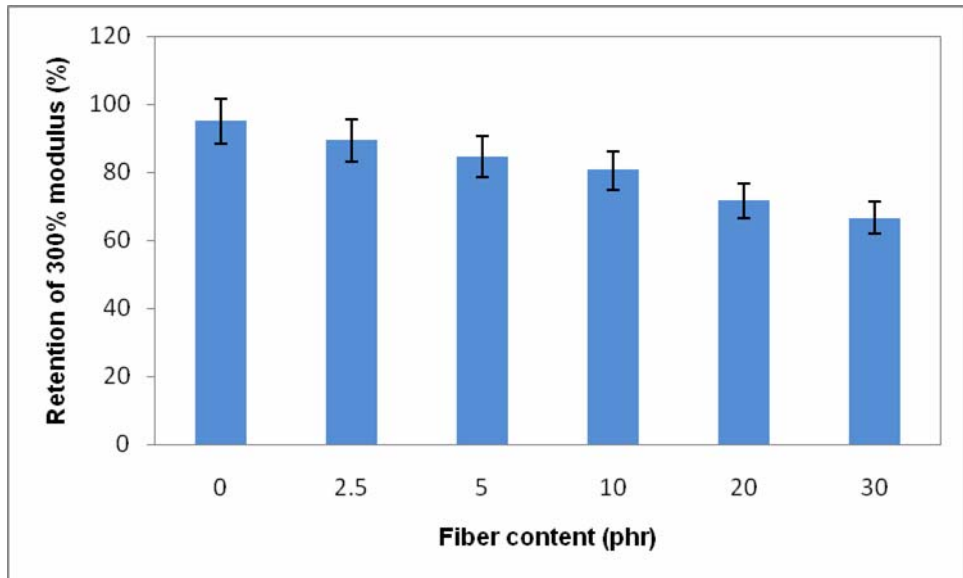
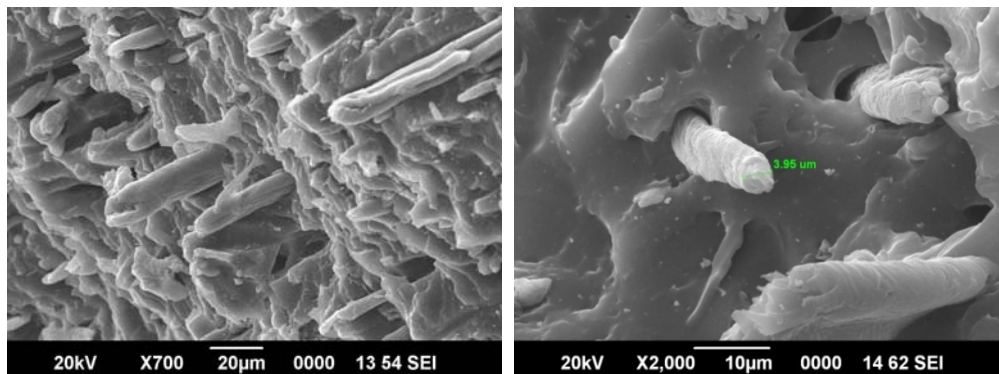


Figure 4.24 Variation of retention in modulus with fiber content

### *Morphological studies*



**Figures 4.25 & 4.26 SEM photographs of tensile fracture surfaces of NR/coir microfiber composites**

SEM photographs of the tensile fracture surface of the NR/Coir composite with 10 phr fiber loading is shown in figures 4.25 and 4.26. Good dispersion of fibers is evident from the figure establishing the effectiveness of latex stage processing. The fibers are arranged in perpendicular direction to the fracture surface confirming effective orientation. It can be seen that the fibers are not debonded from the matrix indicating strong interaction between the fibers and the matrix. The roughness of the fracture surface also indicates better interaction between the fibers and the matrix, which is confirmed by the improved mechanical properties of the composites.

#### **4.A.4 Conclusions**

Chemically treated coir macro fibers were used to prepare short fiber composites through latex stage processing. The fibers were found to reduce strength of the composites with increase in fiber content. Microfibers in the diameter range of 8 -11 µm and length 350 -550 µm were prepared from chemically treated coir macro fibers by mechanical size reduction. Microfibers in the pulp form were again subjected to chemical treatments. Eco-friendly

coir microfiber-natural rubber composites were prepared through latex stage processing method. Morphological studies reveal a composite with well dispersed micro fibers in the rubber matrix. Cure characteristics and mechanical properties of the composites were evaluated. The mechanical properties of the composites were showing a maximum at 10 phr fiber loading presumably due to the better dispersion of fibers in the rubber matrix. Tensile strength, modulus and tear strength of the composites were improved by 22%, 76% and 122% respectively compared to the nonreinforced composites. Abrasion loss and resilience decreases with fiber content while hardness and compression set decreases with fiber content. Ageing resistance of the composites decreased with fiber content due to the lower thermal stability of the composites. The coir microfibers prepared from coir by chemical and mechanical means was found to be a good reinforcing agent for the natural rubber.

**Part -B**

**Dynamic Mechanical Studies of Coir Microfiber Reinforced Natural Rubber Composites**

**4.B.1 Introduction**

The RPA 2000 Rubber Process Analyzer is a very versatile dynamic mechanical rheological tester (DMRT). The RPA has been proven to be an effective raw polymer tester, a processability tester for mixed rubber stocks, an advanced cure meter, and a DMRT for measuring post cure dynamic properties. The RPA 2000 measures the viscoelastic properties of rubber compounds in torsional shear. Thorough rubber compound characterizations are made through frequency, strain, and temperature sweeps. Here we subjected the uncured and cured fiber compounds to varying strains in a single sweep. The complex modulus values of the compounds were plotted against strain.

Dynamic mechanical analysis in a Dynamic Mechanical Analyzer is a very powerful technique which allows for determination of mechanical properties (modulus and damping), detection of molecular motions (transitions), and for the development of morphology relationships (crystallinity, molecular weight, crosslinking, etc). [23] Martins and Mattoso [24] studied dynamic mechanical properties of powdered tire rubber/short sisal fiber composites and reported that incorporation short sisal fibers to the tire rubber matrix increased both the storage and the loss moduli and the increase is higher for composites with chemically treated fibers. Effect of matrix's type on the dynamic properties for short fiber-elastomer composite were studied by Ashida and Naguchi [25]. Ashida et al [26] investigated the dynamic moduli and  $\tan \delta$  for nylon-CR and PET-CR composites with unidirectional short fibers.

Here the dynamic mechanical properties of coir microfiber reinforced composites prepared through latex stage processing are investigated. Rubber Process Analyzer is used to study the variation of dynamic modulus in a strain sweep mode for both uncured and cured compounds. Dynamic mechanical analyzer is used to study the dynamic moduli and  $\tan \delta$  in temperature and frequency sweep modes.

#### 4.B.2 Experimental

5 cm<sup>3</sup> of the uncured fiber mixes were cut using a punch and placed in the sealed biconical cavity of the Rubber Process Analyzer and subjected to strain sweep program. The samples were kept at the test temperature of 60 °C for a preheating time of 4 minutes. It is then subjected to a strain sweep with varying strains of 0.05, 0.1, 0.2, 0.5, 1, 2, and 5 degrees in a single sweep. The complex modulus values obtained were plotted against strain in degrees. For strain sweep studies in cured state, uncured samples were first vulcanized to their respective cure times at 150 °C. The temperature was then reduced to 60 °C and the sample was subjected to strain sweep as above.

TA Instruments DMA Q800 was used to measure the dynamic mechanical properties of the NR-Coir micro fiber composites. Test specimens having a dimension of 30 mm x 3 mm x 2 mm were used in tension mode. Temperature sweep and frequency sweep experiments were conducted. Temperature sweep experiments of the composites were performed from -80 °C to +40 °C. Frequency was set at 1 Hz and amplitude 15 μm. Frequency sweeps were conducted over a frequency range of 1Hz to 63 Hz at 40 °C. The amplitude was fixed at 15 μm.

### 4.B.3 Results and discussion

#### 4.B.3.1 Strain sweep in RPA

Figure 4.27 shows the variation of complex modulus with strain for natural rubber/ coir microfiber composites in the uncured state. At low strains the modulus increases with the fiber content indicating high matrix-filler interaction. With increase in filler content, restriction of the matrix against the shearing action increases, which reflects in the complex modulus. 20 and 30 phr composites show high initial modulus which may be the effect of filler-filler interaction or in other words filler agglomeration. On increase in strain these filler networks break giving lower modulus. Thereafter the modulus stabilizes upto a strain in which filler polymer interaction breaks giving still lower modulus values. 5 and 10 phr composites show almost constant modulus upto a strain of 2 degree indicating better dispersion of fibers. Modulus at high strains is a measure of the matrix-matrix interaction. All of the composites show a tendency to converge to a single value with increasing strain.

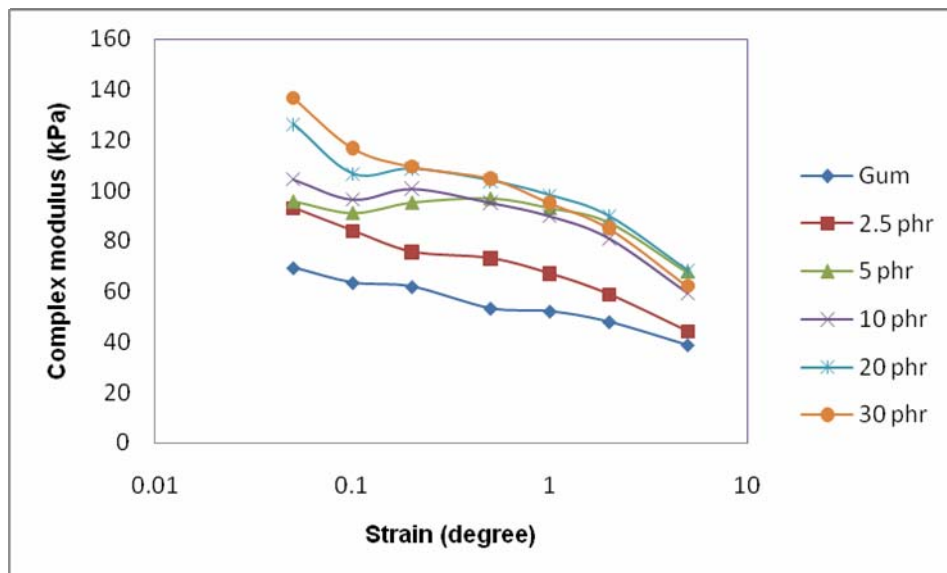


Figure 4.27 Complex modulus Vs strain for composites in Uncured state

Fig 4.28 shows the variation of complex modulus with strain of the composites in cured state. It can be seen that upto 10 phr fiber content, the critical strain above which the composites exhibits Payne effect is almost undistinguishable. Upto this fiber content fiber composites emulate the behaviour of gum composite. This is because of the good fiber dispersion in the rubber matrix at these fiber loadings. In the absence of fiber agglomeration, the decrease of modulus produced as an effect of the breakdown of the fiber network formed in the matrix is limited, ensuring very little in terms of Payne effect[27]. The better mechanical properties at these fiber loadings are also a result of this better fiber dispersion. This supports the effectiveness of latex stage processing method for better dispersion of fibers and ensuing better mechanical properties. As a whole, modulus increases with fiber content. For 20 and 30 phr composites the increase in modulus is much higher. At these fiber loadings the initial modulus shows a considerable decrease at 0.1 degree strain. This is due to the breakdown of fiber agglomeration at these fiber contents. For 20 and 30 phr composites, with increase in strain, Payne effect steps in owing to the breakdown of fiber-matrix network.

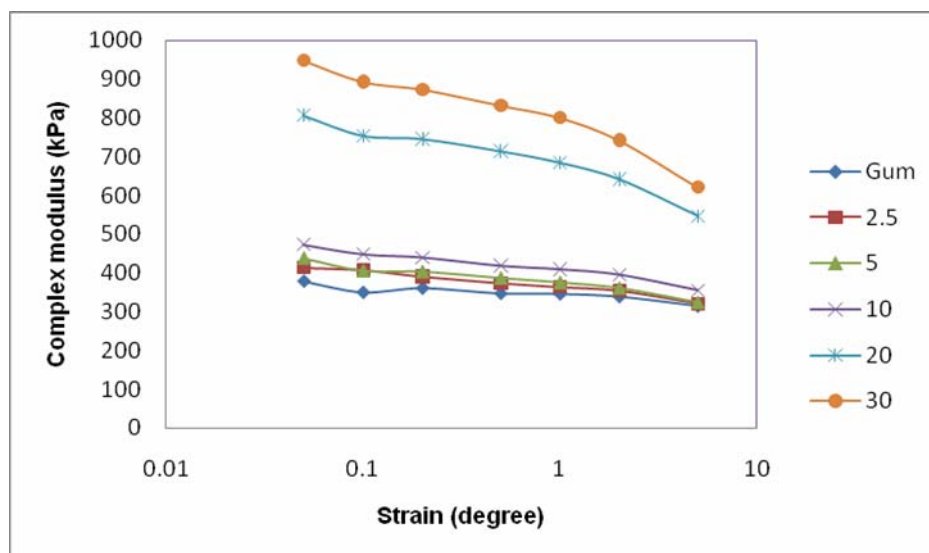


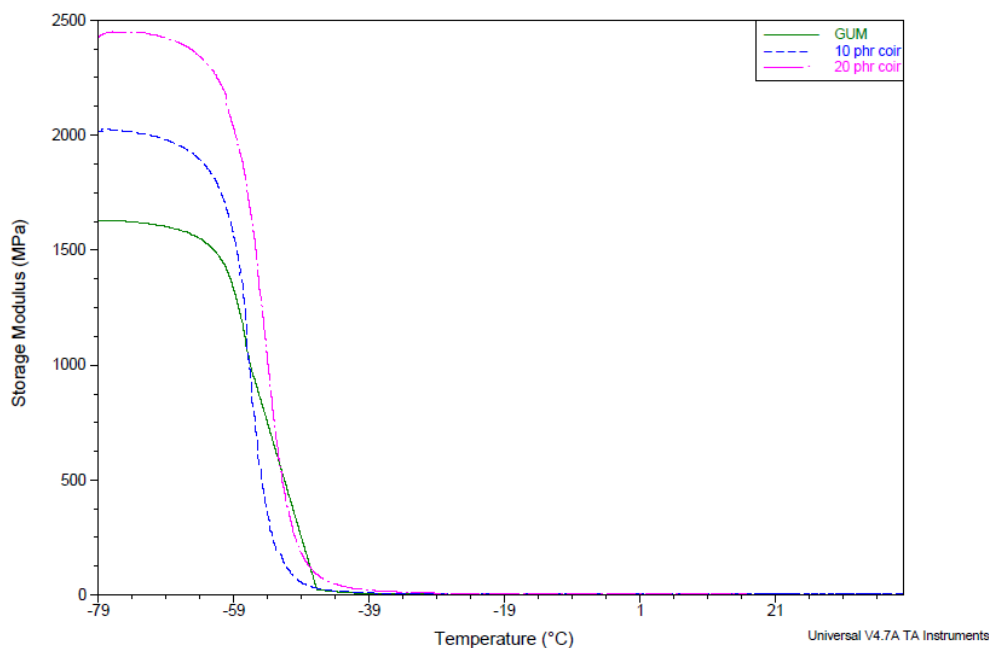
Figure 4.28 Complex modulus Vs strain for composites in Cured state

### 4.B.3.2 Studies in Dynamic Mechanical Analyzer

TA Instruments DMA Q800 was used to measure the dynamic mechanical properties of the NR-Coir composites. Test specimens having dimensions of 30 mm x 3 mm x 2 mm were used in tension mode. Temperature sweep and frequency sweep experiments were conducted. Temperature sweep experiments of the composites were performed from -80°C to +40°C. Frequency was set at 1 Hz and strain amplitude 15  $\mu\text{m}$ . Frequency sweeps were conducted over a frequency range of 1Hz to 30 Hz at 40 °C. The strain was limited to 15 $\mu\text{m}$ .

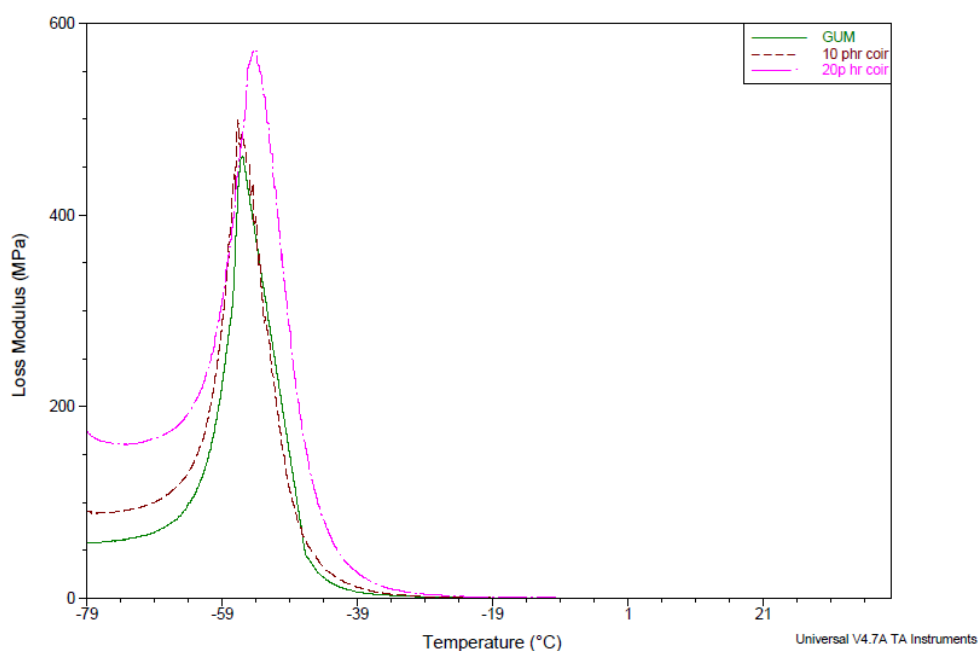
#### 4.B.3.2.1 Temperature sweep studies

Figure 4.29 shows the variation of storage modulus as a function of temperature. It can be seen that fiber composites have higher initial storage modulus compared to gum rubber. The initial modulus increases with fiber content. At the glass transition region the modulus decreases. After glass transition the modulus of all the composites tend to be similar.



**Figure 4.29** Variation of storage modulus with temperature of NR/coir microfiber composites

Figure 4.30 shows the variation of loss modulus with temperature. The glass transition temperature of fiber composites as obtained from loss modulus peaks show not much variation from that of gum rubber except in the case of 20 phr composites. In figure 4.31 the loss modulus peaks are zoomed to get a clear picture of this improvement in glass transition. This is due to reinforcing fibers restricting the segmental mobility of the composites. At 20 phr fiber content the restriction is sufficiently higher so as to make a noticeable change in the glass transition. The loss modulus of the composites increases with fiber content. This may be due to energy being dissipated at the interface between the rubber and fiber. With the increase in fiber content the energy dissipation will also increase.



**Figure 4.30** Variation of loss modulus with temperature of NR/coir microfiber composites

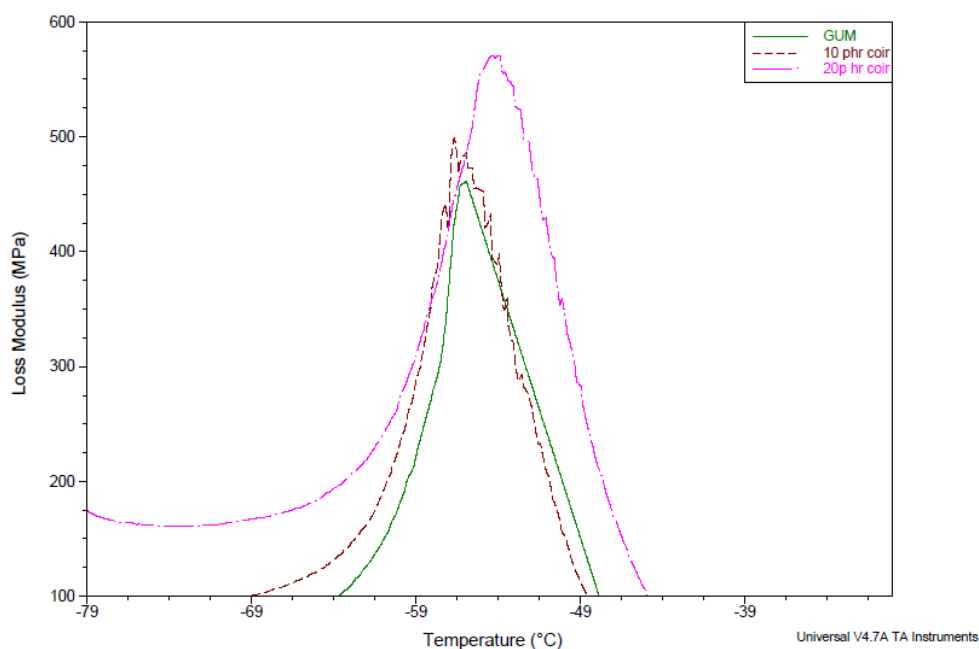


**Figure 4.31** Variation of storage modulus with temperature of NR/coir microfiber composites (Zoomed version)

#### 4.B.3.2.2 Frequency sweep

Figure 4.32 gives the variation of storage modulus ( $E'$ ) with fiber content of the composites. Storage modulus increases with frequency. Beyond a frequency of 14.6 Hz the increase in storage modulus is more pronounced. The increase in frequency is equivalent to decrease in temperature. The rise in modulus beyond this frequency is corresponding to the transition region in a temperature sweep experiment. In between composites it can be seen that  $E'$  increases with fiber content. With the increase in fiber content the rubber matrix gets more and more restricted and this reflects in the storage modulus values.

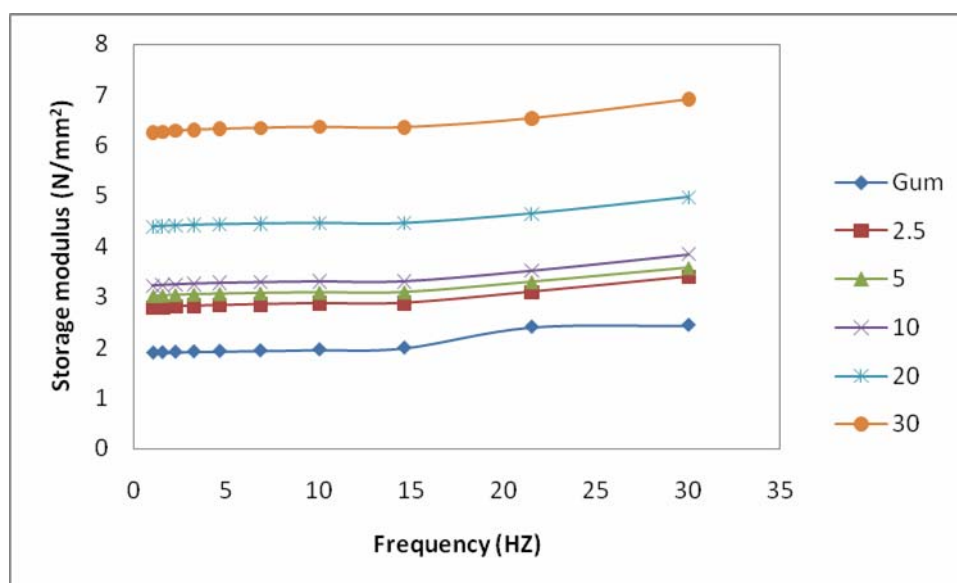


**Figure 4.32 Variation of storage modulus ( $E'$ ) with frequency**

Figure 4.33 shows the variation of loss modulus ( $E''$ ) with frequency of the composites. For all composite,  $E''$  does not change much up to a frequency of 14.6 Hz. Beyond this frequency there is a sharp increase in loss modulus. A peak similar to that in the glass transition region is noted. This also suggests the transition region similar to a temperature sweep profile. In between composites loss modulus increases with increase in fiber content.

Variation of tan delta with frequency is given in figure 4.34. Here also transition region is noted by a peak in the curves beyond the frequency of 14.6 Hz. The peak value decreases with increasing fiber content. As the matrix becomes more restricted the segmental mobility of the rubber molecules will be reduced which is reflected in the lowering of the tan delta peak value.

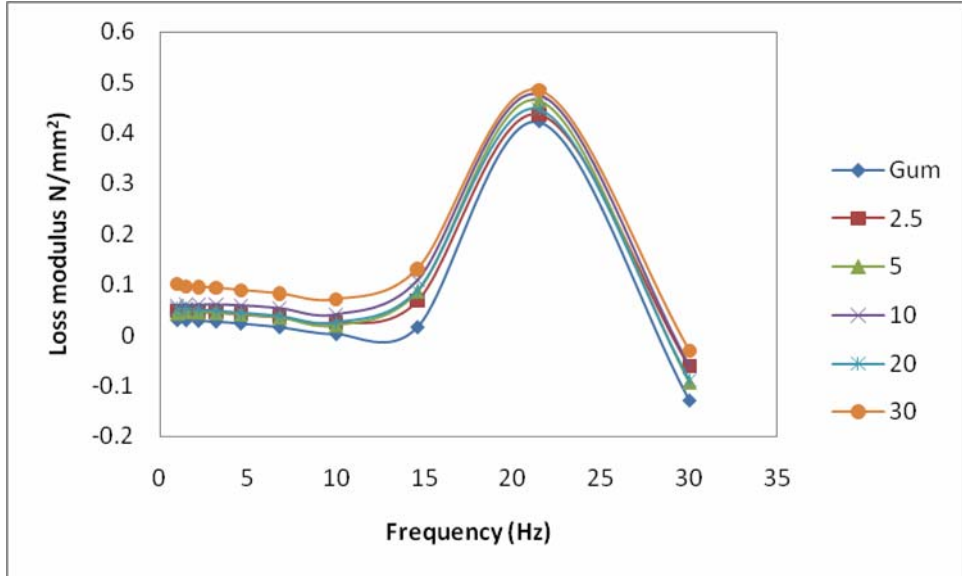


Figure 4.33 Variation of loss modulus (E'') with frequency

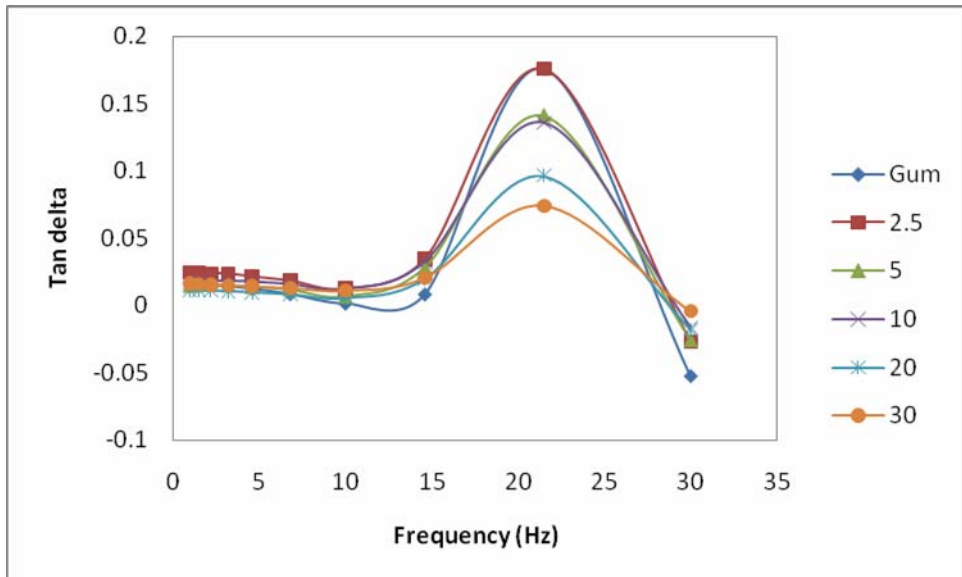


Figure 4.34 Variation of tanδ with frequency

#### **4.B.4 Conclusions**

Strain sweep studies in RPA and temperature and frequency sweep studies in DMA were performed. Strain sweep studies showed that upto 10 phr fiber content dispersion of fibers in the composites is uniform without any fiber agglomeration. At 20 and 30 phr fiber content agglomerations of fibers in the matrix causes considerable decrease in modulus with strains beyond critical strain. Temperature sweep studies in DMA showed an increasingly restrained matrix with increasing fiber content, indicating increased reinforcement. The glass transition of the composites marginally increased with fiber content. Frequency sweep studies also indicated the increase of reinforcement with fiber content. Frequency sweep profiles show a transition region corresponding to the transition in temperature sweep.

**Part -C**

**Thermal Studies**

**4.C.1 Introduction**

Thermal analysis is an important tool in polymer technology to investigate the thermal stability of polymers and composites. Many studies have been carried out to establish the effect of short fibers both natural and synthetic on the thermal stability of the composites. It was found that addition of the carbon nanotubes treated using acid bath followed by ball milling with HRH bonding system, the crystallization melting peak in differential scanning calorimetry curves of NR weakened and the curing rate of NR slightly decreased [28]. Studies by Silva et al. showed that biogenic silica short fibers increased the thermal stability of the silicone rubber matrix [29]. Maya et al. [30] investigated natural rubber composite reinforced using sisal and oil palm fibers. The thermal stability of the composites was seen to increase upon fiber loading and chemical modification. Sobhy and Tammam [31] found that thermal stability is increased upon the addition of wheat husk fiber in EPDM rubber. The effect of the addition of ac,ai' fibers in natural rubber were investigated using thermogravimetric analysis under inert and oxidative atmospheres and differential scanning calorimetry [32]. The addition of the fibers did not influence the thermal stability of the composites or the glass transition temperature. Setua and Mathur showed that addition of short fibers in combination with a proper bonding system could enhance the thermal stability of the elastomer composites [33]. In this section the differential scanning calorimetry, thermal degradation and thermal kinetics studies of the coir microfiber/natural rubber composites prepared through latex stage processing is presented.

## 4.C.2 Experimental

Thermogravimetric analyses were carried out on TGA Q50 of TA Instruments. The samples were heated from ambient to 800°C with a heating rate of 20°C/minute under nitrogen atmosphere. A characterization method proposed by Friedman was used to establish the kinetic parameters. The details of the method are given in the previous chapter. Differential scanning calorimetry of the composites was performed on DSC Q100 of TA Instruments. The experiments were carried out from -80°C to 100°C. The heating rate was 10°C/minute. A nitrogen atmosphere was maintained throughout the experiment.

## 4.C.3 Results and discussion

### 4.C.3.1 Thermogravimetry

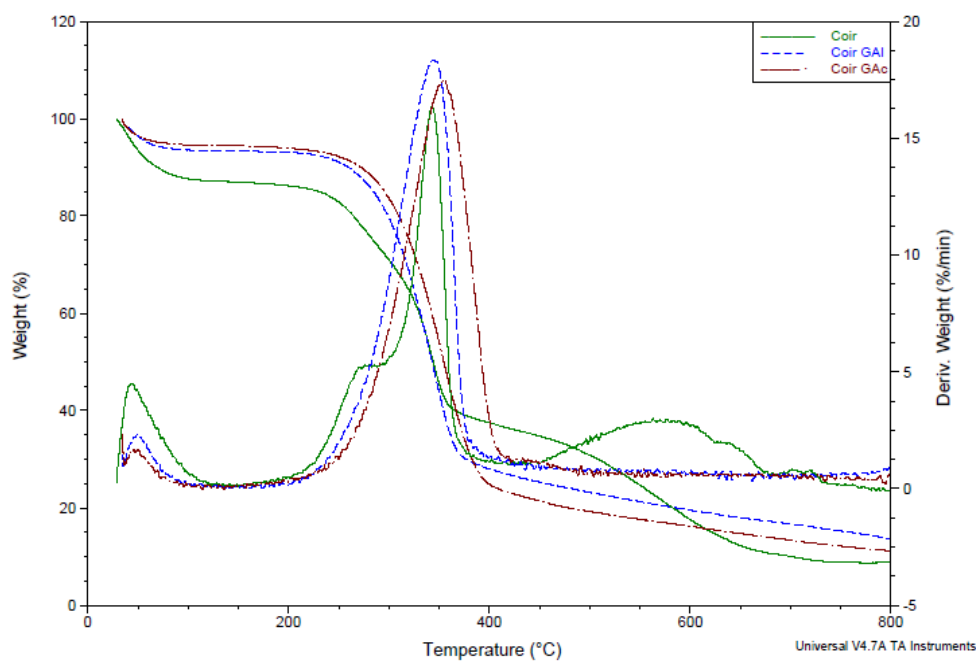
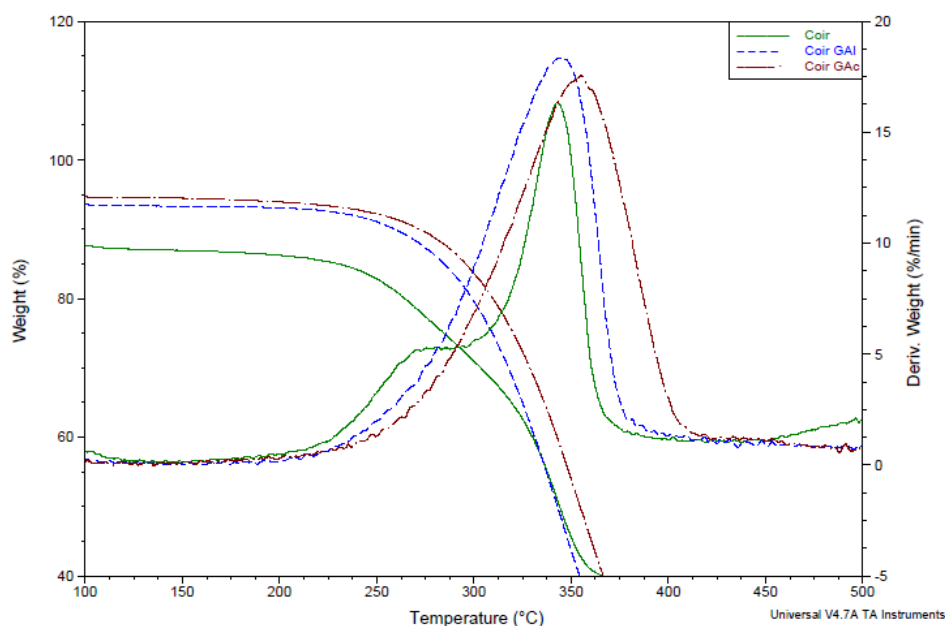


Figure 4.35 TGA and DTG profile of treated and untreated coir fibers



**Figure 4.36 TGA and DTG profile of treated and untreated coir fibers (Zoomed version)**

Figure 4.35 and 4.36 give the thermal degradation behaviour of treated and untreated coir fibers. Coir GAl denotes coir fibers after mechanical size reduction and alkali treatment. Coir GAc denotes size reduced coir after acid treatment. It can be seen that untreated coir has 3 distinct degradations. First degradation is that of hemicelluloses which is shown by a shoulder peak just before the second degradation peak of cellulose. Third peak shows the degradation lignin. There is substantial amount of lignin in the untreated coir. After the alkali treatment the lignin content considerably reduced as evidenced by the disappearance of the peak corresponding to the presence of lignin. Disappearance of the shoulder peak in the DTG curves of treated fibers indicates a reduction in the hemicelluloses content. It can be seen that the onset of degradation of coir fibers shifted to higher temperatures after the alkali treatment. This is due to the removal of partial amount of hemicelluloses which has low thermal stability compared to cellulose. After acid treatment the onset of degradation is further shifted to higher

temperature. This is a result of further removal of hemicelluloses by the acid treatment. The shift in the main degradation peak in the DTG curves shows the improvement in thermal stability of the fibers.

However compared to the vulcanized rubber the thermal stability of the treated coir microfibrer is very less. This can be seen from the TGA curves presented in figure 4.37. It can be seen that the degradation of coir fibers either in treated or untreated form, starts much earlier than the onset of degradation of rubber vulcanizate. So the addition of coir microfibrer to the rubber is bound to reduce the thermal stability of the rubber composites.

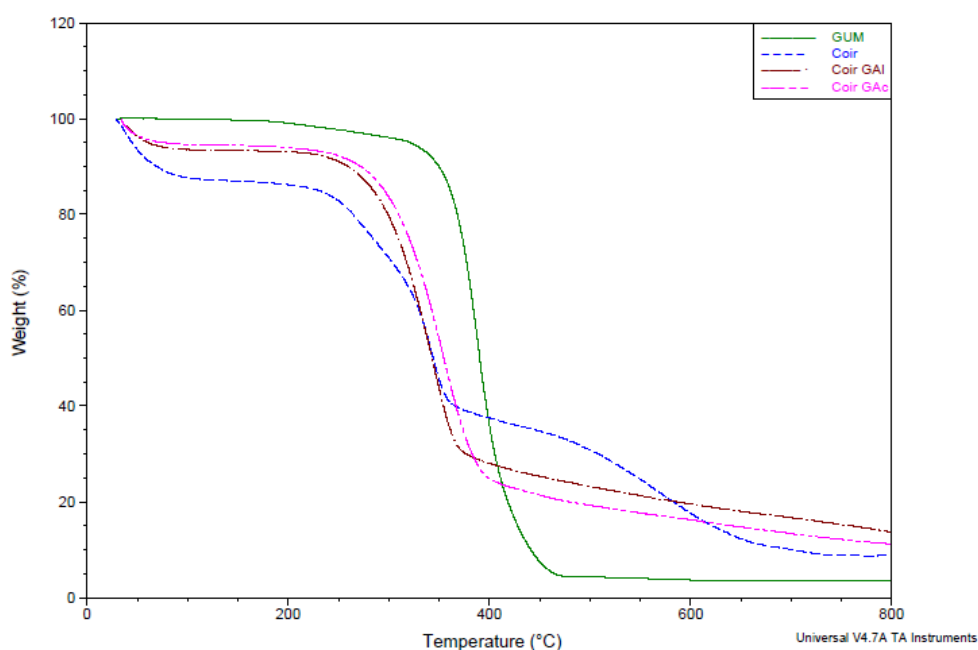


**Figure 4.37 TGA profile of gum rubber and treated and untreated coir fibers**

Figure 4.38 shows TGA and DTG plots of gum and coir reinforced composites. Figure 4.39 is a zoomed version to the graph to make the degradation pattern clearer. It is seen that the addition of coir microfibrer

reduces the onset of degradation of the coir/NR composites. But the peak degradation rate of the composites is reduced in the fiber composites. Table 4.3 gives the onset of degradation ( $T_i$ ), the temperature at which the rate of decomposition is maximum ( $T_{max}$ ), the peak degradation rate, and the residue at  $800^\circ\text{C}$  for the composites. It can be seen that initiation of degradation temperature and temperature at maximum rate of degradation is lower for coir composites compared to the gum rubber. This is due to the presence of coir micro fibers which are comparatively lower in thermal stability. The lignin content in the coir is responsible for the thermal stability of coir. Lignin content determination by chemical means shows that, after the mechanical and chemical treatment the lignin content reduced from 45% to 22.4%. As already discussed the reduced thermal stability of the fiber is responsible for the reduced maximum degradation temperature of the composites.

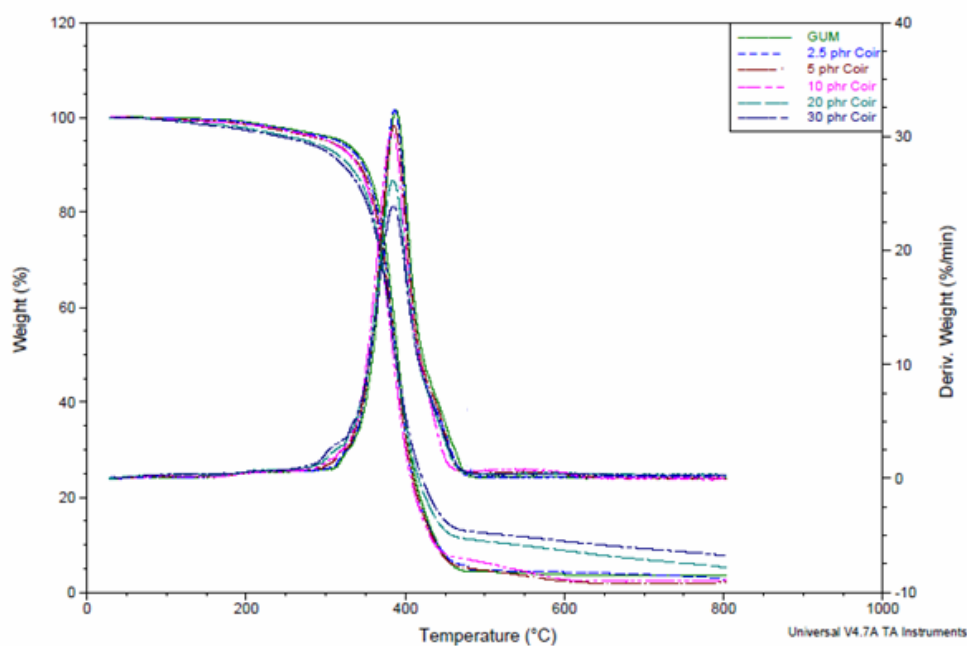


Figure 4.38 TGA and DTG profile of NR/coir micro fiber composites

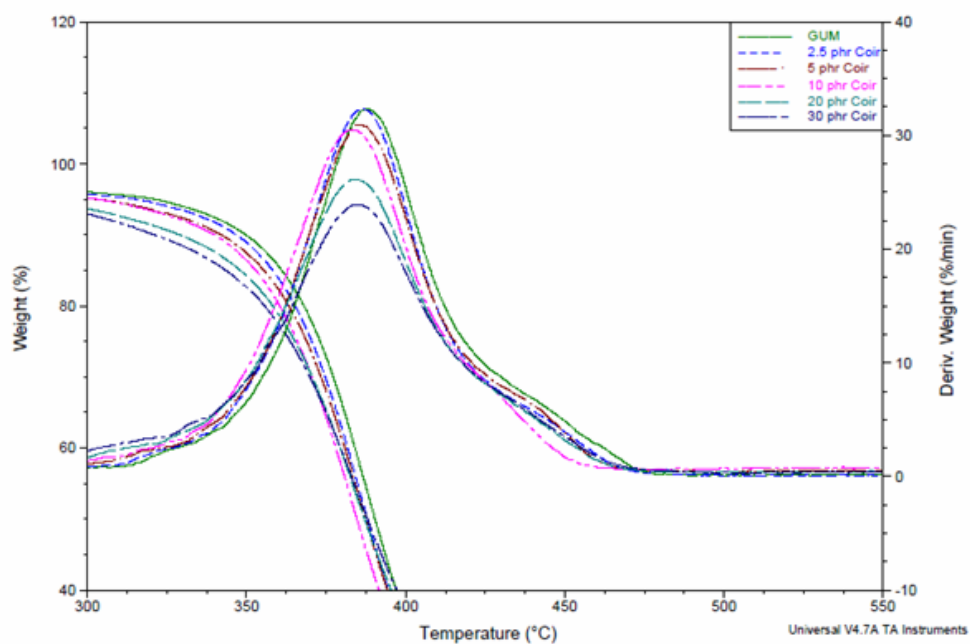


Figure 4.39 TGA and DTG profile of NR/coir micro fiber composites (Zoomed version)

Table 4.3 Degradation parameters of coir microfiber composites

	Ti	Tmax	Rate	Residue
Gum	310.64	388.18	1.587	3.525
2.5	310.37	386.45	1.588	2.835
5	292.23	385.87	1.519	1.998
10	286.63	383.46	1.5	2.547
20	289.9	384.63	1.287	5.309
30	290.08	384.99	1.177	7.761

Friedman method was used to study the degradation kinetics of the coir composites. Figure 4.40 and 4.41 shows typical plots of  $\ln(da/dt)$  vs  $1/T$  and the  $\ln(1-\alpha)$  vs  $1/T$  respectively. It can be seen that plots exhibited good linear

relationship which shows that the thermal degradation of the composites proceeded in good agreement with the Friedman model. Activation energy ( $E_a$ ) and order of the degradation reaction ( $n$ ) of the composites were found from the Friedman plots and are given in Table 4.4.

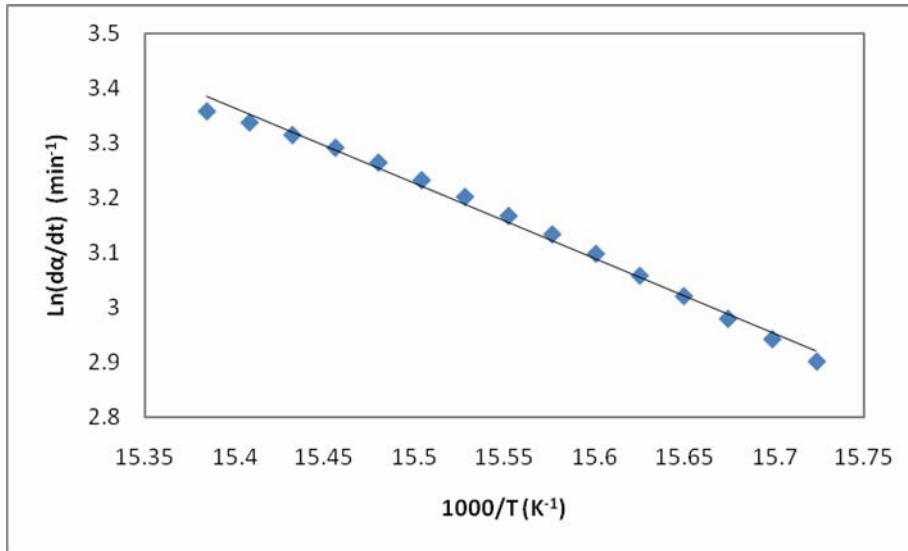


Figure 4.40 Ln( $da/dt$ ) vs  $1/T$  plots in Friedman model

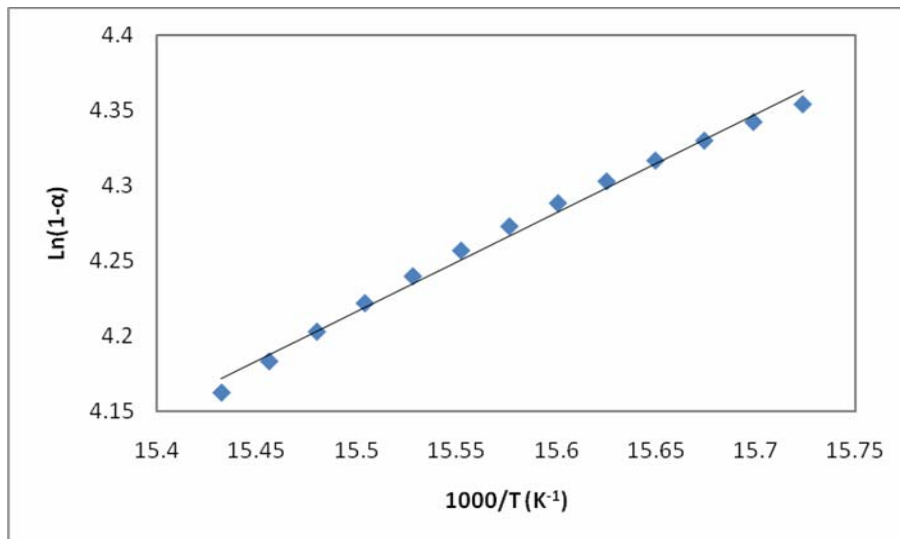


Figure 4.41 Ln( $1-\alpha$ ) vs  $1/T$  plots in Friedman model

**Table 4.4 Kinetic parameters obtained by Friedman method**

	<b>Ea (kJ/mol)</b>	<b>n</b>
Gum	139.209616	2.6980
2.5 phr	138.88537	2.5951
5 phr	126.7885	2.3268
10 phr	114.0847	2.0904
20 phr	110.5595	2.2716
30 phr	106.610422	2.3593

Activation energy of the composites are lower than that of the gum rubber. With the increasing amount of fiber in the composites, activation energy decreases continuously. This confirms the lowering of thermal stability by the addition coir micro fibers with low lignin content.

#### 4.C.3.2 Differential Scanning Calorimetry

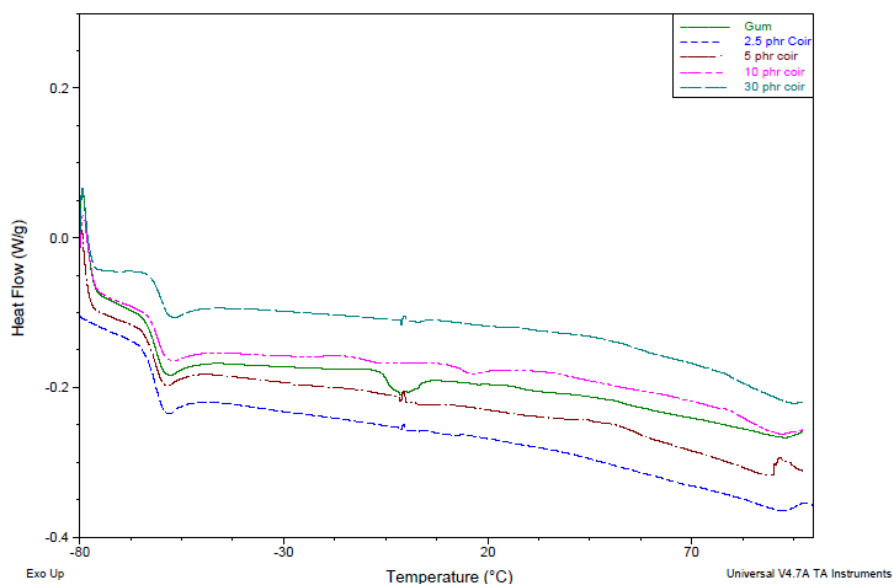
**Figure 4.42 DSC thermograms of NR/ coir microfiber composites**

Figure 4.42 shows the DSC plots of gum and micro-coir reinforced composites. It can be seen that there is a marginal increase in the glass transition temperature of 30 phr fiber composites compared to the gum composite from -61.45 °C to -60.23 °C.

#### **4.C.4 Conclusion**

The chemical treatments and mechanical downsizing of the fibers are effective in removing large amounts of lignin and hemicellulose. The thermal stability of the fiber improved with chemical treatment, but was still much lower compared to the stability of the gum composites. So the incorporation of fibers into the rubber matrix reduces the thermal stability of the composites. Friedman model was used to determine the kinetic parameters of degradation. The activation energy of the composites decreases with fiber content, showing decreased thermal stability. DSC studies showed a marginal increase in T<sub>g</sub>.

#### **References**

- [1] Chakraborty S.K., Setua D.K. and De, S.K., *Rubber Chem. Technol.* **55** (1982) 1286.
- [2] O'Connor, J.E., *Rubber Chem. Technol.* **50** (1977) 945.
- [3] Derringer G.C., *Rubber World*; **165**(2) (1971) 45.
- [4] Sreeja T.D. and Kutty S.K.N. *Polym.Plast.Technol. Eng.*, **42** (2003) 239.
- [5] Rajeev R. S., Bhowmick A.K., De S.K. and Bandyopadhyay S., *J. Appl. Polym. Sci.*; **90** (2003) 544.
- [6] Varghese S., Kuriakose B., Thomas S. and Koshy A.T., *J. Adhes. Sci. Technol.*; **8**(3) (1994) 235.
- [7] Kumar R.P., Amma M.L.G. and Thomas S., *J. Appl. Polym. Sci.*, **58**(3) (1995) 597.
- [8] Kumar R.P. and Thomas S., *Polym. Int.*, **38**(2) (1995) 173.

- [9] Jayaraman K., *Compos.Sci. Technol.*, **63** (2003) 367.
- [10] Sreeja T.D. and Kutty S.K.N., *Int. J. Polym. Mater.*, **52**(3) (2003) 239.
- [11] Bledzki A. K., and Gassan, J., *Carbon*; **24** (1999) 221.
- [12] Saheb D. N. and Jog J. P., *Adv. Polym. Tech.*, **18**(4) (1999) 351.
- [13] Ishida H., *Interfacial Phenomena in Polymer, Ceramic and Metal Matrix Composites*.Elsevier, New York, NY, USA; 1988.
- [14] Amar K.M., Manjusri M. and Lawrence T.D., *Natural Fibers, Biopolymers, and Bio-composites*. CRC Press, Tailor and Francis; 2005.
- [15] Arumugam N., Selvy K.T., Rao K.V. and Rajalingam P., *J. Appl. Polym. Sci.*, **37** (1989) 2645.
- [16] Geethamma V.G., Thomas Mathew K., Lakshminarayanan R. and Thomas, S., *Polymer*, **39**(6-7) (1998) 1483.
- [17] Geethamma V.G., Joseph R. and Thomas, S., *J. Appl. Polym. Sci.*, **55** (1995) 583.
- [18] Medalia A. I. and Kraus G. Reinforcement of elastomers by particulate fillers. In *Science and Technology of Rubber*, J. E. Mark, B. Erman, and F. R. Eirich, Eds., Academic Press, San Diego, Calif, USA, 2nd edition; 1994.
- [19] Tserki V., Matzinos P., Kokkou S. and Panayiotou C., *Composites, Part A*, **36**(7) (2005) 965.
- [20] Dannenberg E. M., Filler choices in the rubber industry the incumbents and some new candidates. *Elastomerics*, **113**(12) (1981) 30.
- [21] Bipinbal P. K., and Kutty, S.K.N., *J. Appl. Polym. Sci.*, **109**(3) (2008) 1484.
- [22] Boldizar A., Klason C., Kuba't J., Na'slund P. and Sa'ha P., *Int. J. Polym. Mater.*, **11** (1987) 229
- [23] Turi Edith A., *Thermal Characterization of Polymeric Materials*, Second Edition, Volume I., AcademicPress, Brooklyn, New York, 1997, P. 980.
- [24] Martins M. A. and Mattoso L. H. C., *J. Appl. Polym. Sci.*, **91** (2004) 670.

- [25] Ashida M., Noguchi T. and Mashimo S., *J. Appl. Polym. Sci.*, **30** (1985) 1011.
- [26] Ashida M., Noguchi T. and Mashimo, S., *J. Appl. Polym. Sci.*, **29** (1984) 661.
- [27] Payne, A.R., *J. Appl. Polym. Sci.*, **6** (1962) 57.
- [28] Sui G., Zhong W.H., Yang X.P., Yu Y.H. and Zhao S.H., *Polym. Adv. Technol.* **19**(11) (2008) 1543.
- [29] Silva V.P., Gonçalves M.C. and Yoshida I.V.P., *J. Appl. Polym. Sci.*, **101** (2006) 290.
- [30] Jacob M., Jose S., Thomas S. and Varughese K.T., *J. Reinf. Plast. Compos.* **25** (2006) 1903.
- [31] Sobhy M.S. and Tammam, M.T., *Int. J. Polym. Sci.* (2010) 1
- [32] Martins M. A., Pessoa J.D.C., Gonçalves P.S., Souza F.I. and Mattoso L.H.C., *J. Mater. Sci.*, **43** (2008) 6531.
- [33] Setua D.K. and Mathur G.N., *Polymer*, **79** (2001) 646.

.....✂.....



## NANOCELLULOSIC FIBER REINFORCED NATURAL RUBBER COMPOSITES

<b>C</b> <b>o</b> <b>n</b> <b>t</b> <b>e</b> <b>n</b> <b>t</b> <b>s</b>	<b>Part -A</b>
	<i>Mechanical properties of NR- Nanocellulosic Fiber Composites</i>
	<b>Part B</b>
	<i>Dynamic mechanical properties of NR- Nanocellulosic Fiber Composites</i>
	<b>Part C</b>
	<i>Thermal studies of NR- Nanocellulosic Fiber Composites</i>

### Part -A

#### Mechanical properties of NR- Nanocellulosic Fiber Composites

##### 5.A.1 Introduction

Cellulose is the most abundant natural material after silica. Because of its renewability, biodegradability, abundance and low cost, cellulose has been tried to be used for many different applications. One of the main areas where extensive research is being carried out is replacing petroleum derived synthetic materials with cellulose. Depletion of the petroleum reserves and danger of global warming has put great thrust on efforts in the substitution of synthetic polymers with natural alternatives. The high strength and mechanical properties of the cellulose makes it a suitable substitute for synthetic fibers.

According to Meier [1] and Heyn [2] elementary fibrils of diameter 3.5 nm formed from the cellulose molecules are universal structural units of natural cellulose. Blackwell and Kolpak [3] also reported the occurrence of elementary fibrils with diameters of approximately 3.5 nm in cotton and bacterial cellulose, thus giving supportive evidence about the basic fibrillar unit in cellulose microfibrils. According to Meier, microfibrils are agglomerates of elementary fibrils and always have diameters which are multiples of 3.5 nm. The bundling of elementary fibrils into microfibrils is caused by a pure physical coalescence as a mechanism of reducing the free energy of the surfaces [4]. The maximum diameter of a microfibril was proposed to be 35 nm.

Natural fibres have been applied as the raw material for the production of a fibrillated material, which was introduced and defined as microfibrillated cellulose (MFC) by Turbak et al. [5] and Herrick et al. [6] Several modern and high-tech nano-applications have been envisaged for MFC.

Over the years, the fibrillated materials have been endowed with various nomenclatures, such as nanofibrillated cellulose, nanofibers, nanofibrils, microfibrils and nanocellulose[7-11]. Here the individual fibrils are in nanometer dimensions and the fibrillated material will be referred to as nanofibrillated cellulose.

In this study nanofibrillated cellulose prepared from Coir fibers is used to prepared composites based on natural rubber. The mechanical, dynamic mechanical and thermal properties are investigated with respect to nanofibril loading.

## **5.A.2 Experimental**

### **5.A.2.1 Materials Used**

Concentrated natural rubber latex (60 DRC) was procured from Njavally Latex Pvt Ltd., Coir microfiber dispersion in water, Zinc oxide, stearic acid, TQ (1,2-dihydro-2,2,4-trimethylquinoline), CBS (cyclohexylbenzthiazylsulfenamide) and sulfur used were of commercial grade. Hexa (hexamethylenetetramine) resorcinol and sodium chlorite were supplied by Merck Ltd, Mumbai. Hydrochloric acid – 3.5 and 5 M solution, Sodium hydroxide – 5% solution.

### **5.A.2.2 Processing**

The chemical composition of the coir fiber is given in Table 5.1 [12]. Coir was subjected to chemical and mechanical treatments to reduce it to micrometer sized short fibers with a diameter range of 8-11 micrometers and an aspect ratio of 35 to 65. The dispersion of coir microfibers in water was taken as the starting material. The details of conversion of coir macro fibers to microfibers are described in previous chapter.

#### **5.A.2.2.1 Bleaching and homogenization**

Bleaching is carried out to remove lignin and hemicellulose which is remaining even after the two successive alkali treatments meted out to the fibers, first, in the macro form and then to the comminuted microfibers in the dispersion. Bleaching was based on a method proposed by Wise et al. [13] which was modified to get nanofibrillated cellulose fibers. To 100 g of water dispersion containing 4% by weight of short coir microfibers 4g of sodium chlorite was added together with 1 ml of glacial acetic acid. The dispersion was kept at 60 °C for 2 hours. Afterwards it was washed free of acid with distilled water. The process was repeated with 2 g of sodium chlorite and 0.5 ml of glacial acetic acid. The bleached fibers were then washed free of acid and homogenized in a

homogenizer (IKA Homogenizer model T25 digital S22) at 16000 rpm for 2 hours to facilitate fibrillation of the material to nanofibrillated cellulose.

#### **5.A.2.2.2 Preparation of composites**

The water dispersion both in bleached and homogenized sates were used as such, in natural rubber latex for composite preparation according to the method described in previous chapters. The dispersions were added to concentrated natural rubber latex. It was mixed well and coagulated using dilute acetic acid in successive layers. The coagulum obtained was squeezed between rollers to remove water. The sheet obtained was dried in an air oven at 40 °C for three days. Fiber loading was adjusted to get 2.5, 5, 10 and 20 phr of nanofiber in the final composites. The composites were then processed like conventional sheet rubber.

Formulation of the mixes is given in table 5.2. The mixes were prepared according to ASTM D 3182 on a laboratory size two-roll mixing mill. Cure characteristics of the mixes were determined by using Rubber Process Analyzer model RPA 2000 at 150°C. Nano fibers were oriented in the mill direction by passing through tight nip in the mill at the end of the mixing process. The thin sheets obtained were cut in the required dimensions and stacked one above the other to the desired volume. The sheets were vulcanized at 150<sup>0</sup>C under a pressure of 180 kg/cm<sup>2</sup> in an electrically heated hydraulic press to their respective cure times. The samples obtained were tested for mechanical properties according to relevant ASTM standards.

#### **5.A.2.2.3 Scanning electron microscopy**

The dispersions at bleached and homogenized stages were examined with scanning electron microscopy using 6390LA JEOL instrument. A drop of

dispersion was placed on the carbon tape and allowed to evaporate the water completely. The samples were gold plated to suppress specimen charging.

An ultra-high resolution FE-SEM (Hitachi S-4800) employing a cold field emission electron source was also used for structural analysis. A drop of the dispersion was placed on the carbon tape and allowed to evaporate the water completely. Prior to FE-SEM imaging, samples were vacuum dried and specimen charging was suppressed by coating with gold (3 nm thickness) using an Agar HR sputter coater. The accelerating voltage was 1kV current 10uA. The surface was scanned to study the fiber characteristics and to determine the dimensions.

#### **5.A.2.2.4 Atomic force microscopy**

Dispersion of the nanofibrillated material after homogenization process was cast into a sheet. The smooth surface of the sheet was probed with AFM in non contact mode. The instrument used was Agilent 5500 AFM.

#### **5.A.2.2.5 X-ray diffraction**

The homogenized sample was cast into a sheet. A small portion was cut from the sheet and used for HRXRD using the instrument PANalytical XPert Pro High Resolution X-Ray diffractometer. The scan range was from 5 to 80 2 $\theta$ .

**Table 5.1 Chemical composition of Coir**

Cellulose	32–43%
Lignin	40–45%
Hemi-cellulose	0.15–0.25%
Pectins and related compounds	3–4%
Moisture Content	8

**Table 5.2 Formulation of the mixes**

<b>Ingredients</b>	<b>Phr</b>
NR	100
Fiber	2.5, 5, 10 &20
Zno	4
Stearic acid	2
TQ	1
CBS	1
Sulphur	2
Hexa	1.6
Resorcinol	2.5

### 5.A.3 Results and discussions

#### 5.A.3.1 Fiber characterization

##### 5.A.3.1.1 Lignin content

**Table 5.3 Lignin content**

<b>Lignin content (%)</b>	
<b>Unbleached</b>	<b>Bleached</b>
22.4	0.74

Lignin content of the fibers are given in table 5.3. When the microfibers in the pulp form were bleached the lignin content was reduced from 22.4% to 0.74%. This drastic decrease in the lignin content was expected to reduce the bonding between the fibrils in cellulose and rendering a nanofibrillated material, which was confirmed by SEM and AFM.

**5.A.3.1.2 Infrared spectroscopy**

**5.A.3.1.3 Scanning electron microscopy**

**a). After bleaching**

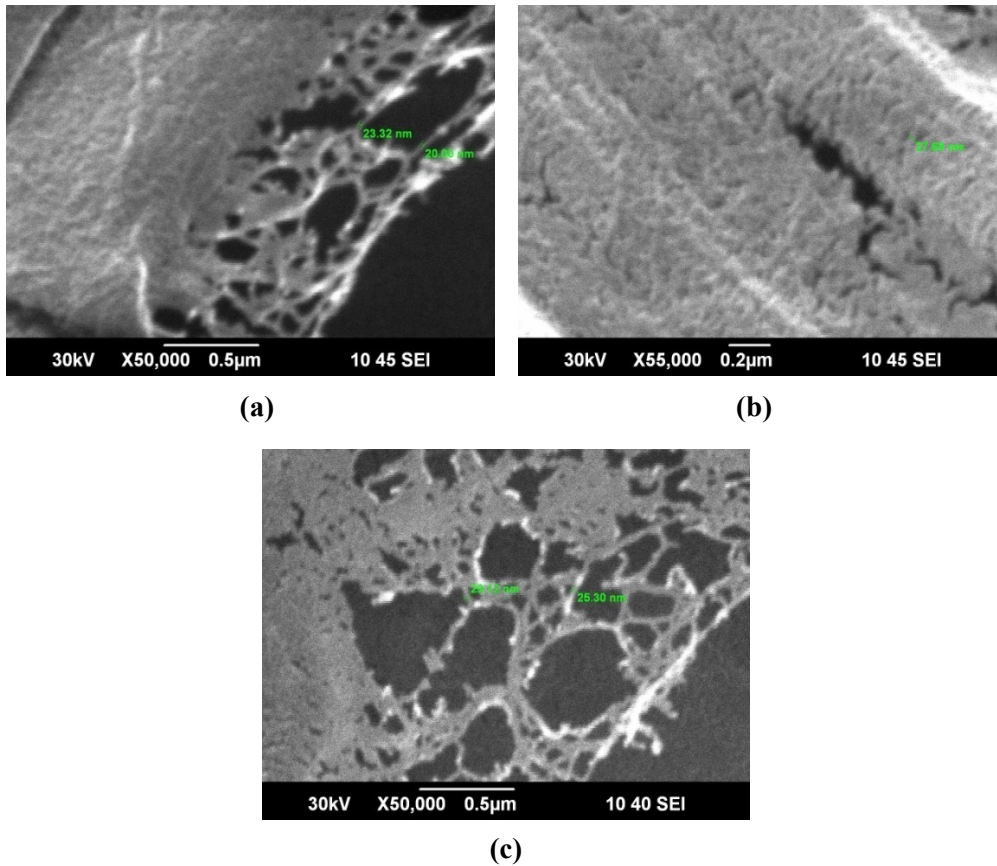


**Figure 5.1 (a, b and c) SEM images of the bleached fibers**

Figures 5.1a, 5.1b and 5.1c show the morphology of the bleached fibers as seen through scanning electron microscope. After the removal of the lignin content the microfibrils separate into fibrils of nanometer dimension. As can be seen from the images fibrils are still retained in a network like structure. This is due to the small amount of lignin and hemicellulose remaining in the fibers and high intermolecular hydrogen bonding between the cellulose molecules. Further separation of the fibrils in the loose

network can be achieved through high shearing forces applied in the homogenization process. Since the bleached fibers themselves are in a state of considerable fibrillation, the fibers in bleached stage as such were used to make composites, in the hope of completing the fibrillation by the shear forces developed in the mixing process. Bleached fibers were incorporated into natural rubber in latex stage by the process described earlier.

**b). After homogenization**

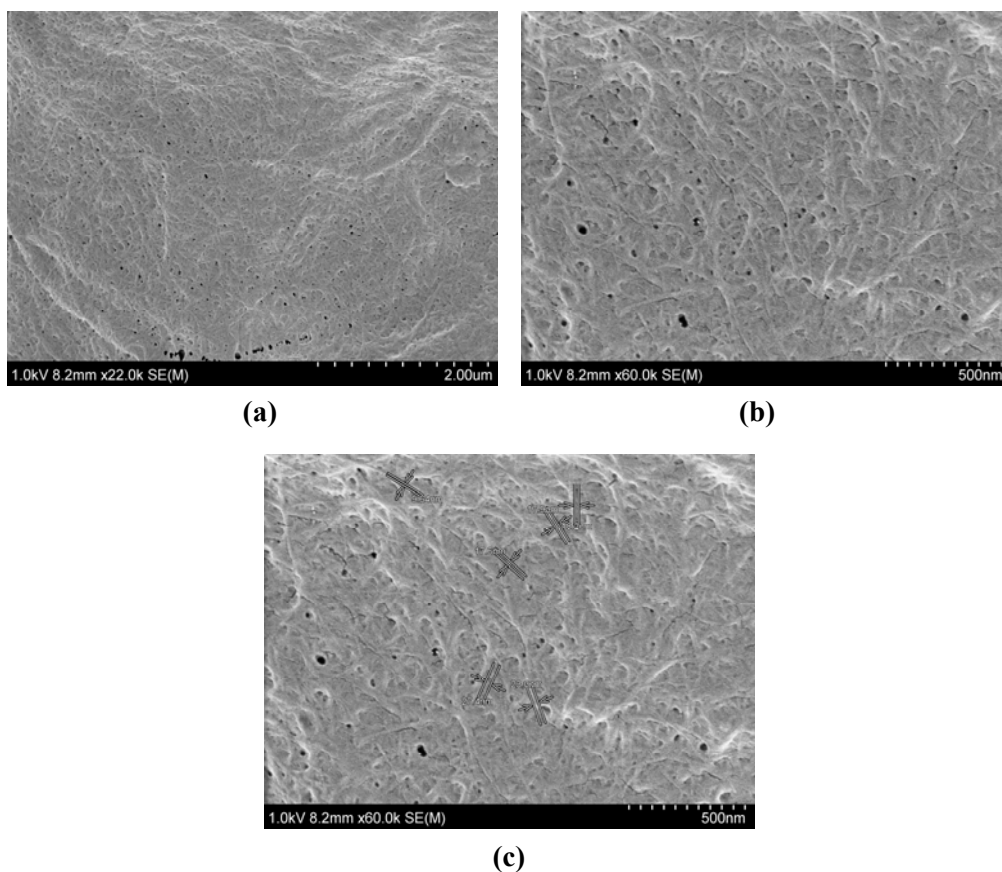


**Figure 5.2 (a, b and c) FESEM images of Homogenized fiber**

Figures 5.2a, 5.2b and 5.2c show the FESEM images of homogenized fiber. It can be seen that, uniform fibrillation is more evident in the homogenized sample. The cellulose fibers get separated into individual fibrils of diameter about 18 nm. The shear forces in the homogenizer make the fibrillation more efficient. The distribution and dispersion of these fibrils in the rubber matrix will be more efficient. Better dispersion of fibrils will result in better reinforcement of the composites.

#### **5.A.3.1.4 Atomic force microscopy**

AFM images of the nanofibrillated cellulose after homogenization are shown in Figures 5.3(a, b, c and d). 5.3(a) and 5.3(b) show 2D images in 1  $\mu\text{m}$  and 500 nm scans respectively. Figures 5.3(c) and 5.3(d) show the 3D images. The nanofibrillated state of the fibers can be clearly seen in the images. The diameter of the fibrils is nearly 20 nm. The fibrillation is seen to be uniform throughout the sample. Since the fibers were in an entangled state the length of the fibers could not be measured from the images.

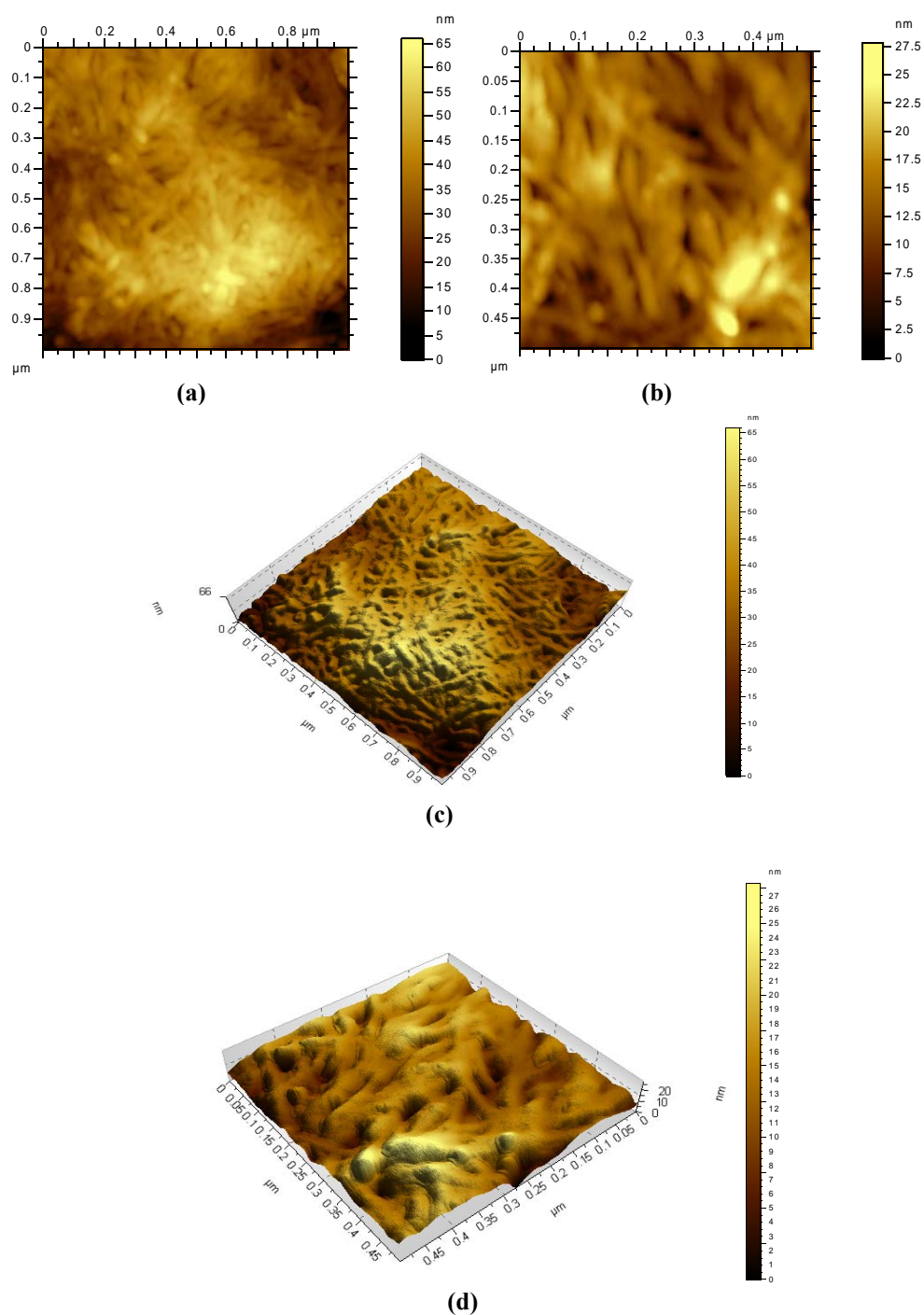
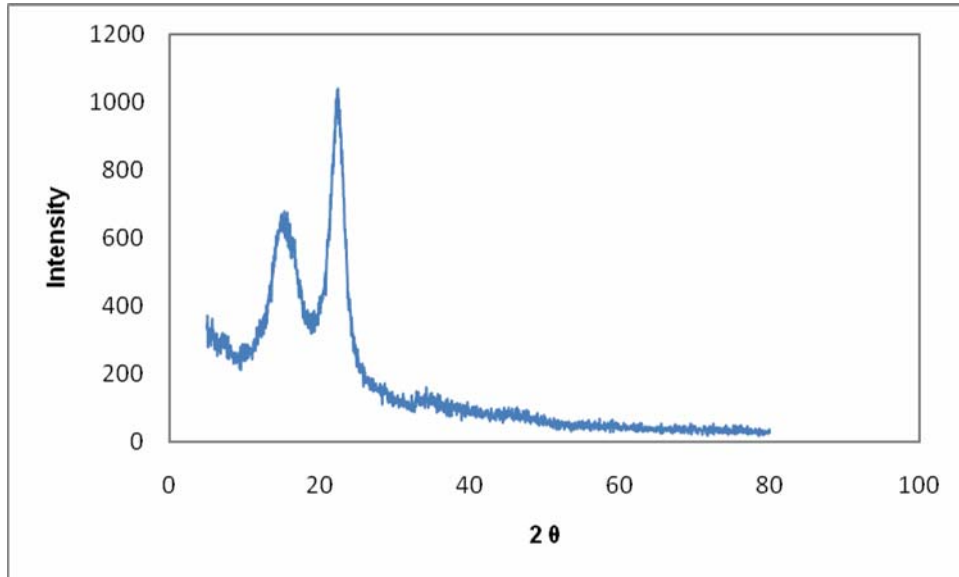


Figure 5.3 (a, b, c and d) AFM images of nanofibrillated cellulose after homogenization

### 5.A.3.1.5 X-ray diffraction



**Figure 5.4 X-ray diffraction pattern of nanofibrils after homogenization**

XRD spectrum of nanofibrillated cellulose after homogenization is given in figure 5.4. The spectrum is similar to that of Whatman- 1 filter paper reported by Das et al. [14]

The crystallite size was calculated by using the Scherrer equation,

$$L_{h,k,l} = K\lambda/b\cos\theta$$

where,  $K = 0.94$ , [15] and was found to be 5.17 nm which is close to the crystallite size reported for filter paper.

### 5.A.3.2 Composite characterization

Composites of nanofibrillated cellulose after bleaching are designated as BL and those after homogenization are designated as HO. This sample designation is followed throughout.

### 5. A.3.2.1 Cure characteristics

#### 5. A.3.2.1.1 Cure time and scorch time

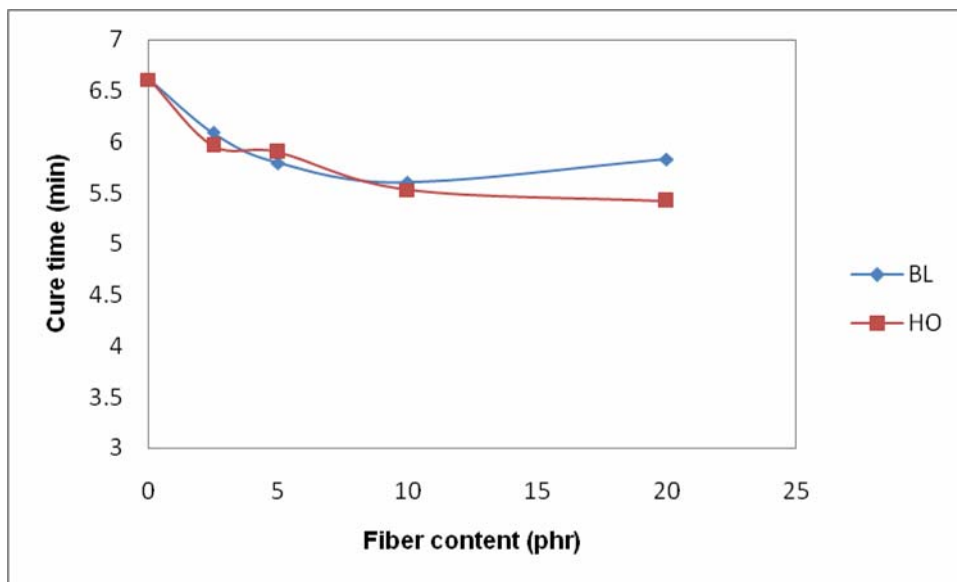


Figure 5.5 Variation of Cure time with fiber content

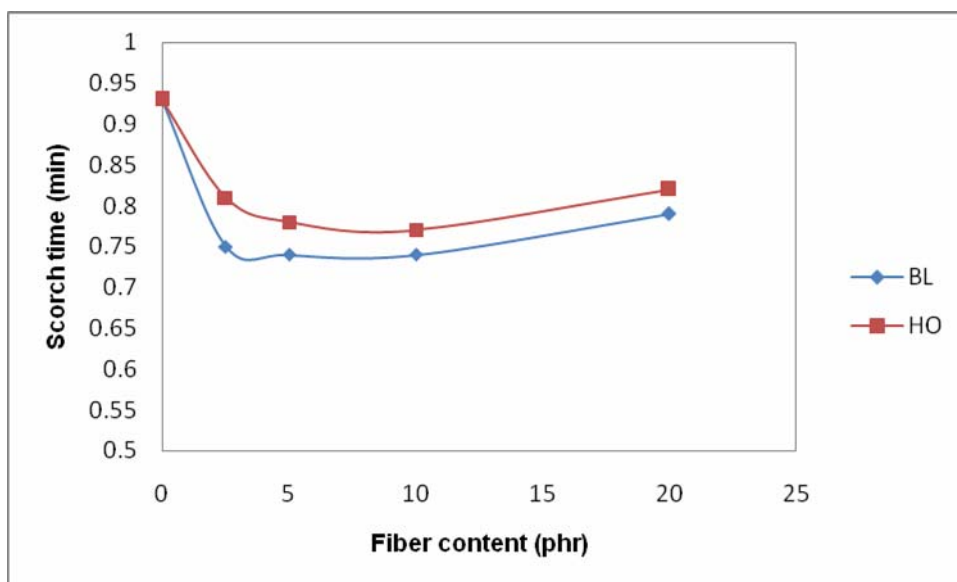


Figure 5.6 Variation of Scorch time with fiber content

Figure 5.5 shows the variation of cure time with fiber content of the composites containing bleached and homogenized fibers. The cure time is found to be reduced in both the cases with a leveling effect at higher fiber content. The reduced cure time indicates a marginally higher rate of cure reaction in the presence of the nanofibers.

The variation of scorch time with nanofiber content is shown in Fig. 5.6. The reduced scorch time in the case of composites containing nano fibers indicates a relatively fast onset of cure reaction. This may be due to relatively higher heat generation during processing of these composites. With the fibers in, the matrix becomes stiffer leading to higher heat generation during shearing process.

#### 5.A.3.2.1.2 Differential torque

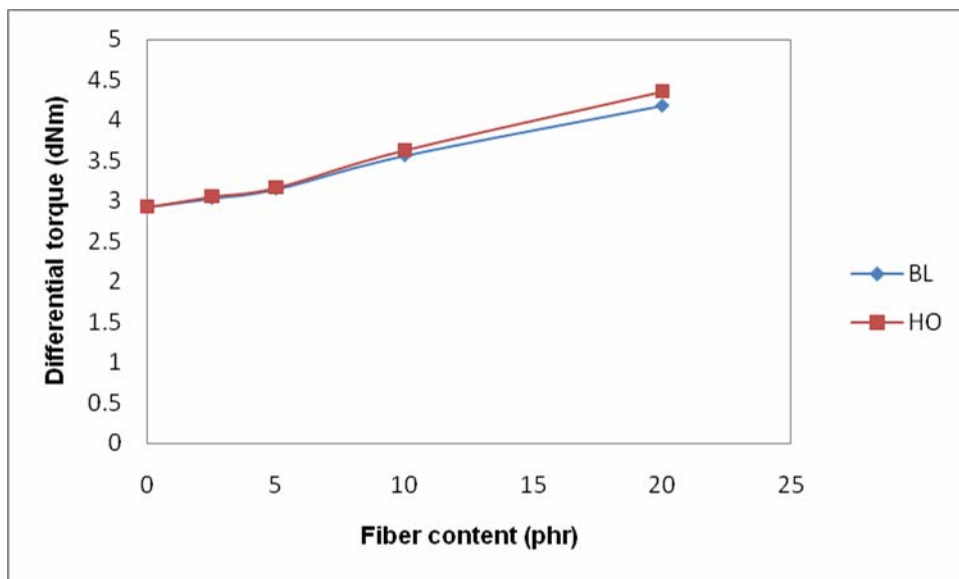


Figure 5.7 Variation of Differential torque with fiber content

Figure 5.7 shows the variation of differential torque, which is the difference between maximum and minimum torque experienced in Rubber Process Analyzer during cure time determination. It can be considered as a measure of crosslink density or stiffness of the composites. The differential torque increases linearly with the fiber content showing the increasingly restrained nature of the rubber matrix upon fiber loading, due to the reinforcing ability of the fibers. Homogenized (HO) and bleached fiber (BL) composites show almost similar variation with increasing fiber content

### 5.A.3.2.2 Mechanical properties

#### 5. A.3.2.2.1 Tensile strength

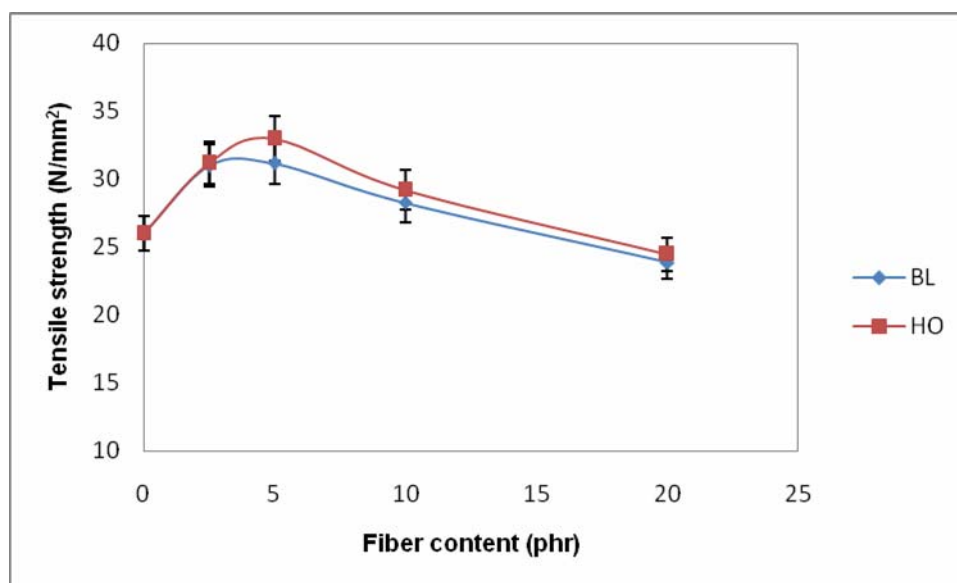
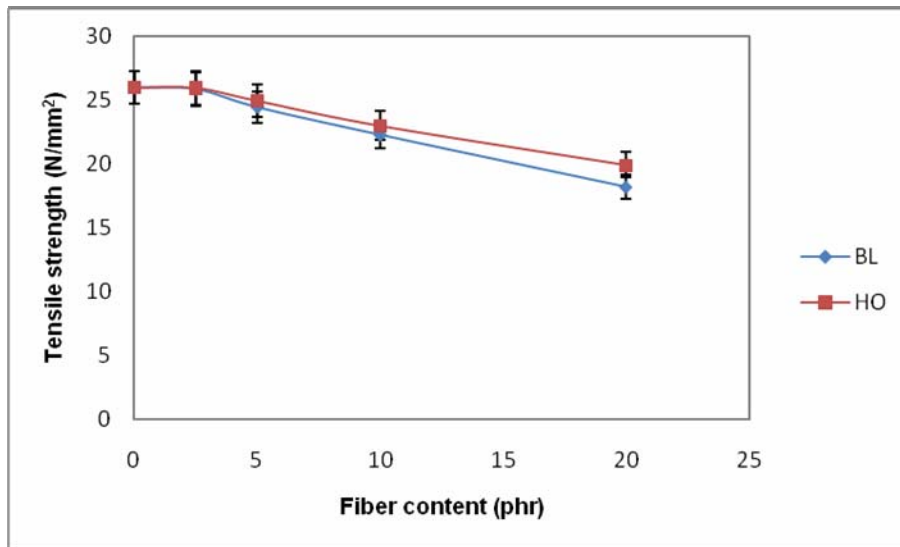


Figure 5.8 Variation of tensile strength (Longitudinal) with fiber content



**Figure 5.9 Variation of tensile strength (Transverse) with fiber content**

The effect of the nanofibers on the tensile strength of the composites in longitudinal direction is shown in figure 5.8. For both BL and HO composites tensile strength increases with fiber content upto 5phr loading. On further loading of fibers, tensile strength decreases. As evident from the SEM and AFM images the fibers in the bleached and homogenized sample are in a state of nanofibrillation. Though the fibers are separated they still maintain a network like consistency. Due to the high shearing forces in the developed during the mixing of the composites the network structure breaks and the fibrils get distributed throughout the matrix in a uniform fashion. This can be clearly observed from the SEM pictures of the fracture surface of the composites (figures 5.20(a), 5.20(b), 5.21(a) and 5.21(b)). The increased surface area of the cellulose fibrils facilitates a large number of sites for bonding with the rubber matrix through the insitu formed resorcinol formaldehyde bonding agent. This naturally will increase the reinforcement of the matrix and results in increased tensile strength of the composites. Beyond the loading of 5 phr, dispersion of fibrils in the rubber matrix may not be sufficient causing agglomeration of the

fibrils. At large strains the fiber- fiber interaction in these agglomerates may not be sufficient to hold them together and cracks will initiate. These cracks will act as points of stress concentration. At higher strains the composite break at these points giving lower tensile strength values without realizing the full potential of the reinforcement imparted by the cellulose fibrils. The HO composites show marginally better values than BL composites. This is due to better fibrillation in the case of HO composites leading to better dispersion of fibrils in the rubber matrix without agglomeration.

Figure 5.9 gives the tensile strength in the transverse direction of the nano composites. Since the fibrils will be arranged in a direction perpendicular to the application of tensile load effective stress transfer will not be taking place. The fibrils will mostly act as diluting constituents to the matrix. With increase in fiber content the dilution of matrix also increases leading to lower tensile strength values.

#### 5.A.3.2.2.2 Modulus

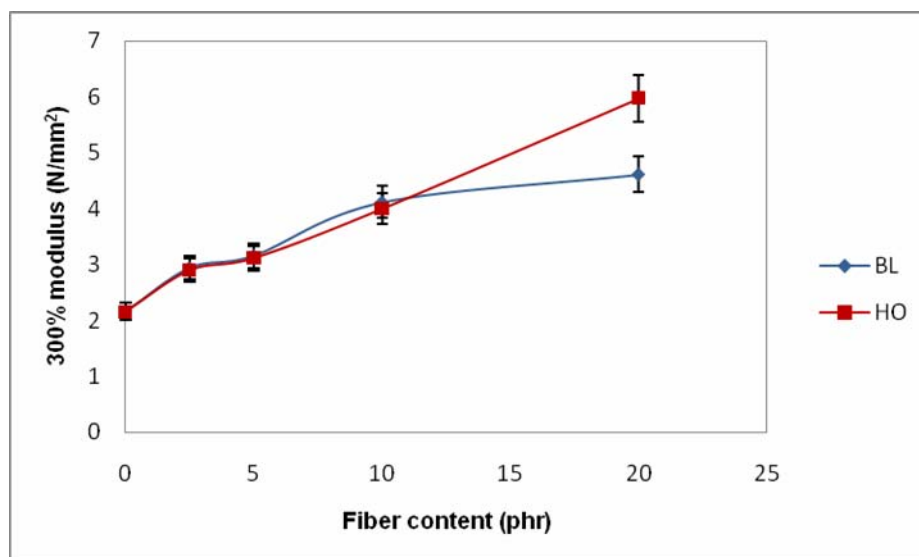
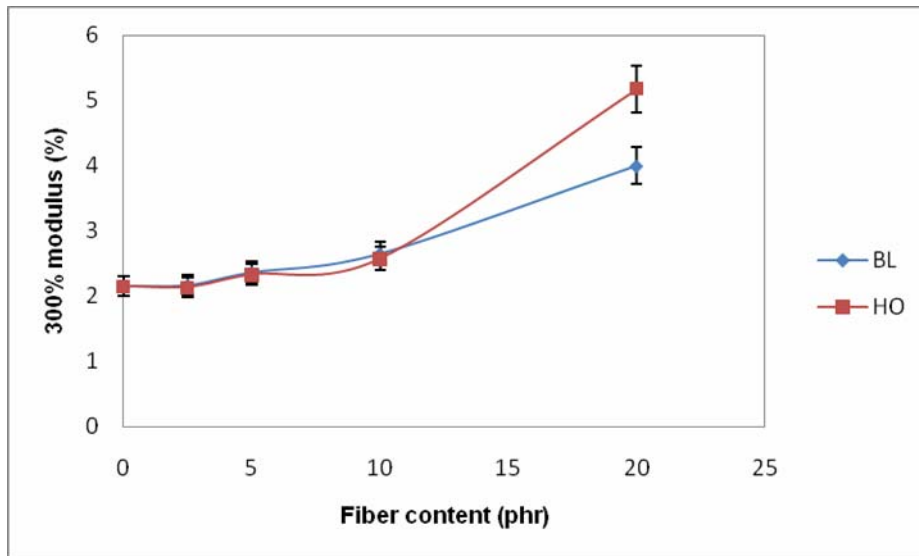


Figure 5.10 Variation of modulus (Longitudinal) with fiber content



**Figure 5.11 Variation of modulus (Transverse) with fiber content**

Figure 5.10 shows the variation of modulus of the BL and HO composites with fiber content. The modulus goes on increasing with fiber content unlike in the case of tensile strength where the property decreases beyond a loading of 5 phr. The modulus which is measured at low strains is not affected by the stress concentration at agglomerates of fibrils at higher fiber loadings which causes the reduced tensile strength at higher elongations. At the fiber loading of 20 phr, HO composite shows considerable improvement in modulus over that of BL composites. The better dispersion and resulting improved reinforcement in the case of HO composites is the reason for this behavior.

Figure 5.11 shows the modulus of composites in the transverse direction. Modulus increases with fiber content, but the increase is lower compared to the modulus in longitudinal direction. The fibers arranged in transverse direction also contribute to the stiffening of the matrix, but at a lower scale. In transverse modulus also HO composites show higher values than BL composites. This is due to the better dispersion of fibrils in the composites.

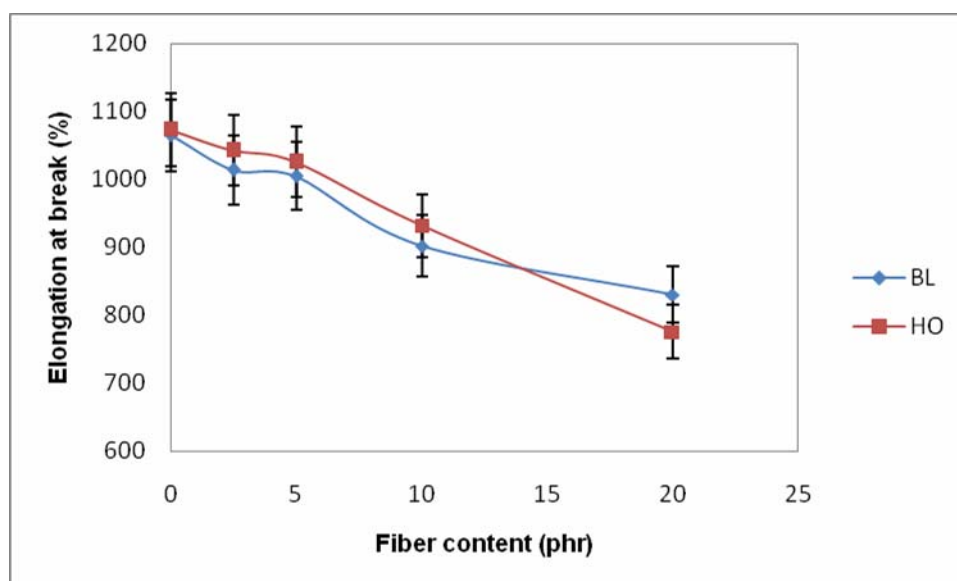


Figure 5.12 Variation of elongation at break (Longitudinal) with fiber content

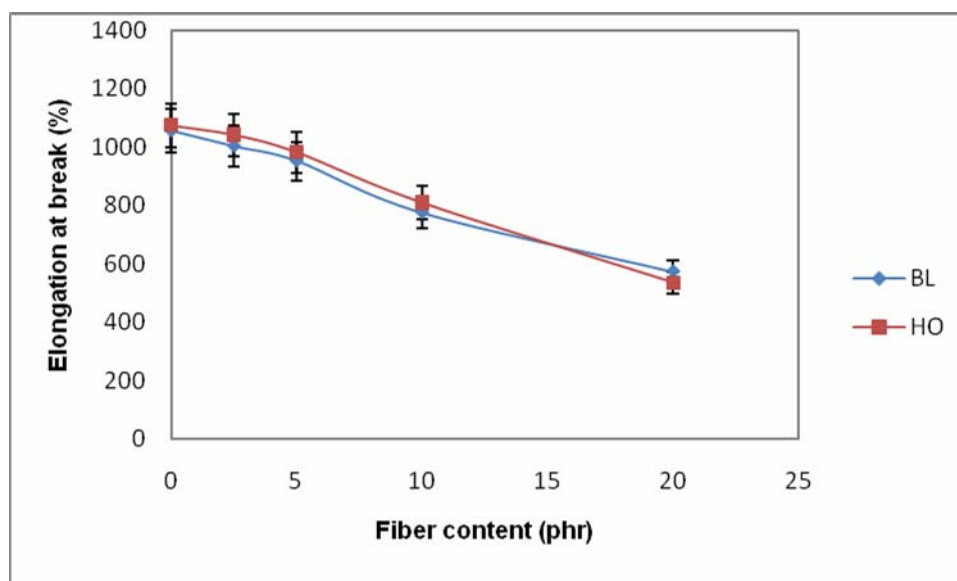


Figure 5.13 Variation of elongation at break (Transverse) with fiber content

Elongation at break in longitudinal direction is plotted against fiber content in figure 5.12. Elongation at break steadily decreases with fiber

content. The decrease is caused by the higher reinforcement imparted to the matrix by the cellulosic fibrils. The large decrease at 10 and 20 phr fiber loading may be due to premature failure of the composites by the crack propagation, originating from the agglomerates of fibrils at these loadings.

Figure 5.13 shows the variation of elongation at break in transverse direction with fiber content. The elongation decreases with fiber content. The values are lower than that in the longitudinal direction. The fibrils in the transverse direction are less effective in stress transfer and will get debonded from the matrix at lower elongations than the fibrils arranged in longitudinal direction leading to premature failure.

#### 5.A.3.2.2.4 Tear strength

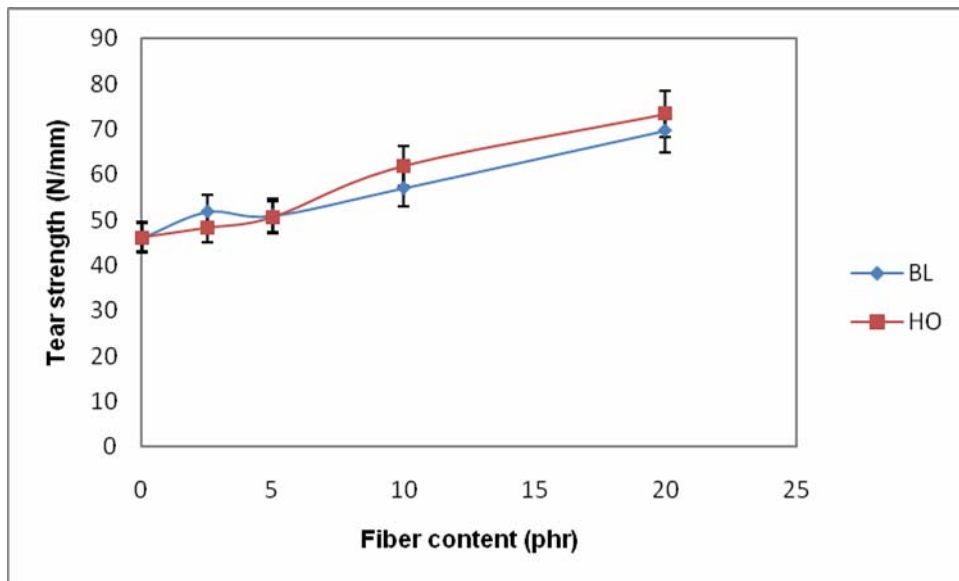
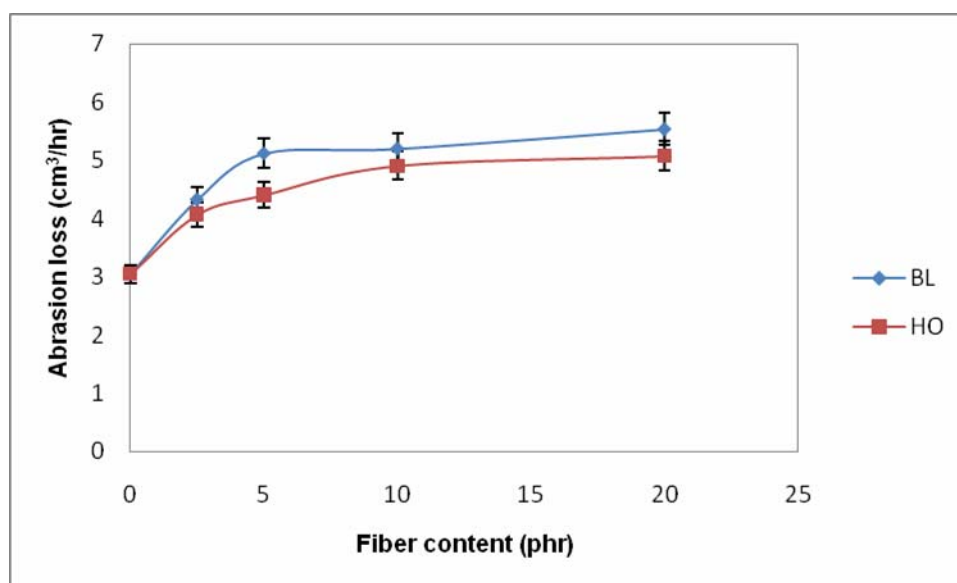


Figure 5.14 Variation of tear strength with fiber content

Figure 5.14 shows the variation of tear strength of BL and HO composites with fiber content. The tear strength increases with fiber content. The crack propagation direction in the tear strength experiment is in

perpendicular to the direction of arrangement of fibrils. With increase in fiber content the resistance to crack propagation will be increased leading higher tear strength values.

#### 5.A.3.2.2.5 Abrasion loss



**Figure 5.15** Variation of abrasion loss with fiber content

Figure 5.15 shows the effect of fiber content on abrasion loss. In contrast to other type of fibers the abrasion loss increases with increasing fiber content. The cellulosic fibers in the nanofibrillated state with very low lignin content may be more prone to abrasion than the rubber matrix. The increasing amount of fiber will increase the amount of material being abraded resulting in higher abrasion loss. The chances of fiber agglomeration are more in BL composites. At these agglomerates abrasion loss will be more compared to areas with well dispersed fibrils. So the BL composites show higher abrasion loss than HO composites.

### 5.A.3.2.2.6 Hardness

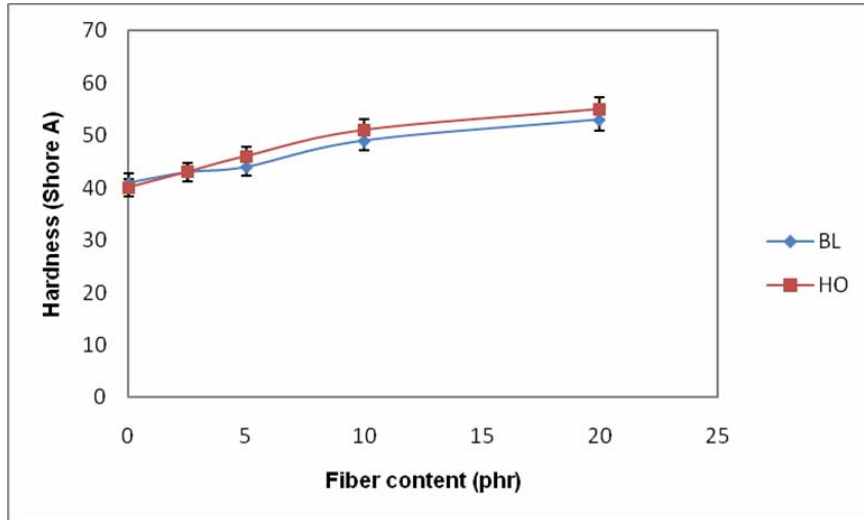


Figure 5.16 Variation of hardness with fiber content

Figure 5.16 shows the variation of hardness with fiber content. For both type of composites hardness increases with fiber content, HO composites being marginally better. This may be due to better dispersion of fibrils and resulting better reinforcement in HO composites.

### 5.A.3.2.2.7 Resilience

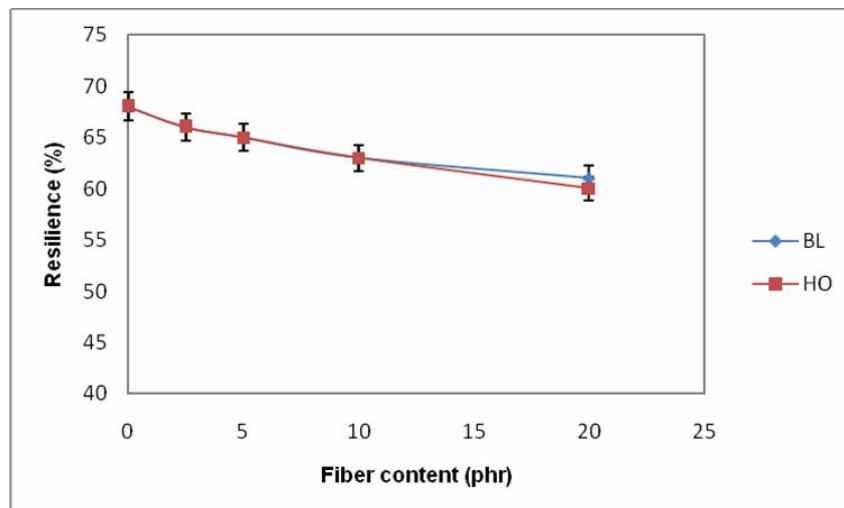


Figure 5.17 Variation of resilience with fiber content

The effect of fiber content on resilience of the composites is given in figure 5.17. Resilience decreases with increase in fiber content. This may be due to energy being dissipated at the fiber matrix interface. At higher fiber content the interfacial area will be dissipating more energy, giving lower resilience.

### 5.A.3.2.3 Ageing resistance

Ageing resistance of the composites reinforced with nanofibrillated cellulose is given in figures 5.18 and 5.19. Figure 5.18 gives the retention percentage of tensile strength and figure 5.19 retention percentage of modulus of the composites. For the gum composites the retention percentage of tensile strength is more than 100%. This may be due to the post curing of resorcinol formaldehyde remaining unreacted in the vulcanized composites. With increase in fiber content the retention percentage decreases due to the lower thermal resistance of cellulosic fibrils. This is supported by the behavior of composites in thermal analysis. In the case of modulus the retention percentage initially decreases and then increases until 10 phr fiber content. At lower elongations in which moduli are measured, the decrease in properties of the cellulosic fibrils due to ageing is less pronounced.

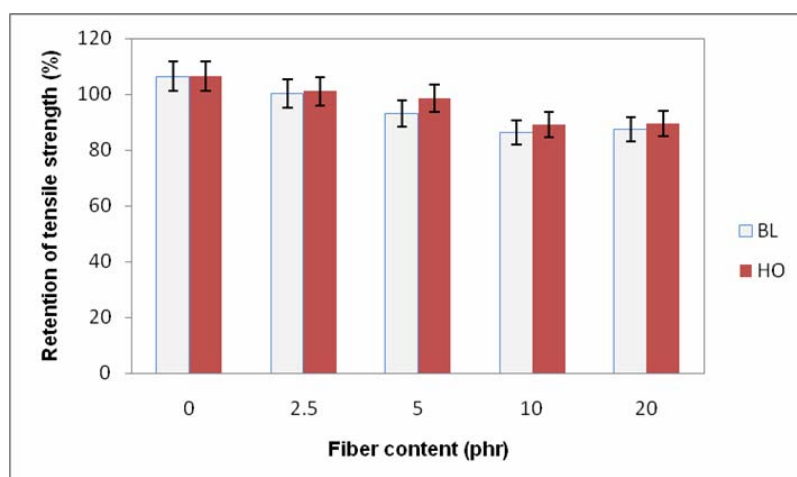


Figure 5.18 Variation of retention in tensile strength with fiber content

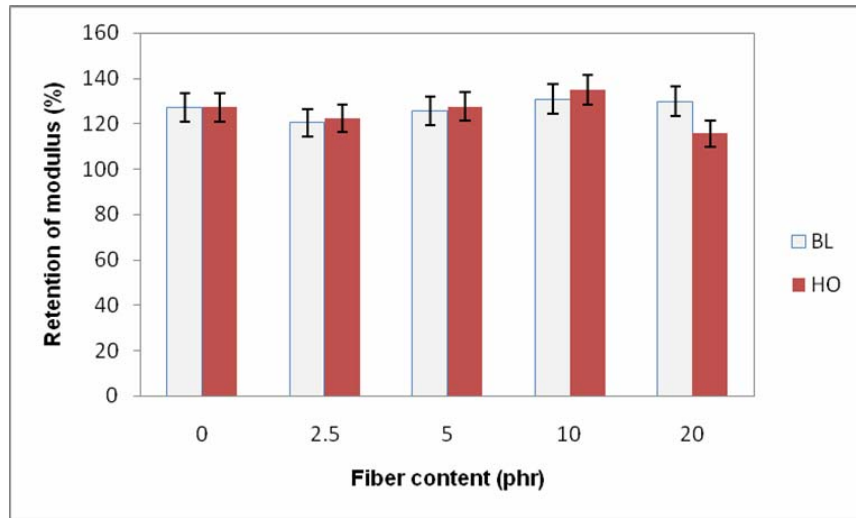


Figure 5.19 Variation of retention in modulus with fiber content

#### 5.A.3.2.4 SEM Analysis

##### a). Composites of nanofibrillated cellulose after bleaching

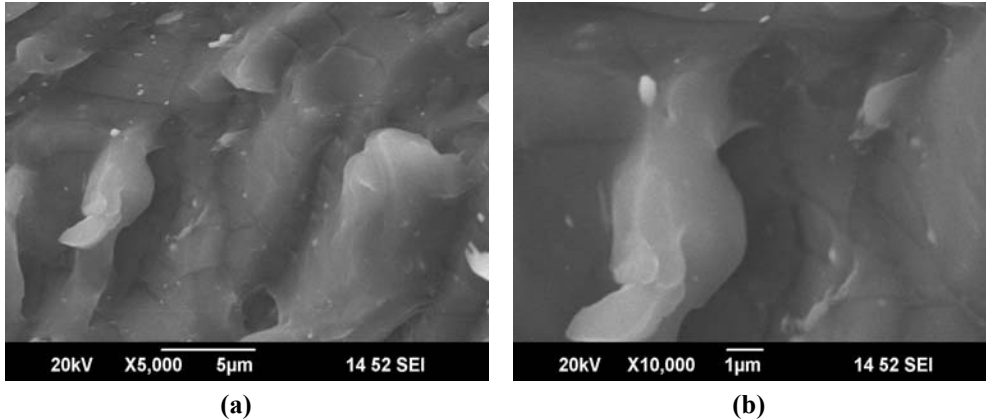
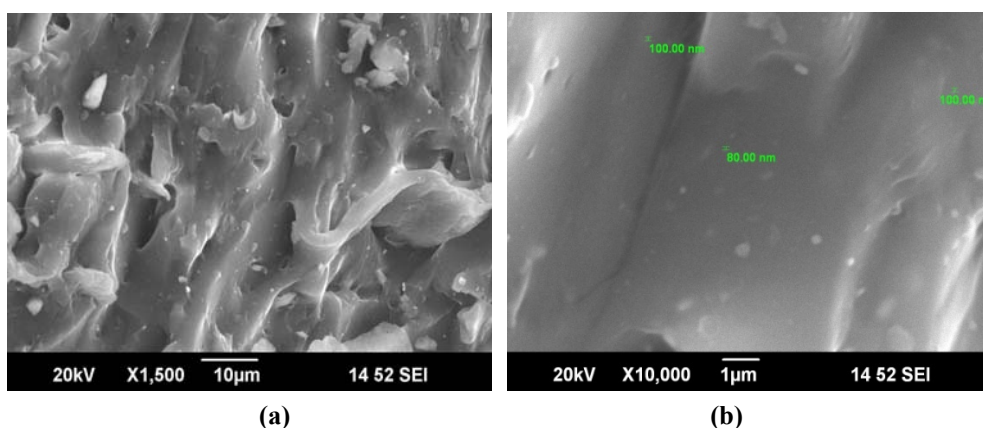


Figure 5.20 (a and b) Tensile fracture surface of composites of nanofibrillated cellulose after bleaching

The tensile fracture surface of the vulcanized NR/nanofibrillated cellulose (after bleaching) composites with 5 phr fiber loading was analyzed by scanning electron microscopy. From the SEM images (Figures 5.20a and 5.20b) it can be seen that the fibers which were in a network consistency were

separated into individual fibrils and dispersed uniformly in the rubber matrix. As expected the high shear forces developed during the mixing process play their part in the separation and distribution of fibrils throughout the matrix. This fine distribution of high strength nano fibrils improved the mechanical properties of the composites.

**b). Composites of nanofibrillated cellulose after homogenization**



**Figure 5.21 (a and b) Tensile fracture surface composites of nanofibrillated cellulose after homogenization**

Figures 5.21(a) and 5.21(b) show tensile fracture surface of the vulcanized NR/nanofibrillated cellulose (after homogenization) composites with 5 phr fiber loading. It can be seen that the fibrils are well dispersed and distributed throughout the matrix. The fracture surface of HO composites is rougher and jagged compared to BL composites. This is due to better dispersion of homogenized fibrils and ensuing better properties compared to bleached fibrils.

#### 5.A.4 Conclusions

Nanocellulosic fibers were extracted from coir fibers through a simple cost effective process of bleaching and homogenization. After bleaching the lignin content in the sample was reduced to 0.74 % facilitating nanofibrillation.

Morphological studies of the bleached sample showed a state of limited nanofibrillation. The bleached samples were subjected to homogenization for complete fibrillation of the material. FESEM and AFM studies revealed that uniform fibrillation could be achieved and the fibrils were of about 18 nm in diameter.

The nanofibrillated cellulose both in bleached and homogenized state were used to reinforce natural rubber composites through latex stage processing method. Cure characteristics and mechanical properties of these composites were evaluated. The addition of nanocellulosic fibers reduced the cure time and scorch time indicating a faster cure reaction. Differential torque increased with fiber content indicating a more restrained matrix.

Mechanical properties of the composites were improved by the addition of nanofibers. Tensile strength showed a maximum at 5 phr fiber loading in the longitudinal direction. Elongation at break decreased with fiber loading. Modulus and tear strength increased with fiber content. The properties were lower in the transverse direction. Hardness and abrasion loss increased with fiber loading while resilience decreased. Ageing resistance of the composites decreased in general with fiber content.

Morphological studies of the fracture surface of the composites revealed a matrix with well distributed and dispersed nanofibrils. The composites homogenized samples showed a rougher fracture surface indicating better reinforcement.

Nanofibrillated cellulose obtained from coir is an effective reinforcing material for natural rubber composites.

**Part -B**

**Dynamic mechanical properties of NR- Nanocellulosic Fiber Composites**

**5.B.1 Introduction**

There have been many studies on the dynamic mechanical properties of short natural microfiber reinforced rubber composites. Abdelmouleh and Boufi [16] studied dynamic mechanical and thermal properties of composites materials based on four different cellulose fibres (raw and chemically modified) as reinforcing elements in low density polyethylene and natural rubber. Maya [17] et al. studied the dynamic mechanical properties of sisal/oil palm hybrid fiber-reinforced natural rubber composites and found that storage modulus and loss modulus increased with fiber loading. Dynamic mechanical behavior of short coir fiber- natural rubber composites was studied by Geethamma et al. and found that interfacial bonding affects damping properties of composites [18]. Rabu and Wirjosentono studied dynamic properties and swelling behaviour of bamboo fiber filled natural rubber composites [19]. Coming to the effect of nanofillers on dynamic mechanical properties of elastomer composites, Sui et al. [20] studied pretreated carbon nanotube/natural rubber composites using DMA. Thomas et al. looked into the effect of phenol functionalization of carbon nanotubes on properties of natural rubber nanocomposites [21]. Effect of cellulose nanofibers isolated from bamboo pulp residue on mechanical and dynamic mechanical properties of vulcanized natural rubber [22] was studied by Visakh et al.

In this section the effect of nanofibrillated cellulose on the dynamic mechanical properties of natural rubber composites prepared through latex stage processing is presented. RPA and DMA were used as the tools for the

study. Dynamic mechanical properties in cured and uncured state were examined using RPA. DMA was used to study the vulcanized composites.

## **5.B.2 Experimental**

5 cm<sup>3</sup> of the uncured fiber mixes were cut using a punch and placed in the sealed biconical cavity of the Rubber Process Analyzer and subjected to strain sweep program. The samples were kept at the test temperature of 60 °C for a preheating time of 4 minutes. It is then subjected to a strain sweep with varying strains of 0.05, 0.1, 0.2, 0.5, 1, 2, and 5 degrees in a single sweep. The complex modulus values obtained were plotted against strain in degrees. For strain sweep studies in cured state, uncured samples were first vulcanized to their respective cure times at 150 °C. The temperature was then reduced to 60 °C and the sample was subjected to strain sweep as above.

TA Instruments DMA Q800 was used to measure the dynamic mechanical properties of the NR-nanofibrillated cellulose composites. Test specimens having a dimension of 30 mm x 3 mm x 2 mm were used in tension mode. Temperature sweep and frequency sweep experiments were conducted. Temperature sweep experiments of the composites were performed from -80°C to +40°C. Frequency was set at 1 Hz and amplitude 15 μm. Frequency sweeps were conducted over a frequency range of 1Hz to 30 Hz at 40 °C. The amplitude was fixed at 15 μm.

## **5.B.3 Results and Discussion**

### **5.B.3.1 Strain sweep studies in RPA**

Figure 5.22 shows the variation of complex modulus with strain in RPA, for natural rubber/nanofibrillated cellulose (after bleaching), composites in uncured state. At very low strains, the modulus is an indication of filler-filler interaction or filler agglomeration. The gum composites have the lowest

modulus and the lowest decrease in modulus with strain. With increase in fiber content, modulus at low strain increases indicating filler agglomeration. For 10 phr and 20 phr composites initial modulus is much higher but drops to a much lower value on higher strains. This may be due to the breakdown of fiber agglomeration at higher strains. For 2.5 and 5 phr composites, initial modulus is low. For these composites the decrease in modulus with strain is also low. The lower initial modulus indicates better fiber dispersion in the case of these composites. For each compound modulus decreases with strain amplitude. At large strains the modulus values all composites tend to converge towards a single value showing Payne effect [23]. At high amplitudes of strain breakdown of the fiber-rubber network occurs leading to a drop in modulus of composites towards that of the gum composites.

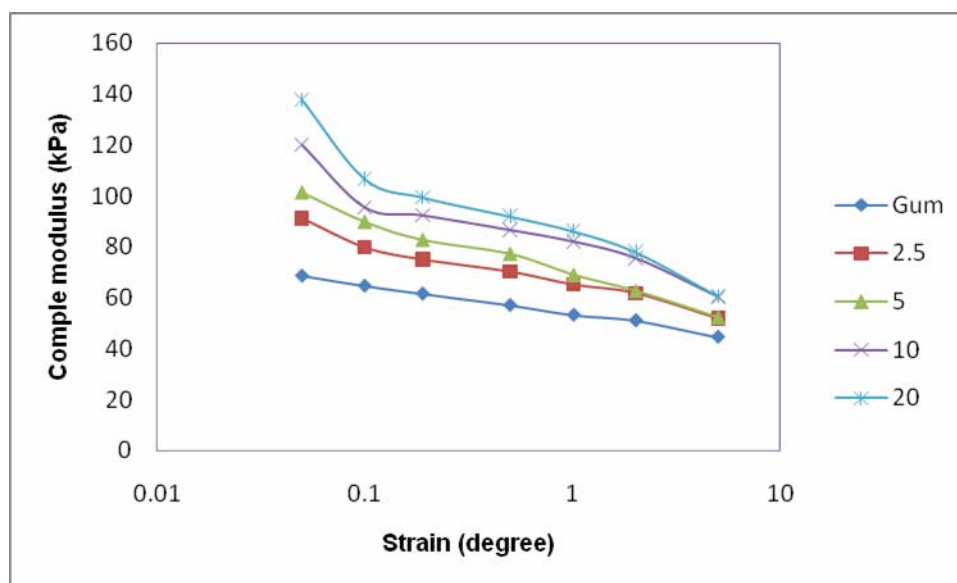


**Figure 5.22** Variation of complex modulus with strain in composites of nanofibrillated cellulose after bleaching in Uncured state

Figure 5.23 shows the response of modulus towards strain in uncured state in the case of natural rubber/nanofibrillated cellulose (after homogenization) composites in RPA. Here also modulus at very low strain is higher for 10 and 20 phr composites. The drop in modulus with strain is also higher for these composites. This indicates fiber agglomeration at these fiber loadings and breaking of fiber- fiber network at higher strains. 2.5 phr and 5 phr composites show lower initial modulus than 10 and 20 phr composites which indicates better dispersion of fibers in these composites. Interestingly, 5 phr composites show higher modulus at moderate values of strain, which is even higher than those of 10 and 20 phr composites at these strains. This may be due to better dispersion of fibers and formation of a network of fibers within the matrix which induces a stiffening of the matrix. This is supported by the better mechanical properties of 5 phr composites.

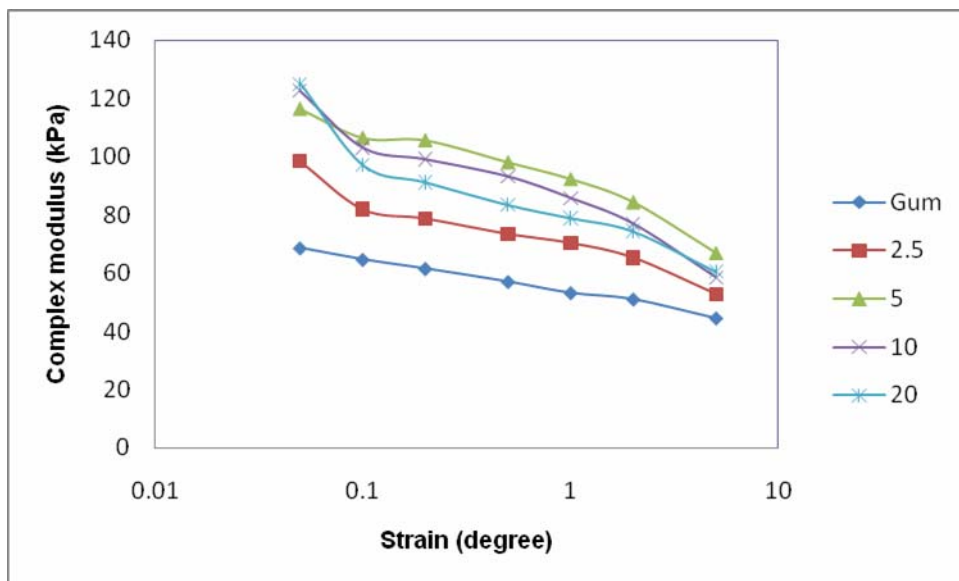


**Figure 5.23** Variation of complex modulus with strain in composites of nanofibrillated cellulose after homogenization in Uncured state

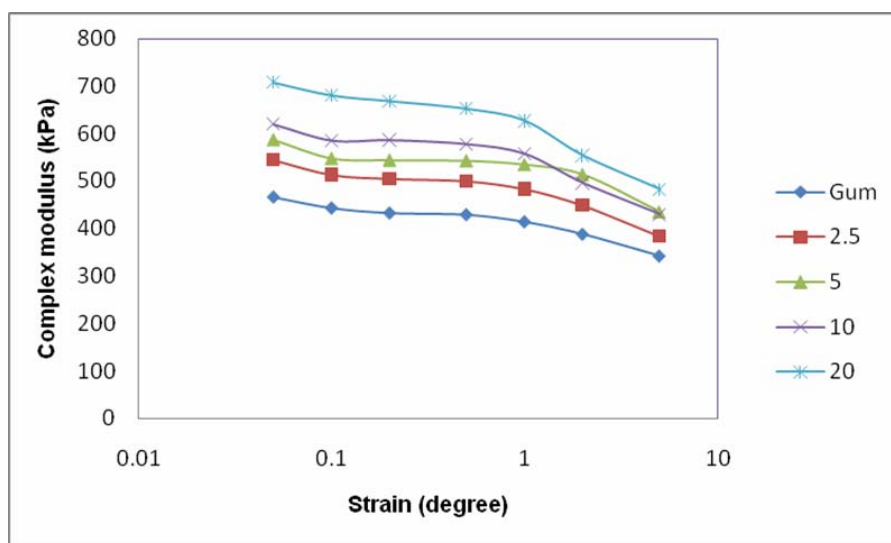


Figure 5.24 Variation of complex modulus with strain in composites of nanofibrillated cellulose after bleaching in Cured state

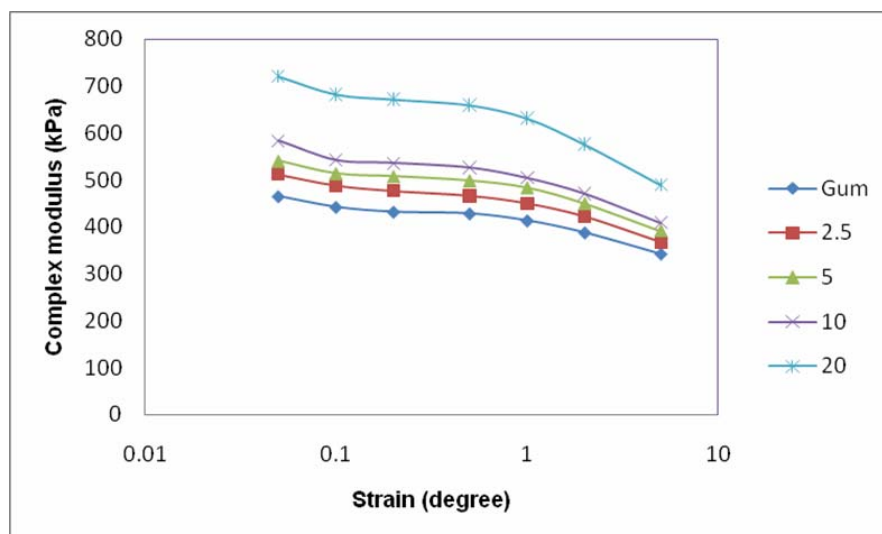


Figure 5.25 Variation of complex modulus with strain in composites of nanofibrillated cellulose after homogenization in Cured state

Figures 5.24 and 5.25 show the variation of complex modulus with strain in RPA, of composites of nanofibrillated cellulose after bleaching and homogenization respectively. In the linear viscoelastic region there will not be

much change in modulus with increase in strain [24]. There is strain amplitude called critical strain above which modulus starts to decrease. For all the composites except 5 phr BL composite the critical strain is at 1 degree. This is due to the breakdown of fiber network formed in the matrix. The better dispersion in the case of 5 phr composites may be the reason for higher critical strain. In HO composites the 2.5 and 5 phr composites show almost similar behavior as that of gum composites. This indicates the better dispersion of fibrils in these composites.

For all composites the initial modulus increases with fiber content. The initial modulus of 2.5 phr and 5 phr HO composites is lower than that of 2.5 phr and 5 phr BL composites. This shows better dispersion of fibrils in HO composites compared to BL composites.

### 5.B.3.2 Studies in DMA

#### 5.B.3.2.1 Temperature sweep studies

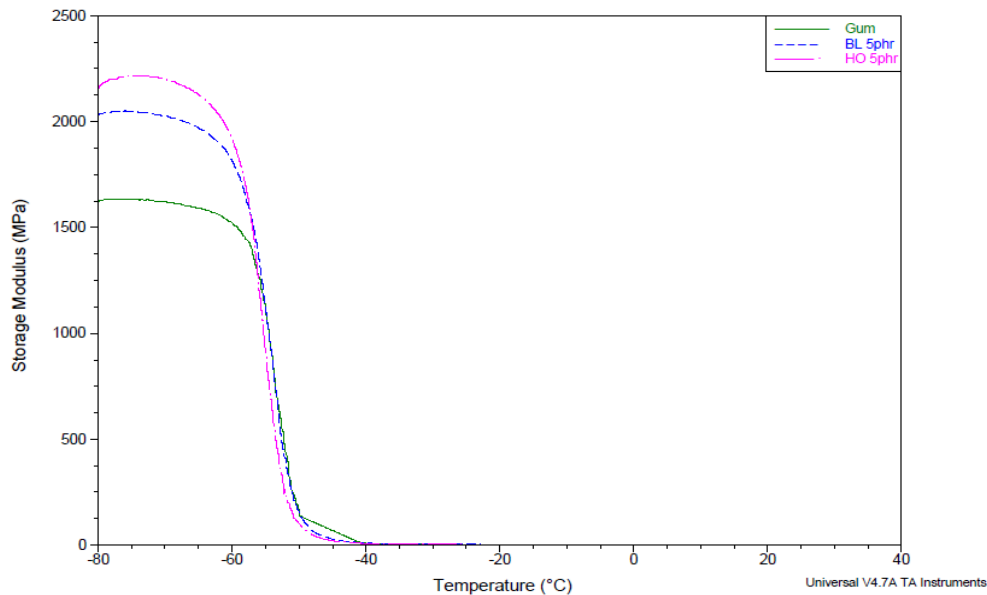
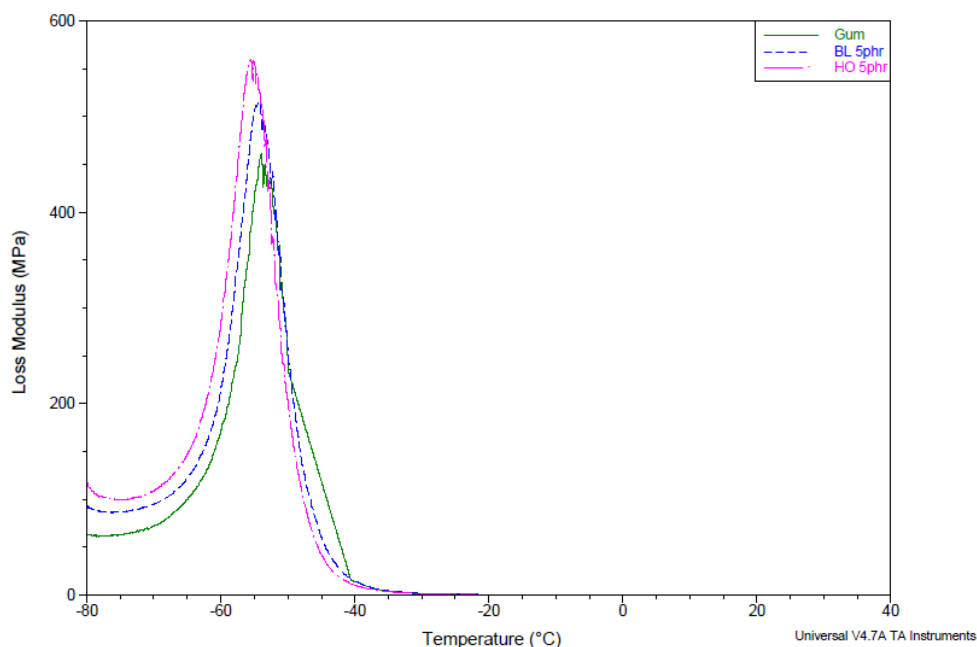


Figure 5.26 Variation of storage modulus with temperature of NR/nanofibrillated cellulose composites

Variation of storage modulus with temperature of NR-nanofibrillated cellulose composites is shown in figure 5.26. Storage moduli of both BL and HO composites containing 5 phr of nanofibrillated cellulose are compared with gum composites. Storage modulus values below glass transition temperature are high which reduces during the transition. Both BL and HO composites show higher storage modulus than gum composite. Between them HO composites show higher storage modulus than BL composites. This is due to the better dispersion and ensuing better reinforcement of HO composites. The variation in loss modulus of the composites is shown in figure 5.27. Loss moduli of the nanofiber composites are higher than that of the gum composites. This is due to the dissipation of energy at fiber rubber interface. HO composites due to their better dispersion have higher interfacial area and correspondingly higher loss modulus than BL composites. The loss modulus peaks at the glass transition temperature are more or less similar indicating no change in the glass transition temperature.



**Figure 5.27** Variation of loss modulus with temperature of NR/nanofibrillated cellulose composites

### **5.B.3.2.2 Frequency sweep studies**

#### **a). Composites of nanofibrillated cellulose after bleaching**

Figure 5.28 shows the variation of storage modulus with frequency of the bleached fiber composites. Composites are marked with numerical values of their fiber content. Theoretically, increasing the frequency has same effect of decreasing the temperature on the composites. At low temperature, storage modulus will be high. At the transition region there is a large decrease in storage modulus. At the rubbery plateau the modulus remains constant. Accordingly, with increase in frequency, storage modulus increases. There is a large increase in the storage modulus beyond a frequency of 14.6 Hz. This could be equated to the transition region of the composites. Corroborating trend is observed in the cases of loss modulus (figure 5.29) and  $\tan \delta$  (figure 5.30) also. Both show a maximum at frequencies beyond 14.6 Hz and then decreases. This can be considered similar to their behavior at the transition region. Between composites, storage modulus increases with fiber content. The composites emulate the same trend as in the case of tensile modulus. Even though the tensile strength decreases beyond a fiber content of 5 phr, at low strains as that encountered in frequency sweep tests the modulus goes on increasing with fiber content. The loss modulus at lower frequencies also increases with fiber content. With increase in fiber content the loss at fiber-fiber and fiber matrix interface increases. At the transition frequencies with increase in reinforcement the loss modulus and  $\tan \delta$  peaks register lower values at maximum.  $\tan \delta$  values decreases with decrease in segmental mobility. Reinforcement by the fibers is hindering the segmental mobility of the molecular chains and as a result  $\tan \delta$  of reinforced composites show marked decrease from gum or non reinforced composites.

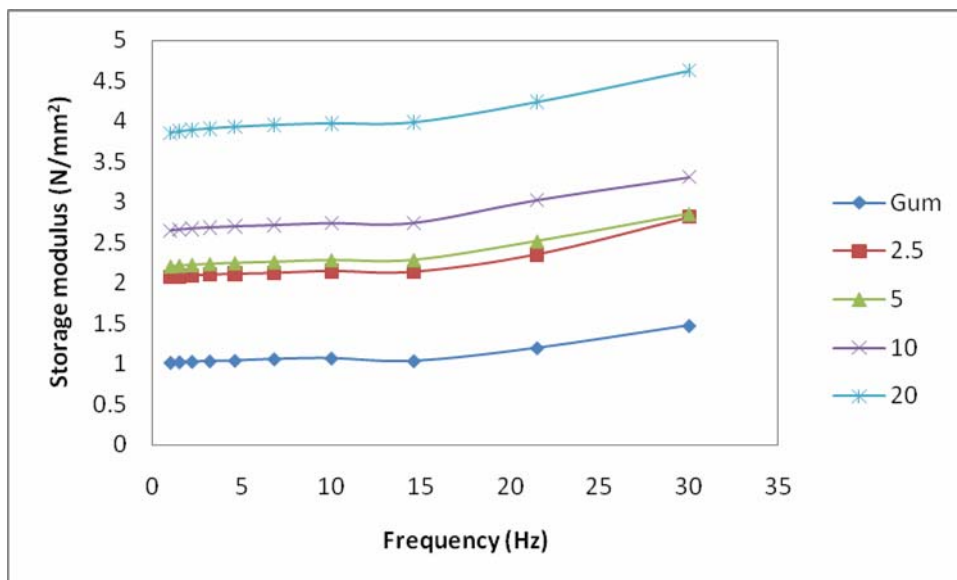


Figure 5.28 Variation of storage modulus with frequency of BL composites

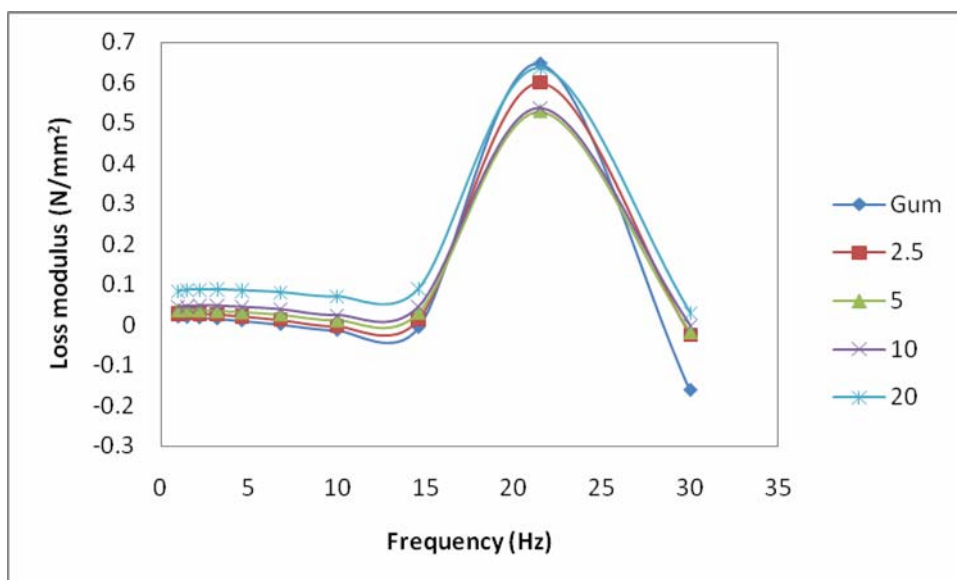


Figure 5.29 Variation of loss modulus with frequency of BL composites

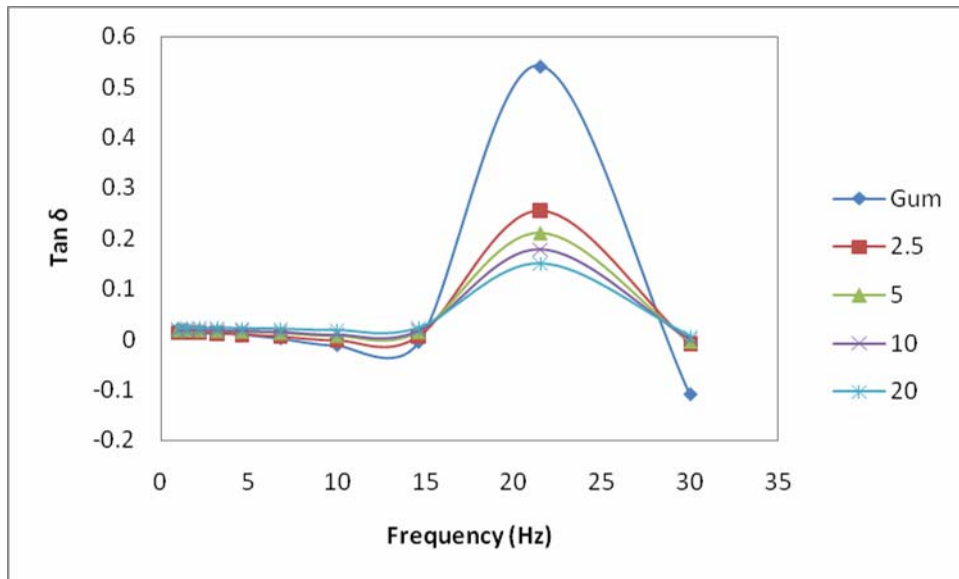


Figure 5.30 Variation of  $\tan \delta$  with frequency of BL composites

**b). Composites of nanofibrillated cellulose after homogenization**

Figure 5.31 shows the variation of storage modulus with frequency in the case of homogenized composites. The composites emulate similar response to frequency as that of bleached fiber composites. Storage modulus increases with frequency. At a frequency of 14.6 there is considerable increase in the slope of storage modulus curve, indicating the transition region. The loss modulus (figure 5.32) and  $\tan \delta$  (figure 5.33) show a maximum beyond this frequency and then decreases. In between composites fiber composites show increased storage modulus than gum composites and modulus increases with fiber content. Compared to bleached fiber composites homogenized fiber composites exhibits better storage modulus. The separation of fibrils during homogenization and consequent better dispersion of fibrils throughout the matrix may be the reason for the betterment.

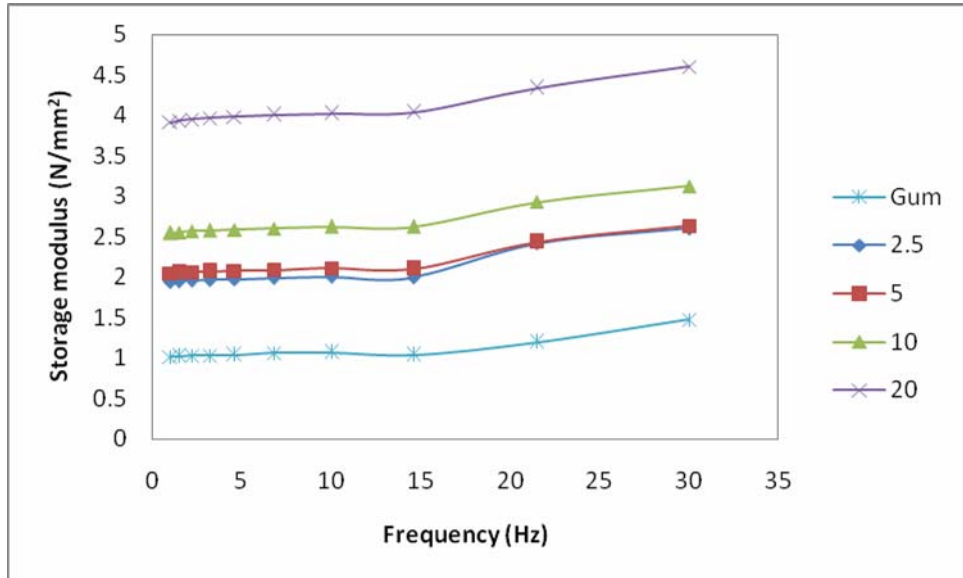


Figure 5.31 Variation of storage modulus with frequency of HO composites

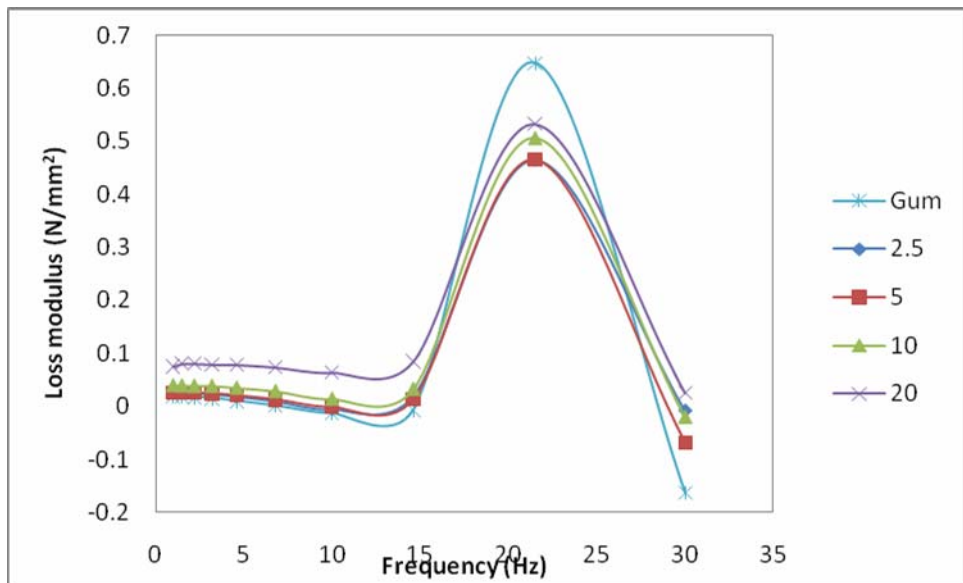


Figure 5.32 Variation of loss modulus with frequency of HO composites

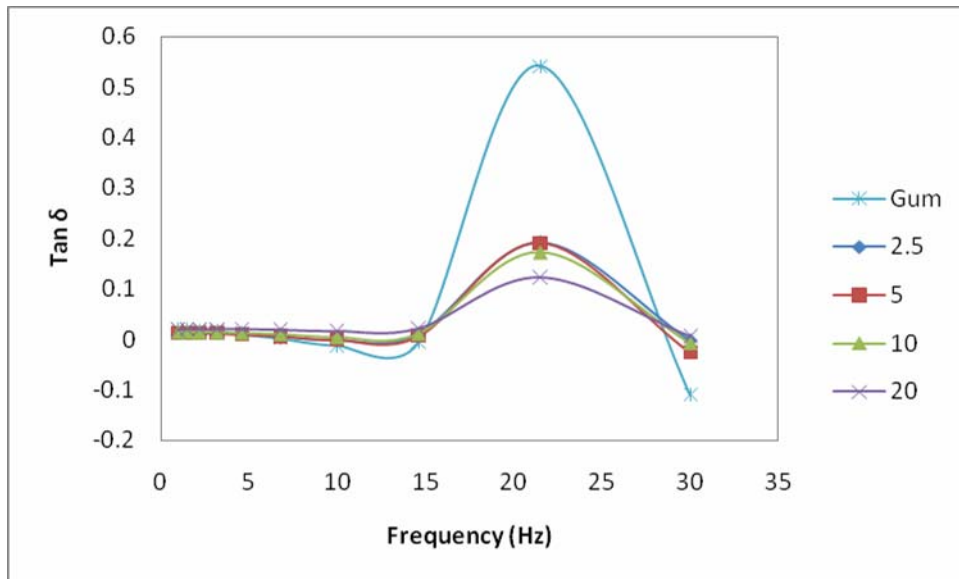


Figure 5.33 Variation of  $\tan \delta$  with frequency of HO composites

#### 5.B.4 Conclusions

Strain sweep studies were conducted in RPA to determine effectiveness of fiber dispersion and fiber rubber interaction. The moduli at lower strains revealed probable fiber agglomeration at higher loadings. 5 phr composites showed better dispersion. Homogenized samples show improved dispersion than bleached samples. Strain sweep studies in cured state indicated better fiber-matrix interaction in the case of 5 phr composites.

Dynamic mechanical properties of the composites were conducted with respect to temperature and frequency. Temperature sweep studies showed restrained matrix even at 5 phr fiber loading indicating improved reinforcement. Frequency sweep studies showed improvement in modulus with fiber content indicating better reinforcement. No appreciable change in glass transition temperature was observed. Frequency sweep studies indicated the increase of reinforcement with increased fiber content. Frequency sweep profiles show a transition region corresponding to the glass transition of the composites.

**Part -C**

**Thermal studies of NR- Nanocellulosic Fiber Composites**

**5.C.1 Introduction**

Many studies have been conducted to understand the effect of nanocellulose fibers and whiskers on the thermal properties of polymer composites. Oksman et al. [25] used cellulose nanowhiskers (CNW) separated from microcrystalline cellulose (MCC) to reinforce polylactic acid and found that CNWs were more sensitive to degradation compared to MCC. Petersson et al. [26] studied the thermal properties of poly(lactic acid)/cellulose whiskers nanocomposites. They also noticed that CNWs degraded faster than MCC from which they were separated and poly(lactic acid)/CNW composites degraded sooner than poly(lactic acid). Bondeson et al. [27] found that utilization of bio-based nanoparticles improves water vapor barrier, mechanical properties, and thermal stability without affecting the transparency of the biopolymers to any great extent. In studies by Pandey et al. cellulose whiskers extracted from grass were used to reinforce Polylactic acid. Thermogravimetric studies showed that the thermal stability of the composites gradually decreased with increasing filler load in the matrix [28]. Effect of cellulose nanofibers isolated from bamboo pulp residue on thermal stability of vulcanized natural rubber was studied by Visakh et al. [23]

In our studies cellulosic fibers in the nanofibrillated state extracted from coir were used to reinforce natural rubber composites. The nanofibrillated material after two different stages of extraction namely bleaching and homogenization were used in the composites. These composites were analyzed for thermal properties using Differential Scanning Calorimetry (DSC) and Thermogravimetry (TGA) to study the effect of the reinforcing fibers on the glass transition temperature and on thermal stability.

## 5.C.2 Experimental

Thermogravimetric analyses were carried out on TGA Q50 of TA Instruments. The samples were heated from ambient to 800°C with a heating rate of 20°C/minute under nitrogen atmosphere. A characterization method proposed by Friedman was used to establish the kinetic parameters. The details of the method are given in the previous chapter.

Differential scanning calorimetry of the composites was performed on DSC Q100 of TA Instruments. The experiments were carried out from -80°C to 100°C. The heating rate was 10°C/minute. A nitrogen atmosphere was maintained throughout the experiment.

## 5.C.3 Results and discussion

### 5.C.3.1 Thermogravimetry

#### a). Composites of nanofibrillated cellulose after bleaching

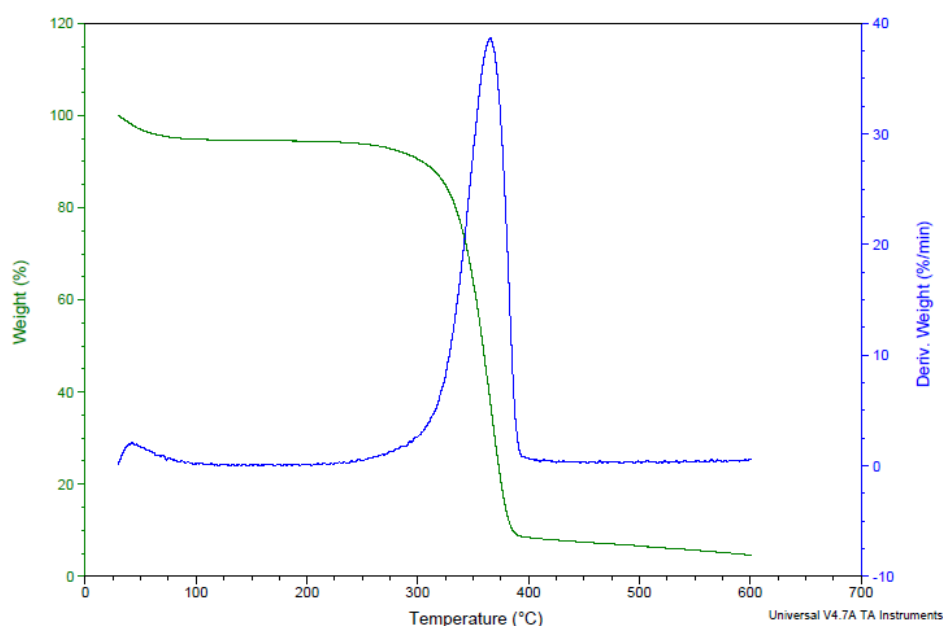


Figure 5.34 TGA and DTG profile of nanofibrillated cellulose after bleaching

Figure 5.34 gives the TGA and DTG profile of nanofibrillated cellulose obtained after bleaching and figure 5.35 that of nanofiber/NR composite. Table 5.3 gives the onset of degradation ( $T_i$ ), the temperature at which the rate of decomposition is maximum ( $T_{max}$ ) and the peak degradation rate for the bleached fiber and its composites. It can be seen that the onset of degradation for the nanocellulose is much lower than that of the gum rubber composite. It is also observed that the onset steadily decreases with increasing amount of nanofibrillated cellulose in the composites. The lower thermal stability of the nanofibrillated cellulose compared to the gum rubber vulcanizate, causes the early onset of thermal degradation in composites. With increase in the fiber content the onset shifts to lower temperatures (Figures 5.35 and 5.36). Though the shift in the onset of degradation is considerable, the shift in the peak degradation temperature between gum and nanofiber composites is only marginal. All of the fiber composites show more or less similar temperature at maximum degradation. Though the difference in the onset of degradation between gum composite and bleached fiber is nearly 100 °C the difference in peak degradation temperature is about 35 °C only. This shows that in cellulosic fibers, once degradation starts, the average rate of degradation is lower compared to gum rubber composite. So the presence of fibers does not alter the peak degradation temp to any great extent. This reduced average rate of degradation is also responsible for the decrease in the peak degradation rate of the composites with increasing fiber content.

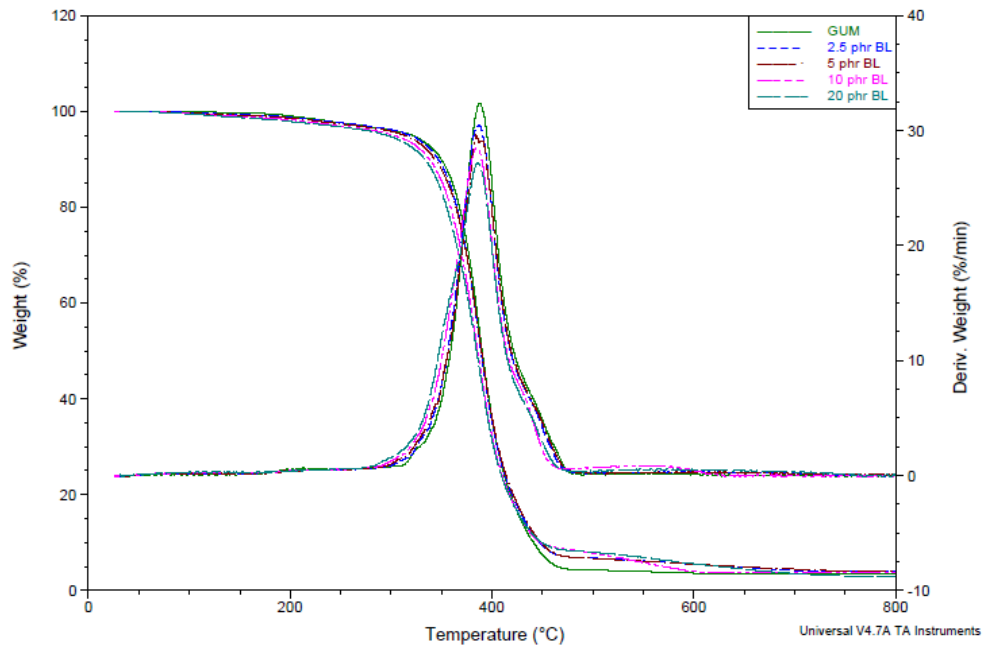


Figure 5.35 TGA and DTG profile of NR/nanofibrillated composites after bleaching

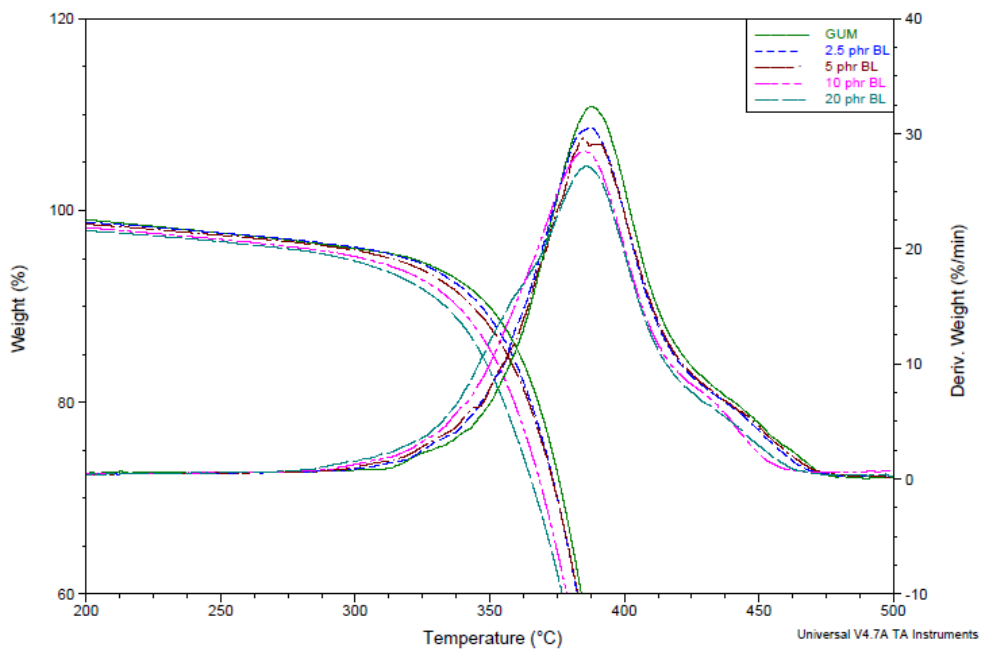
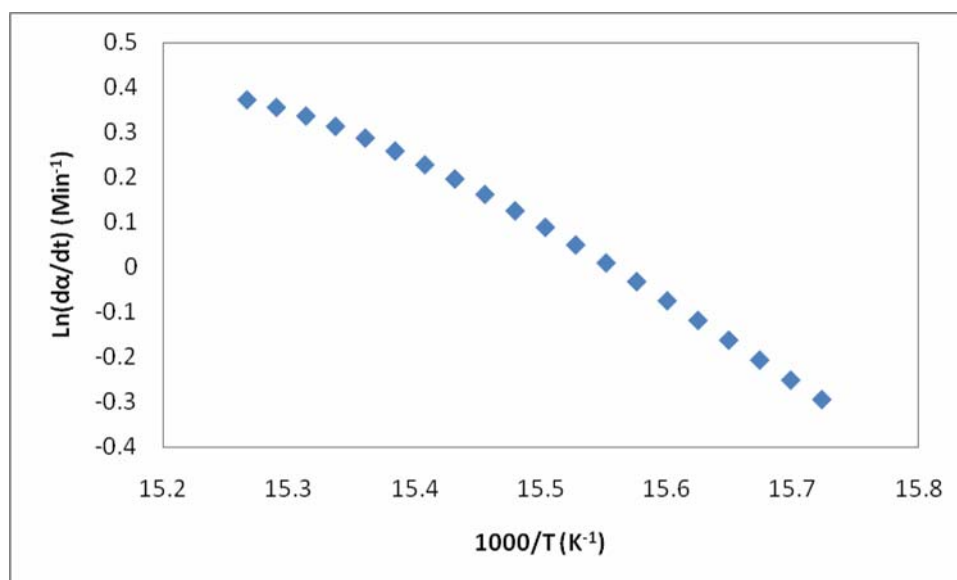


Figure 5.36. TGA and DTG profile of NR/nanofibrillated composites after bleaching (Zoomed version)

**Table 5.3 Degradation parameters of nanofiber and BL composites**

	Ti (°C)	Tmax (°C)	Rate (%/°C)
Nanofiber alone	212.8	353.2	1.46
Gum composite	310.6	388.1	1.58
2.5 phr composite	298.5	386.6	1.49
5 phr composite	290.1	387.0	1.44
10 phr composite	287.5	385.0	1.40
20 phr composite	279.5	386.0	1.33

Friedman method was used to study the degradation kinetics of the bleached fiber composites. Figures 5.37 and 5.38 show typical plots of  $\ln(d\alpha/dt)$  vs  $1/T$  and the  $\ln(1-\alpha)$  vs  $1/T$  respectively. It can be seen that plots exhibited good linear relationship which shows that the thermal degradation of the composites proceeded in good agreement with the Friedman model. Activation energy ( $E_a$ ) and order of the degradation reaction ( $n$ ) of the composites were found from the Friedman plots and are given in Table 5.4.

**Figure 5.37  $\ln(d\alpha/dt)$  vs  $1/T$  plot in Friedman method**

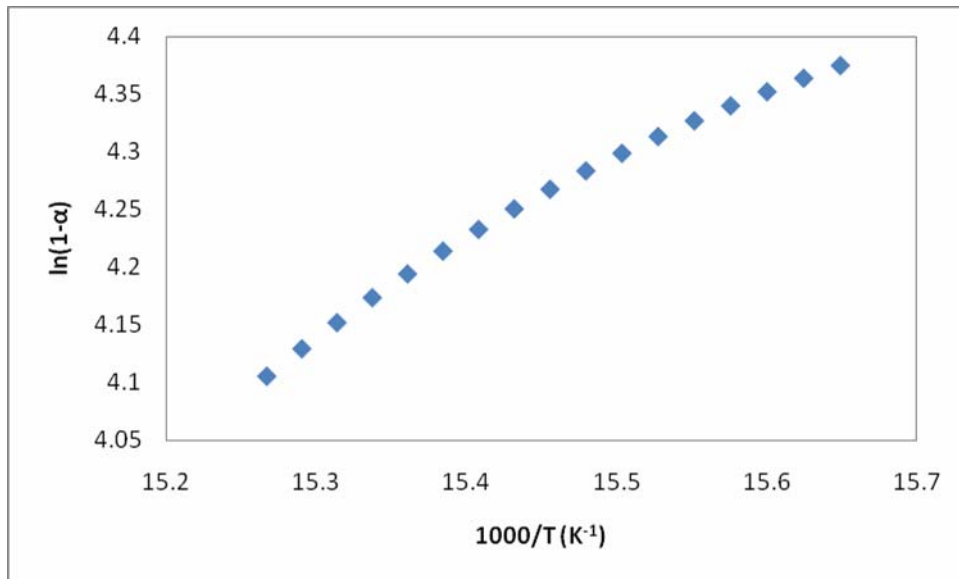


**Figure 5.38 Ln(1- $\alpha$ ) vs 1/T plot in Friedman method**

**Table 5.4 Thermal kinetics parameters of BL composites**

	<b>Ea (kJ/mol)</b>	<b>n</b>
Gum	139.2	2.6
2.5 phr	124.8	2.1
5 phr	120.6	2.1
10 phr	110.0	2.1
20 phr	89.7	2.1

**b. Composites of nanofibrillated cellulose after homogenization**

Figure 5.39 shows the TGA and DTG profile of nanofibrillated cellulose (HO) obtained after homogenization step. As in the case of nanocellulose after bleaching, the HO nanocellulose also degrades at a much lower temperature than the gum rubber composite. The addition HO nanocellulose to the rubber matrix results in lower onset of temperatures for the composites. This decrease in thermal stability can be observed in figures 5.40 and 5.41. Table 5.5 gives the thermal degradation parameters of the nanofiber and HO composites. Peak

degradation temperatures of composites were decreased by the addition of HO fiber. But among the HO composites peak degradation temperature does not vary to any appreciable extent. Similar behavior was observed in BL composites also. Decreased onset of degradation and lower average rate of degradation of the HO fiber may be the cause of this behavior.

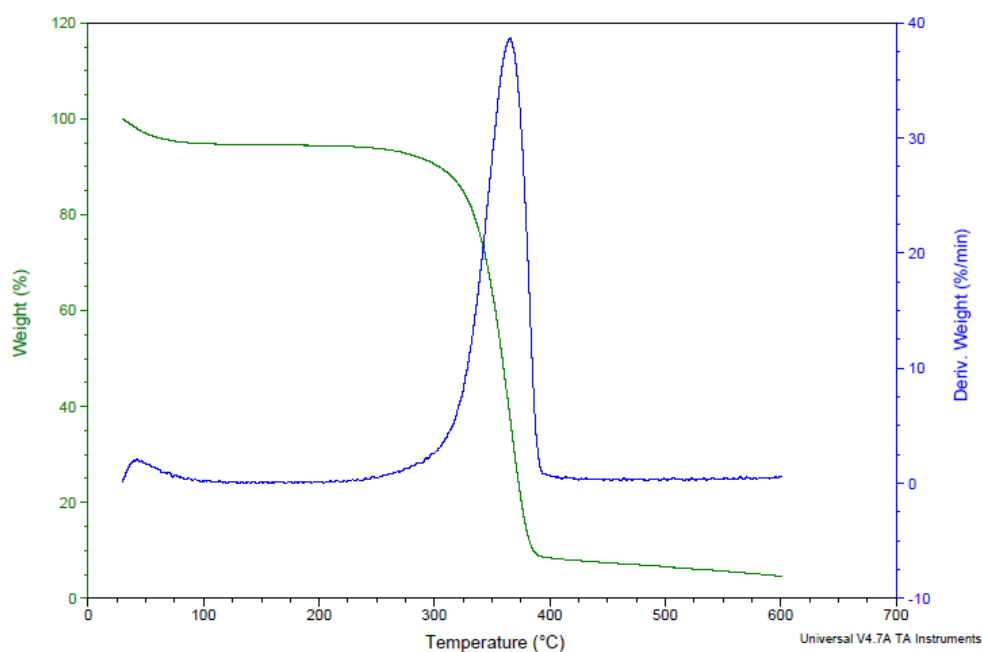


**Figure 5.39 TGA and DTG profile of nanofibrillated cellulose after homogenization**

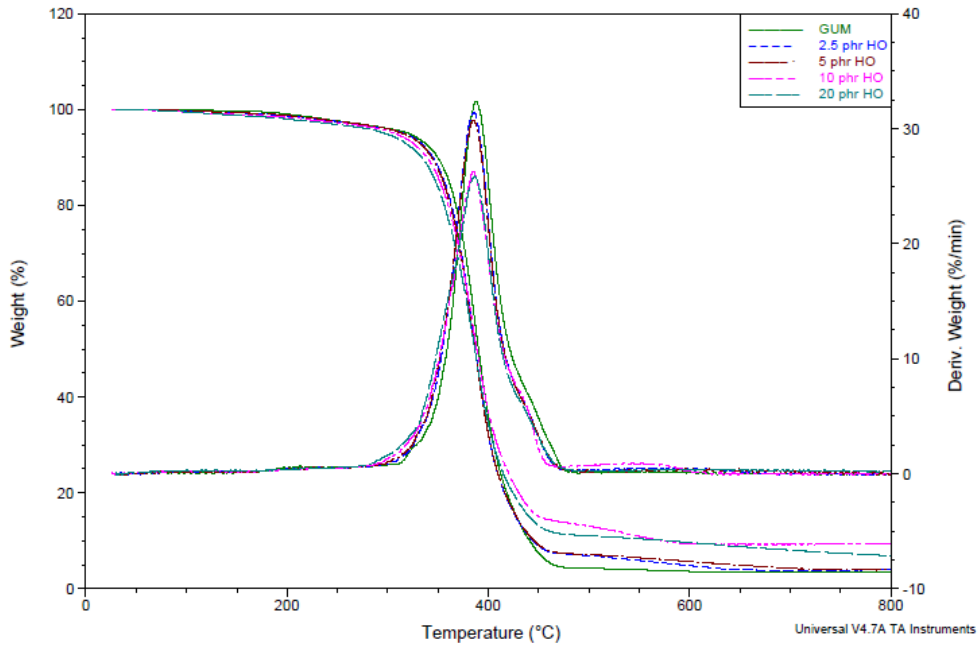


Figure 5.40 TGA and DTG profile of NR/nanofibrillated composites after homogenization

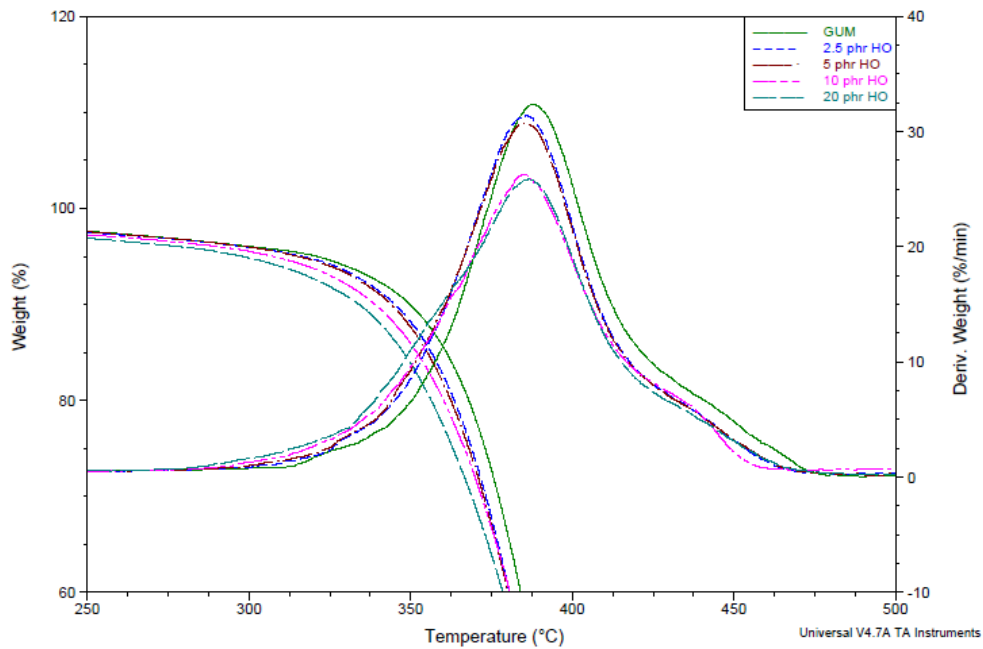


Figure 5.41 TGA and DTG profile of NR/nanofibrillated composites after homogenization (Zoomed version)

**Table 5.5 Degradation parameters of nanofiber and HO composites**

	Ti (°C)	Tmax (°C)	Rate (%/°C)
Fiber alone	213.6	353.0	1.47
Gum composite	310.6	388.1	1.58
2.5 phr composite	299.0	385.5	1.54
5 phr composite	294.8	385.5	1.51
10 phr composite	285.1	385.4	1.28
20 phr composite	279.7	386.4	1.26

Thermal kinetic parameters of the composites obtained by applying Friedman model is given in table 5.6. It can be seen that the activation energy of the composites decreases with increase in fiber content. This is in tune with the thermal stability of the composites as observed from TGA traces. The order of the degradation reaction almost remains constant among nanofiber composites.

**Table 5.6 Thermal kinetics parameters of HO composites**

	Ea (kJ/mol)	n
Gum	139.2	2.6
2.5 phr	130.0	2.1
5 phr	122.6	2.1
10 phr	113.2	2.1
20 phr	93.7	2.2

### 5.C.3.2 Differential Scanning Calorimetry

Figures 5.42 and 5.43 shows the DSC thermograms of BL and HO composites respectively, in comparison with gum composite. It can be seen that the glass transition as obtained from the DSC analysis is similar for all composites.

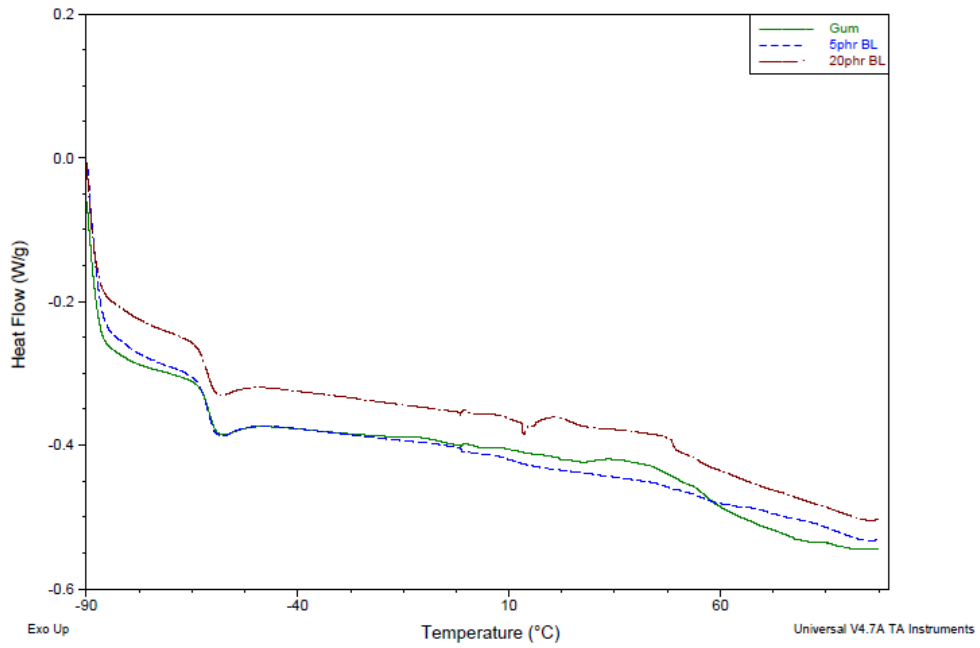


Figure 5.42 DSC thermograms of NR/nanofibrillated cellulose after bleaching

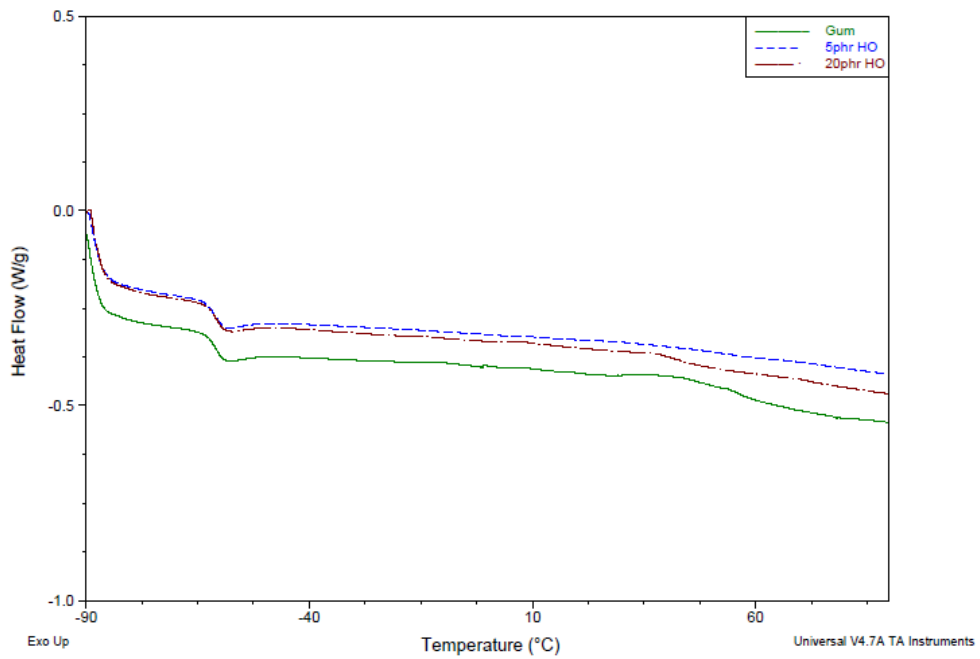


Figure 5.43. DSC thermograms of NR/nanofibrillated cellulose after homogenization

### 5.C.4 Conclusions

The thermal stability of the bleached and homogenized fibers were much lower compared to that of the gum composites. So the incorporation of the nanofibrillated cellulose into the rubber matrix reduces the thermal stability of the composites giving lower onset of degradation. Friedman model was used to determine the kinetic parameters of degradation. The activation energy of the composites decreases with fiber content showing decreased thermal stability. DSC studies showed no appreciable change in glass transition temperatures of the nanocomposites compared to gum composites.

### References

- [1] Meier H., Pure and applied chemistry **5** (1962) 37.
- [2] Heyn A.N., J. Ultrastruct. Res., **26** (1969) 52.
- [3] Blackwell J. and Kolpak F.J., **8**(3) (1975) 322.
- [4] Peterlin A. and Ingram P., Textile Res. J. **40**(4) (1970) 345.
- [5] Turbak A.F., Snyder F.W., Sandberg K.R., J. Appl. Polym. Sci. Appl. Polym. Symp. **37** (1983) 815.
- [6] Herrick F.W., Casebier R.L., Hamilton J.K. and Sandberg K.R., J. Appl. Polym. Sci. Appl. Polym. Symp., **37** (1983) 797.
- [7] Siqueira G., Bras J. and Dufresne A., Biomacromolecules, **10**(2) (2009) 425.
- [8] Mörseburg K. and Chinga-Carrasco G., Cellulose, **16**(5) (2009) 795.
- [9] Ahola S., Österberg M. and Laine J., Cellulose, **15**(2) (2008) 303.
- [10] Gardner D.J., Oporto G.S., Mills R. and Samir MASA, J. Adhesion. Sci. Technol. **22** (2008) 545.
- [11] Abe K., Iwamoto S. and Yano H., Biomacromolecules, **8**(10) (2007) 3276.

- [12] Amar K.M., Manjusri M. and Lawrence T.D., Natural Fibers, Biopolymers and Bio-composites. CRC Press, Taylor & Francis; 2005.
- [13] Wise L. E., Murphy M., and D'Addieco A. A., Paper Trade Journal, **122** (1946) 35.
- [14] Das K., Ray D., Bandyopadhyay N.R. and Sengupta S., J. Polym. Environ. **18** (2010) 355.
- [15] Revol J.F. et al. Can. J. Chem. **65** (1987) 1724.
- [16] Abdelmouleh M. and Boufi S., Compos. Sci. Technol. **67** (2007) 1627.
- [17] Jacob M., Francis B. and Thomas S., Polymer, (2006) 671.
- [18] Geethamma V.G., Kalaprasad G., Groeninckx G. and Thomas S., Composites, Part A, **36**(11) (2005) 1499.
- [19] Rabu M. and Wirjosentono B., Polym. J. **10** (2001) 377.
- [20] Sui G., Zhong W.H., Yang X.P., Yu Y.H. and Zhao S.H., Polym. Adv. Technol. **19** (2008) 1543.
- [21] Thomas P.S. et al., J. Appl. Polym. Sci., **124** (2012) 2370.
- [22] Visakh et al. BioResources **7**(2) (2012) 2156.
- [23] Payne AR. In: Kraus G, editor. Reinforcement of elastomers. New York: Interscience; 1965. p. 69.
- [24] Dick J. S., and Pawlowski H., Rubber World, January, 1995
- [25] Oksman K., Mathew A.P., Bondeson D. and Kvien, I., Compos. Sci. Technol., **66**(15) (2006) 2776.
- [26] Petersson L., Kvien I. and Oksman K., Compos. Sci. Technol., **67** (2007) 2535.
- [27] Syre D., Oksman P., and J K., Biobased Mater Bioenergy. **1**(1) (2007) 372.
- [28] Pandey J. K., Lee C. S. and Ahn S., J. Appl. Polym. Sci., **115** (2010) 2493.

.....✉.....



## POLYANILINE COATED MICRO AND NANO FIBER CONDUCTING COMPOSITES BASED ON NATURAL RUBBER PREPARED THROUGH LATEX PROCESSING

<b>Contents</b>	6.1 <i>Introduction</i>
	6.2 <i>Experimental</i>
	6.3 <i>Results and Discussion</i>
	6.4 <i>Conclusions</i>

### 6.1 Introduction

During the past two decades, conducting polymers and conducting polymer composites have been the subject of intensive research and development. Polyaniline (PANI) is one of the most studied conducting polymers due to its high electronic conductivity, redox and ion-exchange properties, excellent environmental stability and ease of preparation from common chemicals [1,2,3,4]. It is relatively inexpensive, has three distinct oxidation states with different colors and has an acid/base doping response. These properties make PANI a promising material for applications such as actuators, super capacitors and electrochromics. They are suitable for manufacture of electrically conducting yarns, antistatic coatings, electromagnetic shielding, and flexible electrodes. Conducting polymers are also suitable for shielding electromagnetic radiation and reducing or elimination of electromagnetic interference because of their relatively high conductivity and dielectric constant and ease of tuning of these properties through chemical processing and doping [5,6,7]. Reports on the high shielding efficiency of polyaniline, in comparison with that of copper triggered active research, in tuning of it by chemical processing with different dopants [8,9].

There have been efforts to get conducting polymers in fiber form. For this either the conducting polymers were made into fibers or fibers were coated with conducting polymers. Conductive coating of the fibers has been prepared by direct surface coating or by in situ polymerization on textile substrates [10,11,12,27-29]. Polyamides, polyesters, carbon fibers and kevlar are commonly used to produce conducting fibers. Commonly used conductive materials are polythiophene, polyaniline or polypyrrole [13,14].

Incorporation of conducting additives into an elastomer matrix will combine electronic conductivity of the additive with elasticity and other useful mechanical properties of the rubber matrix [15,25]. Several reports deal with the development of such conducting materials by employing conducting carbon black as the conducting additive [16,26] and their potential. In recent years, conducting polymers with highly extended conjugated electron systems in their backbones have attracted great interest due to their electrical, electrochemical and optical properties [17]. Conducting blends of elastomer and polyaniline have several potential applications, especially as pressure sensors. A blend of PANI and nitrile rubber (NBR) has been prepared by coating a platinum working electrode with a thin film of nitrile rubber and polymerizing aniline by the potentiodynamic method [18]. Nitrile rubber and polyaniline were also blended by cold mixing in a 'calender'. PANI was doped with different dopants. All samples were electroactive and presented similar conductivities [19].

Studies have been conducted on the incorporation of conducting polymer coated short fibers into the elastomer matrix to impart good mechanical and electrical properties to the composites. Saritha et al. prepared composites of natural and chloroprene rubbers with conducting short nylon fibers [20,21].

Polypyrrole coated short nylon fibers were also used to prepare elastomeric composites based on natural rubber [22].

In all these works conducting polymer and coated fiber were incorporated to the dry rubber. If both of these additives are added in the latex stage advantages in terms of better dispersion of conducting polymer and short fiber and lower breakage of the short fibers could be achieved. So efforts have been made to polymerize insitu, the conducting polymer in the latex containing short fibers. Our own group earlier reported the polypyrrole coated short nylonfiber/natural rubber composites prepared by in situ polymerization in latex [23].

In this chapter the insitu polymerization of polyaniline in latex containing fibers, to prepare conducting elastomer composites is discussed. Fibers used were of micro and nano size, separated from coir through the processing method discussed in the previous chapters. Mechanical properties, DC electrical conductivity and microwave characteristics of the conducting elastomer composites are discussed. This chapter envisages another application of latex stage processing of the composites.

## **6.2 Experimental**

### **6.2.1 Materials**

Concentrated natural rubber latex (60 DRC) was procured from Njavally Latex Pvt Ltd. Vulcastab VL was supplied by Rubber Research Institute of India, Kottayam. Coir fibers procured locally were chopped to approximately 6mm length. Zinc oxide, stearic acid, TQ (1,2-dihydro-2,2,4-trimethylquinoline), ZDBC (zinc dibutyldithiocarbamate) and sulfur used were of commercial grade. Aniline monomer was purified by distillation and stored in the absence of light. Ammonium peroxydisulphate was supplied by Merck Specialities Pvt. Ltd., Mumbai.

### 6.2.2 Preparation of composites

Weighed amount of concentrated latex was diluted to 20% dry rubber content. 10 % Vulcastab stabilizer based on dry rubber content was added to the latex. The coir fiber was processed as per the methods given in previous chapters to prepare micro and nano fiber dispersions. Calculated amount of fiber dispersions were added to the diluted latex. Amount of fiber was varied as 10, 20, and 30 phr for microfiber composites and as 5, 10, 20 and 30 phr for nanofiber composites. Aniline monomer was then added in calculated amount for the formation of 70 phr of polyaniline by insitu polymerization. The latex mixture was stirred and an aqueous solution of ammonium peroxydisulphate was added. The monomer to oxidant ratio was 1:1. To this mixture 1 molar solution of hydrochloric acid was added with stirring. Numerous local coagulations appear within the latex. The latex was kept undisturbed for 6 hours. The coagulated latex was then filtered, washed thoroughly with distilled water and dried at 50°C for 24 hours.

**Table 6.1 Formulation of the mixes**

<b>Ingredients</b>	<b>Phr</b>
NR	100
Polyaniline	70
Fiber	20
ZnO	4
Stearic acid	2
TQ	1
ZDBC	1.5
Sulphur	2

The dried sheet was used for compounding according to ASTM D 3182 in a two- roll mill as per the Formulation given in Table 6.1. Since an

accelerator capable of curing the rubber stock at room temperature is used, all the mixes were vulcanized at 90°C for 1 hour in an electrically heated hydraulic press under a pressure of 180 kg/cm<sup>2</sup>.

### **6.2.3 DC electrical conductivity**

The DC electrical conductivity of the samples were measured by a two-probe method using a Keithley 2400 source-measure unit, which is a fully programmable instrument capable of sourcing and measuring voltage or current simultaneously with accuracy. A constant current source was used to pass a steady current through one of the probes and the voltage across the other was measured. The measurements were done at room temperature. The conductivity of the sample was calculated by the following formula:

$$\sigma \text{ (S / cm)} = (I/V) \cdot (l/A)$$

where,  $\sigma$  is the electrical conductivity, I is the current through the probe in amperes, V is the voltage across the probe in volts, l is the spacing between the probes in centimeters and A is the area of contact of the probes with the sample in centimeter square.

### **6.2.4 Measurement of microwave properties**

The microwave characteristics of the prepared conducting polymer composites were studied using cavity perturbation technique. The experimental set up consists of a ZVB20 vector network analyzer, sweep oscillator, S-parameter test set and rectangular cavity resonator. The measurements were done in S (2.5 –4 GHz) band frequencies at room temperature (25°C). The dimensions of S band rectangular wave-guide used in the measurements were 34.5 cm X 7.2 cm X 3.4 cm. Photograph of the network analyzer is shown in figure 6.1.



**Figure 6.1 Setup for the measurement of microwave properties**

The quality factor  $Q_0$  of the cavity and resonance frequency  $f_0$ , in the unperturbed conditions were measured. The samples in the form of thin rectangular rods, the length of which equals the height of the cavity, so that both the ends of the specimen are in contact with the cavity walls, were used. The samples were inserted into the cavity through a slot and positioned at the maximum electric field. The resonance frequency,  $f_s$ , and loaded quality factor,  $Q_s$ , of the samples were measured. Knowing the volume of cavity,  $V_c$  and volume of sample,  $V_s$  the dielectric permittivity and dielectric loss were calculated.

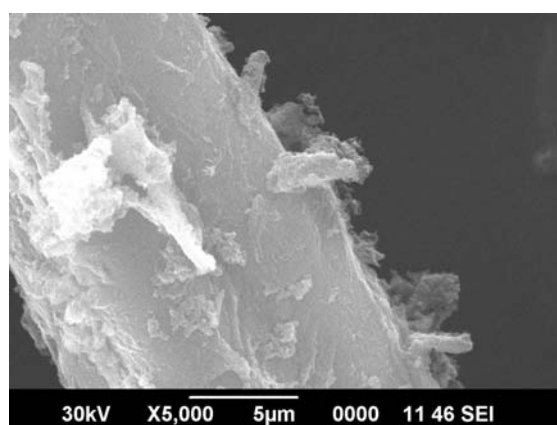
$$\text{Dielectric permittivity, } \left[ \frac{f_0 - f_s}{2f_s} \frac{V_c}{V_s} \right]$$

$$\text{Dielectric loss } \left[ = \frac{V_c}{4V_s} \left[ \frac{Q_0 - Q_s}{Q_0 Q_s} \right] \right]$$

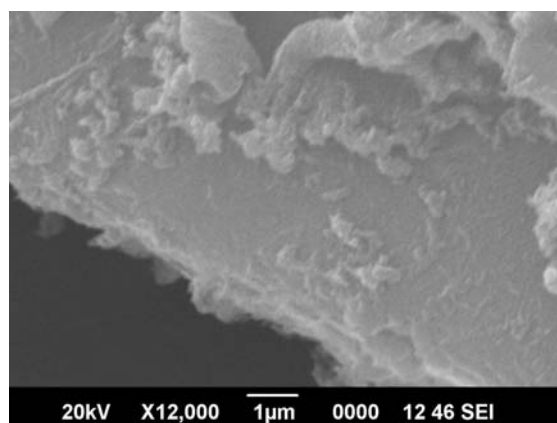
## 6.3 Results and Discussion

### 6.3.1 SEM Analysis

SEM images of the microfiber surface coated with polyaniline are shown in figures 6.2(a) and 6.2(b). It can be seen that a uniform coating of polyaniline is formed on the microfiber surface.



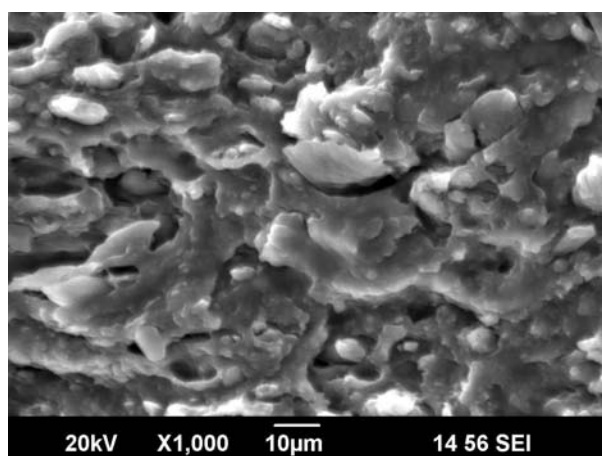
(a)



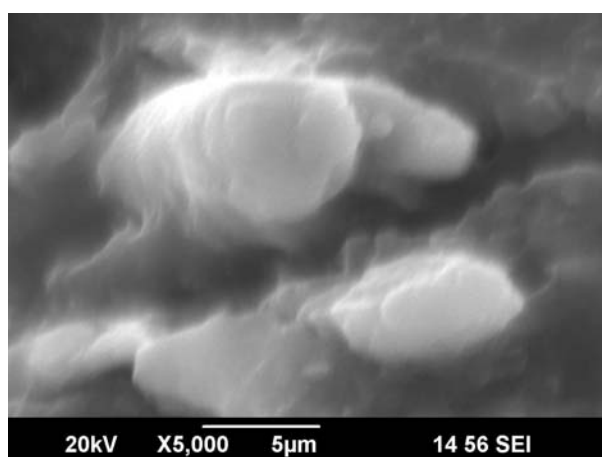
(b)

**Figure 6.2(a & b) Pani coated surface of microfiber**

Tensile fracture surface of the polyaniline/polyaniline coated fiber/ natural rubber composite is shown in figures 6.3(a) and 6.3(b). The uniform distribution of polyaniline and polyaniline coated microfibers in the rubber matrix can be seen.



(a)



(b)

**Figure 6.3 (a & b) Tensile fracture surface of the polyaniline/polyaniline coated fiber/ natural rubber composite**

## **6.3.2 Mechanical properties**

### **6.3.2.1 Tensile strength**

Tensile strength of the polyaniline/polyaniline coated fiber/ natural rubber composites as a function of fiber content is given in figure 6.2. The tensile strength gradually decreases with increasing fiber content for both micro and nano fiber composites. In the case of micro and nano fiber composites discussed in the previous chapters, the tensile strength increases due to improved

interaction between the fiber and matrix through the presence of a bonding agent. In the absence of a bonding agent the interaction between non polar rubber and the polar fiber will be minimum. The presence of another polar material in the form of polyaniline will increase the incompatibility. So the fibers will not contribute to the reinforcement and will act as diluting constituent for the matrix. At high strains the fibers will be debonded from the matrix. The voids formed will be acting as stress concentrators leading to the early failure of the composites. Among the composites the nano composites show better tensile strength than micro composites due to the lower size and better dispersion the former case.

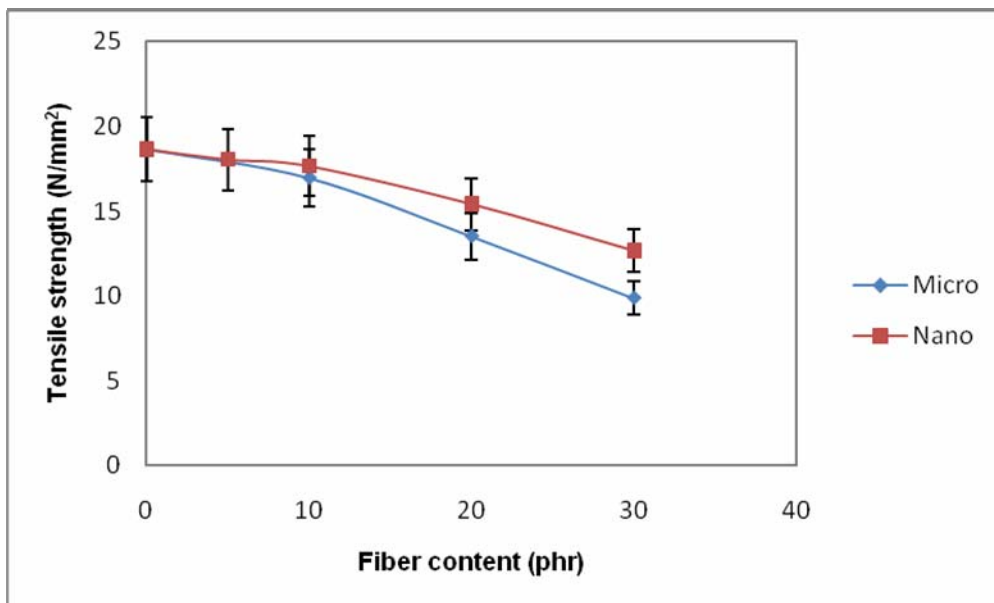


**Figure 6.3 Variation of tensile strength with fiber content**

### 6.3.2.2 Modulus

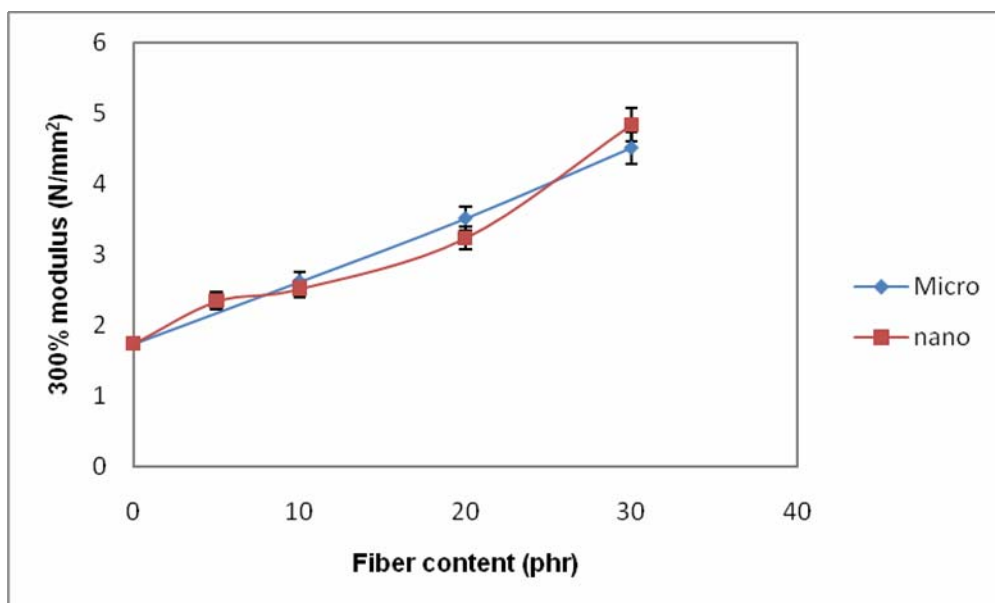
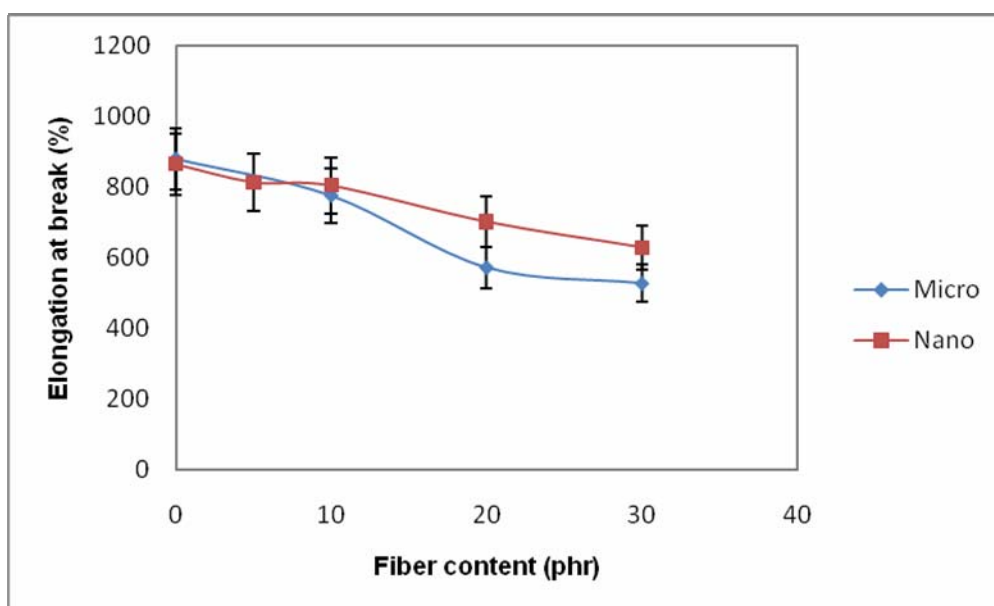


Figure 6.4 Variation of modulus with fiber content

Figure 6.3 shows the variation of modulus with fiber content. Since the modulus is measured at lower elongations the incompatibility of the fibers and polyaniline with the matrix does not affect the values to a great extent. The modulus increases with fiber content for both micro and nano composites.

### 6.3.2.3 Elongation at break

Figure 6.4 shows the elongation at break of the composites. Elongation decreases with fiber content. Decrease in elongation is larger for micro composites. The defects formed during the application of tensile load will be larger in the micro composites than in nano composites. These defects will accelerate the failure process giving lower elongation at break for the micro composites.



**Figure 6.5** Variation of elongation at break with fiber content

### 6.3.3 DC electrical conductivity

The conductivity of polyaniline is compared with polyaniline coated micro fiber and polyaniline coated nano fiber in Table 6.2. It can be seen that conductivity of PANI coated microfiber is one order of magnitude lower than pure PANI. Interestingly the nanofiber shows a much reduced conductivity compared to that of the micro fiber. Conductivity was 3 orders of magnitude lower than that of micro composites. The much finer size of the nano fibers increases their surface area by many orders of magnitude. So nano fibers require more amount of PANI for good uniform coating on their surface. When same amount of PANI was coated on both samples microfiber sample pellets acquire a continuous conducting path more easily, which is reflected in the conductivity of the samples.

**Table 6.2 conductivities of PANI and PANI coated nano and micro fiber**

<b>Conductivity (S/cm)</b>		
<b>Pani</b>	<b>Pani/Micro</b>	<b>Pani/Nano</b>
$4.610 \times 10^{-1}$	$2.08332 \times 10^{-2}$	$7.37607 \times 10^{-5}$

The conducting behavior of micro and nano fibers are almost repeated in the conducting elastomer composites of polyaniline/polyaniline coated fibers (figure 6.5). The micro fiber composites exhibit conductivities two orders of magnitude higher than nanofiber composites especially at 30 phr fiber content. The lower conductivity of the PANI coated nanofibers may be the reason for this interesting behavior. The higher surface area of the nanofibers may require more amount of PANI for uniform coating on the entire fiber surface. So the chance of forming a continuous conducting path through the matrix is diminished, giving lower conductivity for composites. In microfiber composites the coated fibers will be in touch with each other giving a continuous path for electrical conduction through the matrix. Due to their higher sizes the surface area of the micro fibers will be less compared to nanofibers. So for the same volume of fibers the area to be coated with PANI is lower for microfiber. The remaining PANI will be retained in the matrix giving a continuous path for conduction. So the microfiber composites offer higher DC conductivity than nanofiber composites. Similar studies conducted with short nylon fibers, through dry rubber stage processing gave conductivity values which were decreasing with fiber content [20]. The improper dispersion of fibers may be the problem in dry rubber processing of fiber composites. This verifies the suitability of latex stage processing to make conducting composites.

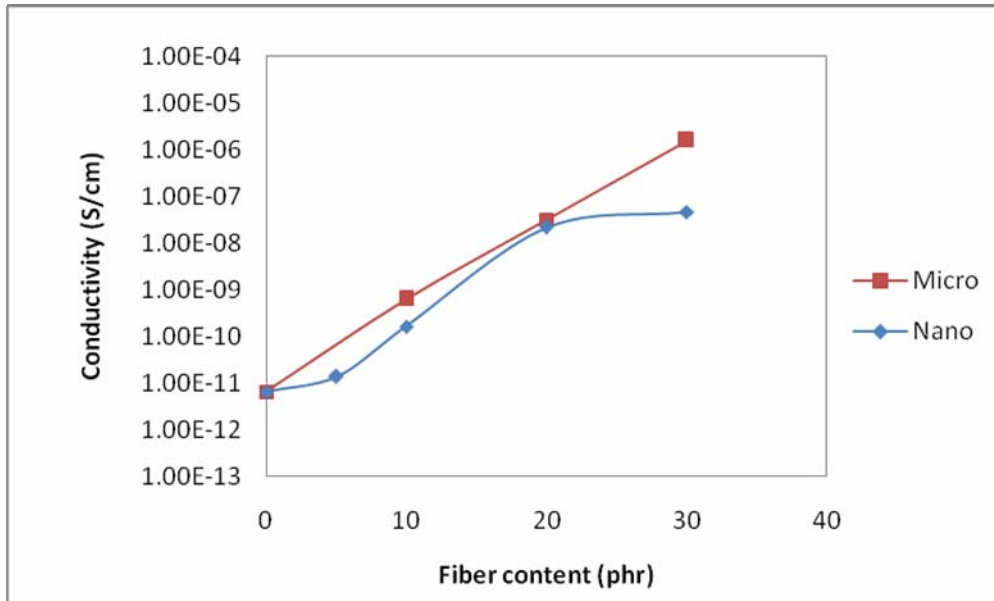


**Figure 6.6 Variation of conductivity with fiber content**

### **6.3.4 Microwave characteristics**

#### **6.3.4.1 Dielectric permittivity**

Figure 6.6 and figure 6.7 show the variation dielectric permittivity with fiber content for micro and nano fiber composites respectively. For micro composites the dielectric permittivity increases with fiber content almost linearly. In the case of nano composites it increases upto 10 phr fiber loading and then remains almost constant. According to Koops [24], the dielectric permittivity is inversely proportional to the square root of resistivity. As discussed in the previous section, conductivity of the microfiber composites increases considerably with fiber content. For nano composites the increase in conductivity with fiber content is lower especially at higher fiber content. The permittivity also behaves in a similar fashion.

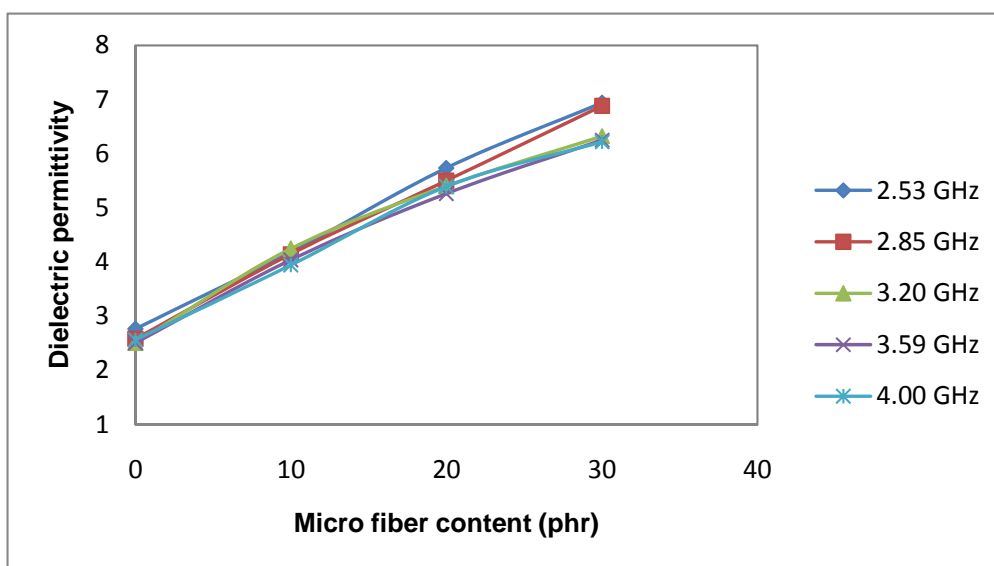


Figure 6.7 Variation of dielectric permittivity of composites with loading of microfiber

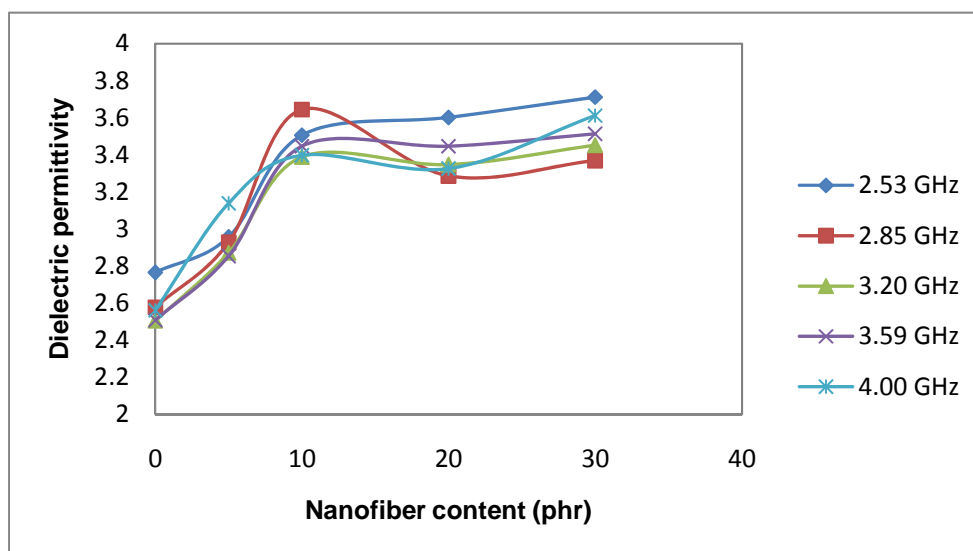
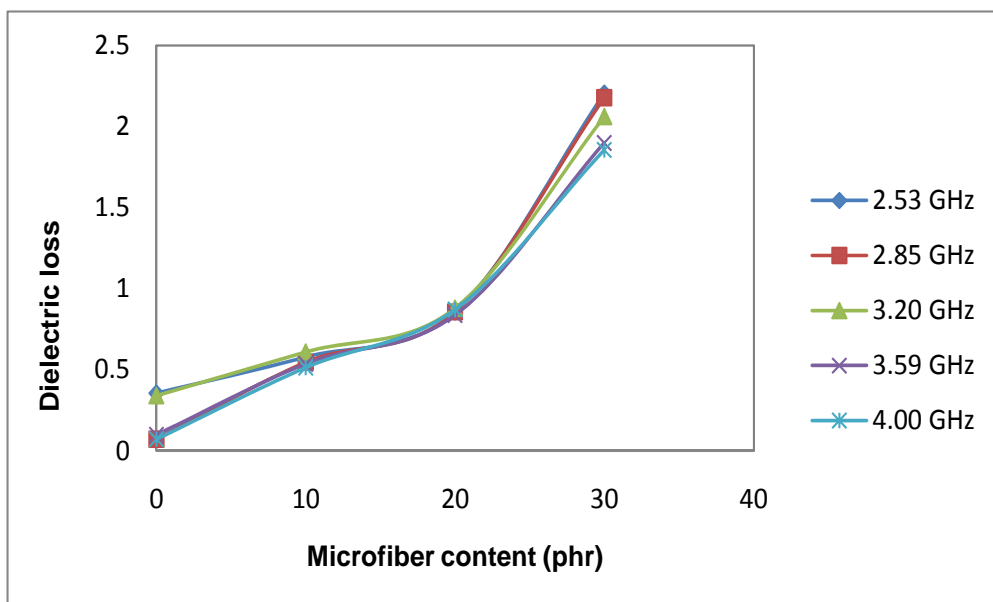


Figure 6.8 Variation of dielectric permittivity of composites with loading of nanofiber

### 6.3.4.2 Dielectric loss

The variations of dielectric loss with fiber loading in micro and nano composites are given in Figures 6.8 and 6.9 respectively. Microfiber composites show a steady increase in dielectric loss with fiber content. In the case of nanofiber composites dielectric loss increases considerably upto 10 phr fiber loading. Thereafter the increase in loss is minimal. The electromagnetic radiations when passing through a conducting composite medium with dispersed particles, some part gets reflected from the particles. If the particles are in a fiber shape the reflection will be happening from each point on the conducting fiber surface giving considerable loss. The coated fibers in elastomer matrix are responsible for the higher loss in this case. The increased dielectric loss of microfiber composites can be effectively utilized in EMI shielding applications.



**Figure 6.9** Variation of dielectric loss with loading of microfiber

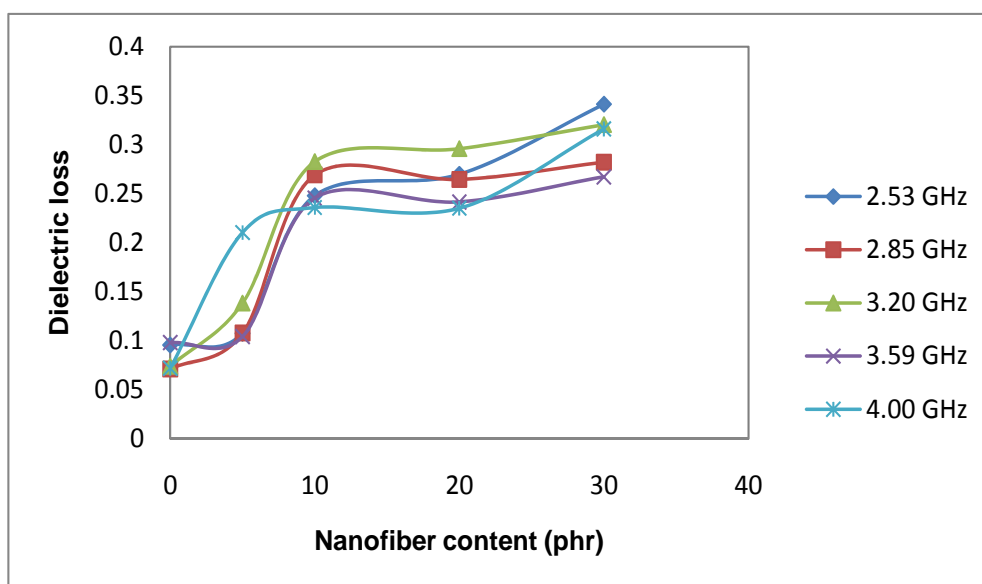


Figure 6.10 Variation of dielectric loss with loading of nanofiber

## 2.4 Conclusions

Conducting composites based on natural rubber were made using micro and nano fibers extracted from Coir, a natural fiber. The composites were prepared through latex stage processing, a novel method for the preparation of elastomer composites. The composites were evaluated for mechanical and electrical properties. With increasing fiber content, tensile strength and elongation at break were decreasing while modulus was increasing. DC conductivity of the polyaniline coated fibers, in pellet form, was less than that of pure polyaniline. In the case of elastomer composites, with increase in fiber content, the conductivity increases. The increase was higher in the case of microfiber composites.

Dielectric permittivity and dielectric loss of the elastomer composites increases with increasing fiber content. Microfiber composites show continuous increase in permittivity and dielectric loss with fiber content. For

nanofiber composites increase in the above properties is observed upto a fiber loading of 10 phr. Thereafter the properties do not change to any appreciable amount.

The increased dielectric loss with fiber content in the case of microfiber composites can be utilized to make elastomer based flexible EMI shielding materials.

### References

- [1] Gospodinova N. and Terlemezyan L., *Prog. Polym. Sci.*, **23** (1998) 1443.
- [2] Kang E., *Prog. Polym. Sci.*, **23** (1998) 277.
- [3] Trivedi D.C., in *Handbook of Organic Conductive Molecules and Polymers*, vol. 2, ed. by Nalwa HS. Wiley, Chichester, pp. 505–572 (1997).
- [4] Stejskal J., in *Dendrimers, Assemblies, Nanocomposites*, MML Series, vol. 5, ed. by Arshady R and Guyot A. Citus Books, London, pp. 195–281 (2002).
- [5] Joo J., Oh E-J. and Epstein A.J., *Mol. Electron. Devices*, (1995)107.
- [6] Joo J., and Epstein A.J., *Proc. Conference on Plastics for Portable Electronics*, Las Vegas, NV, 5-6 January, 140-149 (1995)
- [7] Kohlman R.S., Min Y.G., MacDiarmid A.G., and Epstein. A.J., *Proc. Soc. of Plastics Engineers Annual Technical Conference (ANTEC)* 1412-1416, ( 1996)
- [8] Lee C.Y. et al. *Synth. Met.*, **102** (1999) 1346.
- [9] Joo J. et al. *Mol. Cryst. Liq. Cryst. Sci. Technol., Sect. A*, **316** (1998) 367.
- [10] Gregory R.V., Kimbrell W.C. and Kuhn H.H., *Synth. Met.* **28** (1989) 823.
- [11] Gregory R.V., Samuels R.J. and Hanks T. National Textile Center annual report. <http://www.furman.edu/~hanks/ntc/>.
- [12] SarithaChandran A. and Narayanankutty S.K., *J. Mater. Res.*, **24** (2009) 2728.

- [13] Heisey C.L., Wightman J.P., Pittman E.H. and Kuhn H.H., *Text. Res. J.* **63** (1993) 247.
- [14] Byun S.W., and Im, S.S., *Synth. Met.* **57** (1993) 3501.
- [15] Anand J., Palaniappan S. and Sathyanarayana D., *Prog. Polym. Sci.*, **23** (1998) 993.
- [16] Wan Y., Xiong C., Yu J. and Wen D., *Compos. Sci. Technol.*, **65** (2005) 1769.
- [17] Ellis J.R.. In: Skotheim TA, editor. *Handbook of conducting polymers*. Vol. 1, New York; Marcel Dekker Inc, 1986, p. 489.
- [18] Tassi E.L. and De Paoli M.-A., *J. Chem. Soc., Chem. Commun.* 155 (1990).doi:10.1039/c39900000155
- [19] Vallim M.R., Felisberti M.I. and De Paoli M-A., *Proceedings 16th ReuniaoAnual da SBQ, Caxambu, 1993*, p. QM-22.
- [20] Saritha C. A., and Narayanankutty S.K., *Polym.-Plast. Technol. Eng.* **50** (2011) 443.
- [21] SarithaChandran A. and Narayanankutty S.K., *Eur. Polym. J.***44** (2008) 2418.
- [22] Pramila Devi D.S., Jabin T., Kutty S.K.N., *Polym.-Plast. Technol. Eng.* **51**(8) (2012) 823.
- [23] Pramila Devi D.S., Bipinbal P.K., Jabin T. and. Kutty S.K.N., *Mater. Des.* **43** (2013) 337.
- [24] Koops C.G., *Phys. Rev.*, 83 (1951) 121.
- [25] Granero A. J., Wagner P., Wagner K., Razal J. M., Wallace G. G. and In het Panhuis M., *Adv. Funct. Mater.*, **21**(5) (2011) 955.
- [26] Yi W., Wang Y., Wang G. and Tao X., *Polym. Test.*, **31**(5) (2012) 677.
- [27] Molina J., Esteves M. F., Fernández J., Bonastre J. and Cases F., *Eur. Polym. J.*, **47**(10) (2011) 2003.
- [28] Mattana G., Cosseddu P., Fraboni B., Malliaras G. G., Hinestroza J. P. and Bonfiglio A., *Org. Electron.*, **12**(12) (2011) 2033.
- [29] Patil A. J. and Deogaonkar S. C., *Text. Res. J.*, **82**(15) (2012) 1517.

.....❧.....

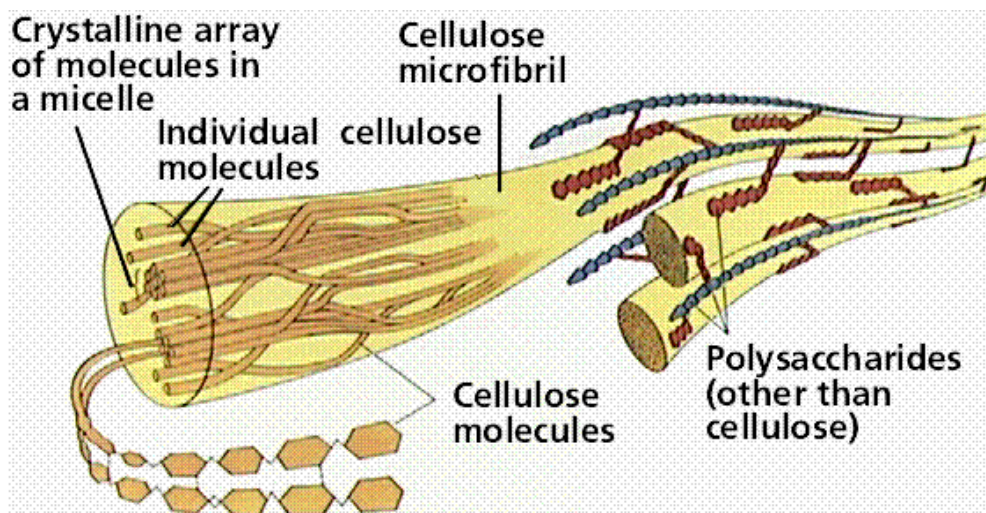
**Response to comments by Examiner in respect of  
Mr. Bipinbal P. K., Dept. of Polymer Science and Rubber Technology,  
Cochin University of Science and Technology**

<b>Chapter 1</b>		
<b>Sl. No</b>	<b>Comment</b>	<b>Response</b>
1	It seems to be fine to add more figures and tables in this part.	Figure included (Appendix A) (Structure of cellulose in plant cell wall)
2	Please add more recent references.	References included. (Page 41 & 42)
<b>Chapter 2</b>		
1	The terms in the equations are not correctly explained	Terms in equations were already explained.
2	Please give the details of chemicals used.	Details of chemicals are included. (Appendix B)
3	The molecular formula of H <sub>2</sub> SO <sub>4</sub> in page 52 is wrongly written	The molecular formula of H <sub>2</sub> SO <sub>4</sub> is corrected.
<b>Chapter 3</b>		
1	It is important to add error bars for the figures.	Error bars were already added except for cure characteristics.
2	The latex and dry stage processing methods need more explanation.	The methods are explained (Appendix C)
3	Author used different formulations for MANR-treated nylon composites and for HRH bonding agents. This needs more clarification	For the MANR treated nylon composites in order to develop good bonding between the fiber and the modified rubber adequate time should be given before crosslinking starts. So a delayed action accelerator (CBS) was used instead of a combination of MBTS and TMTD which was used in composites with HRH bonding agents.
4	Include good explanation for processing energy and fiber breakage analysis.	Explanation is given.
	Evaluation of Processing Energy	Appendix D
	Fiber breakage analysis	Appendix E

5	Please include the comparison of cure characteristics of three types of samples.	Comparison is included (Appendix F)
6	At 10 phr fiber loading the cure time of composite is lower than that of neat. What is the reason behind it?	At the lower fiber content of 10 phr, amines formed as an effect of degradation of the nylon fibers, being alkaline, will accelerate the curing process thus reducing the cure time. With increase in the fiber content the adsorption of accelerators onto the fiber will also increase. This reduces the homogeneous distribution of accelerators throughout the matrix and causes an increase in the cure time.
<b>Chapter 4</b>		
1	Please specify the amount of latex used for the preparation of the coagulum	167g of latex was used to get 100g of dry weight of rubber since the latex used had a dry rubber content of 60.
2	Give the details of the weight of the coir microfiber used? Is it dry weight? Please specify.	The dry weight of coir microfiber is used in the table. Calculated amount of dispersion was used to get the required dry weight.
3	You should avoid the repetition of tables. Table 4.2, Table 4.1 and Table 5.1	The repeating tables have been removed.
4	Table 4.3 is incomplete.	Table 4.3 shows the lignin content in untreated coir and coir after alkali treatments. It is complete by itself.
<b>Chapter 6</b>		
1	Please add more back references to this chapter	References have been added (Page 236)
2	Please give reasons for the microwave characteristics in the section 6.3.4.	Dielectric permittivity: The dielectric permittivity is inversely proportional to the square root of resistivity. As conductivity of the composites increases with fiber content, dielectric permittivity also increases linearly for microfiber composites. For nano composites the increase in conductivity with fiber content

		<p>is lower especially at higher fiber content. The permittivity also behaves in a similar fashion.</p> <p>Dielectric loss: The electromagnetic radiations, when passing through a conducting composite medium with dispersed particles, some part gets reflected from the particles which contribute to the dielectric loss. If the particles are in a fiber shape the reflection will be happening from each point on the conducting fiber surface giving considerable loss. So with increase in the fiber content the dielectric loss also increases. The effectiveness of conducting coating is higher for the microfiber composites compared to the nanofiber composites which reflects in the dielectric loss of the composites.</p>
3	<p>It could have been better to do a comparative study of different properties and thereby state which nanocomposite is showing better result.</p>	<p>If different composites prepared by the latex stage processing are compared with respect to mechanical properties it can be seen that in terms of tensile strength composites of nanofibrillated cellulose are superior since higher tensile strength is achieved with minimum amount of fiber loading. Modulus wise, nylon composites with HRH bonding system perform better. They also excel in ageing resistance. In terms of thermal properties MANR-Treated Nylon composites fare better with higher thermal degradation resistance compared to all other composites.</p>
4	<p>You can mention the future outlook of the synthesized nanocomposites.</p>	<p>Future outlook is included. (Page 244)</p>
5	<p>The author should have performed additional experiments such as Payne effect and Mullin's effect. This could be useful in the future study</p>	<p>Payne effect has been included in the study in the form of strain sweep studies in the Rubber process Analyzer.</p>

## Appendix A



Structure of cellulose in plant cell wall

## Appendix B

### Details of chemicals used

Sl. No.	Chemical	Details
1	<b>Maleic anhydride</b>	S D Fine-Chem Limited, India., Purity $\geq 99.0\%$ , Melting point $51-56\text{ }^{\circ}\text{C}$
2	<b>Hexamethylene tetramine (Hexa)</b>	E-Merck, Mumbai., India., Purity $\geq 99.0\%$ Residue on ignition $\leq 0.1\%$ , Loss on drying $\leq 2.0\%$ , Melting point $280\text{ }^{\circ}\text{C}$
3	<b>Resorcinol</b>	E- Merck Mumbai., India., Purity - $98.5\%$ , Residue on ignition $\leq 0.05\%$ , Loss on drying $\leq 1.0\%$ , Melting point - $109-112\text{ }^{\circ}\text{C}$
4	<b>Silica</b>	Minar Chemicals, Kochi, Density - $2.64\text{ g/cc}$ , BET surface area - $90 \pm 15\text{ m}^2/\text{g}$ , Loss on drying $\leq 5.0\text{ wt.}\%$ , pH $3.7 - 4.7$
5	<b>Aniline</b>	E- Merck Mumbai., India., Purity - $97\%$ , Melting point - $196-198\text{ }^{\circ}\text{C}$

6	<b>Hydrochloric acid</b>	E-Merck Mumbai., India., Purity - 37%, Density - 1.2 g/mL at 25 °C, Boiling point > 100 °C
7	<b>Sulphuric acid</b>	E-Merck Mumbai., India., Assay - 95.0-98.0%, Boiling point - 337°C, Residue on ignition ≤5 ppm
8	<b>Sodium hydroxide</b>	E-Merck Mumbai., India., Purity ≥97.0%, Melting point - 318 °C
9	<b>Ammonium persulphate</b>	E-Merck Mumbai., India., Assay ≥ 98.0%, Residue on ignition ≤0.05%
10	<b>Sodium chlorite</b>	E-Merck Mumbai., India., Assay - 80%
11	<b>Acetic acid</b>	E-Merck Mumbai., India., Density - 1.049 g/mL at 25 °C, Boiling point - 117-118 °C, Melting point - 16.2 °C
12	<b>Valcastab VL</b>	(polyethylene oxide condensate non-ionic stabilizer) was obtained from Rubber Research Institute of India
13	<b>Zinc oxide</b>	Meta Zinc Ltd. Mumbai., Specific gravity - 5.5, Zinc oxide content - 98%, Heat loss (2 hours at 100°C) - 0.5% maximum
14	<b>Stearic acid</b>	Godrej Soaps (P) Ltd, Mumbai., Melting point - 50-69 °C, Acid number -185-210
15	<b>1,2-dihydro 2,2,4-trimethylquinoline (TQ)</b>	Bayer India Ltd, Mumbai., Appearance - Amber to brown granules, Melting point - 80-100°C, Loss on drying (Max) %- 0.30, Ash (Max) % - 0.30
16	<b>N-Cyclohexyl-2-Benzothiazole Sulphenamide (CBS)</b>	Polyolefins Industries Ltd, Mumbai., Specific gravity -1.286 at 20 °C, Melting point -97.5-105 °C
17	<b>Tetramethyl-thiuramdisulphide (TMTD)</b>	NOCIL, Mumbai., Appearance -Light gray powder, Specific gravity - 1.29, Melting point ≥ 142 °C, Heating loss ≤ 0.4%, Ash ≤ 0.3%
18	<b>Zinc diethyl dithiocarbamate (ZDBC)</b>	Merchem Ltd, Kerala., Appearance -White powder, Density - 1.270 g/cc, pH value -neutral
19	<b>Sulphur (S)</b>	Standard Chemical Company Pvt. Ltd., Chennai, India., Purity - 99.0 to 99.5%, Specific gravity - 2.05, Acidity - 0.01, Ash - 0.01 % (max), Melting Point - 115-125 °C, Moisture Content - 0.15% (max)

## Appendix C

### A) Dry stage mixing:

The mixing was done as per ASTM D 3182 on a two roll laboratory size mixing mill. Once a smooth band was formed on the roll, short fibers cut to 6 mm length were added to the small bank formed in the nip. Mixing with intermittent cutting of the stock was continued until the fibers were completely incorporated to the rubber. Then the other ingredients were added in the following order: activators, bonding agent mixture, antioxidant, accelerators and finally sulphur. After complete mixing the stock was passed six times through the tight nip and finally sheeted out at a fixed nip gap so as to orient the fibers preferentially in one direction. Sheets were cut out and stacked one over the other till the required volume is reached.

### B) Latex stage mixing

The concentrated latex was diluted to 12.5% dry rubber content (DRC). Nylon fibers were cut to 6 mm length and separated into individual fibrils by using a jet of compressed air. The separated fibers were spread in an aluminium pan. A layer of latex was spread on the fiber layer so that the fibers are completely wet by the latex. Acetic acid diluted to 8% was sprayed to coagulate the latex. The process was repeated and a sandwich of alternating layers of latex and short fibers were built up until the required fiber content is reached. The coagulum containing the fibers was squeezed between rollers to remove water. The sheet obtained was dried in an air oven at 40°C for three days. Fiber loadings were adjusted to get 10, 20 and 30 phr fiber in the final composites. The composites were then processed like conventional sheet rubber and mixed with other ingredients in a two roll mill.

## Appendix D

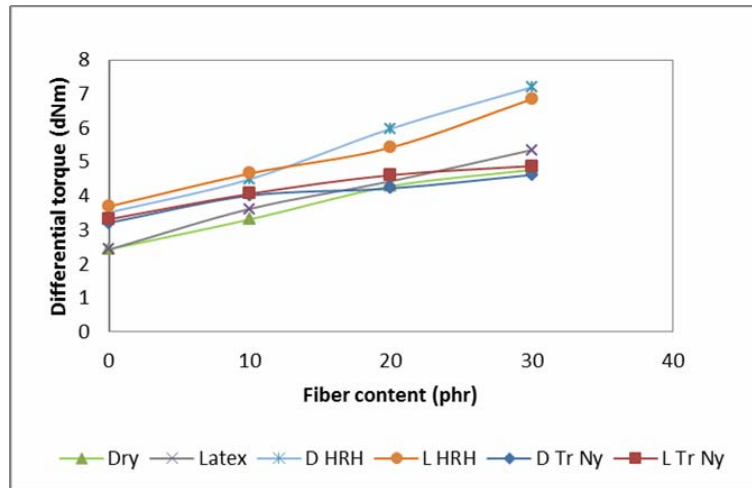
Figure 3.3 shows the integrated energy input during the mixing process in the Rheocord mixer. For both dry rubber and latex stage composites the energy input shows almost a linear increase with time. But for the latex stage composite energy input at any time is greater than the dry rubber composite. The higher energy for mixing in the case of latex stage composites is due to more restrained matrix resulting from better dispersion of fibers. From the figure it can be seen that for the input of

same amount of energy, only shorter mixing time is required for latex stage composites. So, considering the practice of fixing mixing time is in terms of total energy input, shorter mixing time can be fixed for latex stage composites compared to dry rubber composites without compromise in the filler (short fiber) dispersion.

### Appendix E

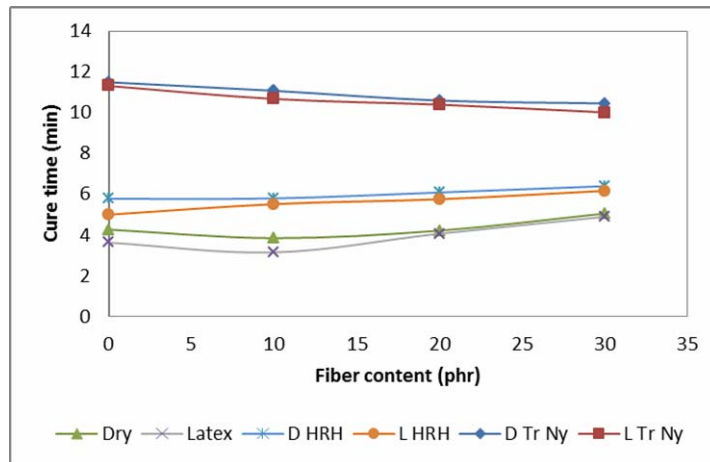
The average length of the cut fibers before mixing was 6mm. Figure 3.4 compares the distribution of fiber length after milling. The figure shows that average fiber length is 1.5 – 2.5 mm in the case of dry rubber compound where as it is 2.5 – 4.0 in the case of latex stage compound. In dry rubber compounds a fraction of 0.31 of the fibers were reduced to a length of 1.5 -2.5 mm compared to the fraction of 0.119 in the case of latex stage compounds. A larger fraction (0.37) could retain a length of 2.5 – 4.0 mm. This confirms lower fiber damage in the case of compounds prepared using latex stage masterbatch. This may be attributed to shorter shear history of the latex masterbatch.

### Appendix F



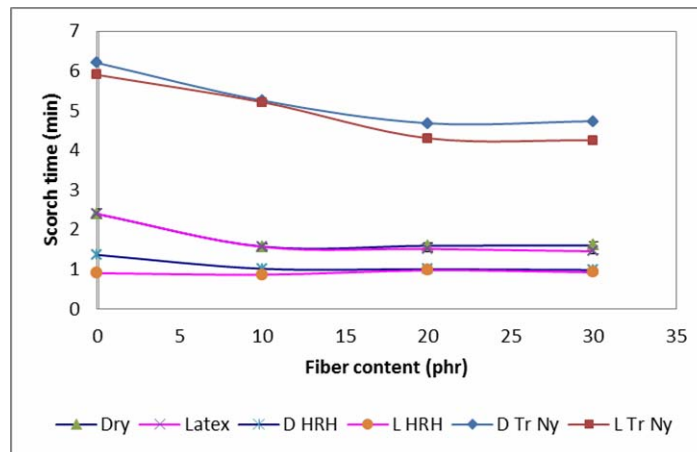
**Figure 1. Variation of differential torque with fiber content**

Figure 1 shows the comparison of differential torque of the nylon fiber composites. In general differential torque increases with fiber content. In between composites differential torque is higher for composites with HRH bonding system indicating higher modulus of these composites.



**Figure 2 Variation of cure time with fiber content**

Figure 2 shows the comparison of cure time for the nylon fiber composites. MANR-treated nylon composites show the highest of all cure times due to the acidic nature of the maleated matrix. Composites with HRH show higher cure time of than that of composites without HRH, may be due to the presence of acidic silca in the matrix. With fiber content, for MANR-treated nylon composites cure time decreases while composites with and without HRH exhibit marginal increase. These effects are caused by the uncombined -NH<sub>2</sub> groups in the former and the adsorption of curatives by the fibers making them unavailable for crosslinking in the latter.



**Figure 3 Variation of scorch time with fiber content**

Figure 3 gives the comparison of scorch time for the nylon composites. Similar to cure time scorch time also is higher for MANR-treated nylon composites compared to composites with and without HRH again due to the same reasons. Composites with HRH show marginally lower scorch time compared to composites without HRH. This may be attributed to the presence of amine functionality in the dry bonding system used.